A comparison of host-parasite interactions between *Toxoplasma gondii* and *Neospora caninum*

Thesis submitted in accordance with the requirements of the University of Liverpool for the degree of Doctor in Philosophy

by

Mariwan Musa Mohammed

May 2015

AUTHOR'S DECLARATION

Apart from help and advice acknowledged, this thesis represents the unaided work of the author

.....

Mariwan Musa Mohammed

May 2015

This research was carried out in the Department of Infection Biology and School of Veterinary Science, University of Liverpool

DEDICATION

I want to dedicate this thesis to my mother, father, sisters and brothers, my wife and my children whom have helped and supported me in my life in the past and especially now during my PhD. Mom and Dad, you are the greatest and the most precious lovers, I can never thank you enough, God bless you.

ACKNOWLEDGEMENTS

First and foremost, I would like to thank my sponsor, Kurdistan Regional Government, ministry of higher education for trusting in me and choosing me as a candidate to study abroad. I would like to thank my supervisors, Professor Jonathan Wastling and Dr Ben Makepeace, for accepting me as a student and for advices and supports during my PhD. I would also like to equally thank Professor Diana William and Dr Jane Hodgkinson, for accepting my application and offering me an offer letter to study in the University of Liverpool. However, there are a lot of other people that generously accepted to help me; this work would not have been the same without Dr Nadine Randle, Dr Dong Xia and Dr Stuart Armstrong, special thanks for your continuous efforts from the beginning to the end of my PhD. Special thanks to Mrs Catherine Hartley for every day support in the laboratory. I would like to thank my PhD advisors, Dr Jane Hodgkinson and Dr Andrew Jackson for their support. I would also like to thank all the colleagues back home and in the UK, especially in Infection Biology; Dr Sarah Vermont, Dr Sarah Altwaim, Dr Corrado Minetti, Dr Patrick Craig, Poom, Kit, Zana, Dashty. I would like also thank Dr Kevin Cham for his nice cooperation to find a tabletop ultracentrifuge on the campus. Also a special thanks to Mr Gregor Govan and Dr Mosavar Farahani from Molecular and clinical cancer medicine, University of Liverpool for their cooperation and assistance concerning the use of the ultracentrifuge. I would like to thank Dr Marie Phelan from the NMR Centre for Structural Biology, University of Liverpool for the generous gift of cloned genes GRA2 and GRA7 from both *T. gondii* and *N. caninum* and who has taught me a lot about HPLC and also for allowing me to use her lab equipment. I would like to deeply appreciate Mr Kamal Ali for unprecedented help and support and in his belief in me by using his villa as a guarantor for my return to home, my sweet home (Kurdistan). I would also like to thank Mr Salam, Mr Arian, Mr Hasan and Mr Sirwan for hosting me on my arrival in the UK and for showing me the beautiful places in the UK.

Finally, special thanks for my brother ‘Sirwan’ and my wife ‘Shaida’ for their patience and support during the entire period of my PhD.

ABSTRACT

A comparison of host-parasite interactions between *T. gondii* and *N. caninum*

Mariwan Musa Mohammed

Toxoplasma gondii and *Neospora caninum* are closely related obligatory intracellular apicomplexan parasites that invade and multiply in almost all mammalian host cells. They cause disease in immunocompromised animals, abortion in the intermediates host and great economic losses to the farming industry. However, there are several biological differences between these parasites, including host range, zoonotic capacity, transmission, virulence and definitive host. What causes these biological differences is not well understood. To fully understand these biological differences, the host-parasite interactions of these parasites have been investigated in this study using several different approaches at the molecular level.

Due to the importance of protein-protein interactions (PPIs) and multiple protein complexes (MPCs) in host-parasite interactions, blue native polyacrylamide gel electrophoresis (BN-PAGE) combined with liquid chromatography tandem mass spectrometry (LC MS/MS) was used to study *T. gondii* and *N. caninum* tachyzoites. Several interesting complexes were identified in *N. caninum* tachyzoites and include mitochondrial complexes, proteasome, glideosome and moving junction molecules that play an important role in the physiology and invasion of host cells. In addition, in *T. gondii* the microneme MIC1/6 complex was found migrated and/or co-associated with the important surface antigen glycoprotein SAG1, which is critical in the initial interaction with host surface peptidoglycan.

In order to understand the direct interactions between parasite secretory proteins such as dense granule proteins (GRA2 and GRA7) and host cell proteins; a pull-down assay has been used to elucidate the binding partners of expressed recombinant GRA2 and GRA7 in both parasites within the host cell lysate. Several methods were applied to purify the recombinant GRA proteins such as affinity chromatography using nickel or cobalt, salting-out, denaturing buffer using urea and reverse phase HPLC. TgGRA2 was successfully purified by HPLC and attempts have been made to study its role in host-parasite interactions using a pull-down assay.

Since these parasites secrete an array of secretory proteins, including kinases, to manipulate host cell responses; phosphopeptide enrichment, combined with LC MS/MS has been used to study the global response in the host signalling pathway through protein phosphorylation and signal transduction in response to infection with *T. gondii* and *N. caninum*. Three important differences were identified; about one-third of the phosphoproteomes of the host cell in response to infection by *T. gondii* and *N. caninum* was different. Approximately 21 % of the phospho-motifs were found differentially enriched between host cells infected with *T. gondii* compared to *N. caninum* infection and finally the pathway analysis showed that a few pathways were differentially enriched between infections with these parasites, such as glycolysis/gluconeogenesis and mTOR signalling pathway in infection with *T. gondii*

but not with *N. caninum*. The differences in the host cell phosphoproteome indicated that these parasites interact with the host cell differently.

As a means of understanding the broader host response to infection with these parasites at the systems biology level, integrated data analyses were performed on quantitative data from the transcriptome, proteome and phosphoproteome of host cells infected with the two parasites. Data analyses showed that host cells produce more proteins in response to infection with *T. gondii* than with *N. caninum* after 36 hours post infection (p.i.). In addition, data analysis showed that *T. gondii* inhibits apoptosis and acute inflammatory responses more when compared to *N. caninum*.

Overall, the results presented in this thesis have provided new insights into the biological differences between *T. gondii* and *N. caninum*. Several interesting differences in host-parasite interactions at both the qualitative and quantitative levels were identified. These interactions are related to the virulence and transmission strategy of the parasites and so are potentially associated with the biological differences between these parasites.

TABLE OF CONTENTS

LIST OF FIGURES

LIST OF TABLES

LIST OF ABBREVIATIONS

AEBSF	4-(2-Aminoethyl) benzenesulfonyl fluoride hydrochloride
AIDs	Acquired immune deficiency syndrome
$Al(OH)_3$	Aluminium hydroxide
AMA1	Apical membrane antigen 1
AP	Affinity purification
BFS	Bovine foetal serum
BN	Blue native
BP	Biological processes
bp	Base pair
Ca^{2+}	Calcium
CBG-250	Coomassie blue G-250
CBP	Calmodulin-binding peptide
CDPK	Calcium-dependent protein kinase
CID	Collision induced dissociation
CO2	Carbon dioxide
Co-IP	Co-immunoprecipitation
DAVID	Database for Annotation, Visualization and Integrated Discovery
DDA	Data dependent acquisition
ddH2O	Double distilled water
DG	Dense granule organelle
DHB	2,5-dihydroxybenzoic acid
DIGE	Difference gel electrophoresis
DNA	Deoxyribonucleic acid
dNTP	Deoxynucleotide triphosphate
DTT	Dithiothritol
EDTA	Ethylenediaminetetraacetic acid
EPEC	Enteropathogenic *Escherichia coli*
ESI	Electrospray ionisation
FC	Fold change
FDR	False-discovery rate
Fe^{3+}	Iron (III)
FIKK	Serine/threonine protein kinase, FIKK family in *Plasmodium falciparum*
FT-ICR	Fourier transform ion cyclotron resonance
g	Gram
Ga^{3+}	Gallium (III)
GAP	Gliding-associated protein
HCl	Hydrochloric acid
HFF	Human foreskin fibroblasts
HP	High purification
Hp90	Heat shock 90 protein
HPLC	High performance liquid chromatography
hr	Hour
HRP	Horseradish peroxidase
Hz	Hertz
IFA	Indirect-immunofluorescence assays
ICC	Ion charge control
IFN-γ	Interferon gamma
IL	Interleukin
IMAC	Immobilized metal affinity chromatography
IMCs	Inner membrane complexes
IMDM	Iscove's Modified Dulbecco's Media
IPA	Ingenuity pathway analysis
IPTG	Isopropyl β-D-1-thiogalactopyranoside
IRGs	Immunity-related GTPases
IT	Ion trap
Kan	Kanamycin

kDa	Kilodalton
KEGG	Kyoto Encyclopaedia of Genes and Genomes
LB media	Luria Bertani
LC	Liquid chromatography
Log	Logarithm
LTQ	Linear trap quadrupole
M2AP	Microneme associated protein
MA	Miliamper
MAPKs	Mitogen-activated protein kinase
mDa	Megadalton
ME49	*T. gondii* type II strain
MgCl2	Magnesium chlorides
MIC	Microneme
min	Minute
MJ	Moving junction
MLC	Myosin light chain
MOAC	Metal oxide affinity chromatography
MPCs	Multiprotein complexes
mRNA	Messenger ribonucleic acid
MS	Mass spectrometry
MSP1	Merozoites surface protein 1 of *P. falciparum*
mTOR	Mammalian target of rapamycin
MW	Molecular weight
MyoA	Myosin A
N. caninum	*Neospora caninum*
NaCl	Sodium chloride
NaH2PO4	Poly-vinylidine fluoride
NaOH	Sodium hydroxide
Nb2O5	Niobium pentoxide
Nc	*Neospora caninum*
NcDPI	*N. caninum* protein disulfide isomerase
NCLIV	*N. caninum* Liverpool strain
NF-κB	Nuclear Factor KappaB
ng	Nanogram
Ni-NTA	Nickel-Nitrilotriacetic acid
nLC	Nanoliquid chromatography
NMR	Nuclear magnetic resonance
NTA	Nitriloacetic acid
NTN	Nano-tubulovesicular network
OD	Optical density
P. falciparum	*P. falciparum*
p.i.	Post infection
PCR	Polymerase chain reaction
pH	Potential of Hydrogen
PKR	Protein kinase RNA-activated
PKs	Protein kinases
PMF	Peptide mass fingerprinting
PMSF	Phenylmethylsulfonyl fluoride
PPIs	Protein-protein interactions
PSM	Peptide spectrum matches
PTMs	Post-translational modifications
PV	Parasitophorus vacuole
RAP	Rhoptry-associated protein in *P. falciparum*
RhopH	High molecular weight rhoptry protein
RNA	Ribonucleic acid
RON	Rhoptry neck protein
ROP	Rhoptry protein
RPKM	Reads Per Kilobase per Million
RPM	Revolution per minute
RT	Room temperature

SAG	Surface antigen glycoprotein
SAX	Strong anion exchange chromatography
SCX	Strong cation exchange chromatography
SDS-PAG	Sodium dodecyl sulphate-polyacrylamide gel electrophoresis
sec	Second
SOC media	Super Optimal broth with Catabolite repression
SP	Signal peptide
SRS	Surface antigen glycoprotein-related sequence
STAT	Signal transducer and activator of transcription
SUMO	Small ubiquitin-related modifier
T. gondii	*Toxoplasma gondii*
T. gondii Me49	*T. gondii* type II strain
T. gondii RH	*T. gondii* type I strain
T. gondii VEG	*T. gondii* type III strain
T25	Tissue culture flasks 25 cm2
TBS	Tris-base salt-Tween-20
TBST	Tris-base salt-Tween-20
TCA	Tricarboxylic acid cycle
TEMED	Tetramethylethylenediamine
TFA	Trifluoroacetic acid
Tg	*Toxoplasma gondii*
Ti^{4+}	Titanium (IV)
TiO2	Titanium dioxide
TOF	Time of flight
UK	United kingdom
V	Voltage
v/v	Volume/volume
w/v	Weight/volume
×	Times
g	Relative centrifugal force
Y2H	Yeast two-hybrid assays
YpkA	Yersinia protein kinase A
ZrO_2	Zirconium dioxide
µl	Microliter
µM	Micromolar
µg	Microgram
µM	Micromolar
$	Dollar currency
%	Percentage
$(NH4)_2SO4$	Ammonium sulphate
[γ-32P]ATP	[Gamma 32 Phosphate] Adenosine triphosphate
>	Greater than
<	Less than
°C	Degree Celsius
1D	One dimensional
2D	Two dimensional

CHAPTER ONE: Introduction

1.1. *Toxoplasma gondii* and *Neospora caninum*

Toxoplasma gondii and *Neospora caninum* are obligatory intracellular protozoan parasites belonging to the Apicomplexa that invade and multiply in almost all mammalian cells. The similarity in morphology between *T. gondii* and *N. caninum* has led to the misidentification of the latter as *T. gondii* until 1984 (Dubey *et al.*, 2002). The Apicomplexa also include pathogens responsible for causing veterinary and medical illnesses: *Eimeria* (coccidiosis) (Lee *et al.*, 2010), *Theileria* (theileriosis) (Perera *et al.*, 2014), *Babesia* (babesiosis) (Homer *et al.*, 2000), *Plasmodium* (the causative agent of malaria) (Gutman and Guarner, 2010) and *Cryptosporidium* (cryptosporidiosis) (Cama *et al.*, 2007; Fayer *et al.*, 1998). The members of this phylum are characterised by the presence of an apical complex (Speer *et al.*, 1999).

1.2. Economic impact of toxoplasmosis and neosporosis

Toxoplasma gondii causes toxoplasmosis, a disease of veterinary and medical importance in almost all parts of the world (Tenter *et al.*, 2000), while *N. caninum* is the causative pathogen of the veterinary disease neosporosis. *T. gondii* is considered a primary disease of humans and sheep (and goat and pigs) (Buxton and Innes, 1995; Dubey, 2003). In sheep, *T. gondii* has been documented as one of the primary causes of infective ovine abortion globally (Dubey and Beattie, 1988). The economic impact of toxoplasmosis in sheep is mainly associated with foetal resorption, abortion, stillbirth and neonatal mortality when infection occurs for the first time during pregnancy. In Uruguay, it has been reported to cause annual loses about 15-32 % of lambs per year which account for wastage of US$1.4-4.7 million (Freyre *et al.*, 1999). Seroprevalence studies of *T. gondii* from sheep all over the world between 1988 and 2009 showed that positive sheep varied from 3-95.7 %, reviewed in Dubey (2009).

In humans, acquired toxoplasmosis in most immunocompetent individuals is self-limiting without showing clinical symptoms (Luft and Remington, 1992). In pregnant women, congenital toxoplasmosis occurs as a result of primary acute infection with *T. gondii* leading to abortion (Montoya and Remington, 2008). In immunocompromised patients, such as those with AIDs, reactivation of chronic

infection in the brain and other tissues can result in necrotising encephalitis or even death with or without clinical symptoms (Dubey *et al.*, 2012; Halonen and Weiss, 2013).

Neospora caninum causes neosporosis mainly in cattle and dogs and is consider as the major causes of abortion in cattle and great economic losses in farm animals worldwide (Dubey, 2003). In the UK, neosporosis has been found as the most frequently diagnosed cause of abortion in dairy cattle; estimated at approximately 12.5 % or 6000 abortions per year (Davison *et al.*, 1999a). A recent UK study of the prevalence in cattle herds showed that > 90 % of herds was seropositive for *N. caninum* (Woodbine *et al.*, 2008). Neosporosis in dogs can affect all ages and causes neuromuscular diseases most frequently in puppy and dogs less than six months old (Barber and Trees, 1996; Weissenböck *et al.*, 1997).

1.3. Life cycles of *T. gondii* and *N. caninum*

The life cycles of *T. gondii* (Figure 1.1) and *N. caninum* (Figure 1.2) are heteroxenous and polyxenous and comprised of three infective stages: the tachyzoites, bradyzoites and sporozoites (Dubey, 2003; Dubey *et al.*, 1998). The morphology and ultrastructure of infective stages are very similar between *T. gondii* and *N. caninum* (Lindsay *et al.*, 1999a; McAllister *et al.*, 1998; Speer *et al.*, 1998; Speer *et al.*, 1999). The definitive hosts are felids and canids for *T. gondii* and *N. caninum*, respectively; they shed environmentally resistant oocysts, which sporulate within 3-5 days of excretion (Dubey *et al.*, 1998; McAllister *et al.*, 1998). After ingestion of oocysts by intermediate hosts, sporozoites differentiate to tachyzoites and invade different cells and tissues. The tachyzoite is the actively moving, invading and multiplying stage, causing disease in almost all kind of host cells except the enteroepithelial cells of the definitive host (Frenkel, 1973). Following the invasion, tachyzoites reside within a non-fusogenic parasitophorous vacuole (PV) (Mordue *et al.*, 1999a) and multiply asexually by repeated endodyogeny (Speer *et al.*, 1999). In response to an increase in the host immunity, tachyzoite convert to slowly proliferating cyst-forming bradyzoites which can survive for many years in a quiescent state in immunocompetent hosts. Once the immunity is compromised, the bradyzoites reactivate and differentiate to tachyzoites which results in the reactivation of infection (Hemphill *et al.*, 2006).

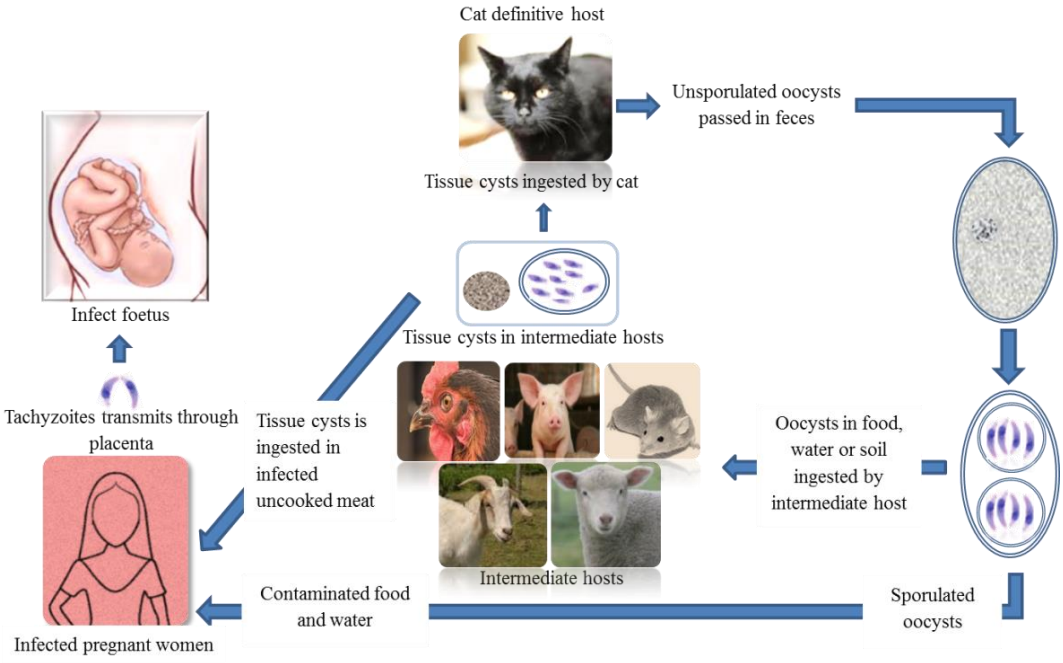

Figure 1.1: Life cycle of *T. gondii*, adapted from Dubey *et al.* (1998).

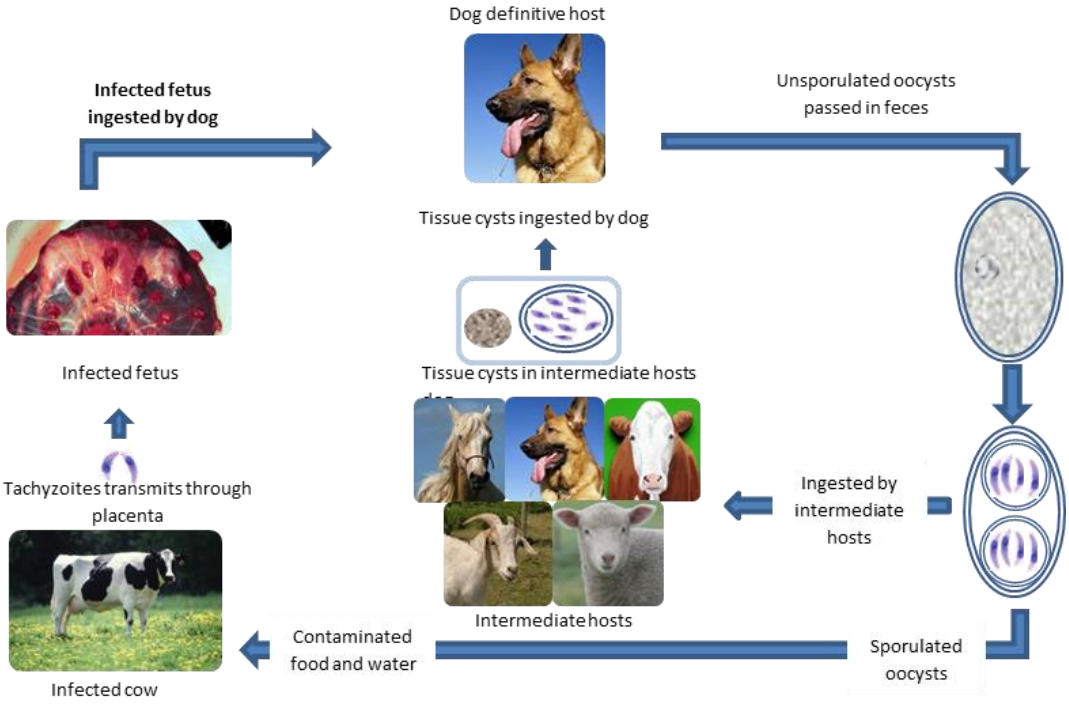

Figure 1.2: Life cycle of *N. caninum*, adapted from Dubey (2003).

1.4. Hosts and transmission routes

With toxoplasmosis, infected cats excrete oocysts in their faeces and contaminate soil, pasture and sources of water (Dubey, 1998); consumption of food and water contaminated with oocysts results in infection of intermediate hosts. Almost all vertebrates including humans, are intermediate hosts (Elmore *et al.*, 2010) and horizontal transmission is the main route of infection which leads to tissue cysts development primarily in the brain and other neural tissues. *T. gondii* is also transmitted vertically in pregnant intermediate hosts following oocyst infection as well as in human through ingestion of undercooked meat containing tissue cysts (Dubey, 2013; Torrey *et al.*, 2013). Naïve cats may acquire the infection orally through the ingestion of animal tissues (intermediate hosts) infected with tachyzoites and tissue cysts as well as food and water contaminated with oocysts (Dubey *et al.*, 1998).

In *N. caninum*, the range of intermediate hosts is narrow compared to *T. gondii*. Canids excrete oocysts which contaminate pasture and transmit horizontally to intermediate hosts such as cattle and other animals like sheep, goats, horses; dogs can also be intermediate hosts (Dubey, 2003; Dubey and Lindsay, 1996). Pigeons were also found infected with *N. caninum* and assumed to play role as natural reservoir host (Mineo *et al.*, 2009). *N. caninum* so far has not been reported to cause infection and diseases in humans (Dubey *et al.*, 2007; McCann *et al.*, 2008). Dogs get infections orally through ingestion of infected animal tissues containing cysts (Cavalcante *et al.*, 2011; Lindsay *et al.*, 1999b; McAllister *et al.*, 1998) by ingesting sporulated oocysts (Bandini *et al.*, 2011) or may become infected by foetal fluids or placental material of infected cattle (Dijkstra *et al.*, 2002a).

N. caninum is mainly transmitted by vertical transmission from the infected pregnant dam to the foetus by crossing the placenta; it can be from acquiring an exogenous infection during pregnancy or reactivation of an endogenous infection (Trees and Williams, 2005). Transplacental transmission has been induced experimentally in dogs (Cole *et al.*, 1995; Dubey and Lindsay, 1989) and reported in naturally infected dogs (Dubey *et al.*, 1988; Dubey *et al.*, 2005). To maintain continuous parasite life cycle in farm cattle; it is believed that both horizontal and vertical transmission routes are necessary in maintaining infection level (Dijkstra *et al.*, 2002b; Williams *et al.*, 2009). However, endogenous infection efficiencies in

dairy herds have been reported to be as high as 78-95 % (Davison *et al.*, 1999b; Paré *et al.*, 1997) and it is considered to be the main transmission route of *N. caninum* (Dubey *et al.*, 2007; Williams *et al.*, 2009).

In general, there are several major biological differences between these parasites as shown in Table 1.1.

Table 1.1. Main biological differences between *T. gondii* and *N. caninum*

Biological difference	***T. gondii***	***N. caninum***	**References**
Host range	Wide	Narrow	(Dubey, 2004; Dubey *et al.*, 2007; Trees *et al.*, 1999)
Zoonotic potential	Yes	No	(Dubey *et al.*, 2007; McCann *et al.*, 2008; Tenter *et al.*, 2000)
Transmission	Mostly horizontally	Mostly vertically	(Davison *et al.*, 1999b; Jones and Dubey, 2010; Williams *et al.*, 2009).
Virulence to host	Strain specific virulence	Reduced virulence	(Lei *et al.*, 2014; Reid *et al.*, 2012; Saeij *et al.*, 2005)
Definitive hosts	Felids	Canids	(Frenkel *et al.*, 1970; McAllister *et al.*, 1998)

1.5. Host cell invasion by *T. gondii* and *N. caninum* and host-parasite interactions

T. gondii and *N. caninum* are obligate intracellular organisms that have to invade host cells successfully in order to survive, grow, multiply and evade the immune system of the host (Besteiro *et al.*, 2011; Hemphill *et al.*, 1996; Ojo *et al.*, 2014). Invasive stages use the apical complex and secretary organelles proteins which sequentially released during host cell invasion resulting in host-parasite interactions, facilitate host cell invasion processes (Carruthers and Sibley, 1997) and recruitment of nutritional resources from the host cell (Coppens *et al.*, 2006). Host-parasite interaction happens during attachment and adhesion of invasive stages to the host cells membrane (Naguleswaran *et al.*, 2002), invasion and PV formation (Besteiro *et al.*, 2011; Besteiro *et al.*, 2009), nutritional resource acquisition,

maintenance of infection, multiplication within PV (Mercier *et al.*, 2005) and manipulation of the host genome (Bougdour *et al.*, 2013).

1.5.1. The apical complex and secretory organelles of the infective stages

Apical complex is the anterior part of the invasive stages consisting of apical rings, polar rings, a conoid, subpellicular microtubules and three invasion-related organelles called rhoptries, micronemes and dense granules (Naguleswaran *et al.*, 2002; Speer *et al.*, 1999). The sequential protein secretions from these organelles (Figure 1.3) help the invasive stages to attach, invade, adapt and establish infection within the host cell (Besteiro *et al.*, 2011; Carruthers and Sibley, 1997; Mercier *et al.*, 2005).

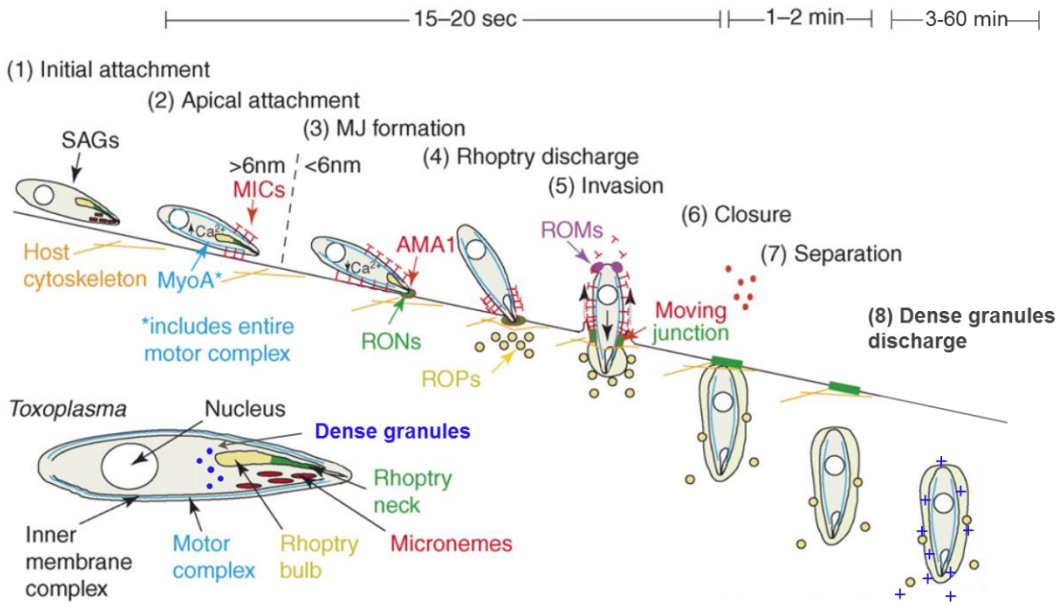

Figure 1.3: Role of secretory organelles in invasion and establishment of infection by *T. gondii*. ROMs: Rhomboid protease(s). Adapted from (Carruthers and Boothroyd, 2007), more information added based on (Bougdour *et al.*, 2014; Carruthers and Sibley, 1997; Mercier *et al.*, 2005).

1.5.1.1. Micronemes

Micronemes are rod-like shape organelle mostly present in the anterior part of the zoites (Dubey *et al.*, 1998). The proteins produce by micronemes are called MIC or MAP (MIC-associated proteins) (Buxton *et al.*, 2002) are expressed by 33 and 38 microneme genes of *T. gondii* and *N. caninum*, respectively (Reid *et al.*, 2012). The

gliding activity of Apicomplexan parasites has been related to the abundance of the micronemes (Tomley and Soldati, 2001). In *T. gondii*, TgMIC2 (Carruthers and Sibley, 1997) and in *N. caninum*, NcMIC3 (Naguleswaran *et al.*, 2002) initiates motility, attachment and invasion of the host cells. In both parasites, apical microneme antigen 1 (AMA1) is one of the main constituents of the moving junction (MJ) complex and plays an important role in host cell invasion (Alexander *et al.*, 2005; Besteiro *et al.*, 2009; Zhang *et al.*, 2007).

In *T. gondii*, microneme proteins have different affinity within the parasite; some of the microneme proteins have transmembrane domains (e.g. MIC2, MIC6 and MIC8) (Di Cristina *et al.*, 2000; Reiss *et al.*, 2001) and others are soluble proteins such as MIC1, MIC3, MIC4 and M2AP. The soluble microneme proteins are targeted to and associate with transmembrane microneme proteins which function as escalator and form complexes, therefore any destruction in any one protein may affect complex formation and affects its partner targeting (Huynh *et al.*, 2003; Reiss *et al.*, 2001). Microneme proteins are characterised by having several different copies of the limited number of adhesive domains which implicated in activities related to host cell interaction and invasion, reviewed in Carruthers and Tomley (2008).

1.5.1.2. Rhoptries

Rhoptries are club-shaped apical complex organelles that consist of a narrow neck portion which extends into the interior of the conoid and connected posteriorly with bulb portion (Dubey *et al.*, 1998). Rhoptry proteins are expressed by 68 rhoptry genes in both *Neospora* and *Toxoplasma* (Reid *et al.*, 2012). The protein secretion/excretion of rhoptries called RON (when the proteins confined to the neck portion), while proteins of the rhoptry bulb compartment refers to as ROP (Besteiro *et al.*, 2011). Rhoptry proteins play important roles in the initial invasion process and in the later stage of invasion, localisation and establishment of intracellular PV (Bradley *et al.*, 2005). RON proteins are released and excreted on to the surface of the target host cell plasma membrane and participate in the formation of the MJ through association with AMA1 (Besteiro *et al.*, 2009).

Structurally ROP proteins are homologues to protein kinases of the mammalian cells (Bradley *et al.*, 2005; El Hajj *et al.*, 2006) and several of these

proteins are active protein kinases whilst others lack the known kinase-like catalytic domain and are expected to be pseudokinases (El Hajj *et al.*, 2006; Lei *et al.*, 2014). In *T. gondii*, ROP18 overexpression was found related to increase in multiplication rate and virulence (El Hajj *et al.*, 2007). Also ROP18 is related to virulence through phosphorylation of the host cell GTPases (IRGs) and prevent destruction of PVM by IF-γ, whereas in *N. caninum* does not seem to play the same role due to pseudogenisation of *ROP18* (Lei *et al.*, 2014; Reid *et al.*, 2012). In *T. gondii* ROP18 is protected from IFN-γ mediated clearance processes by ROP5 in activated macrophages (Behnke *et al.*, 2012). ROP16 is also involved in virulence through phosphorylation of the host signalling pathway (STAT3/6) to modify the early inflammatory response of the host mediated by cytokine, interleukin-12 (IL-12) (Butcher *et al.*, 2011; Ong *et al.*, 2010; Saeij *et al.*, 2007).

1.5.1.3. Dense granules

In *T. gondii* and *N. caninum*, the proteins located in dense granules (DG) and without known homologues and function in other organisms are designated as GRA proteins (Sibley *et al.*, 1991). GRA proteins from *T. gondii* and *N. caninum* are produced by 17 and 15 genes, respectively (Reid *et al.*, 2012). However, the number of identifying GRA proteins is increasing and so far 21 GRA proteins have been identified in *T. gondii* ME49, as reviewed in Mercier and Cesbron-Delauw (2015). DGs are small homogenous vesicle-like structure located at both the apical end and behind the nucleus (Hemphill *et al.*, 1998). DG proteins are secreted at the sub-apical location of the parasite and targeted to the PV by means of typical signal peptides in the N-terminal part of most of the DG proteins (Karsten *et al.*, 1998). The time of secretion of most of the contents of DG proteins occurs within one hour of the invasion and formation of PV (Carruthers and Sibley, 1997; Dubremetz *et al.*, 1993). DG proteins of *T. gondii* are the most intensively studied secretory proteins among members of the Apicomplexa and several orthologues were also identified in *N. caninum* such as NcGRA1 (Atkinson *et al.*, 2001), NcGRA2 (Ellis *et al.*, 2000), NcGRA6 (Liddell *et al.*, 1998), NcGRA7 (Hemphill *et al.*, 1998) and NcGRA14 (Liu *et al.*, 2013). DG proteins have been found to be involved in several important vital processes for the invaded parasites. These processes include nutritional acquisition, providing an environment for the proliferation of parasites, regulating parasite egress

and modulating early immune response to infection (Braun *et al.*, 2013; Cesbron-Delauw, 1994; Coppens *et al.*, 2006; Galinski and Barnwell, 1996; Okada *et al.*, 2013; Travier *et al.*, 2008; Treeck *et al.*, 2011).

1.5.2. Attachment and invasion of host cell

At the early stage of the invasion, intracellular Ca^{2+} levels of the parasite regulates activation of calcium-dependent protein kinases (CDPK1) which is necessary for regulation of the microneme secretions of adhesin such as MIC2, MIC4 and AMA1 (Carruthers and Sibley, 1999; Donahue *et al.*, 2000); they trigger gliding motility, adhesion and invasion of the host cells (Lourido *et al.*, 2010; Nagamune *et al.*, 2008). The first point of host-parasite interaction comes from adhesion following the parasites contact with the host cell surface (Hemphill *et al.*, 1996). *T. gondii* and *N. caninum* interact differently with the artificially produced and naturally occurring host cell surface antigen sulphated proteoglycans (Jacquet *et al.*, 2001; Naguleswaran *et al.*, 2002). *T. gondii* interacts mostly through heparin sulphate, whereas *N. caninum* interacts mostly through chondroitin sulphate (Naguleswaran *et al.*, 2002). In *T. gondii*, adhesion was found to be mediated through binding parasite surface antigens TgSAG3 with the host surface sulphated proteoglycan (Jacquet *et al.*, 2001), while *N. caninum* interact through NcSAG1 and NcMIC3 (Jacquet *et al.*, 2001; Nishikawa *et al.*, 2000). In addition, NcSRS2 was found to interact with host cell surface antigen but not through proteoglycan (Nishikawa *et al.*, 2000). The adhesion process is critical for protein secretion from the invasion organelles (microneme and rhoptries). In *T. gondii*, first contact of tachyzoites with host cell plasma membrane results in secretion of microneme proteins, such as MIC2, onto the surface of the tachyzoites. This allows the parasite to make tight adhesion through anterior part resulting in the protrusion of the conoid which enables rhoptry proteins to pass onto the host cell plasma membrane and consequently moving junction (MJ) formation (Carruthers and Sibley, 1997).

The MJ is an electron-dense, circular tight intersection between the plasma membrane of the apical tip of the invasive zoites and the target host cells (Aikawa *et al.*, 1978; Besteiro *et al.*, 2011). The MJ aids in propelling the parasite into the nascent PV during entry into the host cells (Besteiro *et al.*, 2011; Suss-Toby *et al.*, 1996). Nascent PV formation is a fast process which forms from both the host cell

plasma membrane (excluded from most host surface proteins) and parasite secretory products except microneme; it is critical for protecting the parasites from host cell lysosome (Gendrin *et al.*, 2008; Joiner *et al.*, 1990; Mordue *et al.*, 1999; Sinai *et al.*, 1997). In *T. gondii* apical membrane antigen 1 (AMA1) a type 1 integral membrane protein (Donahue *et al.*, 2000; Hehl *et al.*, 2000) works as a ligand interacting with C-terminal of RON2; RON2/4/5/8 complex, which is secreted from rhoptry neck serves as receptor in the membrane of the host cells during invasion and moving junction formation (Alexander *et al.*, 2005; Besteiro *et al.*, 2009; Collins *et al.*, 2009; Straub *et al.*, 2009; Straub *et al.*, 2011; Tyler and Boothroyd, 2011; Zhang *et al.*, 2007). However, the detail of how MJ plays role in selective sieving of the host membrane protein is not known.

Once the MJ has established, in *T. gondii* ROP1 has been found discharged into the area (Carruthers and Sibley, 1997) and despite the early release of ROPs directly after MICs, ROPs are related to the later stage of invasion and early establishment of the PV formation and infection (Besteiro *et al.*, 2011; Saffer *et al.*, 1992). ROP2/4/18 were found in strands extended from the parasitophorus vacuole membrane (PVM) into the cytoplasm of the host cells were associated with DG protein GRA7 (Alaganan *et al.*, 2014; Dunn *et al.*, 2008).

1.5.3. Maintenance of infection

Following the formation of the nascent PV shortly after invasion, dense granule proteins are secreted into the PV at approximately 20 minutes post invasion (Carruthers and Sibley, 1997). The intravacuolar release of most of the DG proteins is likely responsible for the maturation of the nascent PV and PVM (Mercier *et al.*, 2005; Sibley *et al.*, 1995). Following the invasion, a nano-tubulovesicular network (NTN) forms at the posterior end of the parasite, which later on distribute throughout the PV and connects with the PVM (Sibley *et al.*, 1995). The exact role of this network is not clear, suggesting that it may be important to increase the surface area necessary for transmission of nutrient and waste between the parasite and the host cell (Mercier *et al.*, 2002). However, the exact role of most of the GRA proteins located at the interplay between the host cytosol and the parasite plasma membrane are not known especially in the exchange of nutritional resources and excretion of parasite waste.

Following invasion and establishment of an infection, PV and PVM are modified and decorated by many proteins secreted from the rhoptries and dense granules (Hajj *et al.*, 2006; Mercier *et al.*, 2005; Saffer *et al.*, 1992; Travier *et al.*, 2008). In *T. gondii*, TgGRA15 in type II strain is localised to PVM where involved in positive activation of NF-κB (p65/RelA subunit) and IL-12 production (Melo *et al.*, 2011; Rosowski *et al.*, 2011). However, *T. gondii* plays role in blocking the host apoptotic pathway through inhibition of caspase initiation which is required for NF-κB activation (Payne *et al.*, 2003). TgGRA7 and ROP2/4 were also found to interact in strand-like structure extending from PVM into the host cytosol (Dunn *et al.*, 2008). Furthermore, ROP2 has been shown to be more likely to interact with the mitochondrial import machinery and to associate tight relationship with the host mitochondria (Sinai and Joiner, 2001). In both parasites, several host cell organelles such as mitochondria and endoplasmic reticulum were found surrounding and forming intimate interactions with the PVM in close proximity to the host cell nucleus (Hemphill *et al.*, 2004; Magno *et al.*, 2005; Sinai and Joiner, 2001) and believed that the high affinity could be due to protein-protein interactions (PPIs) between PVM and host organelles (Sinai *et al.*, 1997). Co-fractionation study of infected cell with *T. gondii* showed that GRA3 and ROP2/3/4 were enriched with endoplasmic reticulum (ER) marker calnexin suggested a stable interaction between these membranes (Sinai *et al.*, 1997). In *T. gondii*, DG proteins such as GRA16 and GRA24 were recently discovered to export beyond the PVM into the host cell nucleus to regulate host gene expression (Bougdour *et al.*, 2013; Braun *et al.*, 2013).

In *T. gondii*, previous studies showed that some rhoptry proteins are similar to and behave like host kinases (Saeij *et al.*, 2006; Saeij *et al.*, 2007) such as ROP16 and ROP18 and implemented in phosphorylation of host proteins which is critical in virulence and protection against host immune system (Lei *et al.*, 2014; Ong *et al.*, 2010). While *N. caninum* ROP18 was failed to phosphorylate host cell protein due to its pseudogenisation (Lei *et al.*, 2014; Reid *et al.*, 2012).

Invaded parasites start to egress from infected cell when they occupy almost all the cytoplasmic spaces. Egress is as important as the invasion processes, since the invasion is accompanied by multiplication whilst egress is very critical for propagation in the host from infected cells to non-infected cells leaving the infected

cell to die (Arrizabalaga and Boothroyd, 2004). The intraparasitic Ca^{2+} is critical for invasion and egress (Moudy *et al.*, 2001). Based on the similarity of both processes, it is suggested that they might use the same signalling pathway (Black *et al.*, 2000; Hoff and Carruthers, 2002). However, what is necessary to trigger natural egress is not known.

Though host-parasite interactions have been extensively studied with *T. gondii* infection, less is known about *N. caninum* infection and the differences between these two parasites. The question arises here how *N. caninum* interact with host cell? It is not clear whether *N. caninum* follow the same strategies used by *T. gondii* or uses different ways of manipulating the host cell and host responses. However, there is some evidence showing that protein-protein interactions (PPIs) play an important role in some of the differences between these two species. For example, *T. gondii* and *N. caninum* interact differently with the host cell surface antigen sulphated proteoglycans (Naguleswaran *et al.*, 2002; Naguleswaran *et al.*, 2003) and immunity-related glycoprotein (IRG) of the host cell (Lei *et al.*, 2014; Reid *et al.*, 2012).

1.6. Protein-protein interactions

PPIs are organized direct physical contact between at least two proteins that are regulated in response to stimuli. This physical contact may consequently lead to conformational changes or post-translational modifications (PTMs) which alter the activity, affinity and co-operativity of the binding proteins (Berggard *et al.*, 2007; Ngounou Wetie *et al.*, 2014). PPIs play fundamental roles in controlling all cellular processes such as controlling physical activity, maintaining cellular organization, mediating signal transduction and regulation of metabolic enzymes (Braun and Gingras, 2012; Jones and Thornton, 1995). Thus, to know the function of a particular protein in a cellular environment, it is critical to identify the binding partner of the proteins which requires thorough exploration of total PPIs (interactome) (Braun and Gingras, 2012; Ngounou Wetie *et al.*, 2014). PPIs can be divided based on the lifetime of interactions in to stable and transient or a combination of both (Nooren and Thornton, 2003). Stable PPIs consequently leads to formation of multiple protein complexes (MPCs) under certain conditions, both temporally and spatially (Alberts,

1998); MPCs are important to govern almost all cellular processes (Lasserre *et al.*, 2010).

1.6.1. Protein-protein interactions play an important role in the biology of *T. gondii* and *N. caninum*

In *T. gondii* and *N. caninum*, PPIs play an important role in the invasion and maintenance of infection in host cells; these proteins are derived from both the surface antigens and secretory organelles. While PPIs have been extensively studied with *T. gondii*; less is known about in *N. caninum*.

In *T. gondii*, indirect-immunofluorescence assays (IFA) study of microneme proteins showed that MIC6/1/4 and MIC8/3 are secreted as functional complexes and associate with the parasite plasma membrane (Meissner *et al.*, 2002a), TgMIC6/1/4 complex has been found to play critical roles in host cell attachment and invasion (Zheng *et al.*, 2009). Using pull-down assays, immunoprecipitation and IFA showed that an aldolase forms a bridge between actino-myosin cytoskeleton and the surface adhesin, TgMIC6 (Zheng *et al.*, 2009) and TgMIC2 (Jewett and Sibley, 2003) which play an important role in parasite motility. In *T. gondii*, an immunoprecipitation and blue native (BN)-PAGE study found that MIC2 is associated with M2AP on the parasite plasma membrane necessary for host cell attachment and invasion (Jewett and Sibley, 2004). The *T. gondii* surface antigen TgSAG3 interacts with host cell surface heparin sulphate which is important in mediating adhesion of tachyzoites with host cell surface; this interaction was isolated using pull-down assay and antigen-host cell surface adhesion/coprecipitation assay (Jacquet *et al.*, 2001; Naguleswaran *et al.*, 2002). Moreover, based on immunoprecipitation and/or coimmunoprecipitation and IFA, found that TgAMA1 interact and form complexes with TgRON2/4/5/8 which is critical for MJ formation (Alexander *et al.*, 2005; Besteiro *et al.*, 2009); while TgRON9 and RON10 found to form complexes but do not associate with the MJ formation (Lamarque *et al.*, 2012). In *N. caninum*, surface antigen NcSAG1 and microneme proteins NcMIC1, NcMIC3 and NcMIC4 on the surface of the tachyzoites interact with host cell surface chondroitin sulphate; these interactions were found using a pull-down assay, IFA, antigen-host cell surface coprecipitation assay and solid phase binding assay (Keller *et al.*, 2002; Keller *et al.*, 2004; Naguleswaran *et al.*, 2002; Nishikawa *et al.*, 2000). In addition, NcSRS2

interacts with host cell surface antigen but not through proteoglycan (Nishikawa *et al.*, 2000).

In *T. gondii*, ROP18 is directly involved in phosphorylation of parasite substrate on the PVM (El Hajj *et al.*, 2007). Using IFA and kinase assay, ROP16 and ROP18 were also found involved in phosphorylation of host cell proteins and regulation of parasite virulence (Lei *et al.*, 2014; Ong *et al.*, 2010). ROP4 has also been observed to be phosphorylated on the PVM using [γ-^{32}P]ATP labelling of cellular extracts, but whether the host or parasite kinases are involved in the phosphorylation is not known (Carey *et al.*, 2004). In *T. gondii* infection, ROP2/4 interacts with GRA7 in a strand-like structure extending from the PVM to the cytoplasm of the host cells; GRA7 found phosphorylated only in the presence of infected cells and confirmed using alkaline phosphatase (Dunn *et al.*, 2008). GRA4/6 specifically interact with GRA2 leading to formation of multimeric complex that is stably linked with the NTN (Labruyere *et al.*, 1999). Also, using coimmunoprecipitation TgGRA16 was found form complexes with the host enzymes HAUSP and PP2A necessary for regulation of p53 tumour suppressor pathway and the cell cycle arrest (Bougdour *et al.*, 2013). In addition, these parasites move by a glideosome a multisubunit protein complex forms of interaction of at least five proteins including TgMyoA, MLC1, TgGAP40, GAP45 and TgGAP50 and isolated using immunoprecipitation method (Frenal *et al.*, 2010; Gaskins *et al.*, 2004). These PPIs and complex formation show that *T. gondii* and perhaps *N. caninum* extensively recruit PPIs to invade, establish infection and adaption within the infected host cells.

Despite the success in the identification of protein complexes, these studies were performed to understand individual interactions that happen at a time. However, they cannot be applied for global identification of PPIs compared to some other procedures such as blue native (BN)-PAGE. In addition, stage wide PPIs studies using the native condition of separation of MPCs are necessary to understand the core MPCs happening ubiquitously at a given time that are crucial to maintain cellular organisation.

1.6.2. Methods used to study protein-protein interactions

To study the functions of proteins and understand the biomolecular interaction with other proteins, a method with high efficiency in separation and isolation of different protein complexes is required. Therefore, there are several different methods that can be used to study PPIs including genetics methods such as yeast two-hybrid, biochemical methods such co-immunoprecipitation (Co-IP) and affinity purification (AP), proteomics methods such protein microarrays and gel-based methods such as blue native-polyacrylamide gel electrophoresis (BN-PAGE), bioinformatics methods (Ngounou Wetie *et al.*, 2014) and enrichment methods for PTMs of proteins (Treeck *et al.*, 2011).

1.6.2.1. Blue native-polyacrylamide gel electrophoresis for native isolation of multiprotein complexes

BN-PAGE is a native gradient PAGE technique used for one-step isolation and high resolution separation of enzymatically active protein complexes. Originally, this method was developed for the isolation of mitochondrial membrane protein complexes of the respiratory chain in the enzymatically active form (Fandino *et al.*, 2005; Schagger and Jagow, 1991). BN-PAGE is considered as one of the current most effective technique for the investigation of native protein complexes (Dejgaard *et al.*, 2010). The advantages of BN-PAGE include: firstly, isolation of high molecular MPCs weight between 10 kDa and 10 mDa. Secondly, it can be used for the isolation of whole protein complexes from biological samples such as cells and organelle membrane (Lasserre *et al.*, 2010; Pfeiffer *et al.*, 2003; Schagger, 2001; Wittig *et al.*, 2006) and total cell and tissue homogenates (Schagger *et al.*, 1996; Wittig *et al.*, 2006). Thirdly, BN-PAGE can be performed in most laboratories and is cost effective (Wittig *et al.*, 2006). However, it has to be optimised empirically for each set of different samples.

In this method, non-ionic detergents (digitonin, dodecylmaltoside, triton X-100) are used for the solubilisation of membrane protein complexes and aminocaproic acid is used in the buffers to support the solubilisation (Schagger and Jagow, 1991; Wittig *et al.*, 2006). Unlike SDS-PAGE which separate proteins based on mass/charge ratio, BN-PAGE relies on the size of protein complexes and the negative charge shift which is given by the Coomassie blue G-250 (CBG-250) to the

external of the proteins. Negative charge enables proteins to move from the cathode to the anode in the gradient polyacrylamide gel. In addition, it causes the membrane protein complexes to lose the hydrophobic character upon interacting with the dye which in turn becomes hydrophilic (water-soluble) proteins. The migration of protein complexes slows down with running distances as well as with increasing the gradient of the gel due to the pore size and ultimately the migration of protein complexes stop completely (Wittig *et al.*, 2006). The complexes separated on one dimensional (1D) BN-PAGE are dissociated into the subunit proteins using denaturing Tricine-SDS-PAGE or it can be used directly for functional studies without using SDS-PAGE (Schagger and von Jagow, 1991).

Until recently little research has been done on the complexome of apicomplexan parasites using BN-PAGE. In *T. gondii*, BN-PAGE has been used to characterise the stable protein complexes of MIC2 and M2AP on the plasma membrane of the tachyzoite stage (Jewett and Sibley, 2004). In addition, BN-PAGE has been used successfully to study protein complexes in detergent-resistant membranes of *Plasmodium falciparum* schizonts. Proteins from seven known complexes were identified including MSP-1/7, the low (RAP1/2 and RAP1/3) and high molecular weight rhoptry complexes (RhopH1/H2/H3), and the invasion motor complex (GAP45/GAP50/myosinA) (Sanders *et al.*, 2007). In addition, the whole 20S subunit of proteasome of *P. falciparum* has been isolated using BN-PAGE (Sessler *et al.*, 2012).

1.6.2.2. Pull-down assays for affinity purification of protein complexes

The pull-down assay is a robust way of purifying and identifying individual protein complexes *in vitro* when specific antibody against the bait is not available. The recombinant bait protein is usually expressed fused to different tags such as glutathione S-transferase (GST-fused protein), poly-histidine tail, maltose-binding protein (MBP), calmodulin-binding peptide (CBP) or small peptide epitopes such as FLAG, HA, c-myc. These tags have high affinity to different anti-tag (chemical) ligand such as glutathione, nickel ions immobilized-metal affinity chromatography (IMAC), streptavidin. The anti-tag ligand can be immobilised on solid support such as agarose e.g. sepharose beads. The tag-fused bait is first expressed, purified and either (1) incubated with the lysate containing prey proteins and applied to the

column containing solid support or (2) immobilised on solid support and then incubated with cell lysate containing prey proteins. In either case the bait-prey complex is then eluted with appropriate buffer and analysed using SDS-PAGE and mass spectrometry (MS) (Forler *et al.*, 2003; Miernyk and Thelen, 2008; Orru *et al.*, 2003).

The effect of the tag on the recombinant bait protein is reviewed in (Arnau *et al.*, 2006); the positive effects include improving protein yield, protection of the protein against enzymatic digestion, aids protein refolding and maintain antigenicity and increasing solubility. While, the negative effects include changes to protein conformation, inhibition of enzyme activity, change the biological activity and increases toxicity. The benefits of pull-down assay also include purification not only the pray protein, but also proteins that bind to the prey in a physiological setting (von Mering *et al.*, 2002). It is considered a robust method to isolate and identify protein complexes (Berggard *et al.*, 2007). The weakness of these techniques is unable to detect a less-stable complexes and complexes that dissociate under this setting (Ngounou Wetie *et al.*, 2014). Some of *in vitro* interactions could be non-physiological and only occur as a result of contact with other target during cells lyses preparation which is not happening *in vivo* (Berggard *et al.*, 2007).

Most of the studies performed for studying PPIs in *T. gondii* are based on immunoprecipitation and/or co-immunoprecipitation and IFA using specific antibody produced against the binding partners of the protein complexes. These methods have led to the identification of many protein complexes, such as the TgAMA1/RON2/4/5/8 complex, which is critical for moving junction formation during invasion (Alexander *et al.*, 2005; Besteiro *et al.*, 2009). However, pull-down assays have been used to study *in vitro* PPIs in *T. gondii* and led to the isolation and identification of PPIs between TgMIC2 C-terminal and aldolase critical for parasite motility (Jewett and Sibley, 2003). In addition, it has been also used to identify the interaction of aldolase with C-terminal of TgMIC6 and actin-cytoskeleton of the parasite (Zheng *et al.*, 2009). Also pull-down assays have been used to characterise the binding affinity of recombinant TgSAG3 with heparin sulphate which associates with the surfaces of host cells (Jacquet *et al.*, 2001). Furthermore, affinity chromatography using α-lactose-agarose column has resulted in pull-down and

purification of NcMIC4 from the whole tachyzoite lysate of *N. caninum*; NcMIC4 was found to bind to host cell surface through chondroitin sulphate (Keller *et al.*, 2004).

1.6.2.3. Protein phosphorylation

Precursor proteins are often covalently processed and modified post-translationally through enzymatic cleavage or addition of one or more modifying group to at least one of the amino acids. These modifications determine functional states of the proteins, targeting to its location, fate and interaction with other proteins (Mann and Jensen, 2003). Hundreds of modifications of proteins have been reported (Garavelli, 2004). The most common types of PTMs include cleavage of N-terminal signal peptides, which is necessary for regulation of proteins that enter into the secretory pathway (Jensen *et al.,* 2002), phosphorylation which is implicated in signal transduction and is crucial for regulation of almost all cellular processes (Villen and Gygi, 2008), *N*- and *O*-glycosylation, plays diverse roles within cell such as protein folding (Jensen *et al.*, 2002) and acetylation, which plays a critical role in regulation of eukaryotic transcription (Sterner and Berger, 2000).

Protein phosphorylation is characterised by the addition of at least one phosphoryl group to three hydroxyl-containing amino acids such as tyrosine, serine and threonine (Shi, 2009). It is a reversible process regulated by kinases and phosphatases (Jacot and Soldati-Favre, 2012; Shi, 2009). These enzymes are extensively regulated in response to many stimuli such as metabolites, hormones and growth factors (Zolnierowicz and Bollen, 2000). In response to stimuli, cellular receptors activate specific intracellular protein kinases (PKs) resulting in signal transduction through binding to certain phospho-motif containing protein and subsequent involvement in the corresponding kinase signalling pathway (Pawson, 1995). Subsequently activation of signalling pathway results in multiple PPIs, activation of different enzymes, and regulation of cellular processes such as cell growth, differentiation, development, functions and death (Kondapalli *et al.*, 2005; Pawson, 1995; Shchemelinin *et al.*, 2006; Villen and Gygi, 2008). Thus, genome-based protein phosphorylation (phosphoproteome) studies are critical to understand the overall phosphorylation events happening ubiquitously within cells or organisms (Villen and Gygi, 2008). In addition, it could be also important to make a comparative study of host cell in response to infection with different organisms.

Phosphoproteome is a term applied to the whole set of protein phosphorylations in a given cell (Stern, 2001) and was used for the first time by Alms *et al.* (1999). Phosphoproteomics is a division of proteomics that study the scope and the roles of protein phosphorylation in cells for identification and annotation of proteins that phosphorylates as a result of PTMs (Gomase and Akella, 2009). Thus to study the consequence of a protein phosphorylation in regulation of cellular processes, it is important to understand the following (Zolnierowicz and Bollen, 2000): (1) the identity of the phosphorylated proteins and the amino acid involved in phosphorylation, (2) the responses produced to its phosphorylation, (3) the enzymes involved in the phosphorylation and (4) the mechanisms that determine the activation of these enzymes both spatially and temporally.

Development of enrichment methods for purification of phosphopeptides in combination with MS has opened the way to study phosphoproteome. MS have been exploited for studying protein phosphorylation because of high accuracy, resolution and sensitivity (Le Blanc *et al.*, 2003; Olsen and Mann, 2004). While phosphopeptide enrichment strategy is critical for three reasons: first, low expression level of the phosphoproteins that regulate the cellular activity at a given time (Villen and Gygi, 2008) and second, due to the stoichiometry of a phosphoprotein is less than one percent of the total of that protein (Hunter and Cooper, 1985) and third, due to poor ionisation of phosphopeptides in the mixture containing a non-phosphorylated peptides (Cho *et al.*, 2012). Phosphopeptides enrichment methods, in combination with mass spectrometry, are extensively used as a high throughput method for large scale analysis of phosphoproteome (Pinkse *et al.*, 2004). It has been used successfully in profiling of thousands of phosphoproteins from different organisms such as human (Cho *et al.*, 2012), yeast (Wilson-Grady *et al.*, 2008), Apicomplexan parasites (Treeck *et al.*, 2011) and host cell in response to pathogens (Luo *et al.*, 2014; Wojcechowskyj *et al.*, 2013).

MS-based investigation of global phosphoproteome of *Plasmodium falciparum* schizont stage, intracellular and purified tachyzoites of *T. gondii* has led to the identification of 7835, 11822 and 21498 phosphopeptides, respectively (Treeck *et al.*, 2011). They suggested that protein phosphorylation is a regulatory process that is extensively used in the normal physiology of these parasites and in

host-parasite interactions. The phosphorylated proteins were found belonging to different fractions of the tachyzoites such as nucleus, mitochondrion, apicoplast, cell surface, inner membrane complex and invasion related organelles. Parasite proteins and kinases such as ROP21 and FIKK family secreted into host cell were found phosphorylated suggested that protein phosphorylation is adopted as a strategy to regulate parasite proteins secreted into the host cell and/or host-parasite interactions. However, Treeck *et al.* (2011) did not discuss the phosphoproteome of the infected host cells (at 28 hr p.i) because of data were not generated. A large scale phosphorylation study of blood form of *Trypanosoma brucei* has led to the identification of 852 phosphopeptides; the identified phosphoproteins found involved in crucial biological processes such as signal transduction, DNA and RNA processing, protein production and degradation (Nett *et al.,* 2009). Thus, there is an apparent lack of studies of phosphoproteome of host cell in response to infection with *T. gondii* and *N. caninum*. Therefore, the present study is considered as the first pioneering study investigated phosphoproteome of host cell in response to infection with these parasites.

However, conventional methods such as biochemical (kinase assay and radiolabelling) and genetic (mutation) studies used for analysing phosphoproteins and related enzymes are very important to study individual proteins at a time; they provided important information about the dynamics of proteins and signalling pathway (Gomase and Akella, 2009; Hastie *et al.*, 2006). In *T. gondii*, using conventional methods has led to the identification of several important phosphorylation events; ROP16 and ROP18 have been found involved in phosphorylation of host cell proteins and regulation of parasite virulence (Lei *et al.*, 2014; Ong *et al.*, 2010). Using [γ-^{32}P]ATP labelling of cellular extracts has identified phosphorylated form of ROP4 on the PVM (Carey *et al.*, 2004). In addition, alkaline phosphatase treatment of TgGRA7 which form complexes with TgROP2/4 found that GRA7 phosphorylated only in the presence of infected host cells (Dunn *et al.*, 2008). However, these methods are not effective to study the whole protein phosphorylation and the function of each phosphoprotein within the background of signalling systems (Gomase and Akella, 2009; Villen and Gygi, 2008).

1.6.2.3.1. Immobilised metal affinity chromatography for enrichment of phosphopeptides

IMAC takes the advantage of affinity of a phosphate group to different metals such as iron (III) or (Fe^{3+}) (Andersson and Porath, 1986) gallium (III) or (Ga^{3+}) (Posewitz and Tempst, 1999) or titanium (IV) or Ti^{4+} (de Graaf *et al.*, 2014). IMAC is used for enrichment of phosphopeptides/phosphoproteins from cell lysate containing proteins or a mixture of peptides. In this method, a metal ions such as Fe^{3+} is immobilised to beads such as agarose through ligand such as nitriloacetic acid (NTA) (Neville *et al.*, 1997) and incubated with the phosphopeptides or proteins containing lysate. Bound phosphopeptides or proteins are eluted by washing with phosphate buffer, or by increasing the pH. Phosphopeptide IMAC enrichment can be combined with other enrichment methods such as strong cation exchange chromatography (SCX) (Trinidad *et al.*, 2006; Villen and Gygi, 2008) and strong anion exchange chromatography (SAX) (Nuhse *et al.*, 2003). The combination of SCX and IMAC has been applied successfully to various biological samples such as mouse liver and fly embryos and led to the identification of 5,500 and 13,000 phosphopeptides, respectively (Villen *et al.*, 2007; Zhai *et al.*, 2008) and also to the enrichment of thousands of phosphopeptides from *P. falciparum* schizonts and tachyzoites of *T. gondii* (Treeck *et al.*, 2011). However, the combined use of SCX or SAX with IMAC or TiO_2 is more cost prohibitive than using IMAC or TiO_2 alone.

1.6.2.3.2. Metal oxide affinity chromatography (MOAC) for enrichment of phosphopeptides

MOAC is a form of IMAC and used for the same purpose of IMAC. The metals mostly used are titanium dioxide (TiO_2) (Pinkse *et al.*, 2004) or zirconium dioxide (ZrO_2) (Kweon and Hakansson, 2006), aluminium hydroxide ($Al(OH)_3$) (Wolschin *et al.*, 2005), niobium pentoxide (Nb_2O_5) (Ficarro *et al.*, 2008) in the form of solid bead or coated beads. However MOAC like IMAC does not only enrich phosphopeptide but also frequently found to enrich nonphosphorylated peptides containing multiple acidic amino acid residues (Collins *et al.*, 2007). Studies have found that introducing low pH environment with tryptic peptides during purification decreases nonspecific binding of acidic amino acids through protonation of the carboxylate group (Larsen *et al.*, 2005). *O*-methyl esterification results in blocking of the acidic residues which consequently improved the specificity of the binding of

phosphopeptides (Ficarro *et al.*, 2002). However, *O*-methyl esterification results in partial deamination and methylation of acidic amino acids asparagine and glutamine and the resulted products further complicate MS analysis and interpretation of data (Seward *et al.*, 2004). Selectivity of phosphopeptides binding to TiO_2 is improved by loading 2,5-dihydroxybenzoic acid (DHB) (Larsen *et al.*, 2005). Purification of phosphorylated amino acids using TiO_2 have been further improved by using reducing agents such as phthalic acid which resulted in the very efficient enrichment of phosphoamino acids (Bodenmiller *et al.*, 2007).

TiO_2 alone has been used to enrich phosphorylated proteins of schizont stage of *Theileria annulata* and identified 65 phosphoproteins (Wiens *et al.*, 2014). In addition, using TiO_2 combined with SCX has led to the identification of 10096 phosphorylation sites on 2551 protein groups and quantification of 8275 phosphorylation sites between the bloodstream and procyclic form of *Trypanosoma brucei* (Urbaniak *et al.*, 2013). Furthermore, a combination of in-gel digestion and SAX with TiO_2 identified 2541 phosphorylation sites from phosphoproteome of *Plasmodium falciparum* schizonts (Lasonder *et al.*, 2012). Phosphoprotein analyses of fission yeast using IMAC and TiO_2 found that both of the techniques were resulted in similar profile and in total 2887 distinct phosphorylation sites was identified which assigned to 1194 peptides (Wilson-Grady *et al.*, 2008).

1.7. Mass spectrometric analyses of peptides

Mass spectrometry is a very sensitive and powerful tool for analysing and identifying proteins and peptides from mixtures of different biological samples using variety of MS machines. Examples of these machines are ion trap (IT), triple quadruple, hybrid quadruple/ time of flight (TOF), Fourier transform ion cyclotron resonance (FT-ICR) and hybrid linear IT/FT (ICR or orbitrap) (Collins *et al.*, 2007). The techniques mentioned earlier for isolation and purification of protein complexes and phosphoproteomes can be combined with MS to identify their compositions. Generally, proteins are identified in a mixture using MS for two strategies including protein mapping (peptide mass fingerprinting PMF) and protein sequencing and post-translational modification analysis. Apicomplexan parasites proteome are extensively studied using pre-fractionation and in-gel digestion or gel-free in-solation digestion coupled with MS. Using MS, the proteomes of *T. gondii* and *N. caninum* tachyzoites

has been analysed and hundreds to thousands of proteins have been identified and characterised (Bradley *et al.*, 2005; Sohn *et al.*, 2011; Xia *et al.*, 2008). Proteomics data provide valuable information to interpret transcriptomics data as well as annotation of genome of these parasites (Sohn *et al.*, 2011; Xia *et al.*, 2008). Also thousands of identified proteins by MS from different organisms including apicomplexan parasites are hosted in EupathDB (Aurrecoechea *et al.*, 2013). These databases provide great support for genome-wide proteomics studies in many parasitic organisms such as *T. gondii* and *N. caninum* and ease access by parasitology communities to predict and annotated genes from all over the world.

With tandem MS (MS/MS), proteins are first digested proteolytically into peptides using an enzyme such as trypsin. The resulting peptides are loaded into the HPLC system to separate the peptides; the eluted peptides from HPLC are then ionised by an ionisation source such as electrospray ionisation (ESI) as found on linear trap quadrupole (LTQ) MS (Thermo Finnigan). Using data dependent acquisition (DDA), the mass to charge ratio (m/z) of the ionised peptides is measured, and the most abundant peptides usually 3-10 are selected for fragmentation using collision induced dissociation (CID) and m/z of the resulting ion fragments is measured. The resulting information from mass spectra from each sample are matched to the known peptides called peptide spectrum match (PSM) which then analysed, visualised and interpreted; these analyses are performed using different Bioinformatics tools.

1.8. Bioinformatics and data processing

Bioinformatics tools are used to identify ionised spectral peptides detected by MS. These peptides are identified from an *in silico* database of an organism containing all theoretical peptides. The theoretical peptides are produced from enzymatic digestion (e.g. by trypsin) of the proteome predicted from the genome of the organism of interest. The *in silico* peptides of *Toxoplasma* and *Neospora* as well as several other parasite species are available at the online EupathDB database - http://www.toxodb.org/toxo/(Aurrecoechea *et al.*, 2013). Human *in silico* peptides can be found at http://www.uniprot.org/uniprot/. Following identification of spectral peptides, a cut-off filter is applied to the identified peptides based on the false - discovery rate (FDR) scoring system. The FDR scoring is based on searching the

identified peptides in a real database of the organism against a decoy database which separate nonsense peptides from actual identification. Thus the high the number of the significant peptides per protein the identification of that protein is more confident. There are many different algorithms that are used for identification of mass spectral data from *in silico* peptides such as Mascot (Matrix Science), OMSSA (Geer et al. 2004), PEAKS® (BSI, Waterloo, ON, Canada), and X!Tandem (Craig and Beavis, 2004; Fenyö and Beavis, 2003). The combination of these algorithms can be used to apply more confidence identification.

For quantification of peptides and proteins, spectral data are analysed with quantification software such as Progenesis LC–MS (Newcastle upon Tyne, UK). This software aligns sample spectra replicates and measures the intensities of different peptides and proteins compared to control sample spectra, analysed and processed at the same time with tested sample. The quantified peptides and proteins are then exported into any search engine mentioned earlier containing a database of interested organism for identification of peptides and proteins.

1.9. Systems biology for understanding host cell response to infection with pathogens

Gene expression and protein production are complex processes that controlled by transcriptional, posttranscriptional and epigenetic regulators, which in part regulated by systems that integrate whole biological processes in a given cell or an organism (Braun, 2014). These regulatory interactions may associate with low correlation reported between transcripts and protein abundance (Ghazalpour *et al.*, 2011; Vogel and Marcotte, 2012). Thus, it is important to analyse the gene or protein of interest within the complexes biological system. Conventionally study of cellular components is carried out individually to highlight their biology, which consequently results in generation of very detailed data about a gene to answer a single hypothesis (Wastling and Xia, 2013). However, the advances in technology and generation of genome-wide biological data are progressing toward investigating a system biology as a whole (Wastling *et al.*, 2012). Systems biology integrates different biological data such as genomics, transcriptomics and proteomics generated from the high throughput analytical tool to highlight the functional relationship between differentially expressed genes and protein abundance (Braun, 2014; Wastling *et al.*,

2012). Systems biology is important to understand the biological processes and events happen ubiquitously at a given time or in response to infections (Jovanovic *et al.*, 2015). A systematic approach of host cell response to infection is important to elucidate how pathogens control transcriptome and proteome before and after infection. Understanding systems biology of host cell in response to infection with *T. gondii* and *N. caninum* could help dissect differential host-parasite interactions and the biological differences between the two parasites.

1.10. Aims and objectives of the study

Despite all the available information about the morphology, life cycle, hosts and transmission routes of *T. gondii* and *N. caninum;* the factors responsible for these differences are not known. The question is what causes these differences despite the remarkable similarity in their genome and transcriptome (Ramaprasad *et al.,* 2015; Reid *et al.*, 2012). Thus comparative analysis of these parasites at the molecular level may be crucial to understand these biological differences that could be responsible for host-parasite interaction.

The secretory organelles of *T. gondii* are more extensively studied than those in *N. caninum* leading to understanding some of the important critical processes necessary for movement, invasion, establishment of infection and host cell regulation. However, because the majority of these proteins especially those of DG do not possess homologue in other organisms, the molecular function of these proteins is not understood very well. Based on the homology, *N. Cannon* should have a similar set of proteins to that of *T. gondii* (Reid *et al.*, 2012); but whether and how they participate in the biological differences between these parasites is under investigation. Studying the molecular function of these proteins in *in vitro* and *in vivo* may reveal further differences between these parasites. In addition, investigation of the binding partners of these proteins could help understand their functions.

Toxoplasma gondii and *N. caninum* have been found to use PPIs as a mean to interact, invade, establish infection and modulate host cell responses. The aim of this study was to understand the biological differences between *T. gondii* and *N. caninum* through scrutinising host-parasite interactions. Identifying the PPIs and MPCs of these parasites and genome-wide host cell responses at phosphoproteome level to

infection with these parasites would dissect the biological differences between these parasites.

In chapter two, a native method of separation of MPCs, BN-PAGE combined with LC MS/MS has been used to screen for MPCs in *T. gondii* in order to understand the differences in their complexomes. This is because of the importance of PPIs and MPCs in the normal physiology, invasion and maintenance of *T. gondii*, though less is known about *N. caninum*. Thus, the hypothesis is that host-parasite interactions differ between *T. gondii* and *N. caninum* due to differences in their MPCs.

In chapter three, in order to understand the direct interactions between parasite secretory protein and host cell proteins, a pull-down assay has been used to study the binding partners of recombinant dense granule proteins GRA2 and GRA7 from both parasites within the host cell lysate under physiological settings. There is strong evidence that in *T. gondii*, the dense granule proteins GRA2 and GRA7 play vital roles in the maturation and maintenance of the PV and PVM. This implies that they may play an intermediate role through direct or indirect host-parasite interaction. However, their functions are yet to be fully understood. The hypothesis of this project is that GRA2 and GRA7 may play a different role in host-parasite interaction in infection with both parasites; thus GRA2 and GRA7 can be exploited to study their roles in biological differences between these parasites.

Toxoplasma gondii secretes an array of secretory proteins, including kinases into the host cell during invasion to manipulate host cell responses, but less is known about in *N. caninum*. Therefore, in chapter four a global response in the host cell signalling pathway through protein phosphorylation and signal transduction in response to infection with *T. gondii* and *N. caninum* at 20 hr p.i. was analysed using phosphopeptides enrichment methods combined with LC MS/MS. The hypothesis is that *T. gondii* and *N. caninum* induce different host responses through protein phosphorylation and activation of different signalling pathways.

In order to understand the broader host response to infection with the two parasites at a systems biology level, chapter five looked at the integrative data analyses performed for quantitative data from transcriptome, proteome and

phosphoproteome of host cell infected with *T. gondii* and *N. caninum*. The hypothesis is that studying the comparative system response of host cells to these parasites using quantitative data may uncover the biological differences between these parasites.

CHAPTER TWO: Using blue native polyacrylamide gel electrophoresis to characterize *T. gondii* and *N. caninum* membrane-bound proteins and protein complexes

2.1. INTRODUCTION

Proteomics is an effective method to study and collect biomolecular data about proteins (Lasserre *et al.*, 2010). Proteins extracted from any cell, tissue, organ or whole organism can be analysed directly using liquid chromatography (LC) coupled to mass spectrometry (MS). In addition, mixtures of extracted proteins can be separated based on two dimensional sodium dodecyl sulphate-polyacrylamide gel electrophoresis (2D SDS-PAGE) before analysis with LC MS to obtain information about two-dimensional maps. Despite the fact that these approaches are important in identifying the proteins in a sample, little information is obtained about the molecular function of proteins except that inferred by homology (Lasserre *et al.*, 2010). Therefore, studying protein-protein interactions (PPIs) which play significant roles in almost all of the cellular processes is one way to understand the functional state and molecular mechanisms of proteins. In order to function in a regulatory manner most proteins have to interact with others; these interactions result in the formation of MPCs (Swamy *et al.*, 2006). MPCs can be divided into three types including constitutive (stable) and signal-induced (transient) or combination of both. The stable MPCs are the high abundance and constant, such as multisubunit receptor, proteasome and ribosome. The transient MPCs are of low copy number and temporary, such as binding of activated relay proteins to the activated receptor tyrosin-phosphorylated protein. While protein complexes that characterise by both states include transcription factors. Thus MPCs can be changed in space and time based on the cellular status. The entire complement of MPCs of a cell, tissue or organism is known as the complexome. Understanding complexome is important for mapping of PPIs and better perception of protein function and cellular organisation (Camacho-Carvajal *et al.*, 2004). The complexome is studied by the implementation of different approaches that dissect MPCs directly called complexomics (Camacho-Carvajal *et al.*, 2004).

2.1.1. The role of multiprotein complexes in *T. gondii* and *N. caninum*

Every cell and organism use PPIs and MPCs to maintain cellular processes that are necessary for normal cellular physiology. PPIs in *T. gondii* and *N. caninum* play an important role in the invasion of host cells and the subsequent establishment of the infection, for example, in *T. gondii* it has been found that DG proteins are

stored as both soluble and complex forms (Braun *et al.*, 2008; Labruyere *et al.*, 1999) and are secreted as a soluble form into PV space where they form complexes (more detail is given in Chapter 3) (Mercier *et al.*, 2005). The micronemes and rhoptries also play a storage role for several proteins (Bradley *et al.*, 2005; Soldati *et al.*, 2001; Zhang *et al.*, 2007) and form protein complexes (Lamarque *et al.*, 2012; Saouros *et al.*, 2005). Furthermore, proteins from micronemes have been shown to be excreted and form MPCs on the surface of the parasite and forms tight adhesion through interaction with the host cells surface proteins (Huynh *et al.*, 2003; Keller *et al.*, 2002; Naguleswaran *et al.*, 2002; Rabenau *et al.*, 2001). Also in *T. gondii*, MPCs play important role in the invasion process; microneme protein TgAMA1 is secreted on the surface of the parasite interacts and form complexes with RON2/4/5/8 on the surface of the invading cell which facilitate formation of MJ and internalisation of the parasite (Alexander *et al.*, 2005; Besteiro *et al.*, 2011; Straub *et al.*, 2009; Straub *et al.*, 2011).

Also apicomplexan parasites use a unique way of movement called gliding motility to move within the host, during cell invasion and when they egress from the infected host cells (Gilk *et al.*, 2009). Gliding motility is powered by the glideosome, a macromolecular complex comprising of five protein subunits (Frenal *et al.*, 2010). The myosin heavy chain is one of the subunits of the glideosome which forms the actin-myosin motor; this motor is supported by other proteins such as glycolytic aldolase that links F-actin to the cell surface adhesin complex, MIC2/M2AP (Jewett and Sibley, 2003).

2.1.2. Methods used to study protein-protein interactions in *T. gondii* and *N. caninum*

The sophisticated nature of apicomplexan parasites and technological limitations have hampered complete understanding of the biology of invasion and interaction with host cells despite decades of research. In addition, studies conducted in the last two decades showed that identification of proteins, PPIs and MPCs of different secretory proteins are partly associated with mystery of understanding of these organisms (Alexander *et al.*, 2005; Besteiro *et al.*, 2009; Bradley *et al.*, 2005; Carruthers and Sibley, 1997; Frenal *et al.*, 2010). Several different methods to study PPIs have been used to investigate the functional status of interacting proteins in

apicomplexan parasites. The approaches most frequently used include biochemical methods such as Co-IP and AP. In the former an antibody is raised against a protein to be tested; in the latter either an endogenous protein produced in a normal cell or expressed as a fusion tag in a transgenic cell which is then incubated with antibody to isolate and purify the target protein and its binding partner. In *T. gondii*, Co-IP was used to identify proteins involved in PPIs and MPCs critical for parasite motility such as the glideosome (Frenal *et al.*, 2010), adhesion with the host cell plasmalemma such as the TgMIC4/1/6 complex (Saouros *et al.*, 2005) and for protein involved in MJ and invasion of the host cell such as TgAMA1/RON2/4/5/8 (Alexander *et al.*, 2005; Besteiro *et al.*, 2009). While AP has been used in *T. gondii* to identify the interaction between TgMIC2, TgMIC6 and aldolase critical for parasite motility (Jewett and Sibley, 2003; Zheng *et al.*, 2009).

Other methods include yeast two-hybrid assays (Y2H), in which two proteins to be tested for PPIs are expressed as fusion proteins in yeast. In *T. gondii*, this approach has been used to identify the interacting protein partners of TgROP18 from the host cell, eight novel host cell proteins were obtained (Du *et al.*, 2013). However, co-IP, AP and Y2H are expensive, laborious and can be used only to study one MPC or PPI at a time.

To study the biomolecular interactions of multiprotein complexes, an extraction method that keeps it in its native form is necessary. Thus, blue native/SDS-PAGE (BN/SDS-PAGE) is the most reliable method (Lasserre *et al.*, 2010). BN/SDS-PAGE (Figure 2.1) is a gradient polyacrylamide gel electrophoretic technique that is used for high resolution isolation and separation of enzymatically active MPCs between 10 kDa and 10 mDa especially from biological cells and organelle membranes (Pfeiffer *et al.*, 2003; Schagger, 2001; Wittig *et al.*, 2006). It can be used for the extraction of protein complexes from total cell and tissue homogenates (Schagger *et al.*, 1996; Wittig *et al.*, 2006). Until recently, little research has been done on the complexome of apicomplexan parasites. In spite of that BN-PAGE has been used successfully to study protein complexes in detergent-resistant membranes of *Plasmodium falciparum* schizonts. Proteins from seven known complexes were identified, including MSP-1/7, the low (RAP1/2 and RAP1/3) and high molecular weight rhoptry complexes (RhopH1/H2/H3) and the

invasion motor complex (GAP45/GAP50/myosinA) (Sanders *et al.*, 2007). However, BN-PAGE has not been applied to study the whole membrane-bound proteins and the complexome of apicomplexans.

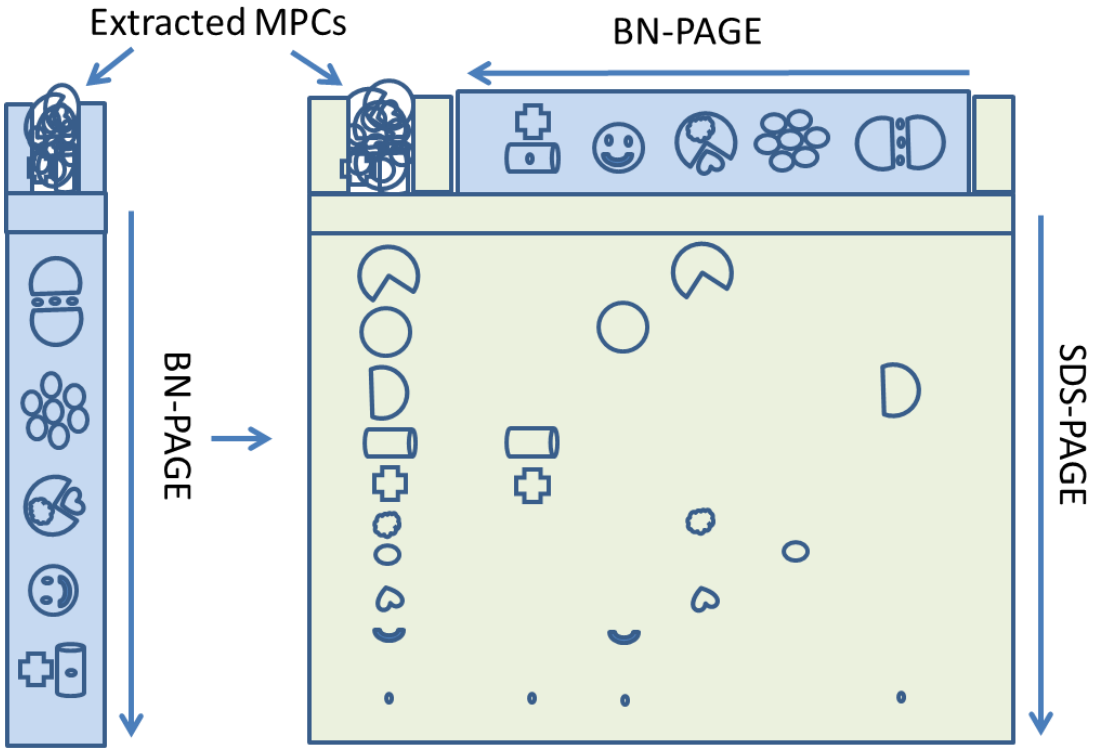

Figure 2.1: Principle of BN-PAGE. A: proteins and MPCs are separated under native conditions in a first-dimension BN-PAGE and b: a gel strip containing proteins and MPCs is prepared under reducing state using SDS and is applied to a two-dimensional BN/SDS-PAGE. The protein subunits of MPCs are separated in the two-dimensional BN/SDS-PAGE gel. MPCs: multiprotein complexes Adapted from (Camacho-Carvajal *et al.*, 2004).

2.1.3. Aims and objectives of the study

The hypothesis is that host-parasite interactions differ between *T. gondii* and *N. caninum* due to differences in their MPCs that comprise the complexomes necessary for parasite physiology, invasion processes and maintenance of infection. A comparative analysis of the complexomes was performed based on the composition of MPCs identified from the tachyzoite stage of *T. gondii* and *N. caninum* using BN-PAGE combined with LC MS/MS.

2.2. MATERIALS AND METHODS

2.2.1. Host cell and parasite maintenance

T. gondii RH strain and *N. caninum* Liverpool strain were maintained twice weekly in culture in monolayers of Vero cells (African Green Monkey Kidney Fibroblast).

2.2.1.1. Vero cell maintenance

Vero cells were maintained in growth medium consisting of IMDM (Iscove's Modified Dulbecco's Media, Lonza) supplemented with 10 % bovine foetal serum (BFS) (Biosera) and 1 % penicillin 10,000 units/streptomycin 10 mg/ml (Sigma). Cells and parasites were incubated at 37 °C in 5 % CO_2 in a humidified incubator.

2.2.1.2. Vero cell passage

Vero cells were passaged once a week. Confluent monolayers of Vero cells were washed with 5 ml PBS-EDTA (Lonza) before detaching the cells with 5 ml of Trypsin-Versene (EDTA) solution (Lonza) for 3-5 min at 37 °C in 5 % CO_2. The cell suspension was collected and transferred to a 50 ml centrifuge tube and centrifuged at 1,000 × *g* for 5 min. The cell pellet was resuspended in 5 ml growth medium where 10 µl were used for cell counting using Neubauer (haemocytometer) cell counting chamber (Marienfeld-Superior). Cells were seeded again at 1×10^5 in 5 ml of growth medium in a tissue culture flask of 25 cm^3 (T25) and infected with the parasites after overnight incubation at 37 °C in the presence of 5 % CO_2.

2.2.1.3. Maintenance of *T. gondii* and *N. caninum* tachyzoites

Parasites were passaged when most of the infected host cells were lysed at about three to four days post infection (p.i.). Infected host cells were detached from the flasks using a 18 mm blade cell scrapper (Falcon®) and collected in a 50 ml centrifuge tube. Parasites were counted before passaging by adding 10 µl of infected cell suspension to haemocytometer chamber. A ratio of 4:1 of parasites to cells was used for maintaining both parasites throughout the experiment.

2.2.1.4. Harvesting of *T. gondii* and *N. caninum* tachyzoites

Infected cells were incubated at the same environment described in section 2.2.1.1. The parasites were harvested four days p.i. when almost all the cells were damaged by the egressed parasites. Parasites purification and harvesting were carried out using 3 μm pore-sizes Nuclepore™ track-etched membranes (Whatman®). Nine T25 flasks of infected cells were scraped with 18 mm blade cell scraper. The scraped host cells infected with *T. gondii* or *N. caninum* were collected in 50 ml centrifuge tubes. Flasks were washed with 5 ml PBS, which was added to the previous collection before centrifuged at 1,500 × *g* for 10 min. The pellets were resuspended in 5 ml growth medium and passage through a 27 gauge needle (Terumo) five times. An additional 25 ml growth medium were added then injected into the filter unit. Another 10 ml of cold PBS was pushed through the filter. The number of the parasites tachyzoites was counted using haemocytometer. Parasites were then centrifuged at 1,500 × *g* for 10 min at 4 °C. The pellet was washed twice with 10 ml cold PBS. Finally the pellet was resuspended in 1 ml cold PBS and centrifuged using bench-top centrifuge (Heraeus) at 16,000 × *g* for 3 min at 4 °C and the pellet was either used directly or kept at -20 °C for future use.

2.2.2. Protein extraction from *T. gondii* and *N. caninum* tachyzoites

Protein extraction was performed in two successive stages; homogenisation to open and break the tachyzoites and solubilisation to extract the membrane-bound protein and multiple protein complexes.

2.2.2.1. Homogenisation of tachyzoites pellet

The homogenization of the tachyzoites pellet was carried out according to a modified protocol of Schagger and von Jagow (1991). All the steps were carried out on ice. A pellet of 2×10^8- 5×10^8 tachyzoites was suspended in 0.5 ml of cold homogenization buffer (440 mM sucrose, 20 mM sodium phosphate, 2 mM EDTA, and 0.1 mM phenylmethylsulfonyl fluoride (PMSF) (Amresco), pH 7.2). Homogenised cells were transferred into pre-cooled 2 ml glass Dounce homogenizer and left on ice for 10 min. The cells were ground three times manually by moving up and down for 30 second each. Homogenized cells suspension were transferred into 1.5 ml eppendorf tube, the homogeniser was washed with 0.5 ml homogenisation

buffer and added to the previous collection followed by centrifugation at 16,000 × *g* for 30 min at 4 °C. The supernatant was discarded and the pellet was washed again with the same homogenization buffer and centrifuged. Finally the pellet was collected.

2.2.2.2. Solubilisation of tachyzoites pellets

The solubilisation of the pellet containing tachyzoites was carried out as previously described (Schagger and von Jagow, 1991). The resulting pellet was resuspended in 92.5 µl of solubilisation buffer containing a non-ionic detergent (750 mM aminocaproic acid (Applichem Lifescience), 50 mM Bis-Tris/HCl (Amresco), 1 mM EDTA (pH 7.0), 10 µg/ml of aprotinin (Amresco), 10 µg/ml of leopeptin (Amresco), 1 mM PMSF and 1 % dodecyl-D-maltoside (Invitrogen)) and incubated on ice for one hour. The supernatant was collected after centrifugation at 16,000 × *g* for 30 min at 4 °C and was used either directly or kept at -80 °C. The protein concentration was determined using Coomassie (Bradford) Protein Assay Kit (Thermo Scientific) as described in section 2.2.3.

2.2.2.3. Optimisation of the solubilisation and homogenisation

2.2.2.3.1. Optimisation of the homogenisation

Three methods of homogenisation were used in order to optimise this step. The first method involved using a Micropestle (Eppendorf) for resuspending pellets, pellet was homogenised for 30 min on ice and shearing forces applied for 30 × 5 min interval. Secondly, sonication was done on ice water for 6 × 5 min cycles using a water bath sonicator (Fisherbrand®) with or without saponin detergent at 0.05%. Samples were cooled for 2 min on ice between each cycle. In the third method, a probe sonicator (Sonics®) was used for 3 min with 30 sec on and 2 min off pulse on ice at 40 % output.

2.2.2.3.2. Optimisation of the solubilisation

The solubilisation of membrane bound proteins and protein complexes were performed by increasing the time and speed of centrifugation. First, the centrifugation time was increased to one hour at 16,000 × *g* at 4 °C. Second, the

centrifugation speed was increased to 100,000 × *g* at 4 °C for 30 min using Optima MAX-XP Ultracentrifuge (Beckman).

2.2.3. Protein assay

Protein concentration was determined using a Coomassie (Bradford) Protein Assay Kit (Thermo scientific). A serial concentration of bovine serum albumin standard proteins at 25 µg/ml, 20 µg/ml, 15 µg/ml, 10 µg/ml, 5 µg/ml and 2.5 µg/ml were used in duplicate along with two duplicate blanks; one of the blanks was set as zero µg/ml. The samples were prepared in serial dilution and in duplicates using doubled distilled H_2O (ddH_2O). Duplicates of 150 µl of each standards and samples were pipetted into a 96-well plate (Fisherbrand®) and 150 µl dye reagent added to each well and mixed thoroughly. The plate was incubated at room temperature for 5 min and the absorbance was measured at 595 nm using Tecan-Infinite® F50 (Tecan Group Ltd.). Sample concentrations were calculated according to the standard curve produced from concentrations of protein standards.

2.2.4. One-dimensional blue native polyacrylamide gel electrophoresis (1D BN-PAGE)

Discontinuous blue native gradient polyacrylamide gel electrophoresis was used for separation of protein complexes and membrane bound proteins of the whole parasite tachyzoite lysate. Bis-Tris gel 3-12 % (BN1001box) or 4-16 % (BN1002box) (Life Technologies) were used for the 1D BN-PAGE. The amount of reagents for casting one Bis-Tris gel (0.16 × 14 × 14 cm) of 4–16 % is shown in Table 2.1.

Table 2.1: 1D BN-PAGE composition and polymerisation conditions. Adapted from (Schagger *et al.*, 1994; Wittig *et al.*, 2006)

Reagent	Stacking gel 3.5 %	Gradient Separation gel	
		4 %	16 %
AB-3 mix (49.5 %)*	0.44 ml	1.5 ml	4.9 ml
Gel buffer (3 ×)**	2 ml	6 ml	5 ml
Glycerol	-	-	3 g
H2O	3.5 ml	10.4 ml	2.045 ml
APS (10 %)	50 µl	100 µl	50 µl***
TEMED	5 µl	10 µl	5 µl***

*AB-mix (acrylamide-bisacrylamide mixture): The 49.5 % T, 3 % C mixture contains 48 g acrylamide/100 ml and 1.5 g bisacrylamide/100 ml. 'T %' is the total concentration of acrylamide-bisacrylamide mixture, 'C %' is referred to the percentage of cross linker form by bisacrylamide to the total amount of monomer (Hjerten, 1962).
**Gel buffer (3 ×): 1.5 M 6-aminocaproic acid, 150 mM Bistris adjusted with HCl to pH 7.0 (4 °C).
***Add fresh. APS: Ammonium persulphate, TEMED: Tetramethylethylenediamine

Depending on the protein concentration of the extracted protein samples, protein loading was varied between experiments, 50-100 µg of protein was loaded per lane. Coomassie blue G-250 (5 %) in 500 mM aminocaproic acid (Invitrogen) was added to the extracted proteins to be run in a ratio so that the concentration of the dye was 1:4 of Dodecyl-D-maltoside. 5 % glycerol was added to the protein samples prior to loading on the gel.

The Cathode running buffer (50 mM Tricine, 50 mM Bistris-HCl pH 7.0, 0.02 % Coomassie blue G-250 and stored at 4 °C) was used only in the upper chamber. The anode buffer (50 mM Tricine, 50 mM Bistris-HCl pH 7.0 at 4 °C) was stored at 4 °C and used in the lower chamber.

Electrophoresis was done using Xcell surelock™ Mini-cell (Invitrogen™). Prepared sample proteins were added to the wells of casted BN-PAGE (each sample added to two wells, one for staining and visualization of the bands and the other one for performing 1D SDS-PAGE. The cathode buffer was added to the upper chamber and the anode buffer to the lower chamber. Electrophoresis was started at 150 volts for 60 min at 4 °C cold room until the protein samples run down to about one third of the gel. Voltage was then increased to 250 V with the current limited to 8-10 mA for 90-120 min.

The gel was removed from the cassette after electrophoresis had finished. The gel cuts into two slices, one for staining with Coomassie blue and the other one for SDS-PAGE. Gel slices for SDS-PAGE was transferred into a small glass Petri-dish

containing 5 ml SDS-sample buffer (12.5 mM Tris, 4 % SDS, 20 % glycerol, 5 mM Dithiothritol (DTT) and 0.02 % bromophenol blue) and incubated for 10 min at room temperature (RT) on a rocking platform. The gel slice was boiled in a microwave for 15 sec at highest temperature set and incubated for 20 min at room temperature (RT) on a gel rocker. The gel slice was then loaded on the stacking gel for the second dimension separation on SDS-PAGE.

2.2.5. Two-dimensional blue native/sodium dodecyl sulfate polyacrylamide gel electrophoresis (2D BN/SDS-PAGE)

Two-dimensional BN/SDS-PAGE was used to analyse the protein subunits separated in the 1D BN/PAGE. Sliced 1D gel of BN-PAGE was laid on a 7 × 8 cm SDS-PAGE gel using plastic cassettes (Invitrogen™). Gels were cast following the recipes listed in Table 2.2 for stacking gel and Table 2.3 for resolving gel. Liquefied Agarose (Bioline) 2 % was used to fix the sliced 1D gel between the plates and covered with SDS sample buffer. Gels were run in running buffer (25 mM Tris, 192 mM glycine, 0.1 % SDS, pH 8.3) at 200 V for 45 min.

Table 2.2**:** Recipe of stacking gel (4 %)

Reagent	**Volume**
ddH_2O	3.025 ml
30 % (w/v) Acrylamide-bisacrylamide (Sigma-Aldrich)	0.65 ml
0.5 M Tris/HCl (pH 6.8)	1.25 ml
10 % (w/v) SDS	50 µl
10 % (w/v) ammonium persulfate (Sigma)	25 µl*
TEMED (VWR)	5 µl*

*****Add fresh

Table 2.3: Recipe of resolving gel (12 %)

Gel Reagent	**Volume**
ddH_2O	3.4 ml
30 % (w/v) Acrylamide-bisacrylamide	4 ml
1.5 M Tris/HCl (pH 8.8)	2.5 ml
10 % (w/v) SDS	50 µl
10 % (w/v) ammonium persulfate	75 µl*
TEMED	7.5 µl*

*Add fresh

2.2.6. Staining of 1D SDS-PAGE

After electrophoresis, gel was fixed in 40 % (v/v) ethanol, 10 % (v/v) acetic acid followed by 25 sec boiling in microwave oven. Gel was then incubated at RT using a gel rocker for 20 min. After fixation, the gel was washed twice in dH_2O for 5 min. The gel was stained overnight using colloidal Coomassie blue G-250 (20 % (v/v) methanol, 0.08 % (w/v) Coomassie Brilliant Blue G-250, 0.8 % (v/v) phosphoric acid, 8 % (w/v) ammonium sulphate).

2.2.7. In-gel trypsin digestion

Slices of gel from 1D BN-PAGE and 2D BN/SDS-PAGE were excised using clean glass Pasteur pipettes. Slices were placed in 0.5 ml microcentrifuge tubes and each gel plug was estimated at 10 µl. The plugs were destained twice in 10 µl destaining solution (50 mM ammonium bicarbonate/50 mM of acetonitrile) and incubated at 37 °C for 10 min. Proteins were reduced using 50 µl of 9.85 mM of dithiothreitol (VWR) in 25 mM ammonium bicarbonate and incubated at 37 °C for 30 min. DTT was removed and discarded. Alkylation step was carried out in 50 µl of 55 mM of iodoacetamide (Sigma) in 25 mM ammonium bicarbonate in the dark for 30 min at RT. After iodoacetamide had removed and discarded, 10 µl of 100 % acetonitrile was added and incubated at 37 °C for 15 min. The solvent was removed and discarded, while the plugs were incubated to evaporate at 37 °C for 10 min. 10 µl of diluted sequencing grade trypsin (Sigma) containing 100 ng trypsin in 25 mM ammonium bicarbonate was added to the gel plug and incubate at 37 °C for one hour. Further 10 µl of 25 mM ammonium bicarbonate was added and incubated at 37 °C overnight. The reaction of trypsin digestion was stopped by adding 2 µl of 2.6 M formic acid. Finally, digested samples were centrifuged at 13,000 × *g* for 1 min and the supernatant was transferred to a new tube and kept at -20 °C.

2.2.8. Liquid chromatography (LC)-MS/MS and data analysis

The LC-MS/MS work for 1D BN-PAGE and 2D BN/SDS-PAGE in-gel digestion was carried out by Dr. S. Armstrong, University of Liverpool. Peptide mixtures were analysed by on-line nanoflow LC using the nanoACQUITY-nLC system (Waters) coupled to an Amazon ion trap mass spectrometer (Bruker Daltonics) equipped with the manufacturer's CaptiveSpray ion source. The analytical

column (nanoACQUITY UPLCTM BEH130 C18, 15 cm 75 μm, 1.7 μm capillary column) was maintained at 35 °C and a flow-rate of 500 nl/min. The gradient consisted of 3-40 % acetonitrile in 0.1 % formic acid for 30 min, followed by a ramp of 40-85 % acetonitrile in 0.1 % formic acid for 3 min. Full scan MS spectra (m/z range, 300-2,000) were acquired by the Amazon in enhanced resolution mode at a resolution of 20,000. Analysis was performed in data-dependant mode. The top 5 most intense ions from MS1 scan (full MS) were selected for tandem MS by collision induced dissociation (CID). The ICC target was set at 200,000. Raw Amazon files were converted to mzML using the CompassXport 3.0.5 tool (Bruker). Peptide identifications were established using the Mascot (version 2.3.02, Matrix Science) (http://www.matrixscience.com) search engine against a custom database separately that contained predicted proteomes from *T. gondii* ME49 strain and *N. caninum* Liverpool strain (ToxoDB, *Toxoplasma* Genomics Resource, Version 11). Mascot search parameters were set with precursor mass tolerance 0.5 Da and fragment mass tolerance of 0.5 Da. Carbamidomethylation of cysteine (C) was set as a fixed modification and oxidation of methionine (M) was included as a variable modification. One missed tryptic cleavage was permitted. Cleavage was done by trypsin, which cuts C-term side of K and R (Lysine and Arginine, respectively) unless next residue is P (Proline). A significance threshold of $p < 0.05$ was applied to the Mascot search results and ion scores < 31 were omitted. Proteins were considered as valid with protein score ≥ 50 with at least two unique peptides. The NCBI basic local alignment search tool (BLAST) (Altschul *et al.*, 1997) in the Gene bank (http://blast.ncbi.nlm.nih.gov/Blast.cgi) and in the ToxoDB databases (ToxoDB, *Toxoplasma* Genomics Resource, Version 11) were used to investigate for orthologous proteins.

2.3. RESULTS

2.3.1. Homogenisation and solubilisation optimisation and one-dimensional blue native polyacrylamide gel (1D BN-PAGE)

Different methods of optimisation were used to obtain the best protein extraction and gel resolution for MPCs from whole tachyzoite lysates. These included different homogenisation tools (Dounce homogeniser, micropestle, water bath sonication and probe sonicator) and spin time/speed.

Initially a glass Dounce homogeniser was used for homogenisation, the 10 cm 4-16 % gradient 1D BN-PAGE gel loaded with 100 µg of protein extract resulting from solubilisation (section 2.2.2.1) of *N. caninum* tachyzoites and Vero cells is shown in Figure 2.2a. Results showed that streaking and background staining of the BN-PAGE were the main problems that hampered visualisation of the bands resulted from the migration of proteins and MPCs.

Modifications to the previous run were applied to the homogenisation, centrifugation time and gradient gel concentration. Tachyzoites were incubated on ice for 30 min and a micropestle was used to apply shearing force to the tachyzoites manually every 5 min. Centrifugation was performed at 16,000 × *g* for 30 min at 4 °C for the homogenised fraction and one hour for the solubilised membrane bound proteins. The result of 3-12 % 1D BN-PAGE gel was loaded with 100 µg of extracted protein from *T. gondii* and *N. caninum* is shown in Figure 2.2b, which has exhibited apparent improvement in resolution despite a milder background staining issue.

To further optimise the visualisation of the 1D BN-PAGE gel, water bath sonication was used in the homogenisation step. Ultracentrifugation at 100,000 × *g* at 4 °C for 30 min was also applied to differentially solubilise the membrane bound proteins and protein complexes. The resulting 1D BN-PAGE gel which was loaded with 50 µg of extracted protein from *T. gondii* and *N. caninum* is shown in Figure 2.2c, which exhibited better visualisation of the bands with less background staining. Less background staining could be related to the amount of protein loaded (50 µg) (Figure 2.2c) which is half the amount used compared to previous gels (100 µg) per each well (Figure 2.2b). However, better efficiency of homogenisation measured by

number and intensity of bands on gel is still to be achieved. In addition, detergent was used at a low concentration in the homogenisation buffer (Figure 2.2d), which could help break the cells and release more soluble proteins for further enrichment of membrane bound proteins. Saponin (0.5 % v/v) was added to the homogenisation buffer and 6 × 5 min water bath sonication was used. The resulting 1D BN-PAGE gel loaded with 18 µg of extracted protein from *T. gondii* and *N. caninum* (because of low amount of protein yield that recovered from this method) is shown in Figure 2.2d, which showed very weak protein bands suggesting that detergent treatment might resulted in the loss of proteins during protein extraction.

A probe sonicator was used in conjunction with ultracentrifugation to increase the recovery of more membrane bound protein and reduce background staining. The probe sonicator was used for 2 × 30 sec (74 Hz) at 40 % amplitude output. The 1D BN-PAGE gel, which was loaded with 50 µg of extracted protein from *T. gondii* and *N. caninum*, is shown in Figure 2.2e. However, it seems that sonication by probe sonicator has made no obvious improvement than water bath sonication concerning the gel resolution.

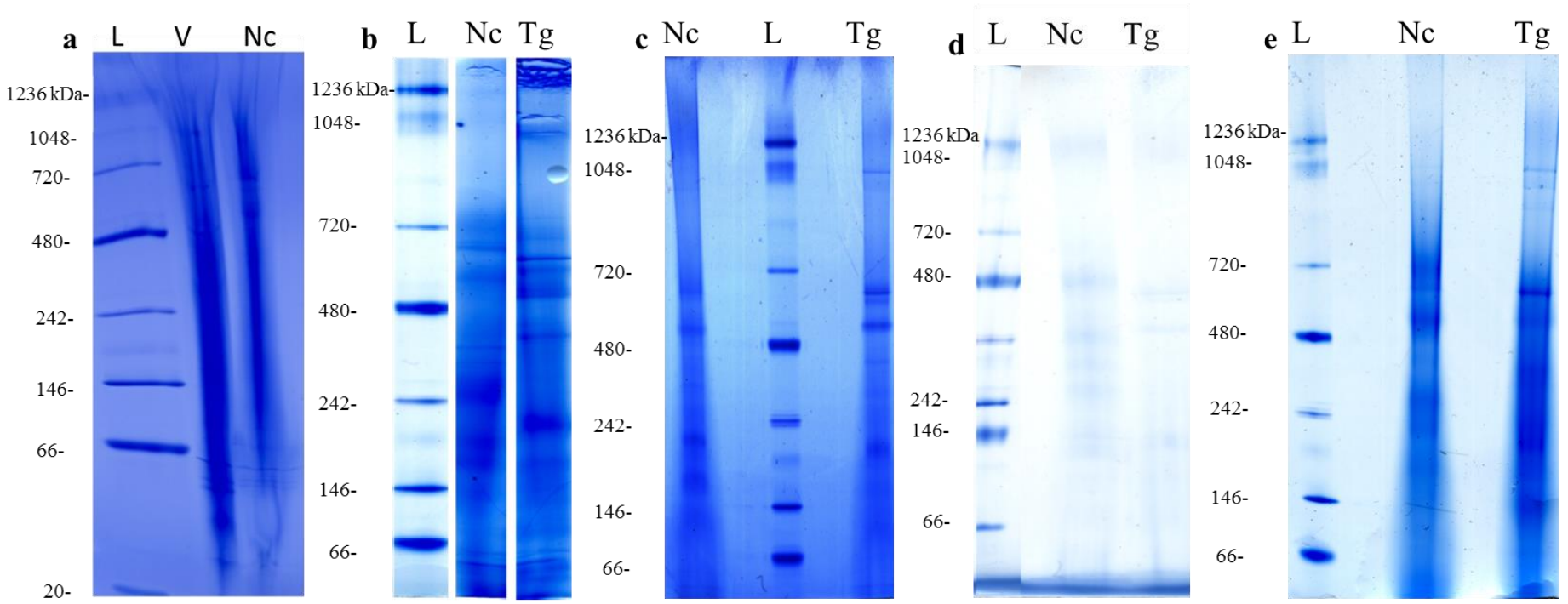

Figure 2.2: Optimisation of 1D BN-PAGE gel from tachyzoites lysate of *T. gondii* and *N. caninum*. Different methods were used to extract and optimise the 1D BN-PAGE from tachyzoites lsate of *T. gondii* and *N. caninum* as described in section 2.3.1. L: protein standard labelled with the molecular weight of each protein. V: Vero cells, Nc: *N. caninum* tachyzoites and Tg: *T. gondii* tachyzoites. Protein loading varied between experiments: Lane a (V and Nc) and lane b (Nc and Tg) contain 100 µg of the extracted proteins; lane c (Nc and Tg) contains 50 µg; lane d (Nc and Tg) contains 18 µg and lane e (Nc and Tg) contains 50 µg.

2.3.2. 1D BN-PAGE of whole tachyzoite multiprotein complexes of *N. caninum* and *T. gondii*

Gel slices from 1D BN-PAGE of *N. caninum* (Figures 2.3a, slice 1-5) and *T. gondii* (Figure 2.4a, slice 1-11) were analysed with mass spectrometry. Protein was considered to be significant identifications with at least two or more unique peptides and with Mascot protein score of ≥ 50. Two or more proteins when co-existed in the same gel spot were considered as potential PPIs (because PPIs is more likely to be exist in the presence or co-existing of two or more protein in 1D BN-PAGE). The results from *N. caninum* and for *T. gondii* gels are shown in Table 2.4 and 2.6, respectively.

2.3.3. 2D BN/SDS-PAGE of whole tachyzoite multiprotein complexes of *N. caninum* and *T. gondii*

Gel strips from 1D BN-PAGE of *N. caninum* and *T. gondii* samples (Figures 2.3a and 2.4a, respectively) were applied to the 2D SDS-PAGE (Figure 2.3b and 2.4b, respectively). 2D BN/SDS-PAGE showed that protein subunits were separated and 32 and 13 gel slices of the separated protein on the gels from *N. caninum* (Figure 2.3b) and *T. gondii* (Figure 2.4b), respectively, were analysed by mass spectrometry. The results from *N. caninum* gel and *T. gondii* results are shown in Table 2.5 and 2.7.

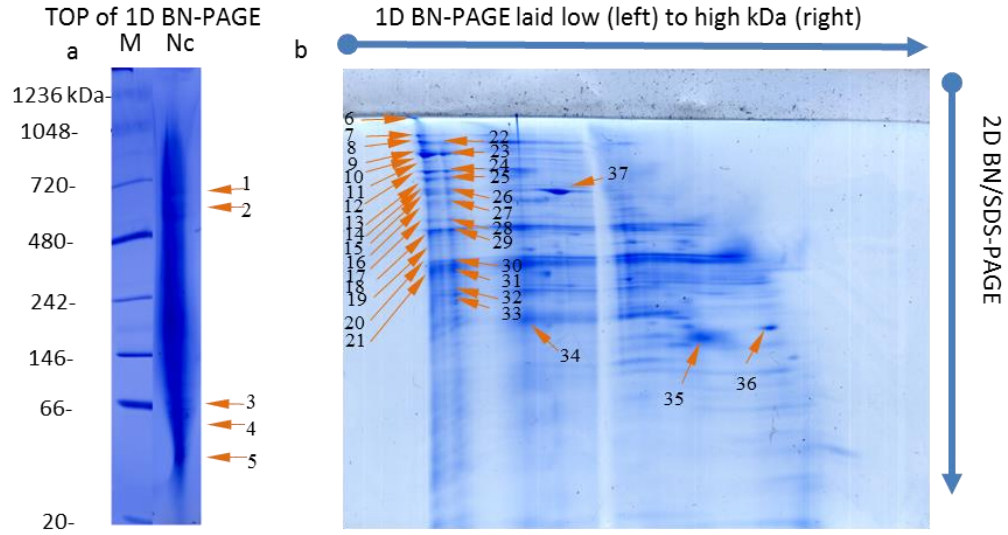

Figure 2.3: 2D BN/SDS-PAGE of differentially purified membrane proteins and complexes of *N. caninum*. a) 1D BN/PAGE: M) protein standard, Nc) 100 µg of *N. caninum* tachyzoite lysate, b) 2D BN/SDS-PAGE. 1-37 with arrows indicate locations of the gel cut for in gel digestion and mass spectrometry analysis.

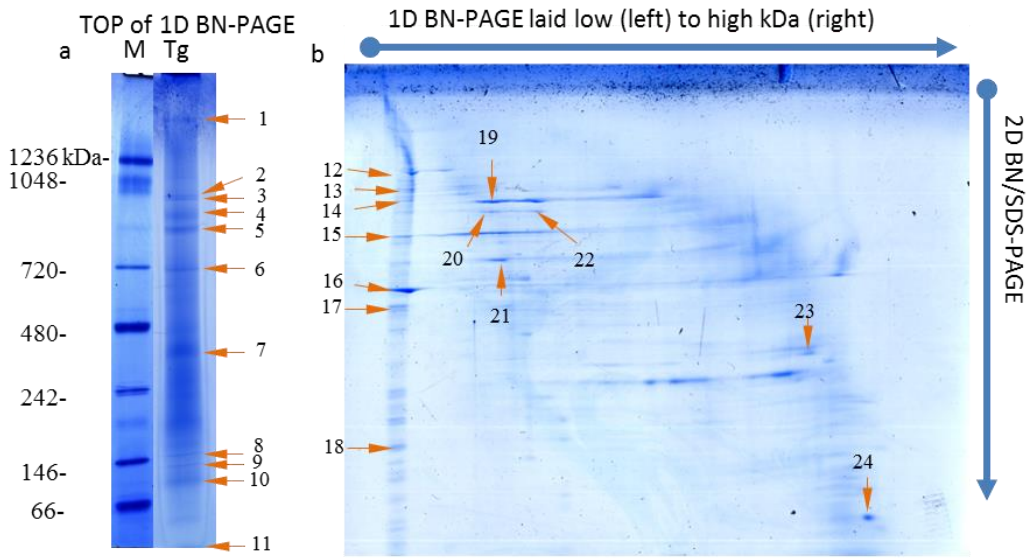

Figure 2.4: 2D BN/SDS-PAGE of differentially purified membrane proteins and complexes of *T. gondii*. a) 1D BN/PAGE: M) protein standard, Tg) 100 µg of *T. gondii* tachyzoite lysate, 2) 2D BN/SDS-PAGE. 1-24 with arrows indicate locations of gel cut for in gel digestion and mass spectrometry analysis.

2.3.4. In-gel digestion and mass spectrometry of 1D BN-PAGE and 2D BN/SDS-PAGE from *N. caninum* and *T. gondii*

The detail of the results from mass spectrometry of 1D BN-PAGE and 2D BN/SDS-PAGE (Figure 2.3 and 2.4) from *N. caninum* and *T. gondii* are shown in Appendix in Tables I and II, respectively. These tables show the total number of proteins identified from each spot analysed by MS, including all the proteins that were considered significant based on the threshold applied by the Mascot software. Mascot scoring is based on the ions score of individual peptide which is -10log(*P*), where *P* is the probability that the observed match of a peptide is a random event. Ions scores > 31 of an individual peptide indicate the identity or extensive homology ($p<0.05$).

Neospora mass spectrometry results from 1D BN-PAGE (Figure 2.3a) and 2D BN/SDS-PAGE (Figure 2.3b) based on the custom filters applied in section 2.3.2 are shown in Tables 2.4 and 2.5, respectively. Results showed that several protein subunits were identified in each slice suggesting that they could be associating with each other. Several of these proteins were identified as “hypothetical protein”, “conserved hypothetical protein”, or “unspecified product”. The sequences of these

proteins were searched for protein orthologue using BLAST® and ToxoDB (Version 11) and one of the orthologue proteins name from *T. gondii* ME49 strain (the most completed genome sequence annotation) was chosen (Tables 2.4 and 2.5).

Results from 1D BN-PAGE (Table 2.4**)** showed that isolated protein bands contained multiple proteins. *N. caninum* gel slice 1 (Figure 2.3a) consisted of nine significantly identified proteins; three of them were members of the glideosome (NCLIV_048570, NCLIV_049900 and NCLIV_029420), two of the proteins were from the proteasome (NCLIV_065750 and NCLIV_048880), from mitochondria (NCLIV_022220), rhoptry (NCLIV_001970), and from other compartments (NCLIV_034460 and NCLIV_019110).

On the other hand, proteins identified from gel slice 2 (Figure 2.3a) were from different subcellular locations such as rhoptry (NCLIV_001970), plasmalemma (NCLIV_033230 and NCLIV_032770) and HSP90-like protein, related protein (NCLIV_019110). While gel slice 3 (Figure 2.3a) was composed of five protein subunits including actin (NCLIV_003440), subtilase enzyme (NCLIV_021050), protein disulfide isomerase (NCLIV_011410), 14-3-3 protein homolog (NCLIV_024820) and putative 40S ribosomal protein S18 (NCLIV_047630). Five protein subunits from gel slice 4 (Figure 2.3a) were identified which include phosphoglycerate kinase 1 (NCLIV_011270), protein disulfide isomerase (NCLIV_011410), 14-3-3 protein homolog (NCLIV_024820), ribosomal protein RPL8 (NCLIV_021080) and putative cAMP-dependent protein kinase (NCLIV_017370).

Results from 2D BN/SDS-PAGE of *N. caninum* from spot 6-21 separated on straight line down on the gel; these spots could contain protein subunits of MPCs and/or co-migrated proteins to the same band (Figure 2.3b and Table 2.5), identified six proteins RON1, RON2, RON3, RON5, RON8, and a ROP2 family member (NCLIV_054120, NCLIV_054120, NCLIV_048590, NCLIV_064620, NCLIV_055360, NCLIV_070010 and NCLIV_001970, respectively) that belong to the rhoptries. In addition three protein subunits were identified from gel slice 14 (Figure 2.3b): putative myosin heavy chain (NCLIV_003050), subtilisin (NCLIV_021050) and TgRON5 (NCLIV_055360). While in analysed gel spots 22-

33 (Figure 2.3b and Table 2.5), RON2, RON3, RON5, ROP2 family member and ROP40 (NCLIV_012920) also were identified and they all belong to rhoptries. Also gel slice 34 (Figure 2.3b) showed three proteins (NCLIV_050470, NCLIV_022220, NCLIV_061940) from the mitochondria were associated with each other and with rhoptry ROP2 family member (NCLIV_001970), glideosome GAP45 (NCLIV_048570) and putative cAMP-dependent protein kinase (NCLIV_017370). While spot 35 only contained one significant protein, Putative microneme protein MIC3 (NCLIV_010600).

Table 2.4: Protein complexes and/or co-existed proteins identified from 1D BN-PAGE protein bands (Figure 2.3a) from *N. caninum* tachyzoite lysates. Proteins listed are from individual gel spot that contains two or more proteins (PPIs is more likely to be exist in the presence or co-existing of two or more protein in 1D BN-PAGE). Protein was considered to be significant identifications with at least two or more unique peptides and with Mascot protein score of ≥ 50.

Gel slice no.	Protein ID accession	Protein description	Protein score	*T. gondii* orthologue (Protein ID accession)*
1	NCLIV_034460	Hypothetical protein	341	Cell division cycle 48 protein (TGME49_273090)
	NCLIV_001970	Unspecified product	171	TgROP2 family member**
	NCLIV_048570	Conserved hypothetical protein	151	Gliding-associated protein 45 (GAP45) (TGME49_223940)
	NCLIV_049900	Hypothetical protein	106	Myosin A (TGME49_235470)
	NCLIV_065750	Alpha 2 subunit of 20S proteasome (ISS), related	99	-
	NCLIV_029420	Putative myosin light chain MLC1	98	-
	NCLIV_019110	HSP90-like protein, related	73	-
	NCLIV_048880	Proteasome subunit beta type-7, related	73	-
	NCLIV_022220	Hypothetical protein	51	Mitochondrial-processing peptidase beta subunit, putative (TGME49_202680)
2	NCLIV_032770	Hypothetical protein	112	Vacuolar proton-translocating ATPase subunit, putative (TGME49_232830)
	NCLIV_019110	HSP90-like protein, related	105	-
	NCLIV_033230	SRS domain-containing protein	91	-
	NCLIV_001970	Unspecified product	67	TgROP2 family member
3	NCLIV_011410	Protein disulfide isomerase	227	-
	NCLIV_024820	14-3-3 protein homolog	97	-
	NCLIV_021050	Unspecified product	77	Subtilase family serine protease, putative (TGME49_204050)
	NCLIV_047630	Putative 40S ribosomal protein S18	62	-
	NCLIV_003440	Actin, related	53	-
4	NCLIV_011410	Protein disulfide isomerase	274	-
	NCLIV_017370	Putative cAMP-dependent protein kinase regulatory subunit	92	-
	NCLIV_021080	Hypothetical protein	72	ribosomal protein RPL8 (RPL8) (TGME49_204020)
	NCLIV_011270	Hypothetical protein	69	Phosphoglycerate kinase 1 (TGME49_318230)
	NCLIV_024820	14-3-3 protein homolog	52	-

* Orthologue name of *T. gondii* protein for uncharacterised *N. caninum* proteins (hypothetical protein, unspecified product and conserved hypothetical protein). Dash sign (-) indicates that the protein is characterised in the database of *N. caninum*. **Accession number for ROP2 family member is not given as ROP2 family comprises several members with similar protein sequences.

Table 2.5: Protein identified from 2D SDS-PAGE (Figure 2.3b) differentially purified from *N. caninum* tachyzoite lysates. Proteins listed are from individual gel spot that contains significantly identified protein. Protein was considered to be significant identifications with at least two or more unique peptides and with Mascot protein score of ≥ 50.

Gel slice no.	**Protein ID accession**	**Protein description**	**Protein score**	***T. gondii* orthologue (Protein ID accession)***
8	NCLIV_070010	Hypothetical protein, conserved	209	TgRON8 (TGME49_306060)
	NCLIV_042820	DNA FLJ58099, highly similar to *Homo sapiens* clathrin, heavy polypeptide-like 1 (CLTCL1)	99	-
	NCLIV_031970	Hypothetical protein	59	Pre-mRNA splicing factor PRP8, putative (TGME49_231970)
9	NCLIV_007800	Unspecified product	86	Hypothetical protein (TGME49_253370)
	NCLIV_042820	cDNA FLJ58099, highly similar to *Homo sapiens* clathrin, heavy polypeptide-like 1 (CLTCL1),	53	-
10	NCLIV_042820	cDNA FLJ58099, highly similar to *Homo sapiens* clathrin, heavy polypeptide-like 1 (CLTCL1)	243	-
	NCLIV_070010	Hypothetical protein, conserved	177	TgRON8 (TGME49_306060)
	NCLIV_048590	Unspecified product	135	TgRON3 (TGME49_223920)
12	NCLIV_064620	Unspecified product	215	TgRON2 (TGME49_300100)
13	NCLIV_064620	Unspecified product	200	TgRON2 (TGME49_300100)
14	NCLIV_003050	Putative myosin heavy chain	158	-
	NCLIV_021050	Unspecified product	100	Subtilisin SUB1 (TGME49_204050)
	NCLIV_055360	Unspecified product	65	TgRON5 (TGME49_311470)
15	NCLIV_055360	Unspecified product	112	TgRON5 (TGME49_311470)
	NCLIV_019110	HSP90-like protein, related	53	-
16	NCLIV_055360	hypothetical protein	90	TgRON5 (TGME49_311470)
18	NCLIV_001970	Unspecified product	134	TgROP2 family member
19	NCLIV_054120	Unspecified product	98	TgRON1 (TGME49_310010)
20	NCLIV_001970	Unspecified product	165	TgROP2 family member
23	NCLIV_042820	cDNA FLJ58099, highly similar to *Homo sapiens* clathrin, heavy polypeptide-like 1 (CLTCL1)	328	-
	NCLIV_048590	Unspecified product	84	RON3 (TGME49_223920)
24	NCLIV_064620	Unspecified product	270	TgRON2 (TGME49_300100)
26	NCLIV_055360	Unspecified product	134	TgRON5 (TGME49_311470)
29	NCLIV_055490	Heat shock protein 70 (Precursor), related	67	-
30	NCLIV_001970	Unspecified product	235	TgROP2 family member

31	NCLIV_001970	Unspecified product	220	TgROP2 family member
	NCLIV_012920	Unspecified product	63	TgROP40 (TGME49_291960)
33	NCLIV_053580	50S ribosomal protein L4P, related	170	-
	NCLIV_001970	Unspecified product	130	TgROP2 family member
	NCLIV_047530	Conserved hypothetical protein	85	Hypothetical protein (TGME49_225150)
	NCLIV_006180	Putative duplicated carbonic anhydrase	61	-
34	NCLIV_050470	Hypothetical protein	159	Peptidase M16 family protein beta subunit, putative (TGME49_236210)
	NCLIV_022220	Hypothetical protein	124	Peptidase M16, alpha subunit, putative (TGME49_202680)
	NCLIV_048570	Conserved hypothetical protein	96	Gliding-associated protein 45 (GAP45) (TGME49_223940)
	NCLIV_017370	Putative cAMP-dependent protein kinase regulatory subunit	93	-
	NCLIV_061940	Hypothetical protein	88	Eukaryotic porin, putative (TGME49_218280)
	NCLIV_001970	Unspecified product	72	TgROP2 family member
35	NCLIV_010600	Putative microneme protein MIC3	105	-
37	NCLIV_019110	HSP90-like protein, related	436	-

* Orthologue name of *T. gondii* protein for uncharacterised *N. caninum* proteins (hypothetical protein, unspecified product and conserved hypothetical protein). Dash sign (-) indicates that the protein is characterised in the database of *N. caninum*.

Toxoplasma mass spectrometry results from 1D BN-PAGE of (Figure 2.4a) and 2D BN/SDS-PAGE (Figure 2.4b) based on the custom filters applied in section 2.3.2 are shown in Tables 2.6 and 2.7, respectively. Results from the *T. gondii* analysis showed that only gel slices 7 and 9 from 1D BN-PAGE contained more than one protein with potentially interacting proteins. Gel slice 7 contained SAG-related sequence SRS29B (TGME49_233460) and microneme protein MIC6 (TGME49_218520). Gel slice 9 consisted of three proteins including protein disulfide isomerase (TGME49_211680), 14-3-3 protein (TGME49_263090) and ribosomal protein RPSA (TGME49_266060). On the other hand analysis from 2D SDS-PAGE showed only gel slices 12, 19 and 21 contained significantly identified proteins.

Table 2.6: Protein complexes and/or co-existed proteins identified from 1D BN-PAGE protein bands (Figure 2.4a) differentially purified from *T. gondii* tachyzoite lysates. Proteins listed are from individual gel spot that contains two or more proteins (PPIs is more likely to be exist in the presence or co-existing of two or more protein in 1D BN-PAGE). Protein was considered to be significant identifications with at least two or more unique peptides and with Mascot protein score of ≥ 50.

Gel slice no.	Protein ID accession	Protein description	Protein score
7	TGME49_233460	SAG-related sequence SRS29B (SRS29B) or (SAG1)	157
	TGME49_218520	Microneme protein MIC6	66
9	TGME49_211680	Protein disulfide isomerase	304
	TGME49_263090	14-3-3 protein	215
	TGME49_266060	Ribosomal protein RPSA (RPSA)	54

Table 2.7: Proteins identified from 2D SDS-PAGE (Figure 2.4b) of differentially purified from *T. gondii* tachyzoite lysates. Proteins listed are from individual gel spot that contains significantly identified protein. Protein was considered to be significant identifications with at least two or more unique peptides and with Mascot protein score of ≥ 50.

Gel slice no.	Protein ID accession	Protein description	Protein score
12	TGME49_290950	Clathrin heavy chain, putative	406
19	TGME49_244560	Heat shock protein 90, putative	219
21	TGME49_247550	Heat shock protein HSP60 (HSP60)	70

2.4. DISCUSSION

Blue native electrophoresis was used to study the complexome of *T. gondii* and *N. caninum* at the fast growing and multiplying tachyzoite stages. A comparative study of the complexomes of both parasites could help in dissecting the biological differences between these two related organisms.

To date BN-PAGE has not been used to study the complexomes of *T. gondii* or *N. caninum* or in the comparison between them. In this project efforts have been made to optimise the technique so that can be used efficiently to study these parasites and understand their complexomes based on the protein interactions and complexes from total cell lysates, including membrane bound protein complexes. Despite some progress towards optimisation of the technique, technical problems have hampered further improvement in the optimisation.

Proteins of the gel slices from 1D BN-PAGE and 2D BN/SDS-PAGE from *N. caninum* (Figure 2.3) and *T. gondii* (Figure 2.4) were digested with trypsin and analysed using LC MS/MS. The data analysis from this study showed that many proteins were potentially associated together, while some of these associations could be due to non-specific interactions, protein subunits from complexes such as the proteasome and glideosome were found together following 1D BN-PAGE. The identification of proteins from known complexes indicates that some of these interactions were not a consequence of non-specific interactions. In this study, three subunits of the glideosome protein complex TgMyoA-MLC1-GAP45 (NCLIV_049900, NCLIV_029420 and NCLIV_048570, respectively, Table 2.4) were found together which is in agreement with the study of Gaskins *et al.* (2004) on *T. gondii*. The present study is also comparable with the study of Sanders *et al.* (2007), identified the invasion motor complex comprised of (GAP45/GAP50/myosinA) from detergent-resistant membranes of *Plasmodium falciparum* schizonts using BN-PAGE. The glideosome is a macromolecular complex that powers substrate-dependent gliding motility of apicomplexan parasites and is required for migration through the host biological barrier, invasion of host cells, and egress (Keeley and Soldati, 2004). In *T. gondii*, the glideosome is comprised of MyoA (TgMyoA) which is a class XIV member of a family of apicomplexan-specific myosin (Heintzelman and Schwartzman, 1997) and is

associated with myosin light chain (TgMLC1) (Herm-Götz *et al.*, 2002). MyoA is critical for parasite motility within the host, invasion of host cells and egress from infected cells (Meissner *et al.*, 2002b). Previous studied in *T. gondii* found that other subunit were associated with the glideosome such as the gliding associated proteins TgGAP40 (Frenal *et al.*, 2010), TgGAP45 and TgGAP50 (Gaskins *et al.*, 2004). In this study, GAP40 and GAP50 were not identified which might be due to an insufficient centrifugation force (16,000 × *g*) to extract these proteins from inner membrane complexes (IMCs); a high centrifugation force (100,000 × *g*) is required to extract membrane bound proteins solubilised by non-ionic detergent (Wittig *et al.*, 2006). GAP50 is an integral transmembrane glycoprotein and plays an important role as a receptor in the IMCs for TgMyoA-TgMLC1-GAP45 (Gaskins *et al.*, 2004). In addition, TgGAP40 was identified as a polytopic protein of the IMC. The findings of the present study of co-existing TgMyoA-TgMLC1-TgGAP45 subunits of the glideosome together are in agreement with those of Gaskins *et al.* (2004) who found that the glideosome forms in two stages. Initially the TgMyoA-TgMLC1-TgGAP45 complex forms and assembles in the cytosol of an immature daughter parasite, it eventually translocates to the mature IMC were it associates with the membrane anchor TgGAP50 forming the functional glideosome. The final assembly of the functional glideosome is mediated by phosphorylation of the TgGAP45 (Gilk *et al.*, 2009). While the exact role of the recently identified subunit GAP40 in the complex is not known (Frenal *et al.*, 2010).

In the present study, proteasome complex subunits were also found together such as alpha 2 subunit of 20S proteasome (ISS) related protein and proteasome subunit beta type-7 related protein (NCLIV_065750 and NCLIV_048880, respectively) (Table 2.4). In addition, two other proteasome proteins (NCLIV_028230 and NCLIV_017470) were found in the same spot but only contained one peptide per each (Appendix, Table I). The proteasome is a non-lysosomal macromolecular protease of multisubunit proteins present in eukaryotic cells (Bochtler *et al.*, 1999). The proteasome plays an important role in the regulation of various vital cellular processes (DeMartino and Slaughter, 1999). In eukaryotic cells, 26S proteasome comprises of two sub complexes of 20S proteasome the proteolytic core and a 19S regulator which makes the enzyme ATP dependent and specific for proteolysis of ubiqitinated substrates (Ferrell *et al.*, 2000). In *T. gondii*, it

has been shown that the proteasome is located mainly in the cytosol (Paugam *et al.*, 2001). The proteasome plays a critical role in the virulence and regulation of differentiation of parasitic protozoan such as life cycle progression in *Trypanosoma cruzi* (González *et al.*, 1996) and *T. gondii* (Shaw *et al.*, 2000). These studies are in agreement with results from the current work where, in addition to proteasome subunits in *N. caninum*, cell division cycle 48 protein (NCLIV_034460) was also found co-existed together or associated with the complex. This suggests that cell division cycle 48 protein potentially recruited by the proteasome during cell progression of tachyzoite stage. However, presence of proteins of different MPCs together in one gel slice could be due to physical interactions occurring between different complexes resulted from whole tachyzoite solubilisation or just co-migration of proteins to the same molecular size on the BN-PAGE.

In this study the *N. caninum* protein disulfide isomerase NcDPI (NCLIV_011410) (Table 2.4) was found associating/co-localising with different proteins such as ribosomal proteins (NCLIV_021080), 14-3-3 protein (NCLIV_024820) and kinases such as phosphoglycerate kinase 1 (NCLIV_011270) and putative cAMP-dependent protein kinase regulatory subunit (NCLIV_017370). Also in *T. gondii* (Table 2.6), disulfide isomerase (TGME49_211680) was found associating/co-localising with ribosomal proteins (TGME49_266060) and 14-3-3 protein (TGME49_263090). This enzyme functions to introduce disulfide bonds into newly synthesised proteins inside the endoplasmic reticulum mainly on two cysteines situated in close proximity (Oka and Bulleid, 2013). It is a critical step in the folding and maturation of secretory proteins containing disulfide bonds (Matagne and Dobson, 1998) which promote structural stability and enable the assembly of multi-protein complexes (Hogg, 2003). Immunogold-electron microscopy study showed that NcDPI was localised to tachyzoite cytoplasm, microneme and plasma membrane surface (Naguleswaran *et al.*, 2005). They also found that NcDPI was associated with adhesion of tachyzoites with host cell surface membrane and its inhibition reduced host cell surface adhesion; suggested that plays important role in processing of molecules involved in adhesion and invasion of host cell (Naguleswaran *et al.*, 2005). The association of this enzyme could be related to PTMs of these proteins and transform them to the functional state before targeting to a destined location.

In the present study, 2D BN/SDS-PAGE from *N. caninum* based on the orthologue proteins from *T. gondii*, several related rhoptry proteins were identified including RON1, RON2, RON3, RON5, RON8, a ROP2 family member and ROP40 (Figure 2.3b, Table 2.5). These results are in agreement with the proteomic analysis of a rhoptry organelle fractions that have identified several proteins from the rhoptry bulb and neck, as well as many other proteins and enzymes in *T. gondii* (Bradley *et al.*, 2005) and *N. caninum* (Marugán-Hernández *et al.*, 2011). The former found TgRON1, 2, 3, and 4 while the later found NcRON2, 3, 4, and 8 from the analysis. This suggests that these proteins could be associating together inside the rhoptry organelles. In addition RON2, 3, 4, 5 and 8 were found to play important roles in the moving junction formation following attachment of *T. gondii* and *N. caninum* tachyzoites (Alexander *et al.*, 2005; Sohn *et al.*, 2011; Straub *et al.*, 2009). The tight association between these proteins inside the parasite rhoptry and beyond the parasite plasma membrane during invasion processes and its critical role in the moving junction formation suggest that these proteins may form complexes. Complex formation inside rhoptries and secretion as one macromolecule may help the parasite to invade the host cells very quickly and establishment of infection.

In the present study, ROP2 family member from spot 1 of 1D BN-PAGE (Table 3.4) and spot 34 of BN/SDS-PAGE (Table 4.5) was found associating/co-migrating with mitochondrial proteins from *N. caninum*. A recent studied found that ROP18 is associated with a complex containing a ROP2 family member, pseudokinases ROP8/2 and GRA7 on the cytosolic surface of PVM and ROP18 was found to play critical role in the virulence of the parasite following infection of host cell (Alaganan *et al.*, 2014; El Hajj *et al.*, 2007; Lei *et al.*, 2014). Furthermore, a previous study using co-IPs found that TgROP2 family member, pseudokinases ROP2/4 and GRA7 were associating together on strand-like structure extending from PVM and demonstrated that TgGRA7 was phosphorylated only within infected host cell (Dunn *et al.*, 2008). In addition, previous studies showed that in both parasites, several host cell organelles were found in intimate association with PVM near the host cell nucleus such as mitochondria and endoplasmic reticulum (Hemphill *et al.*, 2004; Magno *et al.*, 2005; Sinai and Joiner, 2001) and thought might result from protein-protein interaction between PVM and host organelles (Sinai *et al.*, 1997). TgROP2 has been shown to have more likely to play key role as an interacting

molecules of the parasite with the mitochondrial import machinery of the host cell (Sinai and Joiner, 2001). Finding of the present study suggests that ROP2 family member from *N. caninum* might also interact with mitochondrial protein of the host.

In the present study, spot 7 from 1D BN-PAGE (Table 2.6, Appendix Table II) from *T. gondii* showed that the microneme protein MIC6 (TGME49_218520) and MIC1 interacted/co-localised with SRS29B (TGME49_233460). MIC6 is an escorter transmembrane protein found in oligomeric complex in *T. gondii* comprised of MIC6-1-4 (Saouros *et al.*, 2005). In *T. gondii*, the transmembrane domains of escorter MICs were found playing critical roles in complex formation and directing other soluble microneme proteins to the micronemes (Meissner *et al.*, 2002a; Reiss *et al.*, 2001). On the other hand SRS29B (SAG1) is a surface antigen adhesin that binds through its N-terminal to the surface of the tachyzoites by a glycosylphosphatidylinositol (GPI)-anchor (Jung *et al.*, 2004). It plays an important role in mediating attachment and invasion of host cell through interaction with host surface proteins (He *et al.*, 2002) and in attracting host immunity and maintenance of balance between parasite and host through reducing the virulence of the acute infection caused by *T. gondii* tachyzoites (Boothroyd *et al.*, 1998; Lekutis *et al.*, 2001). Oligomerisation increases the opportunity of proteins from different organelles to makes distinct complexes that facilitate invasion collaboratively (Alexander *et al.*, 2005; Carruthers and Tomley, 2008). Interaction/co-localisation of MIC6, MIC1 and SRS29B in this study may indicate that these proteins together play role in facilitating attachment and invasion of host cell by tachyzoites.

In this study, BN/SDS-PAGE was used to investigate the differences between host-parasite interactions based on the complexome of tachyzoites stage of both parasites. Several different complexes were identified that play important part in gliding motility, attachment and invasion of host cell. However, limitation of access to laboratory instrument for BN/SDS-PAGE has laden further development to understand the complexomes of both *T. gondii* and *N. caninum* and host-parasite interaction. Native MPCs within the parasites both during and after invasion, could help understand the biological differences between these parasites. Therefore, the next step was to fractionate different compartment of tachyzoites using sucrose gradient fractionations before applying to BN-PAGE would be useful to decrease the complexity of the tachyzoites lysate. With a less complex sample the probability of

non-specific interactions occurring between MPCs of different compartment would be lower resulting in better separation of MPCs on the BN-PAGE. It would be important to study the host-parasite interactions based on the PPIs and MPCs of the same compartments or fractions of the tachyzoites from both parasites.

BN-PAGE is a valuable analysis tool to perform screening to identify potential protein binding partners. Potential PPIs can be later analysed further using biochemical analysis and pull-down assay to confirm the presence of interaction. Therefore next project is to study comparative host-parasite interaction based on using the same recombinant proteins from both *T. gondii* and *N. caninum*; and because of the importance and availability of recombinant genes of dense granule proteins GRA7 and GRA2 of both parasites. In addition a potential binding partner of GRA7 which is a ROP2 family member was found associated with mitochondrial proteins of *N. caninum*. However it was not possible to determine which member of the *T. gondii* ROP2 family was the orthologue of NCLIV_001970) as they are very similar in protein sequences. Thus GRA7 was used in pull-down because it is a well-known binding partner of ROP2 family members at the interface between the cytoplasmic face of PVM and host cell organelles (Alaganan *et al.*, 2014; Dunn *et al.*, 2008). While TgGRA2 has been found in gel slice 9 (Figure 2.4a and Table 2.6, Appendix Table I) based on the significant threshold applied by Mascot but no any binding partner was identified. Thus TgGRA2 and TgGRA7 from both parasites will be used to pull-down interacting partner from the host cell.

CHAPTER THREE: Pull-down assay for characterisation of *T. gondii* and *N. caninum* dense granule proteins in host-parasite interactions

3.1. INTRODUCTION

Toxoplasma gondii and *N. caninum* exploit intracellular strategies within infected host cells that help successful establishment of infection and replication. Successful invasion results in formation of PV surrounded by a PVM (Sinai, 2014). PV provides the necessary environment required for replication of the highly multiplying tachyzoite stage and to evade detection and destruction by the host immune system (Besteiro *et al.*, 2011; Mercier *et al.*, 2005; Sinai and Joiner, 1997). The nascent PVM is excluded from most of the host cell membrane proteins at the time of invasion, preventing it being involved in host vesicular traffic and it is non-fusogenic with lysosomes (Gendrin *et al.*, 2008; Mordue *et al.*, 1999). Infective stages employ an array of proteins from secretory organelles that play significant roles in the attachment, invasion, establishment of infection (Carruthers and Sibley, 1997) and the alteration of host cell physiology (Bougdour *et al.*, 2014). Several proteins from each organelle have been characterised and identified with certain critical functions having been assigned for some of them. However, the exact function of most of these proteins is not yet known, particularly most of the secretory proteins of the dense granules (Carey *et al.*, 2000; Mercier *et al.*, 2005). In *Toxoplasma* and *Neospora*, these proteins have been found to be involved in remodelling the PVM and formation of NTN in the PV (Carruthers and Sibley, 1997; Hemphill *et al.*, 1998; Lebrun *et al.*, 2007; Mercier *et al.*, 2002; Michelin *et al.*, 2009; Travier *et al.*, 2008).

3.1.1. Dense granule proteins and their association with parasitophorus vacuoles and the parasitophorus vacuole membrane

The intravacuolar release of the DG proteins is likely responsible for the maturation of the nascent PV (Mercier *et al.*, 2005; Sibley *et al.*, 1995). Following invasion, a NTN forms within 10-20 min at the posterior end of the parasite, which later distributes throughout the PV forming elongated tubules of 60-90 nm in diameter that connect with the PVM (Sibley *et al.*, 1995). DG proteins divided into two groups: firstly, a group with no significant homology to any other known protein (Carey *et al.*, 2000; Fischer *et al.*, 1998) and were named as GRA (Sibley *et al.*, 1991); secondly, a group comprising proteins with homologies to already characterised proteins from other organisms, as reviewed in Mercier *et al.* (2005).

GRA proteins are a group of proteins with small to large molecular weight ranging between 12.8 kDa (e.g. TgGRA5) to 94.2 kDa (e.g. TgGRA10) (Mercier and Cesbron-Delauw, 2015). The number of GRA proteins identified and characterised is increasing, especially in *T. gondii* and *N. caninum*. In *T. gondii* zoites, currently 25 proteins have been known to be stored and localised to the DG organelles including GRA1-GRA10, GRA11-12, GRA14-GRA16, GRA19-25, cyclophilin (CyP18), protease inhibitors (TgPI-1, TgPI-2), Tg14-3-3, *T. gondii* patatin-like protein (TgPL1) and isoforms of nucleotide triphosphate hydrolase (TgNTPasa-I, TgNTPasa-II) reviewed in Mercier *et al.* (2005) (Bougdour *et al.*, 2013; Braun *et al.*, 2013; Masatani *et al.*, 2013; Okada *et al.*, 2013). These proteins are secreted in a soluble form, targeted to either vacuolar matrix (Cy-18, TgPI-1, TgPI-2, TgPL1, GRA1 and GRA2), the NTN (GRA2, GRA3, GRA4, GRA6, GRA7, GRA9, GRA12, GRA14, GRA23, TgNTPasa), the PVM (GRA3, GRA5, GRA7, GRA8, GRA10, GRA14, GRA23) or beyond the PVM into the cytosol of the infected host cells (GRA15, GRA16, GRA24).

In *N. caninum*, several orthologues to *T. gondii* have also been identified and characterised. These include NcGRA1 (Atkinson *et al.*, 2001), NcGRA2 (Ellis *et al.*, 2000), NcGRA14 (Liu *et al.*, 2013), NcGRA6 (Liddell *et al.*, 1998), NcGRA7 (Hemphill *et al.*, 1998). As in *T. gondii*, DGs contain other secretory/ excretory molecules such as nucleotide triphosphate hydrolase-type I (NTPasa I) (Asai *et al.*, 1998) and protease inhibitors (NcPI) (Morris *et al.*, 2004).

3.1.2. Structure and molecular function of dense granules proteins

GRA proteins are characterised by having a short N-terminal hydrophobic signal peptide. GRA1 is a soluble protein that lacks central hydrophobic membrane domain, while most of the GRA proteins contain a central hydrophobic membrane domain, either at least a single hydrophobic alpha-helix transmembrane domain e.g. GRA3, GRA4, GRA5, GRA6, GRA7, GRA8) or multiple amphipathic alpha-helices, such as GRA2 and GRA9, as reviewed from Mercier *et al.* (2005). Recently TgGRA16 and 24 were found to contain internal repeats sequence that contains putative nuclear localisation signals (Bougdour *et al.*, 2013; Braun *et al.*, 2013). GRA proteins are found in both soluble and complex forms within the dense granule matrix (Labruyere *et al.*, 1999; Michelin *et al.*, 2009; Sibley *et al.*, 1995). Following

infection of the host cell by *T. gondii*, DG proteins are secreted as soluble proteins into the PV. These either stay in soluble form e.g. GRA1, GRA16 and GRA24 or subsequently become associated with the NTN and PVM (Bougdour *et al.*, 2013; Braun *et al.*, 2013; Sibley *et al.*, 1995; Travier *et al.*, 2008). GRA2 is secreted within multi-lamellar vesicles and assembles at a posterior invagination of the parasite. In the posterior invagination, NTN first form then distribute in the PV matrix. The NTN forms connections with intravacuolar membranes and GRA2 associates with the NTN as an integral membrane protein (Sibley *et al.*, 1995). Experiments using gene knockout mutants of GRA2 found that the NTN formation is induced by GRA2 (Mercier *et al.*, 2002). The integrity of both amphipathic alpha-helices of GRA2 is essential for precise formation of the network and is further stabilized by GRA6 (Mercier *et al.*, 2002). GRA6 binds to the network via hydrophobic interactions, while GRA4 associates with the NTN established by GRA2 through strong protein–protein interactions (PPIs). Thus, GRA4 and GRA6 specifically interact with GRA2 leading to the formation of a multimeric complex that is stably linked with the NTN (Labruyere *et al.*, 1999). GRA12 cannot be translocated to the parasite posterior invagination in the absence of GRA2 (Michelin *et al.*, 2009). However, GRA9 remains in both the soluble form and the NTN membranes associated form following secretion from anterior end of the parasite without trafficking through the posterior invagination (Adjogble *et al.*, 2004). Other GRA proteins localise at and associate with the NTN to a lesser extent, such as GRA3, GRA5 and GRA7, as reviewed in Mercier *et al.* (2005).

The PVM is similar to the NTN as it is also decorated by several proteins secreted from DG shortly after invasion. These proteins possess at least one transmembrane domain that provides possible membrane anchors. GRA3, GRA5, GRA7, GRA8 were detected as PVM associated proteins (Achbarou *et al.*, 1991; Bonhomme *et al.*, 1998; Carey *et al.*, 2000; Dubremetz *et al.*, 1993; Gendrin *et al.*, 2008; Lecordier *et al.*, 1993). In addition, GRA proteins have been found beyond the boundary of the PVM in fine strands extending from the PVM membrane into the cell cytoplasm that can be detected as early as 15 min p.i. (Coppens *et al.*, 2006; Dubremetz *et al.*, 1993; Dunn *et al.*, 2008; Jacobs *et al.*, 1998). The function and composition of the GRA7-containing strands are unknown (Dunn *et al.*, 2008). GRA1, GRA3 and GRA7 were found associating with these strand-like structures,

however GRA1 was only found associating for only 30 min p.i. (Dubremetz *et al.*, 1993; Dunn *et al.*, 2008). TgGRA7 was also found in a complex consisted of ROP18/8/2; GRA7 was found playing critical role in acute virulence in mice through binding with IRG a6 protein which subsequently leading to IRG inactivation and clearance from PVM (Alaganan *et al.*, 2014). In addition, in the type-II strain of *T. gondii*, GRA15 is secreted into the host cell upon invasion and mediate translocation of NF-κB and induction of IL-12, possibly signifying that GRA proteins also play a role not only as structural components of the NTN and PVM but also as effectors that can modulate host signalling pathways (Rosowski *et al.*, 2011). Furthermore, GRA24 travel to nucleus of the infected host cell leading to nuclear translocation and activation of p38α mitogen activated protein (MAP) kinase through sustained autophosphorylation (Braun *et al.*, 2013). Consequently, activation of the host cell kinase leading to up-regulation of the transcription factors Egr-1 and c-Fos and the associated synthesis of key proinflammatory cytokines (interleukin-12 and the chemokine MCP-1), resulting in control of early parasite replication in vivo (Braun *et al.*, 2013).

3.1.3. Structure of GRA2 and GRA7 in *T. gondii* and *N. caninum*

The primary translation of mature messenger of TgGRA2, TgGRA7, NcGRA2 and NcGRA7 products consist of polypeptides comprising of 185 amino acids (AA) (molecular weight (MW) of 19.8 kDa), 236 AA (25.9 kDa), 211 AA (22.42 kDa) and 217 AA (22.49 kDa), respectively. The secondary structures predicted for these GRAs are shown in Figure 3.1, were based on the protein sequences from *T. gondii* ME49 strain used in the construction of recombinant proteins for TgGRA2 (TGME49_227620), TgGRA7 (TGME49_203310), and from *N. caninum* Liverpool strain for NcGRA2 (NCLIV_045650) and NcGRA7 (NCLIV_021640). Secondary structure predictions of proteins can differ based on the software used. TgGRA2 consists of a signal peptide at AA 1-23, the N-terminal sequence at AA 24-68, amphipathic α-helical regions at AA 69-144 (AA 70–92, 95–110 and 119–139 (Travier *et al.* 2008)) and C-terminal peptide between AA 145-185 (Mercier *et al.*, 1993). The primary structure of TgGRA7 has a putative signal peptide at the N-terminus starting from AA 1–26 (Fischer *et al.*, 1998) as almost all GRA proteins (Braun *et al.*, 2008; Travier *et al.*, 2008). The two hydrophobic regions

spanning AA 5–24 and 181–202, the second one is identified as to be a putative transmembrane region (Fischer *et al.*, 1998).

NcGRA2 (Ellis *et al.*, 2000) has about 50 % protein sequence homology with TgGRA2, the predicted NcGRA2 secondary structure contains three amphipathic α-helical regions spanned residues 70-110, 110-150 and 170-190, unique C-terminal sequence, conserved N-terminus with a signal peptide (WILVVAVGALVGA) identical to TgGRA2 (Ellis *et al.*, 2000). While, NcGRA7 is 36 % identical to the TgGRA7 protein sequence; NcGRA7 contains a signal peptide at 1-25 and a putative transmembrane domain between AA 135-160 (NCLIV_021640) as shown in Figure 3.1.

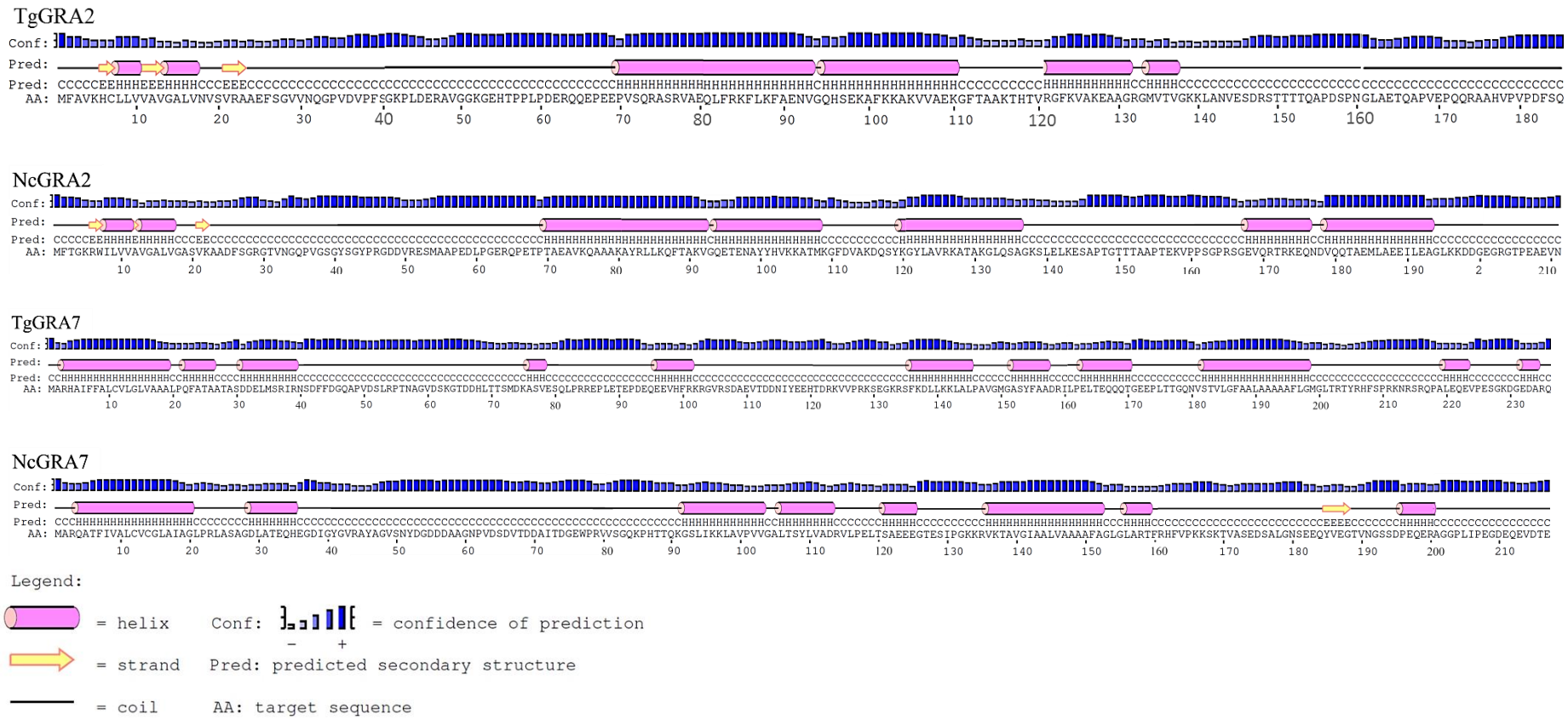

Figure 3.1: Secondary structure prediction of dense granule proteins GRA2 and GRA7 from *T. gondii* (Tg) and *N. caninum* (Nc). Secondary structure prediction was based on the protein sequences used in the construction of recombinant proteins of TgGRA2 (TGME49_227620), TgGRA7 (TGME49_203310), NcGRA2 (NCLIV_045650) and NcGRA7 (NCLIV_021640). The prediction analysis was performed using the Jpred 3 secondary structure prediction server (Cole *et al.*, 2008).

3.1.4. Aims and objectives of the study

There is strong evidence that in *T. gondii*, DG proteins GRA2 and GRA7 play vital roles in the maturation and maintenance of the PV and PVM; implying that they may play intermediate role through direct or indirect host-parasite interaction. However, their functions are not yet known. Therefore, based on the findings from Chapter 2, GRA2 and GRA7 were selected to study comparative host-parasite interactions between *T. gondii* and *N. caninum* because (1) we were interested to study the biology of these GRA proteins using pull-down assay to understand their role in host-parasite interaction and (2) based on the data found in the chapter 2, the presence of binding partner (TgROP2 family members) of GRA7 in *N. caninum* in BN-PAGE analysis (by orthologue) which was found co-existed with mitochondrial proteins. In addition TgGRA2 was co-existed with other proteins but none of the co-existed protein was known to interact with TgGRA2.

The hypothesis of the present study was GRA2 and GRA7 play different role in host-parasite interaction in *T. gondii* and *N. caninum* infection. This study aimed to study a comparative host-parasite interactions using purified recombinant GRA2 and GRA7 proteins from *T. gondii* and *N. caninum* as bait to study their binding partners from host cell lysates using pull-down assay and identified using MS/MS.

3.2. MATERIALS AND METHODS

3.2.1. Cloning of *GRA2* and *GRA7* from *T. gondii* and *N. caninum*

The miniprep of pE-SUMOpro Kan expression vector containing the cloned genes *GRA2* and *GRA7* from both *T. gondii* and *N. caninum* were received from Dr Marie Phelan from the NMR Centre for Structural Biology, University of Liverpool. pE-SUMOpro Kan vector used to enhance gene expression, high recombinant protein yield, increase solubility and folding of hydrophobic protein such as membrane bound proteins. Cloned plasmid DNA with *GRA2* and *GRA7* were produced by GeneArt® Gene Synthesis (Life Technologies) using the following sequences: *T. gondii GRA2* (TGME49_227620) and *GRA7* (TGME49_203310) and *N. caninum* GRA2 (NCLIV_045650) and GRA7 (NCLIV_021640) consisted of 492, 639, 567 and 576 bp, respectively (Table 3.1). In the pE-sumoPro Kan vector, these *GRA* genes are ligated to 6 × histidine-SUMO tag sequence consisting of 320 bp which also expresses with the *GRA* genes upon induction. The full sequence of *GRA* genes is shown in Appendix Table III. The signal peptide (SP) sequences were removed from each of the cloned recombinant genes in expression vector.

Table 3.1: Cloned genes from *T. gondii* and *N. caninum*

Gene name	Accession number[1]	Gene length	Cloned sequence length after removal of SP	Sequence length of removed SP (location in the sequence)
TgGRA2	TGME49_227620	555 bp	492 bp	63 bp (bp 1-63)
TgGRA7	TGME49_203310	708 bp	639 bp	69 bp (bp 1-69)
NcGRA2	NCLIV_045650	633 bp	567 bp	66 bp (bp 1-66)
NcGRA7	NCLIV_021640	651 bp	576 bp	75 bp (bp 1-75)

[1] Information about Gene sequences were obtained from ToxoDB, *Toxoplasma* Genomics Resource, Version 11 (Gajria *et al.*, 2008)

3.2.1.1. Transformation of BL21 (DE3) Competent cells with expression vector containing recombinant genes of GRA proteins

Competent BL21 (Novagen®) cells were transformed with one of the miniprep containing the insert gene of *GRA2* and *GRA7* from *T. gondii* and *N. caninum*. Competent cells (20 µl) were transformed with 1 µl of the plasmid

containing the recombinant gene in a 1.5 ml tube and incubated on ice for 5 min. The cells were heat shocked for 30 sec in a water bath at 42 ºC, then incubated on ice for another 2 min. 80 µl of SOC media (Novagen®) was added to the transfected cells and incubated in shaking incubator at 220 RPM at 37 °C for 1 hr. After incubation, 25 µl of the cells were added onto the surface of LB agar containing 35 µg/ml kanamycin and spread evenly using sterile bent steel rod and incubated overnight at 37 ºC. Several colonies were picked up and cultured in 5 ml LB medium containing 175 µg of kanamycin and incubated overnight at 37 ºC. Transformed colonies were screened by PCR to confirm that they contained the correctly sized inserts.

3.2.1.2. PCR screening of colonies from transformed BL21 (DE3) competent cells

PCRs were performed individually for each cloned gene from transformed competent BL21 in 25 µl reactions containing 1 × PCR buffers containing 15 mM $MgCl_2$, 0.2 mM of dNTP mix (QIAGEN), 0.1 mM from each T7 forward primer (Eurofins Scientific) (5' TAATACGACTCACTATAGG 3') and T7 terminator primer (Eurofins Scientific) (5' GCTAGTTATTGCTCAGCGG 3'), 2.5 U of Taq DNA polymerase (Qiagen). A colony on the growing plate was picked up using sterilised pipette tip and was mixed with the PCR reaction mix. T7 primers add 550 bp to the cloned genes upon amplification. The expected size for the recombinant *TgGRA2*, *TgGRA7*, *NcGRA2*, and *NcGRA7* is 1041, 1188, 1116 and 1125 bp, respectively. The PCR reaction conditions were 94 °C for 1 min; 30 × 94 °C for 1 min, 50 °C for 1 min, 72 °C for 2 min; 72 °C for 10 min.

PCR products were run at 110 V for 30 min on a 1.5 % agarose gel in 1 × TBE (87.5 mM Tris base, 89 mM boric acid, 3 mM EDTA) and stained with SYBR® Safe DNA Gel Stain (Invitrogen).

3.2.1.3. Glycerol stock of transformed competent BL21 (DE3)

The PCR positive colony from transformed competent BL21 with *GRA* genes was grown in LB media overnight in the presence of 35 µg/ml of kanamycin. The grown cells were harvested at 1,500 RPM for 5 min and resuspended in the LB media in the absence of the kanamycin, mixed 1:1 of 50 % autoclaved glycerol

solution homogenised by slow vortexing and were shock frozen using liquid nitrogen and stored at -80 °C for future use.

3.2.2. Recombinant fusion-tagged protein expression

Transformed competent BL21 cells from glycerol stock were grown in LB media or minimal media. Initially, LB media was used to grow transformed cells and express the recombinant GRA proteins. LB media was used in IMAC protein purification and with BugBuster® reagent. Minimal media was used as an alternative to LB media to minimise the expected enzymatic activity from the transformed cells for the rest of the project including IMAC (HisTrap HP column), salting out, HPLC and with urea at pH 8.

Starter cultures of 5 ml of LB media (1 % (w/v) of tryptone, 0.5 % (w/v) yeast extract, 85.5 mM of NaCl in dH_2O, pH 7.5 adjusted with NaOH and sterilised by autoclaving for 15 min at 121 °C) containing 175 µg of kanamycin were inoculated with transformants for each *GRA* gene. The culture was grown in 15 ml loose cap tubes and incubated overnight at 37 °C with shaking at 220 rpm. The starter culture was used to inoculate 250 ml of LB media containing kanamycin (8.75 mg) in a ratio of 1/100 ml.

Minimal media was prepared from the following: M9 salt (42.3 mM disodium phosphate, anhydrous, 22 mM potassium dihydrogen phosphate, 8.5 mM sodium chloride and 18.7 mM ammonium chloride, pH 7.4 adjusted with HCl and autoclaved), 0.4 % (v/v) D-glucose (sterilised by 0.2 µm cellulose acetate filter (Minisart®), 1 mM magnesium sulphate, 10 mM calcium chloride, 166 µM thiamine (sterile filtered) and 100 µl (v/v) PTM-1 salt (consisting of 400 mM boric acid, 30 mM cobalt (II) chloride hexahydrate, 10 mM copper sulphate pentahydrate, 80 mM manganese (II) chloride tetrahydrate, 10 mM zinc sulphate heptahydrate and 5 mM iron (II) suphate heptahydrate (steriled filtered)). The same procedure was used for growing transformants with *GRA* genes in minimal media as performed in LB media.

Transformed competent cells were grown until they reached on optical density (OD) of 0.6-0.7 which took 3 hr in LB medium or 6 hr for minimal medium. The cells were induced to express recombinant proteins using 1 µM of isopropyl β-

D-1-thiogalactopyranoside (IPTG) (Fermentas). After induction, cells were incubated in LB media at 37 °C for 3 hr, or overnight at room temperature in minimal media. After incubation, induced transformants were harvested by centrifugation at 5,000 × *g* for 30 min at 4 °C and supernatant was discarded. Depending on the methods used, the pellet was either used directly or resuspended in 10 ml of lysis buffer (50 mM di-sodium hydrogen phosphate, 150 mM sodium chloride and 20 mM imidazole (Sigma-Aldrich)) for approximately 2 g wet-cell-mass and either used directly or kept at -20 °C for future use.

The expected molecular weight of the recombinant protein (GRA protein plus SUMO-tag (12.41 kDa)) from *T. gondii* TgGRA2 and TgGRA7 are 30.07 kDa and 35.89 kDa respectively. While in *N. caninum*, the expected molecular weight of NcGRA2 and NcGRA7 are 32.55 kDa and 32.37 kDa, respectively (Table 3.2).

Table 3.2: Protein sequences of cloned GRA2 and GRA7 genes from *T. gondii* (Tg) and *N. caninum* (Nc)

Protein name	**Accession number**	**No. of amino acids +/- SP**	**MW of protein kDa +/- SP**	**Protein sequence[1]**
TgGRA2	TGME49_227620	185/164	19.81/17.66	**MFAVKHCLLVVAVGALVNVSV**RAAEFSGVVNQGPVDVPFSGKPLDERAVG GKGEHTPPLPDERQQEPEEPVSQRASRVAEQLFRKFLKFAENVGQHSEKAFKK AKVVAEKGFTAAKTHTVRGFKVAKEAAGRGMVTVGKKLANVESDRSTTTTQ APDSPNGLAETQAPVEPQQRAAHVPVPDFSQ
TgGRA7	TGME49_203310	236/213	25.92/23.48	**MARHAIFFALCVLGLVAAALPQF**ATAATASDDELMSRIRNSDFFDGQAPVDS LRPTNAGVDSKGTDDHLTTSMDKASVESQLPRREPLETEPDEQEEVHFRKRGV RSDAEVTDDNIYEEHTDRKVVPRKSEGKRSFKDLLKKLALPAVGMGASYFAA DRILPELTEQQQTGEEPLTTGQNVSTVLGFAALAAAAAFLGMGLTRTYRHFSP RKNRSRQPALEQEVPESGKDGEDARQ
NcGRA2	NCLIV_045650	211/189	22.42/20.14	**MFTGKRWILVVAVGALVGASVK**AADFSGRGTVNGQPVGSGYSGYPRGDDV RESMAAPEDLPGERQPETPTAEAVKQAAAKAYRLLKQFTAKVGQETENAYYH VKKATMKGFDVAKDQSYKGYLAVRKATAKGLQSAGKSLELKESAPTGTTTA APTEKVPPSGPRSGEVQRTRKEQNDVQQTAEMLAEEILEAGLKKDDGEGRGTP EAEVN
NcGRA7	NCLIV_021640	217/192	22.49/19.96	**MARQATFIVALCVCGLAIAGLPRLA**SAGDLATEQHEGDIGYGVRAYAGVSN YDGDDDAAGNPVDSDVTDDAITDGEWPRVVSGQKPHTTQKGSLIKKLAVPVV GALTSYLVADRVLPELTSAEEEGTESIPGKKRVKTAVGIAALVAAAAFAGLGL ARTFRHFVPKKSKTVASEDSALGNSEEQYVEGTVNGSSDPEQERAGGPLIPEG DEQEVDTE

[1]The underlined and highlight in red amino acid sequences are signal peptides that their DNA coding sequences are not included in the recombinant genes.

3.2.3. Recombinant protein purification

Harvested pellets of induced transformants containing recombinants GRA proteins (from section 3.2.2) were homogenised completely using a clean spatula and vortexing before using in downstream processing for purification of expressed proteins (Figure 3.2).

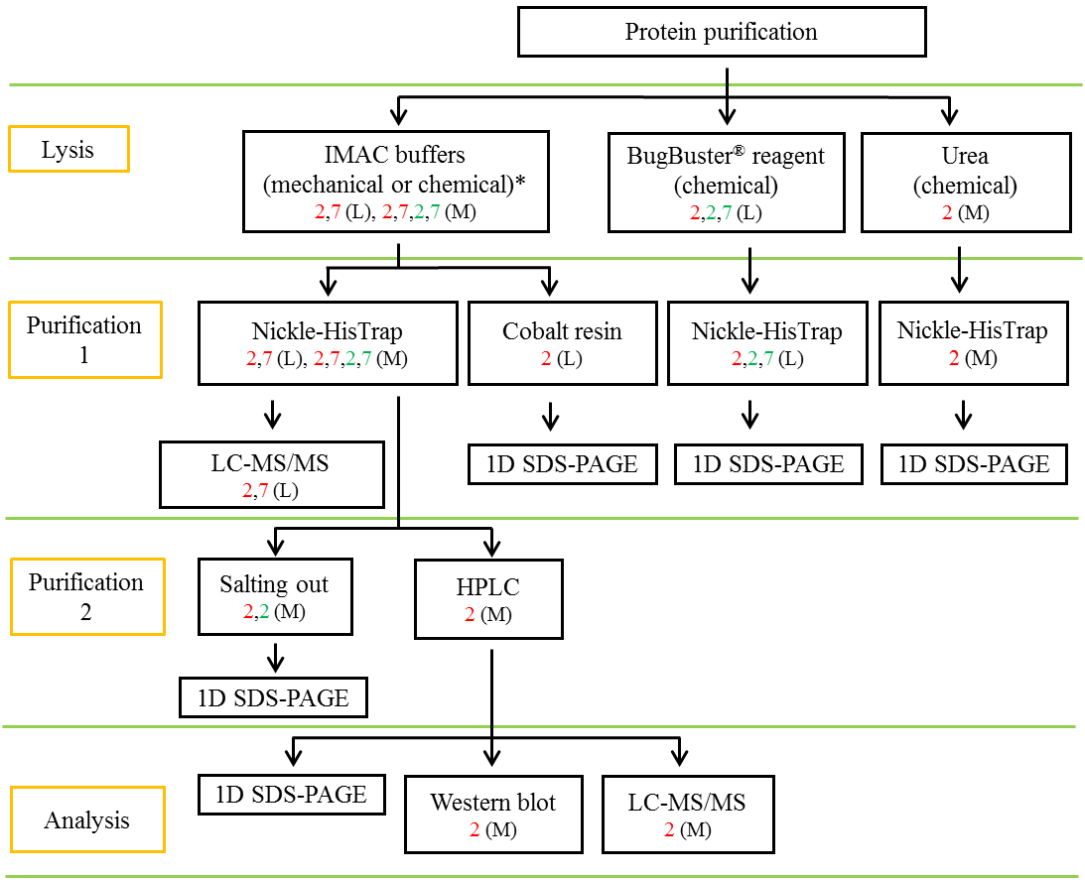

Figure 3.2: Schematic illustration of the optimisation of the recombinant protein purification. The purification procedures were performed in three steps including lysis and two purification steps before data analysis. All steps were performed using TgGRA2. The keys denote the protein/media used at each stage, 2 (TgGRA2), 7 (TgGRA7), 2 (NcGRA2) and 7 (NcGRA7). L: LB media and M: minimal media. *: Mechanical lysis was used with lysis buffer of Nickel-HisTrap HP column.

3.2.3.1. Lysis of recombinant GRA proteins

To optimise conditions for the purification of the recombinant GRA proteins for use as bait in the pull-down experiments, three different lysis methods were used: IMAC, BugBuster and urea (Figure 3.2).

3.2.3.1.1. IMAC lysis for Nickel-Nitrilotriacetic acid HisTrap purification

Cell pellets from induced transformants grown in LB or minimal were homogenised on ice with one tablet of protease inhibitor cocktail, EDTA-free (Thermo Scientific) per 20 ml of lysis buffer (50 mM of di-sodium phosphate, 150 mM of sodium chloride, 10 mM of imidazole, pH 7.5 adjusted by HCl) and lysed on ice using a probe sonicator (SONICS®) for 3 min at 50 % amplitude with 10 sec pulse and off for 30 sec. The lysate was clarified by 20 min centrifugation at 4 °C at 18,000 × *g* and filtered through 0.45 µm syringe filter. The filtrate was kept at 4 °C.

3.2.3.1.2. IMAC lysis for HisPur Cobalt Resin purification

5 ml of IPTG-induced competent BL21 in LB media was transferred to a sterile centrifuge tube, centrifuged at 5,000 × *g* for 5 min and supernatant was discard. The pellet was resuspended in 1 ml of TBS (25 mM Tris-HCl, 150 mM NaCl, pH 7.2) (Thermo Scientific) and transferred to a 1.5 ml microcentrifuge tube and centrifuged at 5,000 × *g* for 5 min and supernatant was discard. The pellet was resuspended in 196 µl of ice-cold TBS per 5 ml of original culture volume. 1 × protease inhibitors cocktail (Sigma) were added per the original culture volume. 200 µl of Pierce Lysis Buffer (Thermo Scientific) (Tris buffered solution of 75 mM NaCl with 1 % of propriety of nonionic detergent) was added per 5 ml of original culture volume. Inverted immediately until thoroughly mixed and incubate on ice for about 30 min with inversion at 10 min interval for 3 ×. After incubation has finished, centrifuged at 12,000 × *g* for 5 min to clarify crude competent BL21 lysate and the supernatant was collected in another microcentrifuge tube and stored on ice at 4 °C.

3.2.3.1.3. BugBuster® lysis for Nickel-Nitrilotriacetic acid HisTrap purification

3.2.3.1.3.1. Preparation of soluble proteins fraction

This fraction consists of soluble protein present in both the periplasm and cytoplasm. Harvested pellets of IPTG-induced competent BL21 in LB media were resuspended in BugBuster lysis buffer at RT. BugBuster lysis buffer consisting of BugBuster reagent, protease inhibitor cocktail EDTA-free (1 tablet per 10 ml) and Benzonase® Nuclease (Novagen®) (25 units Benzonase® Nuclease per 1 ml BugBuster reagent was added and mixed by gentle vortexing) was prepared

immediately before use. 5 ml lysis buffer was used per gram of wet cell pellet (this approximately corresponds to about 2.5 ml per 50 ml culture). The cell suspension was incubated on a shaking platform or rotating mixer at a slow setting for 10–20 min at RT. After incubation, insoluble cell debris removed by centrifugation at 16,000 × *g* for 20 min at 4 °C. The supernatant transferred to a fresh tube and kept at 4 °C and the pellet was processed for inclusion body purification.

3.2.3.1.3.2. Preparation of inclusion body fraction

The pellet from the soluble fraction preparation was resuspended in 2.5 ml of BugBuster reagent containing 1 kU/ml Lysozyme (Novagen®) and incubated at RT for 5 min. 15 ml (6 volumes) of 1:10 diluted BugBuster reagent in ddH_2O were added to the suspension and vortexes gently for 1 min. The suspension was centrifuged at 5,000 × *g* for 15 min at 4 °C. The supernatant was collected and kept on ice at 4 °C.

3.2.3.1.4. Urea lysis for Nickel-Nitrilotriacetic acid HisTrap purification

Protein pellets were lysed under denaturing conditions and resuspended with 10 ml of lysis and equilibration buffer consisting of 100 mM NaH_2PO4, 10 mM Tris/HCl (pH 8.0) and 8 M urea. The suspended cells were stirred slowly for 30 min to lyse completely at RT. The lysate were centrifuged at 16,000 × *g* for 30 min at RT and the supernatant was collected.

3.2.3.2. Purification of recombinant proteins I

3.2.3.2.1. Purification using a Nickel-Nitrilotriacetic acid HisTrap HP column

HisTrap high purification (HP) column (GE Healthcare Life Sciences) 5 ml capacity was used for purification of the recombinant GRA proteins. HisTrap HP columns are prepacked with nickel sepharose high performance for high-resolution purification of histidine-tagged proteins by IMAC. The HisTrap column was washed and equilibrated with 25 ml of washing buffer 1 (50 mM of di-sodium phosphate, 150 mM of sodium chloride, 10 mM of imidazole, pH 7.5 adjusted by HCl). Ice-cold lysate from section 3.2.3.1.1 and 3.2.3.1.3 was loaded onto the Nickel column using syringe and collected in 15 ml tube and named flow-through. The column washed

using 15 ml of washing buffer 1 and the throughput named as wash 1. The column re-washed again with 15 ml washing buffer 2 (50 mM of disodium phosphate, 150 mM of sodium chloride, 40 mM of imidazole, pH 7.5) and named as Wash 2. The protein was eluted from the column using 15 ml of elution buffer (50 mM of di-sodium phosphate, 150 mM of sodium chloride, 500 mM of imidazole, pH 7.5) and saved on ice and named as elution 1. Finally, the column loaded with another 15 ml of elution buffer and saved as before and named elution 2; 10 µl from each fraction was run on an SDS-PAGE as shown in section 3.2.4.1.

For lysate from section 3.2.3.1.4, the histrap HP column was washed and equilibrated with 20 ml of lysis and equilibration buffer (100 mM NaH_2PO4, 10 mM Tris/HCl (pH 8.0) and 8 M urea), 10 ml of the cleared lysate were passed through the column very slowly and the flow through was collected and labelled as flow through. The column then washed with 20 ml of washing buffer (100 mM NaH_2PO4, 10 mM Tris/HCl (pH 6.3) and 8 M urea) and the eluates were collected in 8 fractions of 2.5 ml each. Finally, 20 ml of elution buffer (100 mM NaH_2PO4, 10 mM Tris/HCl (pH 4.5) and 8 M urea) was used to elute the recombinant proteins and the eluates were collected in 4 fractions of 5 ml each; 10 µl from each fraction was run on an SDS-PAGE as shown in section 3.2.4.1.

3.2.3.2.2. Purification using HisPur Cobalt Resin

A wash buffer consisting of 1:1 of TBS to Pierce lysis buffer containing 10 mM imidazole was prepared. The HisPur Cobalt Resin was thoroughly resuspended using a vortex mixer and 50 µl were pipetted into each labelled spin column. The binding capacity of 25 µl of settled HisPur Cobalt Resin (Thermo scientific) is > 250 µg of polyhistidine-tagged protein. 400 µl of the wash solution was added to each spin column and inverted several times to equilibrate the immobilized Cobalt-chelate Resin. Spin column placed in a collection tube and spun at 1,250 × *g* for 30 sec, and the flow-through washing solution was discarded. The latter steps of washing were repeated 5 ×.

Following washing and equilibration, 350 µl of polyhistidine-tagged fusion protein lysate was added to the column and incubated at 4 °C for at least 1 min with gentle rocking motion on a rotating platform. After the incubation, the column placed

into a collection tube and spun at 1,250 × *g* for 1 min and the fraction was labelled as bait flow-through and place on ice at 4 °C. Then the spin column washed with 400 µl of wash solution, inverted several times and spun at 1,250 × *g* for 1 min. The washing step was repeated 5 ×. The fraction was labelled as wash.

The bounded recombinant protein was eluted using elution buffer consisting of washing buffer with 300-500 mM imidazole. 250 µl of the elution buffer was added to the column and incubated for 5 min at RT with gentle rocking on a rotating platform. The column was spun at 1,250 × *g* for 1 min and labelled as Elution 1 and placed on ice. At the end of recombinant protein purification, an SDS-PAGE was performed for each fraction as shown in section 3.2.4.1.

3.2.3.3. Purification of recombinant proteins II

3.2.3.3.1. Purification of recombinant protein by salting out

A second step of purification was applied to eluent prepared by Ni-NTA HisTrap HP column under native condition from section 3.2.3.1.1 using ammonium sulphate salt (VWR) to separate different proteins and reduce complexity based on their solubility. GRA proteins used in this experiment contain multiple hydrophobic membrane domains, so expecting elution of GRA proteins in low concentration of ammonium sulphate salt allowing fractionation and enrichment of GRA protein. Different concentrations of ammonium sulphate were used starting from 10 % to 100 % to purify the recombinant TgGRA2 or NcGRA2 among other proteins that are from competent BL21 expression system. 1 ml was added per each eppendorf tube, 10 eppendorf tubes were label and to each one a concentration was added consisted of 10 %, 20 %, 30 %, 40 %, 50 %, 60 %, 70 %, 80 %, 90 % and 100 % as initial screening to identify the start concentration at which the recombinant protein begins to precipitate. After the ammonium sulphate was added then allowed to mix thoroughly using rotating plate for 1 hr and then centrifuged at 10,000 × *g* for 30 min, the precipitate was collected and 1 ml of TBS buffer pH 7.4 was added to the pellet; then 10 µl from each concentration was loaded on SDS-PAGE. The lowest concentration of ammonium sulphate that caused the recombinant protein to precipitate was then used for further salting out by increasing the concentration by 3

% and again as mentioned earlier centrifuged and resuspended; 10 µl from each concentration was loaded on an SDS-PAGE as shown in section 3.2.4.1.

3.2.3.3.2. High-performance liquid chromatography (HPLC) purification of the recombinant proteins

An HPLC (Varian Prostar 210 Solvent Delivery Module) connected to an analytical column with C18 phase, 5 µm particle sizes, 300 Å pore size, 30 × 4.6 mm (Phenomenex) was used for purification of the eluted recombinant proteins from Ni-NTA HisTrap as second step of purification. Eluted protein samples were desalted prior to loading on the HPLC using PD-10 desalting column (GE Healthcare) according to the manufacturer's instructions. The HPLC column was cleaned each time before use with 30 % acetonitrile in HPLC grade water (VWR), then equilibrated with 95 % of water (solution A) and 5 % of acetonitrile (solution B) for 20 min, sample (2 ml) was loaded onto the column. Proteins were separated using a linear gradient to 75 % solution B for 60 min and finally to 100 % solution B for 20 min. The protein fractions of interest were collected manually at the beginning of the chromatographic peak showed on the screen connected to the HPLC using 1.5 ml eppendorf tube then kept on ice. The recombinant protein was identified using SDS-PAGE, LC MS/MS and western blotting. The protein concentration was determined using Coomassie Plus (Bradford) Assay Kit (Thermo Fisher) and stored at -80 °C after snap freezing with liquid nitrogen.

3.2.4. Analysis of purified recombinant protein and data analysis

3.2.4.1. 1D SDS-PAGE

Proteins fractions from purification steps were run on a 12 % 1D SDS-PAGE for quality control. Gels were run, fixed and stained as described in Chapter 2, sections 2.2.5 and 2.2.6.

3.2.4.2. Western blot analysis for HPLC purified recombinant protein

Purified fractions from HPLC were run on 1D SDS-PAGE in duplicates, one for staining with Coomassie blue and the other to be analysed using western blot. Western blotting was performed to identify the recombinant GRA proteins based on the presence of SUMO-tag; because of anti GRA proteins were not available

commercially. Anti SUMO-tag antibodies (Abcam) were used to identify recombinant proteins via Semi-dry transfer western blot using Semiphor Transphor Unit (Amersham Bioscience). Poly-vinylidine fluoride (PVDF) transfer membrane (EMD Millipore Corporation) were used for immunoblotting the transferred proteins. PVDF were activated using 100 % methanol for 1 min and equilibrated in SDS-PAGE transfer buffer (25 mM Tris/HCl (pH 8.3), 192 mM glycine and 20 % methanol. Four pieces of 0.83 mm thick filter paper (Thermo Scientific) were saturated for 5 min in the transfer buffer. The SDS-PAGE gel was placed on PVDF and sandwiched between the filter papers and placed on the surface of positive electrode. The negative electrode was placed on the top of the sandwiched layers and run according to the manufacturer's instruction for 1 hr at 20 V and 45 mA. After the run has finished, the PVDF membrane was blocked for 1 hr at RT using blocking buffer consisted of 5 % (w/v) of skimmed milk powder (Tesco) in TBST (50 mM Tris-HCl (pH8.3), 150 mM NaCl, 0.5% (v/v) Tween-20 (Sigma). The membrane was washed 5 × for 5 min each with TBST buffer. A specific rabbit polyclonal anti-SUMO3 antibody (Abcam) was used to detect the expressed recombinant proteins. The primary antibody was diluted 1:10,000 in 5 % (w/v) of skimmed milk in TBST. The PVDF membrane was incubated for overnight at 4 °C. The membrane was washed 5 × for 5 min each with TBST buffer. Anti-Rabbit IgG conjugated to horse radish peroxidase (HRP) produced in goat (Sigma-Aldrich, Inc.) was used to detect anti-SUMO3 antibody, diluted 1:10,000 in 5 % (w/v) of skimmed milk in TBST. PVDF membrane was incubated with later dilution for 1 hr at RT. Finally the membrane was washed 5 × 5 min with TBST buffer. The secondary antibody were detected through the activity of horseradish peroxidase (HRP)-conjugated using Clarity™ Western ECL Substrate kit (Bio-Rad Laboratories, Inc.), diluted 1:1 ratio and added to the blot, and incubate for 5 min. The membrane was imaged with a ChemiDoc™ MP Imaging System (Bio-Rad Laboratories, Inc.).

3.2.4.3. In-gel trypsin digestion, LC-MS/MS and data analysis

In-gel trypsin digestion, LC-MS/MS (using the Bruker Amazon ion trap mass spectrometer) and data analysis were performed for purified recombinant proteins from section 3.2.3.1.1 (TgGRA2 and TgGRA7) and 3.2.3.3.2 (TgGRA2) according to protocols described in Chapter 2, sections 2.2.7 and 2.2.8. In addition to the *Toxoplasma* database and Uniprot *E.coli* (UniP_EcoliK12_Feb 2015) databases were also used in the Mascot search. DNA coding sequence of SUMO tag was added to the database using SUMO fusion protein sequence used in the pE-SUMOpro Kan. Proteins with more than two unique peptides matched the criteria applied by Mascot (individual ion score of peptides > 32 indicate identity or extensive homology ($p < 0.05$)) and protein score of ≥ 50 were considered as significant identification.

3.2.5. Pull-down assay using purified recombinant TgGRA2

Pull-down assay was carried out using HisPur Cobalt Resin kit (used also for purification of recombinant GRA protein) for recombinant TgGRA2 protein purified by HPLC. Vero host lysate was used as prey protein(s) to identify host binding partner(s) of the TgGRA2 protein.

3.2.5.1. Immobilisation of purified TgGRA2

A total of 100 µg of TgGRA2 that was previously purified by reverse phase HPLC was added to the column for use as a bait protein. A 10 µg aliquot of the recombinant protein was run on an SDS-PAGE as control. The remaining steps of bait immobilisation were carried out as for purification of recombinant bait protein in section 3.2.3.2.2.

3.2.5.2. Preparation of prey proteins from Vero cell lysate

Vero cells were grown as described in Chapter 2, section 2.2.1.1. A total of 2×10^7 Vero cells were transfer to a sterile 1.5 ml tube and homogenised with 1,200 µl of washing buffer 1 without imidazole (section 3.2.3.2.2) containing protease inhibitor cocktail EDTA-free (Sigma) (the protease inhibitor cocktail consists of 4.16 mM of 4-(2-Aminoethyl) benzenesulfonyl fluoride hydrochloride (AEBSF), 3.2 µM of aprotinin, 200 µM of bestatin, 56 µM of E-64, 8 µM of leupeptin and 6 µM of pepstatin A). The homogenised suspension was pipetted up and down and incubated

on ice at 4 °C for 40 min. After incubation, the suspension spun at 12,000 × *g* at 4 °C for 10 min. The supernatant was collected and imidazole was added to a final concentration of 10 mM and thoroughly mixed by inverting the tube and kept at 4 °C on ice.

3.2.5.3. Prey protein capture from host cell lysate

A total of 700 µl (200 µg proteins) of the cell lysate was added to the column from section 3.2.5.1 containing immobilised recombinant TgGRA2 and incubated at 4 °C with rocking motion on a rotating platform for 1.30 hr. The sample was centrifuge at 1,250 × *g* for 1 min and the flow through labelled as prey flow-through and place on ice. 400 µl of wash solution added and inverted several times to mix thoroughly and centrifuge at 1,250 × *g* for 1 min. The washing step was repeated five times.

3.2.5.4. Bait-prey elution

The elution of TgGRA2-prey complex was performed following the elution stage of the protocol described in section 3.2.3.2.2 for purification of recombinant protein. The bound recombinant protein was eluted using elution buffer consisting of washing buffer 1 (section 3.2.3.2.2) with 300-500 mM imidazole. A total of 250 µl of the elution buffer was added to the column and incubated for 5 min at RT with gentle rocking on a rotating platform. The column was spun at 1,250 × *g* for 1 min and eluent was placed on ice. The elution fraction was concentrated (10 ×) beside the non-concentrated elution due to low protein binding in the elution fraction. StrataClean resin (Agilent Technologies) was used for concentration of the eluent and 2 µl was added to 100 µl of the protein solution in 1 ml tube and diluted by 500 µl of dH_2O, vortexed for 1 min and centrifuged for 2 min at 5,000 rpm. The supernatant was discarded and 10 µl of SDS-PAGE sample buffer was added and heated at 95 °C for 5 min then loaded on SDS-PAGE as described in 3.2.4.1.

3.3. RESULTS

3.3.1. PCR screening of colonies from transformed BL21 (DE3) competent cells containing recombinant *GRA2* and *GRA7* from *T. gondii* and *N. caninum*

PCRs were performed individually for cloned *GRA2* and *GRA7* of *T. gondii* and *N. caninum* from transformed competent BL21 to identify correctly cloned genes. A 1.5 % agarose gel was performed to identify the amplified PCR product from the transformants colonies (Figure 3.3). The expected size for the recombinant *TgGRA2* is 1041 bp and *TgGRA7* is 1188 bp. On the other hand, the expected size of recombinant genes for *NcGRA2* and *NcGRA7* are 1116 bp and 1125 bp, respectively. The results of the PCR showed that both the *GRA2* and *GRA7* from *T. gondii* and *N. caninum* are at the expected sizes.

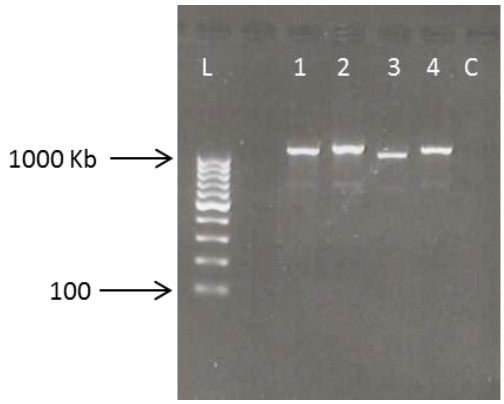

Figure 3.3: PCR products of the *T. gondii* and *N. caninum* colonies run on 1.5 % agarose gel. 1: *TgGRA2* and 2: *TgGRA7*. 3: *NcGRA2* and 4: *NcGRA7*. L: 100 bp DNA ladder and C: negative control.

3.3.2. Expression of the recombinant GRA proteins from *T. gondii* and *N. caninum*

Transformed competent BL21with *TgGRA2*, *TgGRA7*, *NcGRA2* and *NcGRA7* before and after induction by IPTG for 3 hr in LB media (Figure 3.4A) and for overnight in minimal media (Figure 3.4B and C) were analysed using SDS-PAGE (Figure 3.4). Figure 3.4B and C shows that the induced competent BL21 lysate

contains additional protein bands indicating that the cloned recombinant *TgGRA2* and *TgGRA7*, *NcGRA2* and *NcGRA7* genes were expressed.

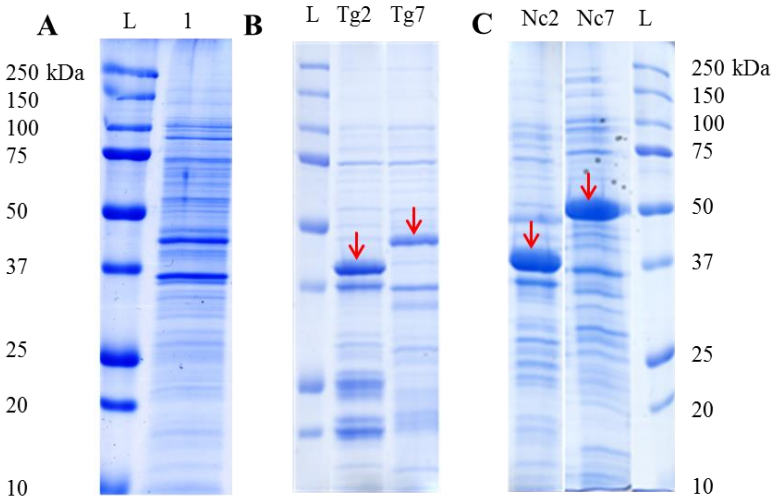

Figure 3.4: Expression and purification of recombinant proteins of *T. gondii* and *N. caninum*. A1: BL21 cell lysate before induction, B: TgGRA2 and TgGRA7 elution fraction after expression and C: NcGRA2 and NcGRA7 elution fraction after expression. Tg2 (TgGRA2), Tg7 (TgGRA7), Nc2 (NcGRA2) and Nc7 (NcGRA7). L: protein standard labelled with protein molecular weight. Red arrows in B and C indicate location of expressed TgGRA2, TgGRA7, NcGRA2 and NcGRA7, respectively. The gels were stained using colloidal Coomassie stain. BL21 cell was grown and induced in LB media (A) and minimal media (B and C). Ni-NTA HisTrap HP column was used for purification of the recombinant protein.

3.3.3. Purification of recombinant proteins

Several different approaches were taken to obtain the cleanest/purest recombinant GRA proteins from *T. gondii* and *N. caninum*. Recombinant GRA2 and GRA7 proteins from both parasites were expressed but TgGRA2 was used most frequently as candidate through all the procedures used for protein purification in this project from transformants grown in either LB or minimal media as explained in section 3.2.2 and Figure 3.2.

3.3.3.1. Purification of recombinant proteins using immobilized metal ion affinity chromatography

Figure 3.5 shows 1D SDS-PAGE of eluted recombinant protein fractions from TgGRA2 and TgGRA7 purified by Ni-NTA HisTrap HP. Several bands of

proteins migrated along the eluted protein fraction indicating that proteins of different molecular sizes were co-eluted. The bands indicated in Figure 3.5 were analysed by MS and the results confirmed to be TgGRA2 and TgGRA7 (Table 3.3). The expected molecular weights of the recombinant proteins (GRA protein with SUMO-tag) were 30.7 kDa and 35.89 kDa for TgGRA2 and TgGRA7, respectively.

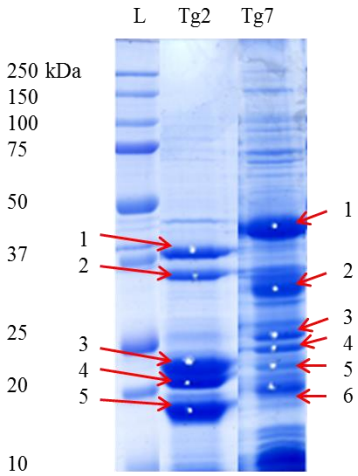

Figure 3.5: Purification of recombinant proteins of *T. gondii*. Tg2: TgGRA2 elution, TG7: TgGRA7 and L: protein standard labelled with protein molecular weight. Proteins were expressed in BL21 cells in LB media and gels stained with colloidal Coomassie blue. Protein spots Tg2.1-5 and Tg7.1-6 were excised from TgGRA2 and TgGRA7, respectively. Each spot was tryptically digested and analysed by LC-MS/MS.

Mass spectrometry analysis of recombinant TgGRA2 and TgGRA7 (Table 3.3) showed that the bands analysed from the SDS-PAGE (Figure 3.5) contained peptides from TgGRA2 or TgGRA7 as well as peptides from a variety of *E. coli* proteins and SUMO-tag. The expressed TgGRA2 and TgGRA7 were identified in numerous bands as shown in Table 3.3. Migration of recombinant proteins to different molecular size on the 1D SDS-PAGE may indicate that these proteins were broken down at some point after expression. Protein degradation may occur either following expression by enzymatic activity of the transformed BL21 or during preparation and purification of the recombinant proteins.

Table 3.3: Mass spectrometry analysis of recombinant GRA2 and GRA7 from *T. gondii*. Mass spectrometry and data analysis using Mascot of different fraction of IMAC purification of poly-histidine SUMO-tagged protein of *T. gondii* GRA2 and GRA7 from in-gel digestion of protein bands by trypsin from Figure 3.5

Gel spot no.	Protein accession	Protein description	Protein score	No. of peptide sequence	Protein mass (kDa)	Protein coverage %
Tg2.1	SUMOTag	SUMO tag	216	2	12402	16
	P0ACJ8|CRP_ECOLI*	cAMP-activated global transcriptional regulator CRP	188	3	23907	16
	TGME49_227620	Dense granule protein GRA2 (GRA2)	142	4	19960	19
Tg2.2	P02931|OMPF_ECOLI	Outer membrane protein F	525	9	39420	26
	P0ACJ8|CRP_ECOLI*	cAMP-activated global transcriptional regulator CRP	329	6	23907	29
	SUMOTag	SUMO tag	80	2	12402	30
	TGME49_227620	Dense granule protein GRA2 (GRA2)	66	2	19960	8
Tg2.3	SUMOTag	SUMO tag	168	2	12402	16
	P0A7V8|RS4_ECOLI*	30S ribosomal protein S4	143	4	23623	20
	P60438|RL3_ECOLI*	50S ribosomal protein L3	139	3	22341	18
	P02931|OMPF_ECOLI	Outer membrane protein F	121	3	39420	9
Tg2.4	P0ACJ8|CRP_ECOLI*	cAMP-activated global transcriptional regulator CRP	331	7	23907	35
	SUMOTag	SUMO tag	234	2	12402	30
	P0A7V3|RS3_ECOLI*	30S ribosomal protein S3	143	3	26078	17
	TGME49_227620	Dense granule protein GRA2 (GRA2)	76	3	19960	25
	P0A7V8|RS4_ECOLI*	30S ribosomal protein S4	68	3	23623	12
Tg2.5	P0ACJ8|CRP_ECOLI*	cAMP-activated global transcriptional regulator CRP	407	6	23907	32
	SUMOTag	SUMO tag	205		12402	37
Tg7.1	TGME49_203310	Dense granule protein GRA7 (GRA7)	540	5	26071	23
	P0A853|TNAA_ECOLI *	Tryptophanase	406	10	53250	22
	SUMOTag	SUMO tag	315	2	12402	30
	P0AG30|RHO_ECOLI*	Transcription termination factor Rho	249	5	47143	12
	P02943|LAMB_ECOLI	Maltoporin	135	3	50106	8
	P0A7V3|RS3_ECOLI	30S ribosomal	104	2	26078	8

		protein S3				
Tg7.2	P61889|MDH_ECOLI*	Malate dehydrogenase	295	5	32599	22
	P0CE47|EFTU1_ECOLI*	Tryptophanase	226	5	53250	13
	P0AFH8|OSMY_ECOLI	Osmotically-inducible protein Y	119	3	21172	26
	TGME49_203310	Dense granule protein GRA7 (GRA7)	182	2	26071	8
	P0ABK5|CYSK_ECOLI*	Cysteine synthase A	116	2	34636	7
	P0A6F5|CH60_ECOLI*	60 kDa chaperonin	115	4	57575	11
	P0A7K2|RL7_ECOLI	50S ribosomal protein L7/L12	104	2	12399	27
	P0A850|TIG_ECOLI	Trigger factor	59	2	48274	7
	P0A6F9|CH10_ECOLI	10 kDa chaperonin	54	2	10492	28
Tg7.3	P0A7V3|RS3_ECOLI*	30S ribosomal protein S3	919	7	26078	35
	P0A9K9|SLYD_ECOLI*	FKBP-type peptidyl-prolyl cis-trans isomerase SlyD	239	3	21293	17
	P62707|GPMA_ECOLI*	2,3-bisphosphoglycerate-dependent phosphoglycerate mutase	131	3	28650	15
	P69441|KAD_ECOLI*	Adenylate kinase	125	4	23739	21
	P0A853|TNAA_ECOLI*	Tryptophanase	119	5	53250	14
	P0A8P6|XERC_ECOLI*	Tyrosine recombinase XerC	114	3	34015	11
	P32664|NUDC_ECOLI*	NADH pyrophosphatase	113	2	30123	7
	P0A7V0|RS2_ECOLI*	30S ribosomal protein	113	3	26895	14
	TGME49_203310	Dense granule protein GRA7 (GRA7)	74	2	26071	8
	P0ACK8|FUCR_ECOLI*	L-fucose operon activator	74	2	27684	9
	P0A7L0|RL1_ECOLI	50S ribosomal protein L1	69	2	24825	12
	P0AGJ2|TRMH_ECOLI*	tRNA (guanosine(18)-2'-O)-methyltransferase	69	2	25609	12
Tg7.4	P0A7V8|RS4_ECOLI*	30S ribosomal protein S4	364	9	23623	45
	P60438|RL3_ECOLI*	50S ribosomal protein L3	360	5	22341	25
	P0A7V3|RS3_ECOLI*	30S ribosomal protein S3	231	4	26078	20
	P0A9K9|SLYD_ECOLI*	FKBP-type peptidyl-prolyl cis-trans isomerase SlyD	127	3	21293	17
	P0AFZ3|SSPB_ECOLI*	Stringent starvation protein B	115	3	18362	19
	P0AFM6|PSPA_ECOLI	Phage shock protein	98	3	25588	15

	*	A				
	TGME49_203310	Dense granule protein GRA7 (GRA7)	96	2	26071	8
	P0ACA3|SSPA_ECOLI *	Stringent starvation protein A	90	2	24457	12
	P0A908|MIPA_ECOLI *	MltA-interacting protein	85	2	27924	10
	SUMOTag	SUMO tag	84	3	12402	37
	P0A917|OMPX_ECOLI	Outer membrane protein X	75	2	18759	15
Tg7.5	P0ACJ8|CRP_ECOLI*	cAMP-activated global transcriptional regulator CRP	1724	13	23907	50
	P60723|RL4_ECOLI*	50S ribosomal protein L4	180	3	22184	18
	P0A7V3|RS3_ECOLI*	30S ribosomal protein S3	120	2	26078	8
	P0A9K9|SLYD_ECOLI *	FKBP-type peptidyl-prolyl cis-trans isomerase SlyD	120	2	21293	12
	TGME49_203310	Dense granule protein GRA7 (GRA7)	114	2	26071	10
	P64588|YQJI_ECOLI*	Transcriptional regulator YqjI	98	2	23954	10
	P0A6N4|EFP_ECOLI	Elongation factor P	67	2	20746	10
	P0ADK0|YIAF_ECOLI *	Uncharacterized protein YiaF	61	2	25872	10
Tg7.6	P0A7V3|RS3_ECOLI*	30S ribosomal protein S3	207	4	26078	22
	P0A9K9|SLYD_ECOLI *	FKBP-type peptidyl-prolyl cis-trans isomerase SlyD	167	3	21293	17
	SUMOTag	SUMO tag	127	3	12402	37
	P0AG55|RL6_ECOLI*	50S ribosomal protein L6	103	2	19060	12
	P0CE47|EFTU1_ECOLI*	Elongation factor Tu 1	101	3	43538	9
	P0A853|TNAA_ECOLI *	Tryptophanase	90	3	53250	11

*Indicates that these proteins contain at least three histidine or cysteine or both in their amino acid sequences

As an alternative and more robust way of purifying recombinant protein, cobalt is recommended for more specific interaction with histidine tagged recombinant protein, so HisPur™ cobalt resin was used for recombinant TgGRA2 (Cobalt resin showed slightly better purification compared to Nickel based IMAC based on 1D SDS-PAGE (Figure 3.6A). However, the recombinant TgGRA2 was not pure due to degradation and/or co–elution of several proteins of the BL21 cells during purification as confirmed by LC-MS/MS (Table 3.3).

In order to understand whether time of induction play roles in decreasing the production of degraded recombinant protein and/or co-eluent and obtaining the pure recombinant protein, the induction time was reduced from 3 hr to 90 min. The *TgGRA2* gene was expressed and results show that fewer proteins were eluted and to some extent better purification was achieved (Figure 3.6B). However at this point the eluent containing recombinant TgGRA2 cannot be used in pull-down assay because of other degraded/co-eluent proteins present and thus further purification is required to get pure recombinant protein.

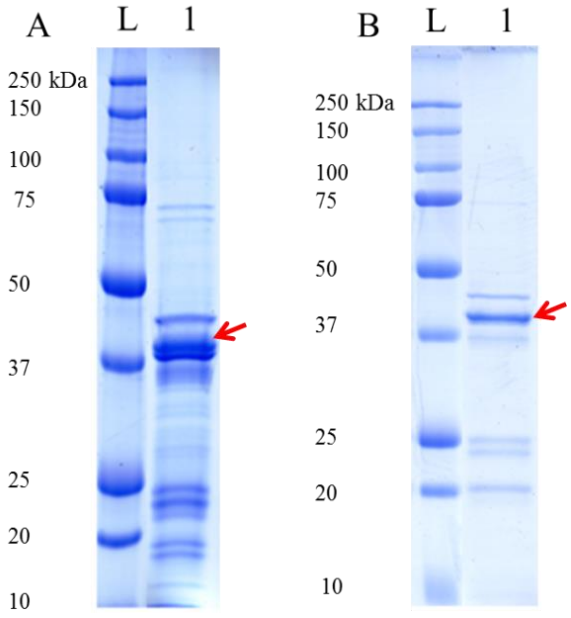

Figure 3.6: Purification of the recombinant protein of *T. gondii* GRA2 using HisPur cobalt resin kit. Recombinant *TgGRA2* induced for 3 hours (A1) or 90 min (B1), L: protein standard. 10 µl of the elution was used and stained with colloidal Coomassie stain. Arrows show the expressed recombinant TgGRA2 protein. LB media used to grow the competent BL21.

Despite the fact that a complete protease inhibitor was added before lysis, proteolytic break down of the recombinant protein cannot be excluded as TgGRA7 and the SUMO-tag were found on multiple bands on SDS-PAGE gel. LB media was used for growing the transformed cells; enriched growth media may enhance more enzymatic activity and therefore protein cleavage. In order to optimise the purification method used, especially to decrease the possibility of enzymatic lysis and break down of recombinant protein during expression, minimal media (Figure 3.2) was used as described in section 3.2.2 and the 1D SDS-PAGE from recombinant GRA2 and GRA7 of *T. gondii* and *N. caninum* are shown in Figure 3.4B and C. However based on 1D SDS-PAGE (Figure 3.6B and C), there is little or no improvement concerning the number of protein bands that eluted from purification steps as seen with LB media (Figure 3.5). Results indicate that breaking down and/or co-elution of protein with the recombinant protein may be not related to the type of the media used.

It was also noticed from the migration of the major protein bands on 1D SDS-PAGE (Figure 3.4B, C and Figure 3.5), *T. gondii* and *N. caninum* recombinant GRA2 and GRA7 proteins with Sumo-tag migrated to higher molecular mass in SDS-PAGE than predicted from the primary translation product of GRA proteins containing Sumo-tag (Table 3.2). Based on the protein standard, recombinant TgGRA2, TgGRA7, NcGRA2 and NcGRA7 were migrated to 40 and 47, 40 and 50 kDa, respectively. However, the expected molecular weight of the recombinant protein with SUMO-tag (12.41 kDa) from *T. gondii* TgGRA2 and TgGRA7 are 30.7 kDa and 35.89 kDa respectively. While in *N. caninum*, the expected molecular weight of NcGRA2 and NcGRA7 with Sumo-tag are 32.55 kDa and 32.37 kDa, respectively.

3.3.3.2. Protein purification using BugBuster reagents

BugBuster protein extraction reagents were used to purify and separate the soluble proteins from the inclusion bodies as an approach to separate soluble from non-soluble (membrane-bound) proteins after expression. This method allows using only fraction that contains mainly the expressed recombinant protein before further purification and elution using Ni-NTA-HisTrap HP (Figure 3.7). Recombinant

TgGRA2, NcGRA2 and NcGRA7 were expresses in LB media and the results show that still there are more proteins bands co-eluted with the recombinant proteins and great difference was not observed compared to purification with Nickel-Histrap HP only (Figure 3.4B and C and Figure 3.5) without recombinant protein separation by BugBuster reagents.

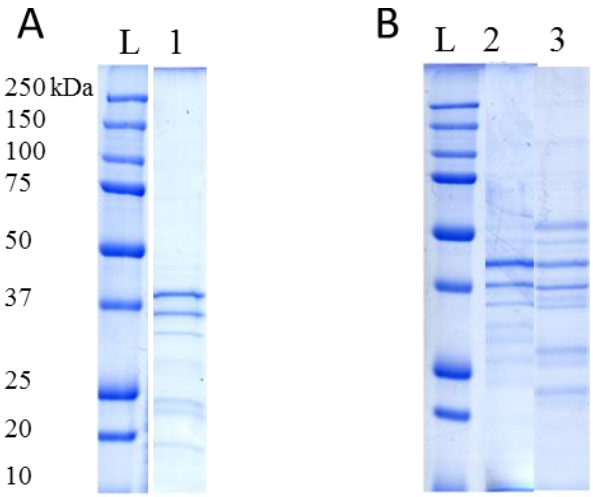

Figure 3.7: Purification of recombinant GRA proteins of *T. gondii* and *N. caninum* using BugBuster protein extraction reagents and Ni-NTA HisTrap HP column. A1: elution of inclusion body fraction of recombinant TgGRA2, B2 and B3: elution of inclusion body fraction of recombinant NcGRA2 and NcGRA7, respectively. L: Protein standard. 10 µl of elution fraction were used. BL21 cells were grown and induced in LB media.

3.3.3.3. Recombinant protein purification under denaturing conditions

Purification of the recombinant TgGRA2 was performed under denaturing conditions using 8 M urea. To stop expected catalytic activity of all the enzymes that might cause degradation of the expressed recombinant proteins. Also urea helps unfolding and separation of interacting proteins from each other including recombinant GRA proteins.

Urea was used as a lysis buffer directly after harvesting cells and the same buffer was applied through the whole processes of the purification with changes in pH during different steps to purify and elute the recombinant proteins (Figure 3.8). Results of 1D SDS-PAGE from different fractions of the purification under

denaturing approach reveal that many proteins co-eluted under denaturing condition as well.

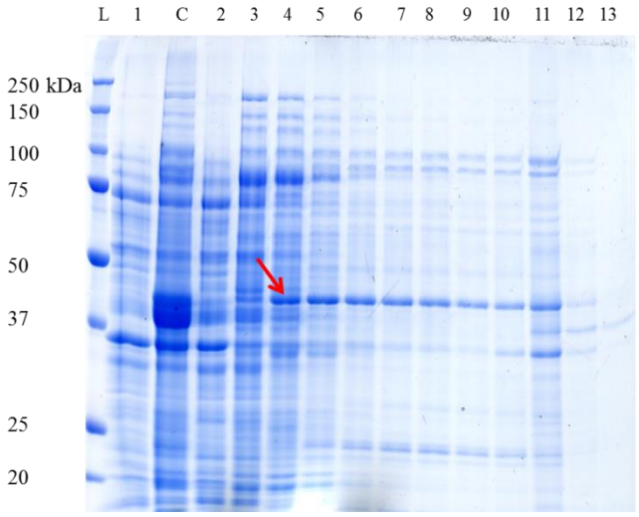

Figure 3.8: Purification of recombinant *T. gondii* GRA2 under denaturing conditions. 10 ml of 8 M Urea buffer was used as lysis buffer and equilibration buffer at pH 8 and passed through the histrap HP column. 1: the flow through was collected in about 1 drop/sec using syringe. 20 ml of the same buffer was used with pH 6.3 as washing buffer and each 2.5 ml collected continuously (2-9). 20 ml of the same buffer used with pH 4.5 as elution buffer and collected as 5 ml per each fraction (10-13). 10 µl was used to run on 1D SDS-PAGE and stained with colloidal coomassie stain. L: protein standard and C: the lysate of induced transformants. BL21 cells were grown and induced in LB media.

3.3.3.4. Purification of recombinant GRA proteins using salting out

Recombinant proteins from bacterial expression systems bind to IMAC and elute under native and denaturing conditions. However several protein bands were co-eluted with the eluent containing the recombinant GRA proteins. An additional step is needed to separate the recombinant GRA proteins from others co-eluted proteins. The solubility of the expressed recombinant GRA proteins (hydrophobic) was exploited to purify it. Ammonium sulphate salt was used to separate different protein based on their solubility in different salt concentrations. After the recombinant proteins had been eluted from IMAC (Ni-NTA HisTrap HP column) they were subjected to the second step of purification (Figure 3.2) using different salt concentration of 10 -100 % (w/v) ammonium sulphate. Based on the hydrophobicity of the protein, soluble protein requires higher concentration of ammonium sulphate

to precipitate than hydrophobic protein. Figures 3.9A and 3.10A show 1D SDS-PAGE of TgGRA2 and NcGRA2 that started to precipitate at 25 % and 20 % of ammonium sulphate, respectively. Further precipitation with more ammonium sulphate was applied to 25 % (Figure 3.9A) and increased to 30 % and 33 % (Figure 3.9B), and also more ammonium sulphate was added to 20 % (Figure 3.10A) and increased to 25 % and 35 % (Figure 3.10B). Results showed better resolution and purification, however, still there are other proteins that co-purified with the recombinant proteins (Figures 3.9B and 3.10B).

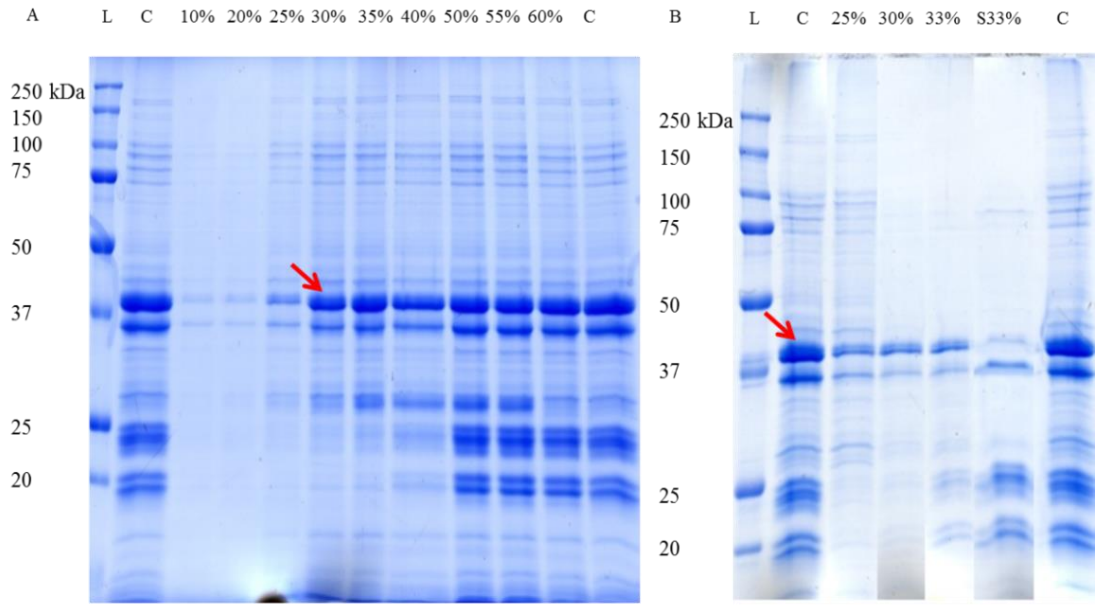

Figure 3.9: Precipitation of recombinant *T. gondii* GRA2 using a successive concentration of solid ammonium sulphate after native purification using imidazole. %: (w/v) concentration of solid ammonium sulphate. B: further fractionation to the 25 % fraction was applied using more solid ammonium sulphate to 30 % and to 33 %. S33 %: supernatant of 33 % fraction. L: protein standard and C: the eluted sample by Ni-NTA HisTrap HP used in the experiment. BL21 cells were grown and induced in LB media.

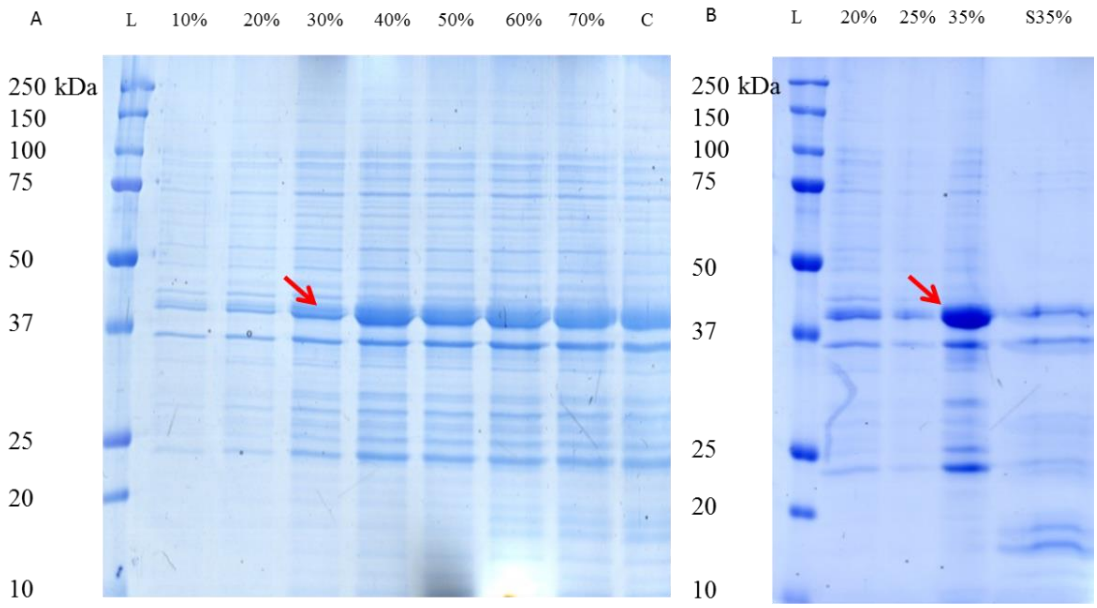

Figure 3.10: Fractionation of recombinant *N. caninum* GRA2 using a successive concentration of solid ammonium sulphate after native purification using imidazole. %: (w/v) concentration of solid ammonium sulphate. B: further fractionation of 20% was applied using more solid ammonium sulphate to 25 % and to 35 %. S35%: supernatant of 35%. L: protein standard with molecular mass. C: the eluted sample by Ni-NTA HisTrap HP used in the experiment. BL21 cells were grown and induced in LB media.

3.3.3.5. Purification of recombinant protein using reverse phase HPLC

Pull down assays require pure protein to be used as bait to understand the physical interaction and function of that particular protein with the prey protein(s). HPLC was used as a second step for purification (Figure 3.2) of recombinant TgGRA2 after elution under native condition using Ni-NTA HisTrap HP column. Figure 3.11a shows a complete graph of an HPLC run during purification of recombinant TgGRA2. One peak was separated (as indicated by the red arrow) and analysed using 1D SDS-PAGE (Figure 3.11b, lane 2) and MS/MS (Table 3.4) and confirmed to be TgGRA2. The Mascot search matched to both SUMO-tag and TgGRA2 with total coverage of 50 % and 47.8 %, respectively. Results indicate that the purified fraction contains recombinant protein that can be used as pure bait to study its interacting partners from both *T. gondii* and host cells.

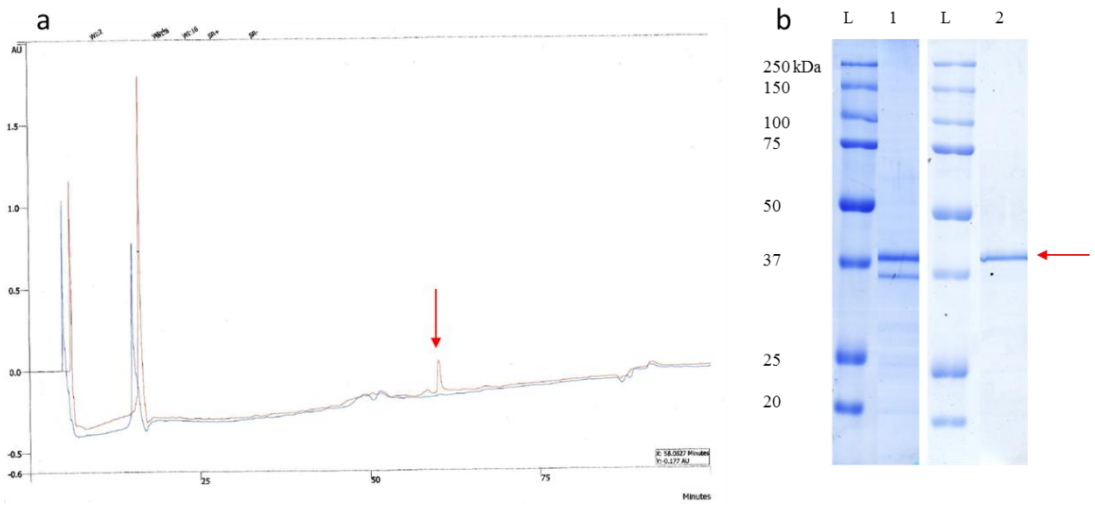

Figure 3.11: Purification of recombinant TgGRA2. a: Graphical representation of the reverse phase HPLC fractionations of the recombinant *T. gondii* GRA2 protein. Eluted fraction of transformants containing recombinant *TgGRA2* gene without induction prepared by Ni-NTA HisTrap HP (Blue graph line) and with induction using IPTG (red graph line). The eluted fractions were desalted using PD-10 and run on HPLC. The arrow shows the peak of recombinantTgGRA2 protein fraction. b: 1D SDS-PAGE of reverse phase HPLC fraction. 1: Elution of recombinant protein *T. gondii* GRA2 under native condition before run on HPLC and 2: after HPLC fractionation using the main peak showed on the graph of the HPLC run fractions (100 µl (10 µg) of the peak fraction was concentrated using 2 µl strata clean beads). BL21 cell was grown and induced in LB media.

Table 3.4: Mass spectrometry analysis of the in-solution digestion of the HPLC fraction of recombinant TgGRA2 protein.

Protein accession	Protein description	Protein score	Protein mass (kDa)	Protein coverage (%)
SUMO Tag	SUMO tag	1007	12402	50
TGME49_227620	Dense granule protein GRA2 (GRA2)	970	19960	47.8

3.3.3.6. Western blot analysis of the HPLC purified recombinant TgGRA2

HPLC purified recombinant TgGRA2 were analysed using western blot to identify the recombinant TgGRA2 protein containing SUMO-tagged-TgGRA2. Results showed that the band purified by the HPLC interacted with the anti-SUMO antibody as shown in Figure 3.12.

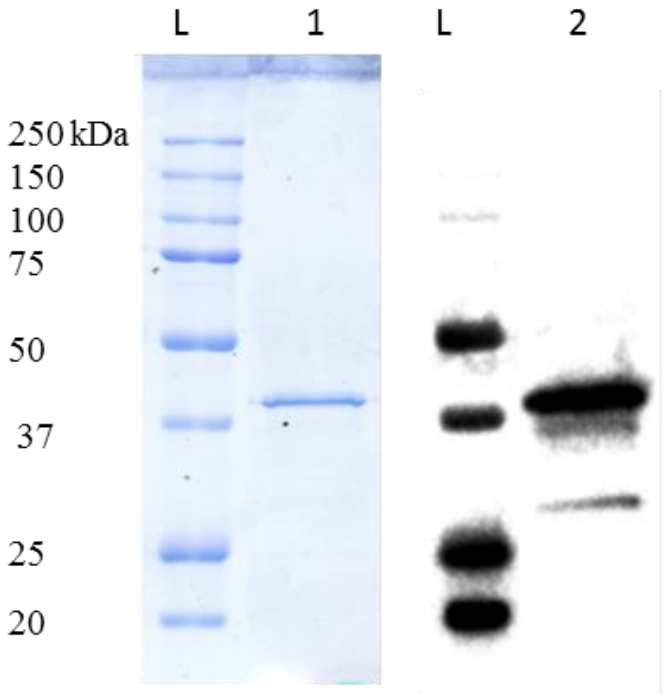

Figure 3.12: Identification of the expressed purified recombinant *T. gondii* GRA2 by western blot. 1: HPLC purified recombinant *T. gondii* GRA2 stained with colloidal Coomassie stain and 2: *T. gondii* GRA2 developed by western blot using anti-SUMO antibody. L: protein standard with molecular weight. BL21 cells were grown and induced in minimal media.

3.3.4. Pull-down assay from Vero cell lysate using HPLC purified recombinant TgGRA2

A pilot pull-down assay was performed to test the ability of the purified HPLC fraction containing recombinant TgGRA2 protein to bind to prey protein from host (Vero) cell lysate. Controls from both HPLC purified recombinant protein TgGRA2 protein and from Vero cells were run beside the experiment using Cobal Resin Kit. Figure 3.13 is 1D SDS-PAGE of Vero cell lysate pulled-down by recombinant TgGRA2 protein, shows that the recombinat TgGRA2 protein is not detected in the elution fraction (Figure 3.13, lane 7 and lane 8). This result was not expected due to the fact that protease inhibitor was added, however SUMO-tag may be cleaved-off from the recombinant TgGRA2 by SUMO enzymes that normally present in euharyotic cell. The experiment could not be repeated because of a lack of recombinant TgGRA2 protein purified by HPLC.

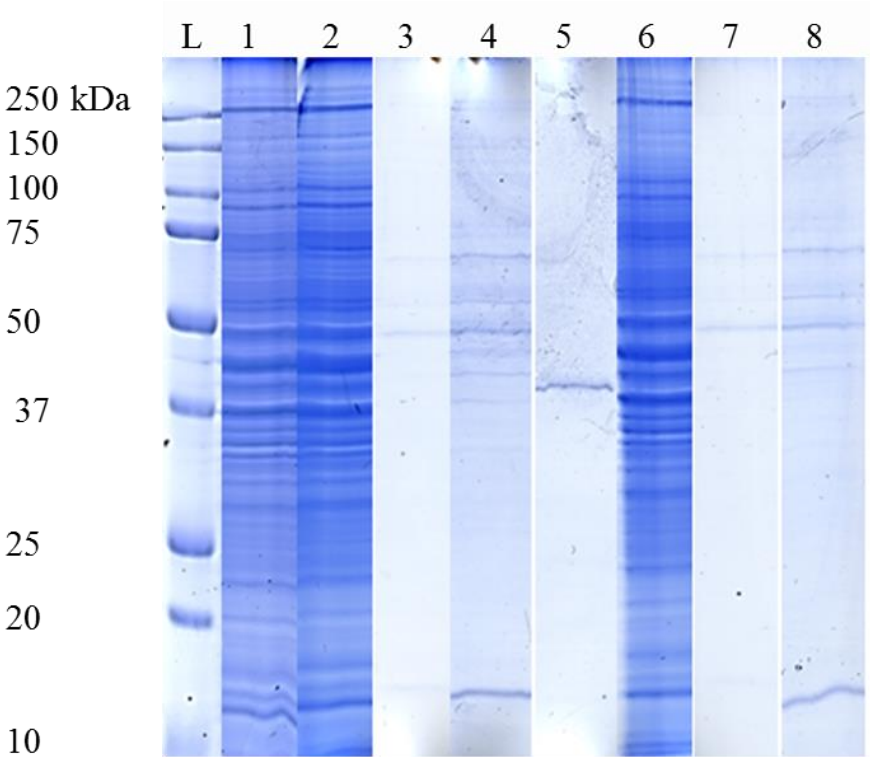

Figure 3.13: Pull-down using recombinant TgGRA2 protein purified by HPLC using cobalt resin kit. 1: Vero lysate (200 µg), 2: Flowthrough, 3:elution of Vero bound protein to IMAC (control), 4:elution from 3 concentrated 10 × by 2 µl of strat clean beads, 5: purified recombinant HPLC fraction of TgGRA2 (10 µl), 6: flowthrough after incubation of recombiant TgGRA2 with Vero lysate, 7: elution of interacting recombant TgGRA2 with binding partners from Vero lysate, 8: elution from 7 concentrated 10 × by 2 µl of strat clean beads.

3.4. DISCUSSION

The present study aimed to dissect the comparative host-parasite interaction using recombinant GRA2 and GRA7 proteins from *T. gondii* ME49 and *N. caninum* Liverpool strain. The expressed proteins are fused to SUMO-tag which enhance gene expression and high protein yield, increases solubility especially membrane bound protein and proper folding of insoluble protein (Butt *et al.*, 2005; Marblestone *et al.*, 2006; Zuo *et al.*, 2005). Due to the location and significance of these proteins in the maturation of PV and PVM, their interactions with the host molecules were investigated to identify differences in host-parasite interactions between *T. gondii* and *N. caninum*.

3.4.1. Recombinant GRA protein purification

Pull-down experiments require using pure recombinant bait proteins to pull-down prey partners. Pure recombinant bait is critical to investigate for high quality interaction and reduces the possibility of nonspecific interaction and false positive results. Thus polyhistidine attached to the SUMO-tag was exploited to purify these proteins using IMAC column (Ni-NTA HisTrap HP and Cobalt HisPur Resin kit). The recombinant GRA proteins were co-eluted with other protein from the endogenous protein of the competent BL21 expression system as shown by MS analysis (Table 3.3). Thus the recombinant GRA proteins require further purification before performing pull-down assay. In addition, the recombinant GRA proteins migrated to different molecular sizes on the SDS-PAGE; which could be due to enzymatic degradation by the expression system and/or (2) degraded during preparation and purification.

The result of this study is comparable to the recent study performed on recombinant *T. gondii* GRA2 and GRA6 (Bittame *et al.*, 2015), they found expression of these membrane related protein very difficult and attempted several vectors before they could get relatively pure recombinant proteins. They used pUET1 expression vector to express the recombinant proteins, which expressed bound to N-terminal S tag of pancreatic ribonuclease and 6 × histidine tag was attached to both terminals. However, they used similar purification method (IMAC) to that used in the present study to purify the recombinant proteins; based on the SDS-PAGE

presented in their study, the recombinant bait proteins were not purified as single band but rather other protein bands with the recombinant protein were migrated to different molecular size, suggested to be due to protein degradation.

In the present study, two problems were required to be solved to purify the bait protein. The first was co-elution of proteins from the bacterial system and the second was migration of the bait protein to different molecular mass location on 1D SDS-PAGE. So to tackle these problems, five different methods were carried out to get pure recombinant GRA proteins.

Firstly, a cobalt Resin kit was used as an alternative to Ni-NTA HisTrap HP column. Cobalt Resin is more specific for binding proteins containing polyhistidine, resulting in high pure recombinant protein elution (Yang *et al.*, 1997). However in the present study, Cobalt IMAC (Figure 3.6) resulted in a nearly similar purification profile to that of the Ni-NTA HisTrap HP purification based on the 1D SDS-PAGE comparison (Figure 3.4B and Figure 3.5). Co-purification of these proteins with recombinant proteins could be due to several reasons; (1) presence of similar sequences within the protein of the bacterial system with rich regions of histidine/cysteine that have high affinity to IMAC (Westra *et al.*, 2001) and/or (2) they interact with sepharose beads on which these IMAC metals (nickel and cobalt) were supported. Based on MS analysis of the sequences of the co-eluted proteins, there is no rich region of histidine/cysteine but rather most of them contain multiple (more than three) histidine and/or cysteines distributed within the protein sequences. Also (3) co-elution of these proteins could be due to non-specific interaction with the recombinant protein either with the SUMO-tag or with the GRA proteins.

Secondly, minimal media was used for growing transformants as an alternative to LB media to decrease the possibility of breaking down of recombinant protein by the enzymatic activity of the expression system. LB media is an enriched media that allows transformants to grow faster than minimal media (Marley *et al.*, 2001), thus it will result in production of basic molecules necessary for maintaining growth. Expression of recombinant GRA proteins in minimal media (Figure 3.4B and) did not result in better purification of recombinant protein than in LB media (Figure 3.5). The reason could be due to (1) the enzymatic activity of the expression

system responsible for lytic activity against the recombinant protein is activated in both media or (2) it might happen during lysis of transformants, preparation and purification of recombinant proteins.

Thirdly, the preparation and purification of recombinant TgGRA2 and NcGRA2 were performed under denaturing condition using 8 M urea. This was to investigate whether migration and degradation of the proteins were related to the lytic activity of the expression system and/or preparation of the recombinant GRA proteins. High concentrations of urea unfold proteins and inactivate enzymes (Bennion and Daggett, 2003; Kumar *et al.*, 2006) which consequently reduces the possibility of enzymatic degradation of the expression system and protein-protein interaction. However the results (Figure 3.8) showed that these proteins are co-eluted with recombinant TgGRA2 and NcGRA2 under denaturing condition as well. The present results suggest that the multiple amino acids such as histidine and/or cysteine within protein sequences of the bacterial system could interact non-specifically with the sepharose bead and allows them to co-elute with recombinant GRA proteins.

Fourthly, as an attempt to separate these co-eluted proteins from recombinant GRA proteins: a second step of purification was applied to the elution fraction of Ni-NTA HisTrap exploiting the solubility of these proteins. Ammonium sulphate salt is used to reduce complexity of a mixture of protein prior to further purification using affinity chromatography (Jain *et al.*, 2004; Kusnadi *et al.*, 1998; Schagen *et al.*, 2000). In the present study, precipitation by ammonium sulphate salt was used to separate the co-eluted (recombinant GRAs from co-eluted *E. coli* protein) proteins from each other. Different concentrations of ammonium sulphate from 10-100 % were used and the results showed that the co-eluent was co-precipitated through most of the concentration applied (Figure 3.9, 3.10). The results indicate that the co-eluted protein may have very close solubility rate in ammonium sulphate to that of the recombinant GRA proteins. As *E. coli* proteins were co-purified with the expressed recombinant protein, the recombinant protein could not be used directly in the experiment without further purification.

Fifthly, in the present study, a second purification step was performed for fraction containing TgGRA2 eluted from Ni-NTA HisTrap HP using reverse phase

(RP) HPLC. This allows separation of the proteins based on their hydrophobicity; the more the hydrophobic protein is the higher the concentration of organic solvent is required to remove it from the solid support. Thus co-eluted protein and the recombinant GRA protein are separated based on their hydrophobicity within organic solvent. The recombinant TgGRA2 was tried and successfully purified. Purified recombinant protein was analysed and identified using different methods (Figure 3.2) such as SDS-PAGE (Figure 3.11b), western blotting (Figure 3.12) and LC MS/MS (Table 3.4). However, technical problem with the HPLC machine hampered the processes of further protein purification.

Another plan which was not attempted due to time constraints was to exploit the SUMO tag as an affinity tag and purifying the bait by co-immunoprecipitation (Co-IP) method. Co-IP is a technique used to identify PPIs through directing a specific antibody against a target protein to indirectly capture the binding partner of the target protein. In this case anti-SUMO antibody is either directly incubated with the lysate of expression system contains unpurified expressed bait or following a purification steps using IMAC. The antibody-bait complex is then purified using protein A or protein G immobilised to solid support. The complex is incubated with host cells lysate containing prey(s). The bait-complex partners can be purified by either protein A or protein G or using IMAC. The antibody-bait complex also can be used directly in far-western blotting. One advantage of this technique is the binding of anti-SUMO with SUMO tag could help protect the SUMO tag from proteolytic degradation by the SUMO enzyme. Another benefit of using anti-SUMO antibody is specifically bind to the SUMO tag that is only present in recombinant bait and in case of any contamination second step purification can be applied exploiting presence of polyhistidine by using IMAC.

3.4.2. Pull-down assay for host cell lysate using *T. gondii* GRA2

Recombinant TgGRA2 purified by reverse phase HPLC was used as bait to pull down prey protein from host cell lysate (Vero cell). However, results showed that the bait protein was not eluted from the elution fraction that should be present alone or with binding partner(s). There are two possibilities for the absence of recombinant TgGRA2: firstly, the bound SUMO-tag to the IMAC was removed by

SUMO-cleaving enzymes that are normally present in host cell of all eukaryotes (Hay, 2007; Johnson, 2004) and washed off from the IMAC during wash steps. Secondly it may interact with other proteins from the cell lysate and led to loss its configuration and binding activity with the IMAC column and swept away by the wash solutions. The pull-down was tried once because of the amount of recombinant protein acquired was very small and that the accessibility of HPLC was not possible. However, these explanations are not explicit unless at least triplicates of the pull-down assay are performed.

3.4.3. *T. gondii* and *N. caninum* GRA2 and GRA7 showed higher molecular weight in 1D SDS-PAGE

In the present study, GRA2 and GRA7 displayed a higher molecular mass in SDS-PAGE analysis (Figure 3.4B and C and Figure 3.5) than predicted from primary translation product produced in native state within the parasites. According to the primary structure of the recombinant TgGRA2, molecular weight should be around 30 kDa (TgGRA2 is 17.66 kDa plus 12.41 SUMO-tag); expressed recombinant TgGRA2 and purified HPLC fraction showed a protein band migrated to about 40 kDa based on 1D SDS-PAGE. In addition, TgGRA7 was found migrated to about 47 kDa. The reason for the higher molecular weight of the recombinant TgGRA2 and TgGRA7 proteins of the present study is not known. It could be due to the structure of these proteins that contain transmembrane domain (GRA7) and multiple amphipathic α-helices (GRA2) from both parasites. These could increase SDS binding amount and slow down its migration in SDS-PAGE (Rath *et al.*, 2009). Also mass shift might be resulted from the addition of SUMO-tag bound to the GRA proteins.

Previous studies showed that the native mature TgGRA2 polypeptide was modified post-translationally through glycosylation (Achbarou *et al.*, 1991; Charif *et al.*, 1990; Darcy *et al.*, 1988; Zinecker *et al.*, 1998). Glycosylation might be due to presence of many serine and threonine residues in the sequence of the GRA2 which provide sites for *O*-glycosylation (Mercier *et al.*, 1993; Zinecker *et al.*, 1998). While in native TgGRA7 the higher molecular mass in SDS-PAGE analysis may be caused by glycosylation of the asparagine residue at amino acid position 213 which may represents a potential *N*-glycosylation site (Fischer *et al.*, 1998). Here we cannot

expect the role of glycosylation as a main cause of mass shift of recombinant GRA proteins; this is due to the fact that there is no evidence of glycosylation of recombinant protein to occur in *E. coli* (Demain and Vaishnav, 2009).

Host-parsite interaction during infection with these parasites could result in different host response to different effector produced from invasion organelles and surface antigenes during infection by *T. gondii* and *N. caninum*. Different responses of host cells to infection can be exploited to study the comparative host-parasites interaction particularly PTMs of protein. PTMs such as protein phosphorylation and analysis of pathways of host cells that respond differntly to infection with these parasites could help understanding the differences in host-parasite interaction.

CHAPTER FOUR: Exploring the comparative phosphoproteome of the host cell response to infection with *T. gondii* and *N. caninum*

4.1. INTRODUCTION

Several biological differences have been found between *T. gondii* and *N. caninum* including host range, zoonotic capacity, transmission, virulence and definitive host (Davison *et al.*, 1999b; Dubey, 2004; Dubey *et al.*, 2007; Lei *et al.*, 2014; McAllister *et al.*, 1998; McCann *et al.*, 2008; Tenter *et al.*, 2000; Williams *et al.*, 2009). Despite these differences the genome and transcriptome of these parasites are remarkably conserved (Reid *et al.*, 2012). Many efforts have been made to study the expression level of transcriptome and proteome of these parasites and host in response to infection (Blader *et al.*, 2001; Nelson *et al.*, 2008; Reid *et al.*, 2012; Xia *et al.*, 2008). A microarray study showed that many host cell genes were modulated in response to infection with *T. gondii*; genes modulated in early infection (1-2 hr p.i.) were found encode proteins involved in immune response to pathogens, while later in infection (> 6-24 hr p.i.) modulated genes were found encode proteins associate with glucose and mevalonate metabolism (Blader *et al.*, 2001). Quantitative gel-based proteomics using two dimensional electrophoresis (2D SDS-PAGE) and difference gel electrophoresis (DIGE) on host cell in response to infection at different time point (6-24 hr p.i.), found that protein expressions and its modification increased with time (with maximum changes at 24 hr p.i.), in response to infection with *T. gondii* (Nelson *et al.*, 2008). Comparative transcriptional analysis of non-infected mice forebrain and *T. gondii* infected samples (acute at 10 days p.i. and chronic stage at 28 days p.i.) revealed high expression of genes associated with innate immune response in infected mice, whereas more than two fold increases in innate immunity-related transcripts was observed in chronic infection than acute stage (Pittman *et al.*, 2014). Nelson *et al.* (2008) suggested that most of the changes in response to infection cannot be revealed by transcriptional studies, but considered protein studies are more robust in interpretation of host response to infection as proteins are 'the true effectors'. The effect of protein can be measured by both the absolute quantities and their functional forms. The functional form of proteins are often due to PTMs that are not analysed directly using transcriptional studies (Nelson *et al.*, 2008). Expression status of genes may not be enough to understand how they fit in different pathways or events involved because of inability to tell actual information about functional status of PTMs of proteins.

4.1.1. Role of post-translational modification of proteins

Analysis of PTMs of protein is one way to understand the functional status of proteins in response to infection and the cellular function they involved. Hundreds of modifications types of proteins have been reported (Garavelli, 2004). Protein phosphorylation is one of the most common types of PTMs which is implicated in signal transduction and is crucial for regulation of almost all cellular processes (Villen and Gygi, 2008). In apicomplexan parasites, protein phosphorylation plays an important role in the regulatory mechanisms within and outside the parasites after invasion of the host cells (Treeck *et al.*, 2011). Thus, the differences between *T. gondii* and *N. caninum* could be beyond the level of protein expression. Using 2D SDS-PAGE, Xia *et al.* (2008) showed that in *T. gondii* tachyzoites, the same protein identification possesses different isoforms and different form of PTMs. Furthermore, DIGE analysis of host cell protein in response to infection with *T. gondii* demonstrated that many of protein changes were resulted from PTMs and protein phosphorylation was found as one of the most important modifications (Nelson *et al.*, 2008). In addition, protein phosphorylation is considered more critical than just transcript and protein expressions for understanding the broader theme of the signalling processes happening ubiquitously in cells at a given time (Gomase and Akella, 2009; Villen and Gygi, 2008). However, PTMs and particularly protein phosphorylation has not been extensively studied in the differences between *T. gondii* and *N. caninum* infected host cells. Dissecting the protein phosphorylations of host cells in response to infection with these parasites could be critical for understanding the comparative host-parasite interactions.

4.1.2. Regulation of host protein through phosphorylation during infection with pathogens

In other pathogens, protein phosphorylation of infected host cells was also found playing important roles in host-pathogen interactions. Immunoblot analysis of *Helicobacter pylori* showed that binding to AGS cells induced tyrosine phosphorylation of two host cell proteins of 145 and 105 kDa and suggested that adhesion consequently leading to signal transduction within the affected cells (Segal *et al.*, 1996). Enteropathogenic *Escherichia coli* (EPEC) induces tyrosine phosphorylation of host cell proteins Hsp90 to initiate cytoskeletal rearrangement

and bacterial internalisation (Rosenshine *et al.*, 1992). Many pathogens were also found using beneficial strategy through interfering with the phosphorylation of the intracellular-signalling pathways of host cell (Bhavsar *et al.,* 2007). *Yersinia* spp. produce kinase-like protein such as YpkA, autophosphorylates and activates in host cells resulting in modulation of host actin cytoskeleton (Prehna *et al.,* 2006). In viral infection, viral effectors subvert the activation of protein kinases of the cell such as PKR, autophosphorylation of PKR is necessary for defences against viral infection and apoptosis (Hasnain *et al.*, 2003).

4.1.3. Phosphorylation of host protein during infection with *T. gondii* and *N. caninum*

Apicomplexan parasites possess rhoptry proteins such as ROP5, 11 and 16 and 18 that are structurally homologue to protein kinases of the mammalian cells (Bradley *et al.*, 2005; El Hajj *et al.*, 2006). Several of these proteins were found as active protein kinases contain kinase-like catalytic domain while others lack the known catalytic trial and are expected to be pseudokinases (El Hajj *et al.*, 2006; Lei *et al.*, 2014). In *T. gondii*, TgROP18 protein was found re-localised at the PVM following invasion and involved in phosphorylation of parasite substrate especially a 70-kDa protein of tachyzoites (El Hajj *et al.*, 2007). Several kinases-like proteins from *T. gondii* such as TgROP16 and TgROP18 were found involved in phosphorylation of host cell proteins directly following invasion and infection within the host environment (Lei *et al.*, 2014; Ong *et al.*, 2010).

Phosphorylation of host cell proteins by *T. gondii* is found related to adaptation and protection from the immune system within the host environment. Regulation of host cell protein phosphorylations by protein kinases from these parasites have been found implicated in virulence of the parasites. In *T. gondii* infection, interferon-induced host cell immunity-related GTPases (IRGs) is loaded onto the formed PVM within the first hour of infection (Khaminets *et al.*, 2010). There are strong evidences of differential host cell protein phosphorylation between *T. gondii* and *N. caninum* infections. For example, IRGs were found phosphorylated by TgROP18 in virulent strain and subsequent protection of PVM from destruction in IFNγ-induced cells, whereas *N. caninum* was found failed to phosphorylate IRGs

due to pseudogenisation of *Neospora* gene *ROP18* (Lei *et al.*, 2014; Reid *et al.*, 2012).

In *T. gondii*, other ROP proteins such as TgROP16 has also been found involved in virulence through direct and strain-specific phosphorylation of the host cell signal transducer and activator of transcription (STAT3/6) signalling pathway (Butcher *et al.*, 2011; Ong *et al.*, 2010; Saeij *et al.*, 2007; Yamamoto *et al.*, 2009). It was found that STAT3 and 6 in HFF cells infected with type I or type III strains at 18 hr p.i. were higher activated than the ones infected with type II strains (Saeij *et al.*, 2007). In IFNγ-induced murine macrophages infected with different strain of *T. gondii*, it was found that ROP16 in type I or type III resulted in high phosphorylation and activation of STAT3; but infection with type II resulted in activation of STAT3 for short time followed by induction of high secretion of IL-12p40, which was thought to be related to different disease outcomes (Saeij *et al.*, 2007). In *T. gondii* infection with type I or type III, direct phosphorylation and sustained activation of STAT6/3 result in modification of early inflammatory response of the host cells mediated by cytokine, IL-12 (Ong *et al.*, 2010; Saeij *et al.*, 2007; Yamamoto *et al.*, 2009).

To understand the critical role of protein phosphorylation in the biological differences between *T. gondii* and *N. caninum* infections, large scale phosphoproteome analyses of the host cell during infection would be very important. Large scale phosphoproteome can be studied using MS/MS to analyse the entire set of the proteomics at any given time with high level of accuracy, specificity and sensitivity (Collins *et al.*, 2007; Gruhler *et al.*, 2005). MS-based investigation of global phosphoproteome of *Plasmodium falciparum* and *T. gondii* led to the identification of 5,000 and 10,000 of new phosphorylation sites, respectively (Treeck *et al.*, 2011). Investigation of protein phosphorylation in host cell in response to infection with these related parasites could play an important role in directing and expanding our understanding toward identifying the factors responsible for the biological differences between *T. gondii* and *N. caninum*.

4.1.4. Aims and objectives of the study:

Despite the significance of host cell phosphorylation events found during infection with both parasites, there is an apparent lack of systematic studies about proteome-wide phosphorylation events of host cell proteins in response to infection. This study aimed to analyse the comparative protein phosphorylation of host cells in response to infection with these parasites at 20 hr p.i using MS-based phosphoproteome approaches.

4.2. MATERIALS AND METHODS

4.2.1. Host cells and parasites maintenance

Human foreskin fibroblasts (HFF) cells were used as host cells for cultivating, maintaining and harvesting both *T. gondii* VEG strain and *N. caninum* Liverpool strain. The HFF cells were maintained and passaged similarly to that of Vero cells as mentioned in section 2.2.1.1 and 2.2.1.2, except that 2×10^5 or 6×10^5 cells were seeded per 25 cm^3 flask (T25) and 75 cm^3 flasks (T75), respectively.

Tachyzoites were maintained as described in section 2.2.1.3 and were harvested as described in section 2.2.1.4.

4.2.2. Time point study

Concurrently, both *T. gondii* and *N. caninum* were grown for 20 hr p.i. in a ratio of 20:1 parasites to initial number of HFF cells seeded. The time point of 20 hr p.i. was chosen because the multiplications of most of the *T. gondii* and *N. caninum* tachyzoites were found at 2^{nd} and 3^{rd} stage of endodyogeny and before egress. A total of 2×10^7 parasites were used to infect the host cells that were maintained for three days following seeding with 1×10^6 cells/T75 flask. At 20 hr p.i., growth medium was discarded and cells were washed with PBS prewarmed to 37 °C. Infected cells were detached using 3 mL of 1 × trypsin free EDTA (SAFC biosciences™) prewarmed to 37 °C and incubated for 2-3 min at 37 °C in 5 % CO_2. Five mL of PBS were added to the detached HFF cells and collected in a 50 ml conical falcon centrifuge tube containing 5 ml of growth media prewarmed to RT. Cell suspension was centrifuged at 1,000 × *g* for 5 min at 4 °C, supernatant was discarded and the pellet was resuspended in 10 ml cold PBS and re-centrifuged at 4 °C. The last step was repeated and the pellet was collected in 1 ml cold PBS in an Eppendorf tube followed by a final centrifuge at 12,000 × *g* for 3 min at 4 °C. The pellets were collected and kept at -80 °C for future use. Uninfected HFF cell samples were collected along with each infected HFF cell sample.

Toxoplasma gondii and *N. caninum* were harvested as described in section 2.2.1.3; the harvested tachyzoites were spiked into the non-infected HFF cells as

control in a ratio of 6:1 parasites per cells for the initial number of parasites used for infection of HFF cell. A total of 1.2×10^8 purified parasites were spiked into non-infected pellet of HFF cells per T75 flask to be used as mock infection samples. Mock infection was used to minimise bias that arise due to the amount of protein used from infected cell and non-infected cell for enrichment with TiO_2.

4.2.3. Protein preparation from harvested samples

Harvested pellets from both infected samples and mocks from 1-2 T75 tissue culture flasks were prepared for phosphoprotein analysis. Each pellet was resuspended in 250 µl of a master mix lysis buffer, which comprised 22.5 mM ammonium bicarbonate, 200 µg of RapiGest™ SF surfactant (Waters), 1 × phosphatase inhibitor cocktail 2 (Sigma), protease inhibitor cocktail-EDTA free (Sigma) (containing 4.16 mM of AEBSF, 3.2 µM of aprotinin, 200 µM of bestatin, 56 µM of E-64, 8 µM of leupeptin and 6 µM of pepstatin A), 100 µM of benzimidine, 200 µM of phenylmethanesulfonyl fluoride, 400 µM of β-glycerophosphate, 400 µM of sodium fluoride and 12 µM of sodium orthovanadate. Pellets were resuspended in master mix lysis buffer and incubated on ice for 30 min. Samples were further lysed and homogenised using probe sonicator (Sonics®) on ice for 5 times for 30 sec pulse (74 Hz) and 1 min off at 40 % amplitudes output. Cell lysates were spun down at 16,000 × *g* for 1 hr at 4 °C and the supernatant was collected and protein concentration was measured using Bradford assay (Thermo scientific).

4.2.4. Protein assay

Protein concentration was estimated by carrying out a Bradford assay from both infected HFF cells and the mock as described in section 2.2.3. An equivalent of 100 µg were taken for global quantification on mass spectrometer separately alongside with 1 mg for enrichment of phosphopeptides using TiO_2 SpinTips (Protea®).

4.2.5. Analysis of sample lysates on an Orbitrap Velos mass spectrometer

4.2.5.1. In-solution digestion and analysis

The required protein amount comprised an equivalent of 100 µg was taken for global quantification separately alongside with 1 mg for phosphopeptides enrichment. Each sample for global quantification was diluted in 25 mM ammonium bicarbonate to a volume of 170 µl before heated at 80 °C for 10 min with a brief vortex at 5 min. Samples were then reduced with 3 mM dithiothreitol and the sample incubated for 10 min at 60 °C. Samples were cooled down to room temperature before alkylation with 9 mM iodoacetamide and incubated for 30 min in the dark at RT. Proteins were then digested with proteomic grade porcine trypsin (Sigma-Aldrich®) at a ratio of 1 µg: 50 µg of trypsin to lysate proteins and incubated overnight at 37 °C. Digestion was stopped by acidification with a final concentration of 0.5 % trifluoroacetic acid and incubated for 45 min at 37 °C. The solution was centrifuged at 13,000 × *g* for 15 min at room temperature. The supernatant was collected where the digest for global quantification was kept at -20 °C for subsequent mass spectrometric analysis and the digestion for phosphopeptides enrichment was further processed using TiO_2 SpinTips kit.

4.2.5.2. Enrichment of phosphopeptides from the digestion

Enrichment of phosphopeptides was performed using TiO_2 SpinTips kit as per the manufacturer's instruction (Protea®). Briefly, SpinTip was washed twice to wet the packing material by adding 100 µl each time of reconstitution and wash solution and then centrifuged at 4,000 × *g* for 5 min. The digestion was reconstituted with equal amount of reconstitution and wash solution. Total volume of 400 µl was divided into two 200 µl aliquots which were loaded to the SpinTip and centrifuged at 4,000 × *g* for 3 min. The flow through was reloaded once to enhance binding then discarded. Retained peptides on the SpinTip were washed four times (twice with 100 µl of the reconstitution and wash solution, and twice with 100 µl of the wash 2 solution) and each time spun at 4,000 × *g* for 3 min. The bounded phosphopeptides were eluted with 200 µl of elution solution, centrifuged at 4,000 × *g* for 3 min. The elution process was repeated once more and the elution solution was combined together before drying off by Concentrator plus (Eppendorf) for 6 hr at room

temperature. Dried off peptides were resuspended in 20 µl recombination buffer containing 3 % acetonitrile and 0.5 % TFA followed by bath sonication for 10 min at 4 °C.

4.2.5.3. Tandem mass spectrometry analysis (Velos –orbitrap)

Mass spectrometry analysis was performed by Dr Stuart Armstrong (Department of Infection Biology, Institute of Infection and Global Health, University of Liverpool) as follows: peptide mixtures from both samples (mock infection and at 20 hr p.i. time point) were analysed by on-line nanoflow liquid chromatography using the nanoACQUITY-nLC system (Waters MS technologies, Manchester, UK) coupled to an LTQ-Orbitrap Velos mass spectrometer equipped with the manufacturer's nanospray ion source. The analytical column (nanoACQUITY UPLCTM BEH130 C18 15 cm × 75 µm, 1.7 µm capillary column) was maintained at 35 °C and a flow-rate of 300 nl/min. The gradient consisted of 3-40 % acetonitrile in 0.1 % formic acid for 90 min then a ramp of 40-85% acetonitrile in 0.1% formic acid for 5 min. Full scan MS spectra (m/z range 300-2000) were acquired by the Orbitrap at a resolution of 30,000. Analysis was performed in data dependant mode. The top 20 most intense ions from MS1 scan (full MS) were selected for tandem MS by collision induced dissociation (CID) and all product spectra were acquired in the LTQ ion trap.

4.2.5.4. Protein identification using multiple search engines

Raw data from mass spectrometric analysis were submitted to PEAKS® Studio (version 7.0, BSI, Waterloo, ON, Canada). The following settings were used for the searches: data refinement was performed with no merged scans, with precursor charge correction and no filtering. InChorus searching was performed including search engines comprised of Peaks, Mascot (Matrix Science), OMSSA (Geer *et al.*, 2004) and X!Tandem (Craig and Beavis, 2004) with a mass tolerance of 10 ppm for the precursor and 0.8 ppm for the fragment ion. Trypsin was used as enzyme specificity; carbamidomethyl cysteine was set as fixed modification, and oxidation of methionine (M), phosphorylation of serine, threonine and tyrosine (STY) were set as variable modifications. Peptides with a maximum of 3 variable modifications and one missed cleavage were allowed. The peptides were searched

for protein identification against locally-installed databases including the annotated protein sequences for *N. caninum* (ToxoDB-9.0_NcaninumLIV_AnnotatedProteins. fasta) and for *T. gondii* (ToxoDB-10.0_TgondiiME49_AnnotatedProteins.fasta) [downloaded from ToxoDB (Gajria *et al.*, 2008)]. UniProt-human reference proteome databases release 2014_02 was used for identification of human proteins (http://www.uniprot.org/). A false discovery rate (FDR) of ≤ 1 % was used as a cut-off for the peptide identifications. Total number of matched phosphopeptides between infection with *T. gondii* and *N. caninum* were presented using a Venn diagram (http://bioinforx.com/).

4.2.6. Pathway analysis

The identified phosphoproteins from HFF cells infected with *T. gondii, N. caninum* or mock infection were submitted to online functional annotation tool DAVID Bioinformatics Resources version 6.7 (Huang *et al.*, 2008). The entries of protein accession number from proteins of interest were submitted as gene lists. In DAVID tool, the KEGG Pathway was chosen for pathway analysis. P-value cut-off ≤ 0.05 was applied to pathways to be considered statistically significant enriched in the annotation categories. The phosphoproteins enriched in each pathway for one parasite were also mapped manually for the other parasite when the same pathway was not statistically enriched, to compare the discrepancies of phosphoprotein coverage.

4.2.7. Phosphopeptide motif analysis

Phosphopeptide motifs were analysed using web-based motif-x programme (Chou and Schwartz, 2011) using default settings. Briefly, the phosphopeptides were queried against background data in international protein index (IPI) human proteome. Each time one AA (S or T or Y) used to identify the motif with +7 and -7 up and down of the selected AA (total of 15 AA). The occurrence of the motif was set to at least 5 × with significant threshold of 0.000001 which correspond to actual alpha-value of approximately 0.0003 by Bonferroni method.

4.2.8. Phosphoprotein quantification

For quantitation of global protein and enriched phosphopeptides, Progenesis LC-MS software from Nonlinear Dynamics (Newcastle upon Tyne, U.K.) was used to carry out label-free quantification. Peptides and proteins quantification using Progenesis LC-MS consisted of several consequent steps. First of all, raw data from Orbitrap Velos mass spectrometer were imported. Once all the data have been imported, the most appropriate reference LC-MS was run to align all the other runs, which were performed by automatic reference run alignment. After the aligned runs have been reviewed, they were filtered in the filtering stage based on charge state and number of isotopes. Monoisotopic spectra with +2 to +7 charges were maintained for analysis while the remaining features that were not matching the filter were removed completely from the analysis. The next stage was study design for analysed runs which reflected biological groupings of the replicates in the original study followed by peptides quantified from both groups. Quantified features were identified at peptides and proteins level by exporting it into PEAKS® software. The analysed data were exported into pep.xml which was later imported into Progenesis LC-MS to match the identified peptides and proteins to the quantified spectra. The quantified spectra were standardised using built in normalisation tool in Progenesis LC-MS. For comparison between host cell infections with *T. gondii* and *N. caninum*, label-free quantification was carried out based on cut-off filters including a p value < 0.05 for significant phosphopeptides quantification and a fold change of > 1.5 to determine the differentially expressed phosphopeptides.

4.2.9. Subcellular localisation and Types of identified and quantified phosphoproteins

Subcellular location and types (based on molecular function) of quantified phosphoproteins were determined using ingenuity pathway analysis (IPA) software (Ingenuity® Systems, Redwood City, CA). In addition, an upstream regulator analysis for pathway or kinases involved in phosphorylation of the quantified phosphopeptides was performed using IPA.

4.3. RESULTS

4.3.1. Comparative analysis of doubling process at 20 hr p.i.

Figure 4.1 shows the growth comparison of tachyzoites based on the doubling processes of *T. gondii* and *N. caninum* in infected HFF cells at 20 hr p.i. Most of the tachyzoites from both parasites were found at 2nd (4 tachyzoites) or 3rd (8 tachyzoites) doubling rounds.

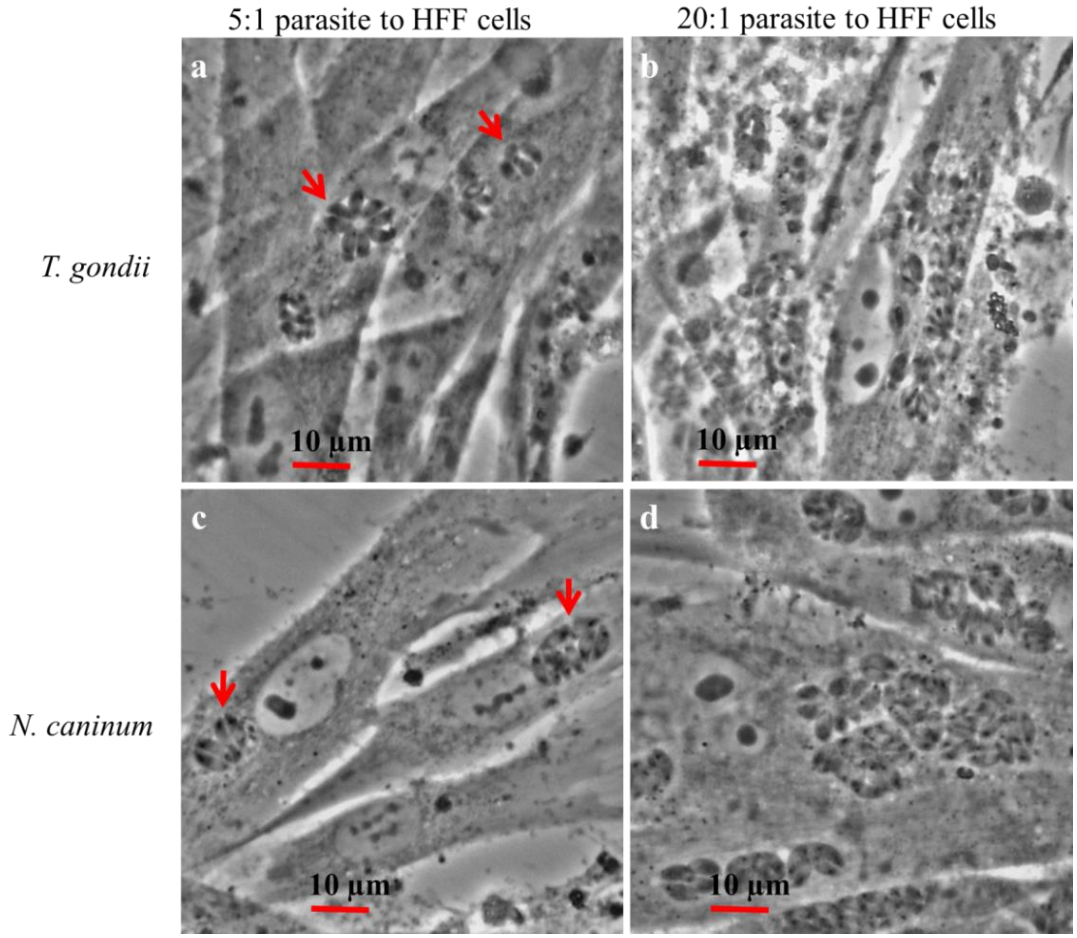

Figure 4.1: The doubling processes of *T. gondii* and *N. caninum* in infected HFF cells at 20 hr p.i. a): HFF cells infected with *T. gondii* VEG strain at a ratio of 5:1 parasites to cells, red arrows shows parasites at the 2nd and 3rd doubling stages at 400 × magnification. b): HFF cells infected with *T. gondii* VEG strain at a ratio of 20:1 parasites to cells at 400 ×. c): HFF cells infected with *N. caninum* Liverpool strain at a ratio of 5:1 parasites to cells, red arrows shows parasites at the 2nd and 3rd doubling stages at 400 ×. d): HFF cells infected with *N. caninum* Liverpool strain at a ratio of 20:1 parasites to cells at 20 hr p.i. at 400 ×. Pictures were taken by AxioCam ERCs % Rev. 2.0 (2 mega pixels) connected to an inverted microscope (Carl Zeiss Microscopy GmbH, Germany) with 400 × magnification.

4.3.2. Total identified peptides and phosphopeptides using TiO_2 and data analysis using PEAKS®

Total numbers of globally identified peptides from HFF cell infected with *T. gondii* and of mock infected with *T. gondii* (containing peptides from both host cell and the parasite) were 17,422 and 16,651, respectively. Total number of identified peptides from HFF cells infected with *N. caninum* and of mocks infected with *N. caninum* (containing peptides from both host cell and the parasite) were 16,415 and 17,250, respectively (Table 4.1).

The total numbers of identified peptides (phosphopeptides and non-phosphopeptides) in the TiO_2 enriched samples from HFF cell infected with *T. gondii* and mocks infection were 5,171 and 3,455, respectively. While total number of identified peptides in HFF cell infected with *N. caninum* and mock infection were 4,556 and 3,043, respectively (Table 4.1).

Table 4.1: Total number of peptides and phosphopeptides identified from global proteome and from TiO_2 enrichment using PEAKS®

Conditions	**Global quantification sample[1]**	**TiO_2 enrichment sample[1]**
HFF cells infected with *T. gondii*	17,422	5,171
HFF cells spiked with *T. gondii*	16,651	3,455
HFF cells infected with *N. caninum*	16,415	4,556
HFF cells spiked with *N. caninum*	17,250	3,043

[1] Including both peptides and phosphopeptides from both HFF cell and the parasites

4.3.3. Enrichment performance of TiO_2 SpinTips kit

The enrichment fold of non-redundant phosphopeptides using TiO_2 SpinTips kit is shown in Table 4.2. The lowest enrichment fold was reported from HFF cell spiked with *N. caninum* and *T. gondii* at 10.52 and 10.54 folds, respectively. A similar enrichment fold was reported from infected HFF cells as well; while the highest enrichment fold was observed from parasite peptides in *N. caninum* and *T. gondii* mock infections at 16.53 and 23.42 folds, respectively.

Table 4.2: The enrichment of non-redundant phosphopeptides identified using TiO_2.

Conditions	Global quantification[1]		TiO_2 Enrichment[2]		Fold enrichment
	Peptides	Phosphopeptides	Peptides	Phosphopeptides	
Parasite peptides in *Toxoplasma* infection	2025	12	285	176	14.67
Host peptides in *Toxoplasma* infection	15242	143	2914	1796	12.56
Parasite peptides in mock infection with *Toxoplasma*	6335	31	632	726	23.42
Host peptides in mock infection with *Toxoplasma*	10203	82	1233	864	10.54
Parasite peptides in *Neospora* infections	1973	12	284	151	12.58
Host peptides from *Neospora* infection	14277	153	2491	1630	10.65
Parasite peptides in mock infection with *Neospora*	5486	34	417	562	16.53
Host peptides in mock infection with *Neospora*	11638	92	1098	968	10.52

[1] The whole cell lysate without TiO_2 enrichment.
[2] The enriched phosphopeptides from each sample using TiO_2 SpinTip kit

4.3.4. Phosphopeptides enrichment from HFF cells using Peaks®

Redundancy in the identified phosphopeptides obtained from the biological replicates of the infected host cells and the mock infection was eliminated. The total number of phosphopeptides from host cells infected with *T. gondii* and *N. caninum* was 1,796 and 1,630, respectively. Total number of phosphopeptides from mock infected HFF cells was 864 and 968 for *T. gondii* and *N. caninum*, respectively (Figure 4.2). Phosphopeptides from HFF cells infected with *T. gondii*, *N. caninum* and mock infections were compared. There are 1101 phosphopeptides overlap between *T. gondii* and *N. caninum* infections (Figure 4.2 a) which accounted for 61.30 % and 67.54 %, respectively. Host cells infected with *T. gondii* and *N. caninum* showed nearly two fold more of phosphopeptides identified than mock infections (Figure 4.2b and c). At the phosphoprotein level, there were 359 phosphoproteins that overlapped between host cells infected with both parasites (Figure 4.3) and 151 phosphoproteins from HFF cells infected with *T. gondii* were

different from infection with *N. caninum*. A total of 101 phosphoproteins were found in infection with *N. caninum* but not in *T. gondii* (Figure 4.3).

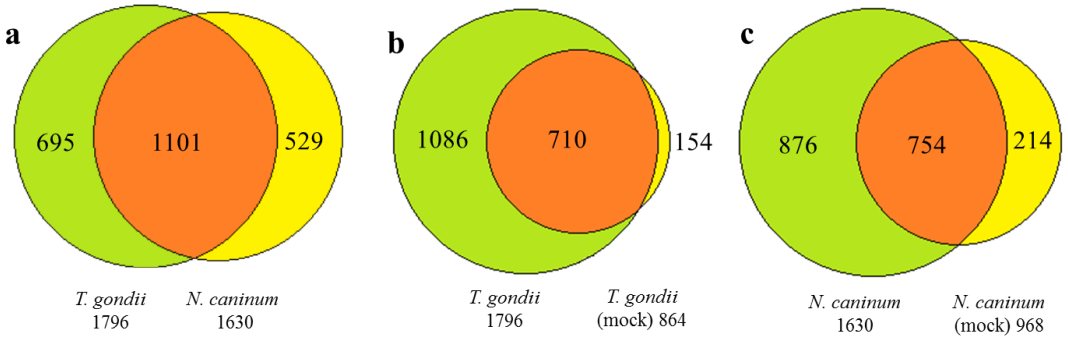

Figure 4.2: Comparison of non-redundant phosphopeptides enriched using TiO_2 from HFF cells. a) HFF cell infected with *T. gondii* and *N. caninum*. b) HFF infected with tachyzoites from *T. gondii* and *T. gondii* (mock) and c) HFF cell infected with *N. caninum* and *N. caninum* (mock).

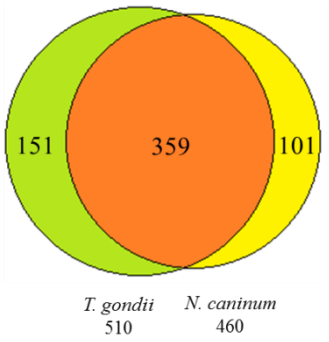

Figure 4.3: Comparison of non-redundant phosphoproteins enriched using TiO_2 from HFF cells infected with *T. gondii* and *N. caninum*.

4.3.5. Subcellular location and types of phosphoproteins

The subcellular locations and types (based on molecular function) of phosphoproteins were analysed using IPA to understand their distribution in response to infection with these parasites. Host cells infected with *N. caninum* and *T. gondii* showed very similar distribution in both subcellular location and types of enriched phosphoproteins as shown in Figure 4.4 and 4.5, respectively.

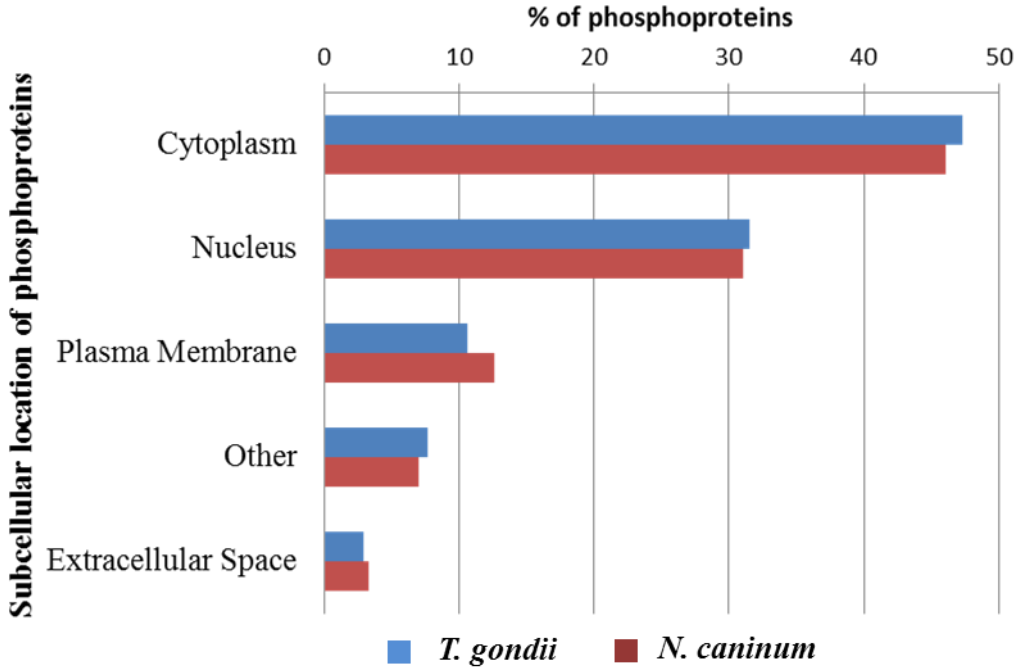

Figure 4.4: Subcellular location of enriched phosphoproteins from host cell infected with *T. gondii* and *N. caninum*.

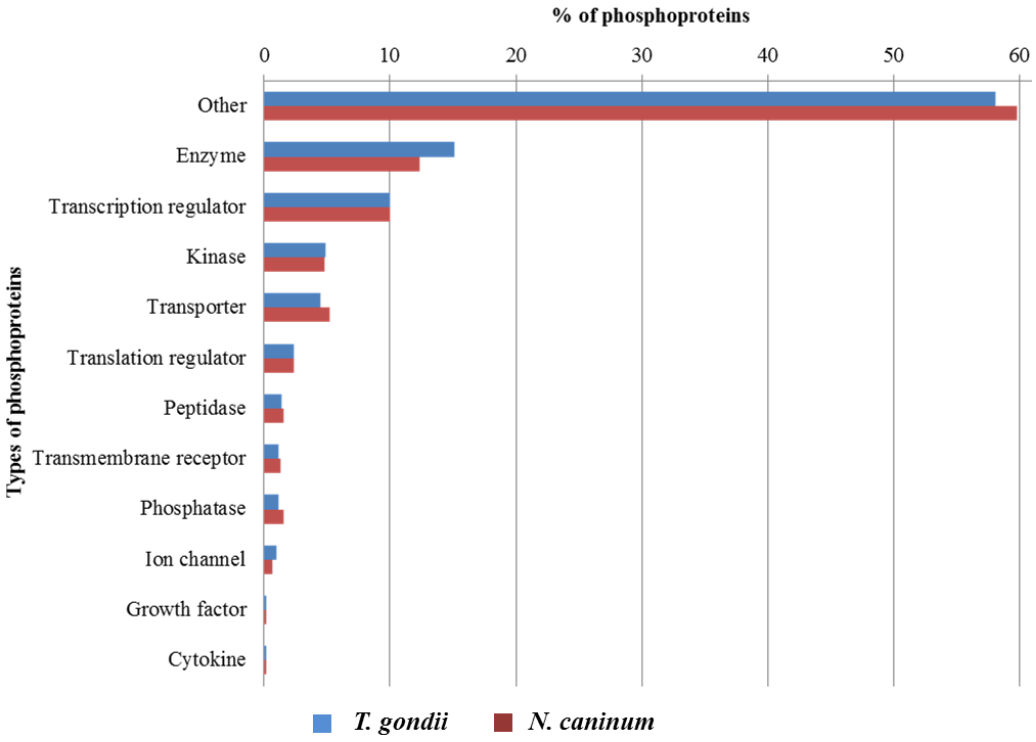

Figure 4.5: Types of enriched phosphoproteins from host cell infected with *T. gondii* and *N. caninum*.

4.3.6. Phosphorylation sites of phosphopeptides identified from infected HFF cells

Investigating phosphorylation sites is important to understand the differences in signalling pathways and the kinases most frequently involved between both infections. Phosphorylated proteins were investigated for differences in phosphorylation sites between the non-infected host cell and host cell in response to infection with *T. gondii* and *N. caninum*. The phosphorylation sites (phosphoserine, phosphothreonine and phosphotyrosine) were found distributed similarly between non-infected and infected host cell with *T. gondii* and *N. caninum* (Table 4.3). However, similar to what was observed at the phosphopeptide level, the highest number of phosphorylation sites were found in infected HFF cells which were nearly two times higher than mock infections (Table 4.3).

Table 4.3: The phosphorylation sites identified in HFF cells infected and mock infected with *T. gondii* and *N. caninum* at 20 hr p.i.

Phosphorylation type	**No. of host phosphosites in *T. gondii* infection /%**	**No. of host phosphosites in mock infection with *T. gondii*/%**	**No. of host phosphosites in *N. caninum* infection /%**	**No. of host phosphosites in mock infection with *N. caninum*/%**
Phosphoserine	1985/85.93	971/88.35	1795/85.6	1083/87.76
Phosphothreonine	310/13.42	121/11	287/13.69	147/11.91
Phosphotyrosine	15/0.65	7/0.64	15/0.72	4/0.32
Total	2310	1099	2097	1234

4.3.7. Motif analysis from enrich Phosphopeptides

Motifs analysis was performed in order to investigate the involvement of different kinases with various phospho-motifs between the two infections. Motif analysis of phosphoserine containing peptides showed differences between host cell infected with *T. gondii* and *N. caninum*. A total of 19 motifs were enriched where four motifs were differentially enriched for each infection as shown in Table 4.4 which is equivalent to 21.05 % differences. On the other hand, phosphothreonine containing peptides showed that only four motifs were enriched where two of them were differentially enriched in *T. gondii* as shown in Table 4.5.

Table 4.4: HFF cell motifs from enriched phosphopeptides of host cells infected with *T. gondii* and *N. caninum* based on the phosphorylated serine amino acid.

s	Motif	Motif score from infection with *T. gondii*	Fold increase	Motif score from infection with *N. caninum*	Fold increase
1	....R..sP.P....	40.67	41.46	40.32	42.70
2	.....P.sP.....	26.10	9.48	27.04	9.87
3	.......sP.....	16.00	4.48	16.00	4.49
4	.......sD.E....	32.00	19.69	32.00	19.00
5	....RR.s.....	22.09	11.98	22.62	12.23
6	....R..s.....	16.00	4.35	16.00	4.40
7	.......sE.E....	30.26	12.94	27.56	12.33
8	.......sSP.....	27.88	9.43	28.55	9.80
9	.......s.E.....	13.39	2.79	9.84	2.55
10	.......s.SP....	20.29	8.42	23.52	10.54
11	.......s....E..	6.44	2.38	6.64	2.60
12	.......sP...R..	24.83	11.47	-	-
13	....R..s.S.....	23.65	10.32	-	-
14	......Rs...S...	13.19	10.97	-	-
15	.......s....D..	8.57	2.93	-	-
16	.....S.sP.....	-	-	24.95	9.02
17	....RS.s.....	-	-	23.44	9.12
18	.......s.DE....	-	-	16.82	17.73
19	.....R.s.....	-	-	8.10	2.79

Table 4.5: HFF cell motifs from enriched phosphopeptides of host cells infected with *T. gondii* and *N. caninum* based on the phosphorylated threonine amino acid.

s	Motif	Motif score from infection with *T. gondii*	Fold increase	Motif score from infection with *N. caninum*	Fold increase
1	.....tP.....	15.95	3.72	16.00	4.41
2	.....SPt.....	15.56	14.51	20.93	18.11
3	....K..tP.....	22.11	20.72	-	-
4	.....tSP.....	14.10	14.74	-	-

4.3.8. Pathway analysis for the enriched phosphopeptides from HFF cells infected with *T. gondii* and *N. caninum*

The identified phosphoproteins enriched from infected HFF cells were submitted to DAVID functional annotation tool for pathway analysis. The results are shown in Table 4.6 and 4.7 for *T. gondii* and *N. caninum*, respectively. Comparing the pathways from both conditions showed that three pathways (mTOR signalling pathway, glycolysis/gluconeogenesis and endometrial cancer) from HFF cells infected with *T. gondii* were not enriched in *N. caninum* infection. Five pathways (erbB signalling pathway, renal cell carcinoma, gap junction, long-term potentiation, and vascular smooth muscle contraction) enriched in *N. caninum* infection were not enriched for *T. gondii* infection (Table 4.8). The detail information about individual proteins involved in the differentially enriched pathway is shown in Table 4.9.

Table 4.6: Pathways enriched in *T. gondii* infection

s	Name of the pathways	P-Value	Gene count	%*	Uniprot genes entry accession number
1	Spliceosome	2.60E-09	21	4.13	Q09161, Q86XP3, P52272, O75643, P49756, Q13573, Q7L014, Q13247, O75494, Q96I25, Q8IWX8, O43290, P08107, P07910, Q9UKV3, O15042, P08621, Q00839, P61978, P09651, Q01130
2	Focal adhesion	1.71E-06	22	4.32	P02751, P08648, P18206, Q9Y490, O96013, P51636, P02452, P21333, Q15942, P35222, O14974, P08123, Q03135, Q14315, P04049, P05412, P50552, Q15746, O15530, P49023, Q9NVD7, Q9NRY4
3	Regulation of actin cytoskeleton	1.92E-04	19	3.73	P02751, P08648, P18206, O96013, O15143, Q8WYL5, P19634, P10398, O14974, P35579, Q14155, P35580, Q8TE77, P04049, Q15746, Q15052, P49023, P25054, Q9NRY4
4	Insulin signalling pathway	0.004335	12	2.36	Q13131, P04049, Q13085, O15530, Q15642, P49815, Q13541, P62753, P10398, P17612, P13861, P10644
5	Pathogenic *Escherichia coli* infection	0.010119	7	1.38	Q92974, O15143, Q9BQE3, P68363, P35222, P19338, Q14247
6	Glycolysis / Gluconeogenesis	0.012888	7	1.38	Q9NR19, P04406, P60174, P06733, P14618, P08559, P17858
7	mTOR signalling pathway	0.026345	6	1.18	Q13131, O15530, P49815, Q13541, P62753, P23588
8	Endometrial cancer	0.026345	6	1.18	P04049, O15530, P25054, P35221, P10398, P35222
9	Arrhythmogenic right ventricular cardiomyopathy (ARVC)	0.036842	7	1.38	P02545, P08648, P15924, P17302, P35221, P35222, P11532
10	Adherens junction	0.038918	7	1.38	O43318, P18206, Q8WWI1, O60716, P35221, P35222, Q07157

*Percentage of genes involved in the pathway from submitted data to the total number of the background genes in the pathway

Table 4.7: Pathways enriched in *N. caninum* infection

s	Name of the pathways	P-Value	Gene count	%*	Uniprot genes entry accession number
1	Focal adhesion	1.51E-07	22	4.81	P08648, P18206, Q9Y490, O96013, P51636, P02452, P21333, Q13177, Q15942, P35222, O14974, P08123, Q03135, Q14315, P04049, P05412, P50552, Q15746, P49023, Q9NVD7, O43707, P15056
2	Spliceosome	3.69E-07	17	3.72	P52272, P49756, Q13573, Q13247, Q9BUQ8, Q8IWX8, Q13435, P07910, O43290, Q9UKV3, O15042, O60508, P08621, Q00839, P61978, P09651, Q01130
3	Regulation of actin cytoskeleton	1.02E-04	18	3.94	P08648, P18206, O96013, Q8WYL5, P19634, P10398, Q13177, O14974, P35579, Q14155, Q8TE77, P04049, Q15746, Q15052, P49023, P62328, O43707, P15056
4	ErbB signalling pathway	0.003008	9	1.97	P04049, P05412, O96013, Q13541, P10398, Q13177, P16333, Q13557, P15056
5	Adherens junction	0.005798	8	1.75	O43318, P18206, Q8WWI1, O60716, P35221, O43707, P35222, Q07157
6	Long-term potentiation	0.012024	7	1.53	P04049, Q14573, P10398, P17612, O14974, Q13557, P15056
7	Vascular smooth muscle contraction	0.013554	9	1.97	P04049, Q14573, Q15746, Q05682, P10398, P17612, O14974, Q9Y6F6, P15056
8	Arrhythmogenic right ventricular cardiomyopathy (ARVC)	0.019995	7	1.53	P02545, P08648, P15924, P17302, P35221, O43707, P35222
9	Pathogenic *Escherichia coli* infection	0.021843	6	1.31	Q71U36, P68363, P16333, P35222, P19338, Q14247
10	Insulin signalling pathway	0.036807	9	1.97	P04049, Q15642, Q13541, P62753, P10398, P17612, P13861, P10644, P15056
11	Gap junction	0.039527	7	1.53	P04049, Q14573, Q71U36, P17302, P68363, P17612, Q07157
12	Renal cell carcinoma	0.047286	6	1.31	P04049, P05412, O96013, P10398, Q13177, P15056

*Percentage of genes involved in the pathway from submitted data to the total number of the background genes in the pathway

Table 4.8: The comparative differences of pathways analysed from phosphopeptides IDs enriched by TiO_2 from HFF cells infected with *T. gondii* and *N. caninum*.

Enriched pathway	**HFF cells infection with *T. gondii***	**HFF cells infection with *N. caninum***
Adherent junction	✓	✓
Arrhythmogenic right ventricular cardiomyopathy	✓	✓
Focal adhesion	✓	✓
Insulin signalling pathway	✓	✓
Pathogenic *Escherichia coli* infection	✓	✓
Regulation of actin cytoskeleton	✓	✓
Spliceosome	✓	✓
Glycolysis/gluconeogenesis	✓	×
MTOR signalling pathway	✓	×
Endometrial cancer	✓	×
ErbB signalling pathway	×	✓
Gap junction	×	✓
Long-term potentiation	×	✓
Renal cell carcinoma	×	✓
Vascular smooth muscle contraction	×	✓

Table 4.9: Pathways differentially enriched from HFF cells infected with *T. gondii* and *N. caninum*.

Pathway	**Gene ID**	**Protein name**	**EC***	***T. gondii***	***N. caninum***
mTOR	Q13131	5'-AMP-activated protein kinase catalytic subunit alpha-1, AMPK1	2.7.11.1	✓	×
	O15530	3-phosphoinositide-dependent protein kinase 1, PDK1	2.7.11.1	✓	×
	P49815	Tuberin, TSC2	-	✓	×
	Q13541	Eukaryotic translation initiation factor 4E-binding protein 1, EIF4EBP1	-	✓	✓
	P62753	40S ribosomal protein S6, RPS6	-	✓	✓
	P23588	Eukaryotic translation initiation factor 4B, EIF4B	-	✓	✓
Glycolysis/ gluconeogenesis	P06733	Alpha-enolase, ENO1	4.2.1.11	✓	×
	P14618	Pyruvate kinase, PKM	2.7.1.40	✓	×
	P08559	Pyruvate dehydrogenase E1 component subunit alpha, PDHA1	1.2.4.1	✓	×
	P17858	ATP-dependent 6-phosphofructokinase, liver type, PFKL	2.7.1.11	✓	×
	Q9NR19	Acetyl-coenzyme A synthetase, ACAS2	6.2.1.1	✓	✓
	P04406	Glyceraldehyde-3-	1.2.1.12	✓	✓

		phosphate dehydrogenase, GAPDH			
	P60174	Triosephosphate isomerase, TPI1	5.3.1.1	✓	✓
Endometrial cancer	P04049	RAF proto-oncogene serine/threonine-protein kinase, RAF1	2.7.11.1	✓	×
	P35221	Catenin alpha-1, CTNNA1	-	✓	×
	P10398	Serine/threonine-protein kinase A-Raf, ARAF	-	✓	×
	P35222	Catenin beta-1, CTNNB1	-	✓	×
	O15530	3-phosphoinositide-dependent protein kinase 1, PDK1	2.7.11.1	✓	✓
	P25054	Adenomatous polyposis coli protein, APC	-	✓	✓
ErbB	P04049	RAF proto-oncogene serine/threonine-protein kinase, RAF1	2.7.11.1	✓	✓
	P05412	Transcription factor AP-1, JUN	-	✓	✓
	O96013	Serine/threonine-protein kinase PAK 4, PAK4	2.7.11.1	✓	✓
	Q13541	Eukaryotic translation initiation factor 4E-binding protein 1, EIF4EBP1	-	✓	✓
	P10398	Serine/threonine-protein kinase A-Raf, ARAF	2.7.11.1	✓	✓
	Q13557	Calcium/calmodulin-dependent protein kinase type II subunit delta, CAMK2D	2.7.11.17	✓	✓
	Q13177	Serine/threonine-protein kinase PAK 2, PAK2	2.7.11.1	×	✓
	P16333	Cytoplasmic protein NCK1, NCK1	-	×	✓
	P15056	Serine/threonine-protein kinase B-raf, BRAF	2.7.11.1	×	✓
Gap junction	P04049	RAF proto-oncogene serine/threonine-protein kinase, RAF1	2.7.11.1	✓	✓
	Q14573	Inositol 1,4,5-trisphosphate receptor type 3, ITPR3	-	✓	✓
	P17302	Gap junction alpha-1 protein, GJA1	-	✓	✓
	P68363	Tubulin alpha-1B chain, TUBA1B	-	✓	✓
	P17612	cAMP-dependent protein kinase catalytic subunit alpha, PRKACA	-	✓	✓
	Q07157	Tight junction protein ZO-1, TJP1	-	✓	✓
	Q71U36	Tubulin alpha-1A chain, TUBA1A	-	×	✓

Long-term potentiation	P04049	RAF proto-oncogene serine/threonine-protein kinase, RAF1	2.7.11.1	✓	✓
	Q14573	Inositol 1,4,5-trisphosphate receptor type 3, ITPR3	-	✓	✓
	P10398	Serine/threonine-protein kinase A-Raf	-	✓	✓
	P17612	cAMP-dependent protein kinase catalytic subunit alpha, PRKACA	2.7.11.11	✓	✓
	O14974	Protein phosphatase 1 regulatory subunit 12A, PPP1R12A	-	✓	✓
	Q13557	Calcium/calmodulin-dependent protein kinase type II subunit delta, CAMK2D	-	✓	✓
	P15056	Serine/threonine-protein kinase B-raf, BRAF	-	×	✓
Renal cell carcinoma	P04049	RAF proto-oncogene serine/threonine-protein kinase, RAF1	2.7.11.1	✓	✓
	P05412	Transcription factor AP-1, JUN	-	✓	✓
	O96013	Serine/threonine-protein kinase PAK 4, PAK4	2.7.11.1	✓	✓
	P10398	Serine/threonine-protein kinase A-Raf, ARAF	2.7.11.1	✓	✓
	Q13177	Serine/threonine-protein kinase PAK 2, PAK2	2.7.11.1	×	✓
	P15056	Serine/threonine-protein kinase B-raf, BRAF	2.7.11.1	×	✓
Vascular smooth muscle contraction	P04049	RAF proto-oncogene serine/threonine-protein kinase, RAF1	2.7.11.1	✓	✓
	Q14573	Inositol 1,4,5-trisphosphate receptor type 3, ITPR3	-	✓	✓
	Q15746	Myosin light chain kinase, smooth muscle, MYLK	2.7.11.18	✓	✓
	Q05682	Caldesmon, CALD1	-	✓	✓
	P10398	Serine/threonine-protein kinase A-Raf, ARAF	2.7.11.1	✓	✓
	P17612	cAMP-dependent protein kinase catalytic subunit alpha, PRKACA	2.7.11.11	✓	✓
	O14974	Protein phosphatase 1 regulatory subunit 12A, PPP1R12A	-	✓	✓
	Q9Y6F6	Protein MRVI1, MRVI1	-	×	✓
	P15056	Serine/threonine-protein kinase B-raf, BRAF	2.7.11.1	×	✓

*Enzyme Commission number

4.3.8.1. Mammalian target of rapamycin (mTOR) signalling pathway

mTOR signalling pathway is one of the pathways that only enriched in *T. gondii* infection. Among the phosphoproteins identified (shown in Table 4.6), three are playing roles in the regulation of the core pathway (AMPK1, PDK1, and TSC2) while the other three (EIF4EBP1, RPS6 and EIF4B) are substrates for the core pathway (Figure 4.6). However, only the last three molecules (EIF4EBP1, RPS6 and EIF4B) have been found phosphorylated in *N. caninum* infection as well.

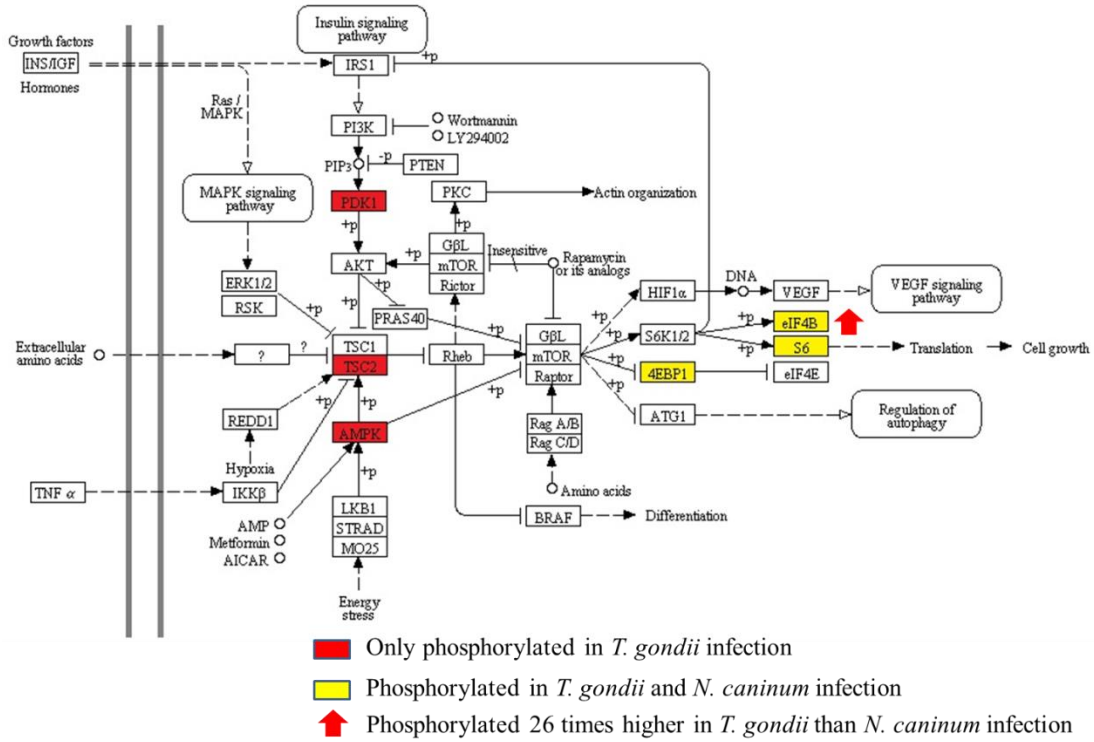

Figure 4.6: mTOR signalling pathway of host cell. Enriched phosphopeptides coverage from host cell infected at 20 hr p.i. with *T. gondii* and *N. caninum*. Red rectangle box: phosphopeptides phosphorylated only in *T. gondii* infection. Yellow rectangle box: phosphopeptides phosphorylated in *T. gondii* and *N. caninum* infection. Pathway is available online on the KEGG pathway site (http://www.genome.jp/kegg/pathway.html).

4.3.8.2. Glycolysis/gluconeogenesis pathway

Pathway analysis showed that more phosphopeptides from HFF cells infected with *T. gondii* were enriched (Table 4.6) in the Glycolysis/gluconeogenesis pathway than *N. caninum* infection at 20 hr p.i. (Figure 4.7).

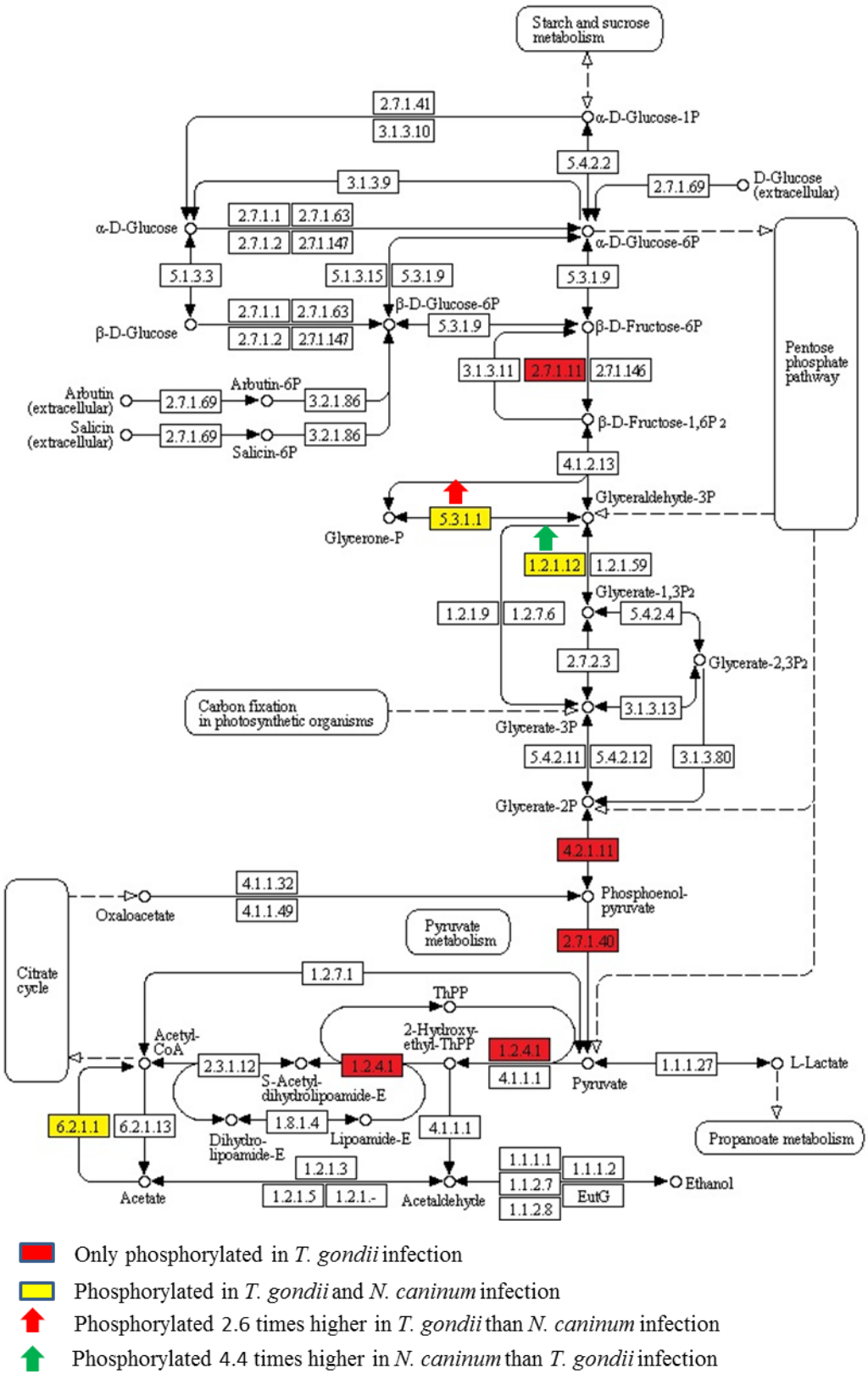

Figure 4.7: Metabolic pathway coverage: Glycolysis and gluconeogenesis. The enriched phosphopeptides from HFF cells infected by both parasites at 20 hr p.i. Red rectangle box: phosphopeptides phosphorylated only in *T. gondii* infection. Pathway is available online on the KEGG pathway site (http://www.genome.jp/kegg/pathway.html).

4.3.9. Phosphopeptides quantification from host cell infected with *T. gondii* and *N. caninum*

In total, 6565 peptides were quantified in TiO_2 enrichment of *T. gondii* and *N. caninum* infections, where 2540 of them were phosphopeptides (Figure 4.8a). When comparing between the two infections, only 397 phosphopeptides were statistically significant ($p < 0.05$) (Figure 4.8b). A total of 95 unique phosphopeptides have showed a fold change of ≥ 1.5 between the two infections (Appendix Table IV). In total, 57 out of 95 phosphopeptides have higher expressions in *T. gondii* infection and the remaining 38 have higher expressions in *N. caninum* (Figure 4.8c, appendix Table IV). Phosphoproteins with high fold changes were observed in *T. gondii* infection that play critical role in cellular process involved in protein productions/translation such as eukaryotic translation initiation factor 4B (EIF4B) and 60S acidic ribosomal protein P1. The EIF4B was increased 26 times in infected cells with *T. gondii* than *N. caninum*. In addition, phosphoproteins with high fold change involved in glycolysis were found in infection with both parasites; triosephosphate isomerase was found in infection with *T. gondii* while glyceraldehyde-3-phosphate dehydrogenase with *N. caninum* infection.

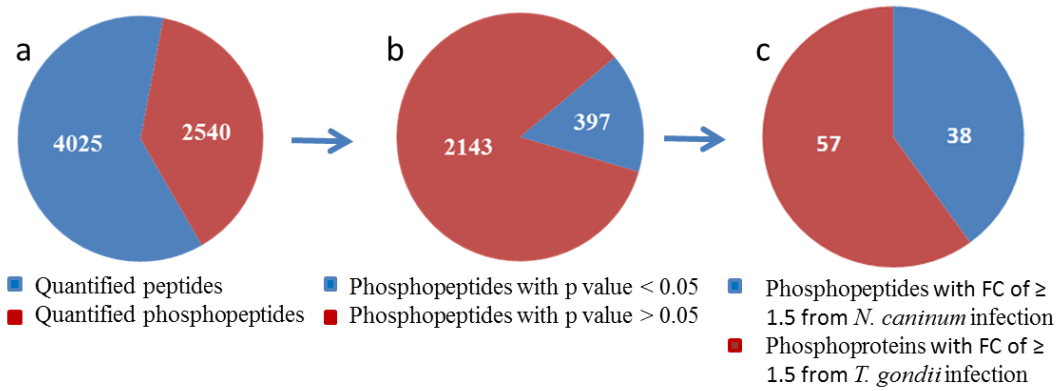

Figure 4.8: Peptides and phosphopeptides enriched from HFF cells infected with *T. gondii* and *N. caninum* at 20 hr p.i. a: total number of quantified peptides and phosphopeptides, b: Total number of significant phosphopeptides with p value < 0.05 and c: Phosphopeptides with fold change (FC) ≥ 1.5.

4.3.10. Upstream regulator analysis of quantified phosphopeptides from host cell infected with *T. gondii* and *N. caninum*

The quantified phosphopeptides were found regulated by different molecules that play vital role in normal cellular physiology. The upstream regulator analyses showed that kinases were distributed similarly between both infections. In addition, transcriptional regulator and enzymes were among the most regulated molecules enriched from infection with *T. gondii* and *N. caninum* as shown in Figure 4.9 and Appendix Table V and VI.

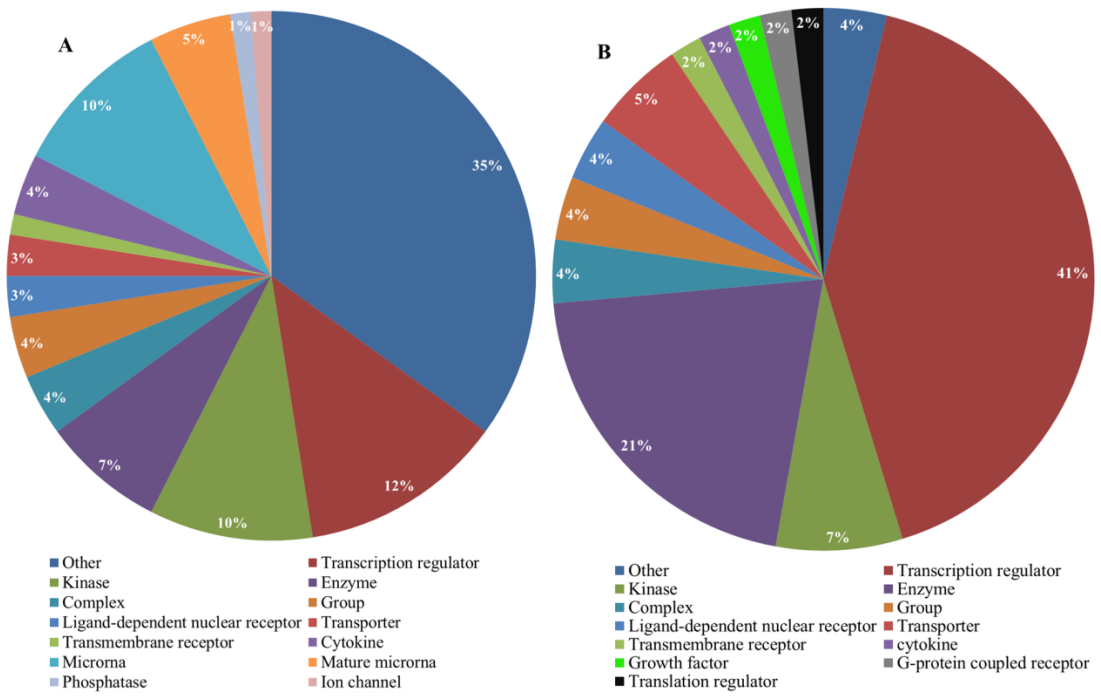

Figure 4.9: Upstream analysis of quantified phosphoproteins. Types of upstream regulator of phosphoproteins quantified from host cell infected by A: *T. gondii* and B: *N. caninum*.

4.4. DISCUSSION

To date there are no large scale host cell phosphoproteome studies in response to infection with *T. gondii* and *N. caninum*. In the present study, the differences in host cell phosphoproteome indicate that these parasites interact with the host cells variably at the phosphoprotein and signal transduction level. Thus, diverse host cell responses of the signalling pathways are potentially responsible for the differences in the biology of these parasites. Enriched phosphoproteomes from host cell infected by *T. gondii* and *N. caninum* showed similarity of 61.30 % and 67.54 %, respectively (Figure 4.2a), where only about one-third of the phosphoproteome was different. In addition, phosphorylation sites and motif analysis from significantly enriched phosphopeptides showed high similarity as well. However, four different motifs were found differentially enriched between infection with *T. gondii* and with *N. caninum*, which is equal to 21.05 %. Furthermore, pathway analysis showed that a few pathways were differentially enriched between infections with these parasites such as glycolysis/gluconeogenesis and mTOR signalling pathway in infection with *T. gondii* but not *N. caninum*. Moreover, similar profiles were also found in subcellular location and types of phosphoproteins identified. The general similarity in host response to these parasites could be related to the fact that the genomes and gene expression of the two parasites are remarkably preserved (Reid *et al.*, 2012). However, small differences could result in great differences in host-parasites interaction, e.g. pseudogenisation of *NcROP18* in *N. caninum* failed to phosphorylate immunity-related GTPases (IRGs) of the host cell that is necessary for protection of PVM from destruction in IFNγ-induced cells (Lei *et al.*, 2014; Reid *et al.*, 2012).

4.4.1. HFF cell intensively responds to infection with *T. gondii* and *N. caninum* through protein phosphorylation

The number of phosphoproteins and phosphorylation sites identified were approximately two times higher in infected HFF cells compared to uninfected cells in the mock infections (Figure 4.2b and c, Table 4.3). These results suggested that infection with *T. gondii* and *N. caninum* actively transduce signals to induce protein phosphorylation of the host cells which modulates host response and adaptation to intracellular environment during infection. In addition, the enrichment of

phosphopeptides from infected HFF cell and mock infections showed similar enrichment fold which indicated an unbiased sampling. The results from this study corroborates the results of a previous study on host response to *T. gondii* infection at different time point; this indicated that protein phosphorylation was actively involved in the modulation of host response (Nelson *et al.*, 2008). In addition, the distribution of types and subcellular localisation (Figure 4.4, 4.5) of identified phosphoproteins from infected host cells showed similar response to infection with these parasites. Furthermore, protein phosphomotifs analysis revealed that these motifs were phosphorylated by similar groups of kinases and potentially involved in the same cellular signalling pathways. Also, upstream analysis regulator of the quantified phosphoproteins showed that they are regulated mostly by kinases, transcriptional regulator and enzymes. However, transcriptional regulator and enzymes were highly processes in *N. caninum* infection than *T. gondii* (Figure 4.9), suggesting that they play different roles in response to infection with these parasites. These results suggest that *T. gondii* and *N. caninum* intensively phosphorylate and modulate host cells and that host cell protein phosphorylations in response to infection with these parasites are generally conserved. However, by using pathway enrichment analysis coupled with quantitative data, it was possible to decipher some interesting differences in host responses following infection with both parasites.

4.4.2. Pathway analysis of HFF cells infected with *T. gondii* and *N. caninum*

Pathway analyses showed that ten and 12 pathways were enriched for HFF cells infected with *T. gondii* and *N. caninum*, respectively.

4.4.2.1. mTOR signalling pathway is a key regulatory metabolic pathway of host cell regulated differently in *T. gondii* and *N. caninum* infections

Mammalian target of rapamycin (mTOR) is a Ser/Thr kinase playing axial contribution in integrating the responses arising from certain conditions such as growth factor signalling, energy stress, nutritional prestige, oxygen tension and regulation of cellular physiology and metabolic processes (Hay and Sonenberg, 2004; Tsalikis *et al.*, 2013; Wullschleger *et al.*, 2006).

4.4.2.1.1. Phosphorylation of downstream substrate of mTOR signalling pathway in *T. gondii* and *N. caninum* infection

Differential phosphorylation of substrates in mTOR signalling pathway indicated that host cells infected by *T. gondii* and *N. caninum* exploit mTOR pathway for selective translation of certain mRNA that are important in translational machinery such as ribosomal protein and elongation factors (Bahrami *et al.*, 2014). Activation of mTOR could ensure continuous synthesis of proteins and enzymes required by rapidly growing and dividing tachyzoites. The result of this study is in agreement with Wang *et al.* (2009), which reported the activation of mTOR signalling pathway in different cell types such as HFF cells, HeLa cells and murine peritoneal exudate macrophages in response to infection with *T. gondii*. In this study, E4-BP1 and S6K substrates (S6 and eIF4B) but not S6K1 were also found in HFF cells infected with *N. caninum* showing similarity in signalling transduction using mTOR pathway. However, quantitative data showed that eIF4B was enriched 26 times more in infection with *T. gondii* than *N. caninum*. In the present study S6K1 was not identified to be phosphorylated in infection with both parasites at 20 hr p.i. which is comparable to the results of Wang *et al.* (2009) that found S6K1 phosphorylated for short time following infection at 2-4 hr p.i. Phosphorylation of eIF4B and S6 but not S6K1 from HFF cells infected with *T. gondii* and *N. caninum* imply that these parasites may have the capability to selectively regulate downstream substrates regardless of the canonical activation of mTOR signalling pathway.

4.4.2.1.2. Phosphorylation of upstream substrate of mTOR signalling pathway in *T. gondii* infection

The PI3K/AKT pathway is an upstream regulator and activator of mTOR signalling pathway, which is activated in response to growth factors and hormones (Laplante and Sabatini, 2012; Petroulakis *et al.*, 2006). The growth factors and hormones activates class I phosphatidylinositol 3-kinase (PI3K) which further leads to phosphorylation (and activation) of PDK1 and AKT with subsequent phosphorylation and inactivation of tuberin (TSC2). Inactivation of TSC2 leads to the activation of Rheb which in turn activates the mTOR signalling pathway (Bai *et al.*, 2007; Li *et al.*, 2004; Shahbazian *et al.*, 2010). In the present study, PDK1, TSC2 and AMPK) were all shown to be phosphorylated during *T. gondii* infection but not

in *N. caninum*, suggesting that PDK1 and TSC2 were selectively activated in the host cell infected by *T. gondii*. The PDK1 and TSC2 were, however, found to be phosphorylated in *T. gondii* infected host cells, but not in uninfected cells, indicating that mTOR signalling pathway was activated upon infection. The results presented here are comparable with that of Wang *et al.* (2009) as the latter authors have not observed AKT phosphorylation in response to *T. gondii* infection as shown in our study. Also, they found that AKT were not associated with *Toxoplasma*-induced activation of mTOR and did not find it to be activated in HFF, 3T3 and HeLa cells. They suggested that AKT activity is not related to the stimulation of mTOR activity in response to infection with *T. gondii* (Wang *et al.*, 2009). Results of the present study suggest that PDK1 activation may lead to phosphorylation of TSC2 independent of AKT activation possibly through other mediators or through kinase-like proteins of parasite origin.

In the present study, AMPK was also found phosphorylated during infection with *T. gondii*. AMPK activation is related to the inhibition of mTOR signalling pathway (Inoki *et al.*, 2003; Zoncu *et al.*, 2011), as well as the regulation of metabolic processes and cellular maintenance (Sanli *et al.*, 2014), stress resistance, apoptosis and glucose metabolism (Greer *et al.*, 2007). In the present study, AMPK activation could be related to the regulation of transcription factors associated with stress but not with inhibition of mTOR due to the fact that pathways associated with energy and protein productions were activated. This finding indicates that HFF cells exhibited more stressful response of *T. gondii* infection than that of *N. caninum*.

Together, results associated with mTOR signalling pathway suggested that *T. gondii* and *N. caninum* potentially phosphorylate host mTOR substrates in a parasite-dependent manner. However, *T. gondii* seems to interact and manipulate more host cells substrates than *N. caninum* infection and induces more host cell response at this time point.

4.4.2.2. Glycolysis/gluconeogenesis is highly regulated in HFF cells infected with *T. gondii*

Once infection is established, growing and dividing parasites must obtain necessary nutrients from the infected host cells. *T. gondii* controls the permeability of

PVM that selectively allows small molecules to diffuse freely from host cytoplasm to PV such as amino acids, sugar, nucleobases and cofactors (Schwab *et al.*, 1994). Cholesterol is also transferred from host to PV exploiting host endo-lysosomal system (Coppens *et al.*, 2006; Coppens *et al.*, 2000).

In this study, pathway analysis showed that phosphoproteins of HFF cells infected with *T. gondii* involved in more metabolic processes than *N. caninum* (Table 4.6). In addition, quantified phosphopeptides were also highly up-regulated in host cell infected with *T. gondii* than with *N. caninum* (Table 4.9, appendix Table IV). Previous study showed that host cell molecules involved in metabolism were highly modulated in response to *T. gondii* infection (Nelson *et al.*, 2008). In this study, seven phosphoproteins identified were assigned to glycolysis/gluconeogenesis pathway in *T. gondii* infection, while only three of them were identified in *N. caninum* infection. The enzymes identified in this study catalyse most of the reactions involved in glycolysis/gluconeogenesis. In addition, acetyl-coA synthase was also phosphorylated which catalyses the formation of acetyl-coA (the citric acid cycle substrate). This result may indicate that host cell intensively responded to high energy demand of *T. gondii* through glycolysis and potentially activation of oxidative phosphorylation to generate more energy.

High energy production is required to fulfil the demand of fast growing and multiplying tachyzoites; these processes are critically involved in the expenditure of cellular energy (Sanli *et al.*, 2014). This is supported by the study of Weilhammer *et al.* (2012), which demonstrated that induction of glycolysis by adding glucose or inducing expression of AKT gene was found responsible for converting permissive cell (cell that allow conversion of tachyzoites to bradyzoites stage) to resistance phenotypes and continuous multiplication of tachyzoites. In addition they showed that glycolytic metabolite such as lactate to play important roles in inhibition of conversion of tachyzoites to bradyzoites in permissive cells (Weilhammer *et al.*, 2012). This study showed that the activation of the glycolysis pathway and energy productions under aerobic condition, which provided complementary evidence to the results of microarray study from Blader *et al.* (2001), which reported that *Toxoplasma*-stimulated transcripts of host cell were up-regulated in anaerobic glycolysis. In addition, modification of the seven enzymes involved in the glycolysis

indicates up-regulation of this pathway during infection with *T. gondii*, a result that is in agreement with previous proteomic and transcriptomics studies of HFF cells infected with *T. gondii* (Blader *et al.*, 2001; Nelson *et al.*, 2008). The modulation of phosphoproteins involved in glycolysis/gluconeogenesis suggests global regulation of host cell metabolism during infection with *T. gondii* more than that induced by *N. caninum* at 20 hr p.i.

4.4.2.3. Host cells expend high energy during infection with *T. gondii* than *N. caninum* could be related to virulence differences and transmission route

In this study, the enrichment of phosphoproteins involved in mTOR pathway, glycolysis pathway and insulin pathway together (Table 4.6) indicated that high energy and proteins production are required for biogenesis and rapidly dividing tachyzoites in *T. gondii* infection comparing to *N. caninum*. This may reflect the urgent needs for *T. gondii* to rapidly multiply enough before the egress. High energy expenditure in cell infected with *T. gondii* potentially determines virulence through modulation of host cells metabolic processes to support tachyzoites replication and early egression. These processes consequently lead to cell death and re-invasion of new neighbouring cells (Hoff and Carruthers, 2002). In addition, high production of energy by the parasite might also determine the virulence of *T. gondii* in host cells compared to *N. caninum*. Song *et al.* (2013) showed that type I strain (RH) up regulate some metabolic pathways involved in ATP production such as pyrimidine biosynthesis, the TCA cycle and pentose phosphate shunt more than the type II strain (Me49) which could be account for the virulence differences between both stains. The higher energy productivity of host cell during infection with *T. gondii* than *N. caninum* potentially related to the virulence and transmission strategy of these parasites.

4.4.2.4. ErbB signalling pathway enriched in *N. caninum* infection may be associated with transmission route of *N. caninum*

ErbB signalling pathway plays important roles in normal physiology of cells and in cancer (Hynes and MacDonald, 2009). This pathway is activated through four members of ErbB family of receptor tyrosine kinases (RTKs) including epidermal growth factor receptor (EGFR or ErbB1), ErbB2, ErbB3, and ErbB4 in response to

different members of the epidermal growth factor family (EGF-family) of peptides (Hynes and MacDonald, 2009). In this study, the downstream substrate of the ErbB2, 3, 4 and EGFR receptor were found phosphorylated. These substrates link RTKs to different intracellular signalling pathways necessary for maintenance of cellular physiology such as proliferation, cell migration, metabolism and survival (Citri and Yarden, 2006; Hynes and Lane, 2005). In addition, ErbB2 and EGFR have been implicated in the development of many types of human cancer (Graus-Porta *et al.*, 1997) through activation of mitogen-activated protein kinase (MAPK), phosphoinositide kinase (PI3K)/AKT, mTOR pathways, proto-oncogene tyrosine-protein kinase (Src kinase) and STAT transcription factors (Egan and Weinberg, 1993; Ming *et al.*, 1994; Sharma and Settleman, 2009; Wieduwilt and Moasser, 2008; Yarden and Sliwkowski, 2001). The greater activation of these pathways in host cell infected by *N. caninum* than *T. gondii* may not be directly related to cancer as there is no evidence that relates *N. caninum* to the cause of cancer in animals. However, these pathways could indicate intimate host-parasite interaction to assure that host cell growth is maintained long enough during infection with minimum exposure to the immune system of the host and apoptosis. Upstream analysis of the quantified phosphoproteins indicates that different kinases such as MAPKs are involved in the phosphorylation of the proteins important for cell survival or death (appendix Table V and VI). Many pathogens modulate the PI3K/AKT survival pathway of the host cell which is primarily associated with activation of antiapoptotic pathways that assure safe place for the pathogens within the host cells (Carter, 2009). Maintenance of the infected host cell by *N. caninum* could be also related to the transmission route through converting tachyzoites to bradyzoites; this process is necessary to maintain the vertical transmission route and allows transmission from infected pregnant mother to subsequent generation.

4.4.3. Conclusion

To summarise, comparative host-parasite interaction has been studied on the host protein phosphorylation in response to infection with *T. gondii* and *N. caninum*. Despite the general similarities that have been identified, a few interesting differences were discovered from phosphorylation sites/ phosphomotifs distribution and quantitative analysis of differential regulations of signalling pathways. The

differences in host protein phosphorylation and modification of signalling pathways, e.g. glycolysis/gluconeogenesis and mTOR signalling pathway potentially associate with the differences in the biology of *T. gondii* and *N. caninum*. High modulation of glycolysis/gluconeogenesis and mTOR signalling pathway during *T. gondii* infection is potentially more associated with the differences in virulence and transmission routes compared to infection with *N. caninum*.

Chapter FIVE: Comparative host cell response to infection with *T. gondii* and *N. caninum* using transcriptome, proteome and phosphoproteome

5.1. INTRODUCTION

Genome, proteome and genome-wide post-translational modification analyses allow for the understanding of functional relationships between genes, mRNAs, proteins and their functional state in both physiological and pathological conditions such as in response to different pathogens. Genomic and transcriptomic analyses provide a global view of how a cell functions as a system in the regulation of gene expression (Komili and Silver, 2008). In addition, the study of genome-wide proteomics is essential for understanding the phenotype and system biology of cellular processes (Cox and Mann, 2011). Conventionally, analyses and attempts to understand different steps elaborated in the regulation of gene expression, RNA transcription-maturation, mRNA processing, nuclear export, translation and degradation were analysed separately; these analyses were based on using biochemical techniques which gave the impression that they function independently (Komili and Silver, 2008).

Protein synthesis is the end product of gene expression; therefore, this suggests that there is a positive correlation between mRNA expression and high protein synthesis. Despite that fact, a number of studies have shown poor correlations between mRNA expression and high protein synthesis. A correlation of approximately 40 % between mRNA expression and protein abundance was reported (De Sousa Abreu *et al.*, 2009; Maier *et al.*, 2009). Furthermore, Shankavaram *et al.* (2007) performed a comparative study of cancer cell transcripts and proteins expression profiling and reported that 65 % of the transcripts and proteins were significantly correlated. Likewise, Lu *et al.* (2007) demonstrated that the correlation between protein abundance and mRNA expression in yeast cells was approximately 73 %. These data suggest that protein abundance cannot be predicted based on mRNA expression alone and that post-transcriptional, translational and PTMs of protein should be considered (Jüschke *et al.*, 2013; Nelson *et al.*, 2008). A poor correlation between mRNA expression and protein level is attributed to three reasons; firstly the regulatory processes involved in the course of gene expression such as microRNAs (miRNAs) interactions, miRNAs is another large family of small RNA of 21-25 nucleotides), secondly due to PTMs of protein resulting in altered half-life of involved proteins, and thirdly the detection method used (Perco *et al.*,

2010). Therefore, it is important to use quantitative systems biology approaches to understand all the processes contributing to gene expression (Jüschke *et al.*, 2013).

5.1.1. Gene regulation of host cell in a host-pathogen interaction system

Gene expression is regulated by several different methods in a signalling-dependent manner from internal or external stimuli. Genes are transcribed to different types of RNAs that are modified post-transcriptionally to produce different functional RNAs by alternative splicing. Genes expression in eukaryotes are controlled both at the gene transcription level and post-translational stages (Figure 5.1) including pre-mRNA splicing and mRNA transport, mRNA translation, mRNA decay (Arraiano and Maquat, 2003) and protein degradation (Jovanovic *et al.*, 2015). Messenger RNA is the most abundant RNA that translates to proteins while miRNAs play a role as negative regulator of gene expression through translational repression and mRNA cleavage, cancer development and probably involved in regulation of different part of cellular processes, as reviewed in (He and Hannon, 2004; Su *et al.*, 2014; Tie and Fan, 2011). Post-transcriptional regulation of gene expression by small RNAs may be partly responsible for the low correlation reported between transcripts and protein abundance (Ghazalpour *et al.*, 2011; Vogel and Marcotte, 2012) and reducing the predictive efficiency of protein expression based on transcripts (Jüschke *et al.*, 2013).

Quantitative analysis of posttranscriptional and translational data are crucial for better understanding of genetic information (Vogel and Marcotte, 2012). Post translational regulation of genes is determined by several factors such as protein modifications and degradation. These modifications determine the status of protein; protein turnover is one of the consequences of these modification (Mann and Jensen, 2003). Degradation of protein is another way that allows proteome of a cell to remodel continuously and especially in response to pathogens (Jovanovic *et al.*, 2015). Pathogens play role as external stimuli through secretion of an array of molecules on/into the cells leading to host cell perturbation and re-programming of host cell genes necessary for evading host immunity, nutritional acquisition and proliferation (Bougdour *et al.*, 2013; Braun *et al.*, 2013; Butcher *et al.*, 2011). Studying host response to infection is critical for understanding the molecular mechanism involved in host-parasite interaction. Studies of integrated systems

biology such as transcriptomics, proteomics and phosphoproteomics of host cell in response to infection with pathogens could be very important to highlight mechanisms underlying infections.

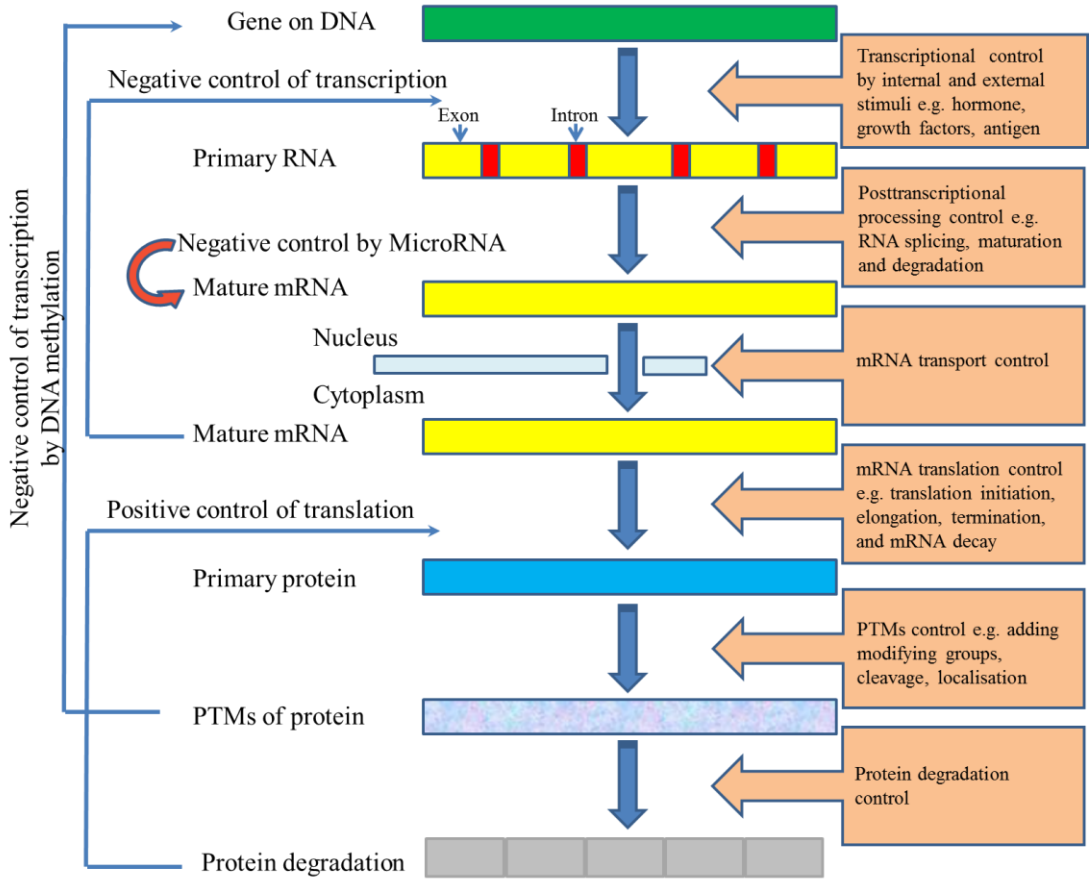

Figure 5.1: Schematic representation of gene regulation in eukaryotes.

5.1.2. Analysis of transcriptome and proteome of host cells in response to pathogens

Transcriptional profiling has been studied in host cells in response to infection with different pathogens. Different pathogens release different arrays of molecules that are associated with host-pathogen interactions. Microarray profiling of host cell in response to *T. gondii* infection has revealed several unknown modulation such as up-regulation of the abundance of transcripts related to immune response and modulation of genes involved in important cellular processes such as metabolism and apoptosis (Blader *et al.*, 2001). In addition, microarray analysis of host immune cells such as macrophages and dendritic cells reveals distinct differences in the regulation of genes in response to different pathogens such as intracellular *T. gondii*, *Leishmania* and *Mycobacterium* and extracellular nematode *Brugia malayi* (Chaussabel *et al.*, 2003). RNA sequencing of mice forebrains in response to infection with *T. gondii* revealed that the majority of the overexpressed transcripts in acute and chronic infections were associated with transcription and translation processes (Pittman *et al.*, 2014). Furthermore, they found that in response to chronic infection, host cells up-regulate transcripts associated with immunity twice more than acute infection. These studies indicate that host cells are remodelled in response to infection leading to modulation of host gene regulation, suggesting that RNA analysis is important to study global gene regulation in response to different pathogens.

Proteomics data analysis is considered a perfect complementary set of transcriptomics analysis of any cell at a given time (Walduck *et al.*, 2004). Genome wide proteome study of host cell in response to infection revealed that host cell proteome is extensively remodelled by pathogens. In response to *T. gondii*, quantitative 2D SDS-PAGE of infected host cell proteome showed that it was consistently changed and the proteins involved in important biological processes were significantly modulated such as glucose, lipid and cholesterol metabolism, mitosis and apoptosis (Nelson *et al.*, 2008). In response to bacterial infection such as *Salmonella enterica* Typhimurium, quantitative proteomic analysis of infected macrophages using mass spectrometry found that the quantified proteins played roles in diverse biological processes implying that they cause global responses (Shi *et al.*, 2009). In addition, in response to intracellular bacteria such as *Mycobacterium*

tuberculosis lipids, quantitative proteomics showed that host proteins involved in innate immune system and lipids metabolic processes were highly up regulated (Shui *et al.*, 2009). However, it is found that protein expression cannot be predicted based on transcripts alone because PTMs of protein and Post-transcriptional regulation of mRNA should also be considered (Jüschke *et al.*, 2013; Nelson *et al.*, 2008; Yang *et al.*, 2015). Recent study of host response to pathogens showed that there is direct relationship between mRNA abundance and protein expression following infection and that the fate of the pre-exited proteins is controlled by protein production and proteolysis (Jovanovic *et al.*, 2015). These studies are inferring that individual analysis of omics is compromised by the fact that none of the analysis produces system wide information about host response to infection. Thus, to understand global response of host cell to infection and how different omics respond relative to each other in response to pathogens; analyses of transcriptome, proteome and phosphoproteome simultaneously provide complementary integrative information at the system level.

5.1.3. Aims and objectives of the study:

Despite close similarity at the genomic and transcriptomic level between the two parasites, there are interesting differences in the host response to infection with *T. gondii* and *N. caninum*. The mechanism of these differences is not known which makes studying the comparative host response on a system biology level a valuable approach to decipher the differences. The present study is aimed to compare host cell responses to infection with *T. gondii* and *N. caninum* at an integrated transcriptomic, proteomic and phosphoproteomic level.

5.2. MATERIAL AND METHODS

5.2.1. Host data collection

Integrated system biology analysis was carried out for HFF cell gene regulation in response to infection with *T. gondii* and *N. caninum* at 36 hr p.i. Transcriptomic and proteomic expression data of host cell were downloaded from HostDB version2.2 (http://beta.hostdb.org/hostdb.b23/getDataset.do?display=detail). Data were generated by Professor Wastling's group at the University of Liverpool and hosted on HostDB. Only a single (averaged) expression value for each mRNA and protein is available on HostDB. To improve statistical power in data analysis, triplicate of host cell proteomes data were provided by Dr Dong Xia, University of Liverpool. Phosphoproteome data used in this chapter were generated in chapter 4.

5.2.2. Time point infection and data generation

According to HostDB, *T. gondii* and *N. caninum* were initially cultured in Vero cells before being used for infection of HFF cells. Confluent monolayer of HFF cells were infected with 1×10^7 tachyzoites of *T. gondii* and *N. caninum* and allowed to grow for 36 hr p.i. Infected HFF cells were collected using a cell scraper.

Transcripts and proteins were prepared from infected HFF cells at 36 hr p.i. and mRNA data were generated using RNA sequencing and individual value for each transcripts was provided in RPKM (Reads Per Kilobase per Million) which is a quantitative approximations of the abundance of target transcripts. Protein data were generated using LC-MS/MS following trypsin digestion and individual values were measured in iBAQ (Intensity Based Absolute Quantification). Generated spectra from LC-MS/MS were searched using Mascot version 2.3 against human protein reference sequence database (UniProt, May 2013).

Quantitative phosphoproteome data were generated as described in chapter 4.

The time point of transcriptome and proteome of host cells in response to infection at 36 hr p.i. and phosphoproteome at 20 hr p.i were chosen based on the same biological conditions where tachyzoites were just about to egress in the culture.

Transcriptomics data were filtered to remove transcripts with zero value. The transcripts of host cell infected with *T. gondii* and *N. caninum* were matched and to avoid ambiguity, only matched transcripts that had unique IDs (one gene expressed to one transcript) was selected and used in the analysis.

Proteome of host cells infected with *T. gondii* and *N. caninum* were matched and only matched host proteins were selected for analysis.

5.2.3. Quantitative data analysis of host cell in response to infection with *T. gondii* and *N. caninum*

Matched transcripts and proteins of *T. gondii* and *N. caninum* were normalised separately using online software Normalyzer (Chawade *et al.*, 2014). Because of the availability of only one replicate of host transcripts, an artificial replicate was generated where individual values of each individual transcripts of original replicate were multiplied by 1.2. Artificial replicates were generated because of the software requirement of at least two replicates from each condition to be processes for normalisation. Following normalisation, the normalisation method with low intra group variation was selected.

Following normalisation, transcripts and proteins were matched based on overlapping IDs. Only matched IDs were used for quantitative analysis of transcripts and proteins in response to infection with *T. gondii* and *N. caninum*.

Fold change (FC) of transcripts and proteins in host cell infected with *T. gondii* to *N. caninum* was calculated and a cut-offs of ≥ 2 FC or < 2 FC were applied to determine significantly increase or decrease in expression, respectively. The IDs that matched the cut-off applied were analysed in DAVID Bioinformatics Resources version 6.7 (Huang *et al.*, 2008) for enrichment of biological process in gene ontology (GOTERM_BP_FAT) enrichment.

Quantified protein data were visualised by scatter (volcano) plot using Minitab software version 17 (Minitab Inc. 2010) to identify the changes in host cell proteins in response to both infection.

5.3. RESULTS

5.3.1. Normalised data from transcriptome and proteome of host cell in response to *T. gondii* and *N. caninum* infection

Transcriptome and proteome from host cell infected with *T. gondii* and *N. caninum* were normalised to reduce biases introduced during sample processing and data generation. Figure 5.2 shows normalised data from host proteome in response to infection with *T. gondii* and *N. caninum*. Normalised VSN-G (Variance stabilising normalisation) shows lowest intragroup variation of PMAD (pooled intragroup median absolute deviation) which is equal to 49 % compared to Log_2 of un-normalised data which is considered as 100 %. Based on the Normalyzer, lower PMAD value compared to Log_2 of un-normalised data suggests better normalization. Although VSG-R has a lower PMAD value, VSN-G was still selected because this method is based on global normalization of the compared groups rather than intragroup normalisation methods separately e.g. VSG-R.

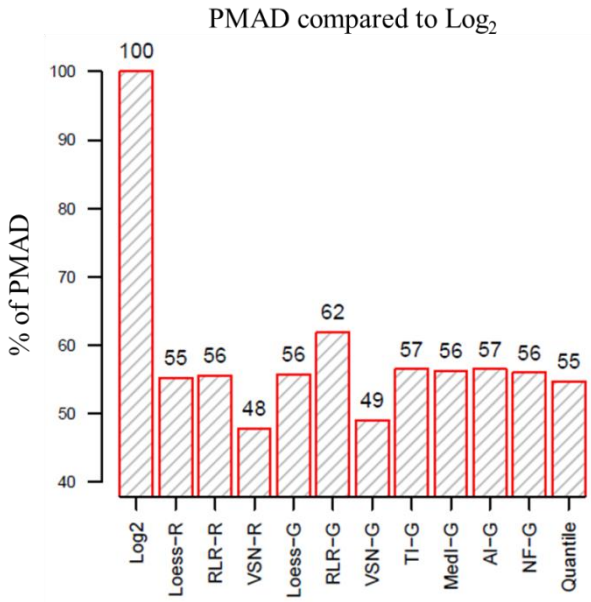

Figure 5.2: Normalisation of proteome of hot cell in response to infection with *T. gondii* and *N. caninum* at 36 hr p.i. Log_2 of PMAD in un-normalised data is considered as 100 %. PMAD: pooled intragroup median absolute deviation. Normalyzer software use several common normalization methods such as LOESS (limma package), Robust Linear Regression (RLR), Variance Stabilizing Normalization (VSN, vsn package), total intensity (TI), median intensity (MedI), average intensity (AI), NormFinder (NF) and quantile (preprocessCore package). The methods used global normalization methods (referred to as 'G'), while those used intragroup normalisation methods separately (referred to as 'R').

5.3.2. Total number of transcripts and proteins identified from analysis of host cell infected with *T. gondii* and *N. caninum* at 36 hr p.i.

After excluding zero values, total number of quantified transcripts in *T. gondii* and *N. caninum* infected host cells was 23635 and 10311, respectively as shown in Figure 5.3a. The differences in the number of transcripts of *T. gondii* and *N. caninum* might have caused by the differences in the cut-off threshold applied for separation of expressed RNA sequence from background noise. In total, 10305 host transcripts were matched between both infections. However, only the genes that had unique transcript were included in this analysis which comprised of 4485 gene IDs. On the other hand, total number of protein quantified from both conditions at the same time point was 926 and 1318 and out of these, 808 host proteins were matched between both infections as shown in Figure 5.3b. There are 403 genes that were matched between transcriptomics and proteomics data which is shown in Figure 5.4.

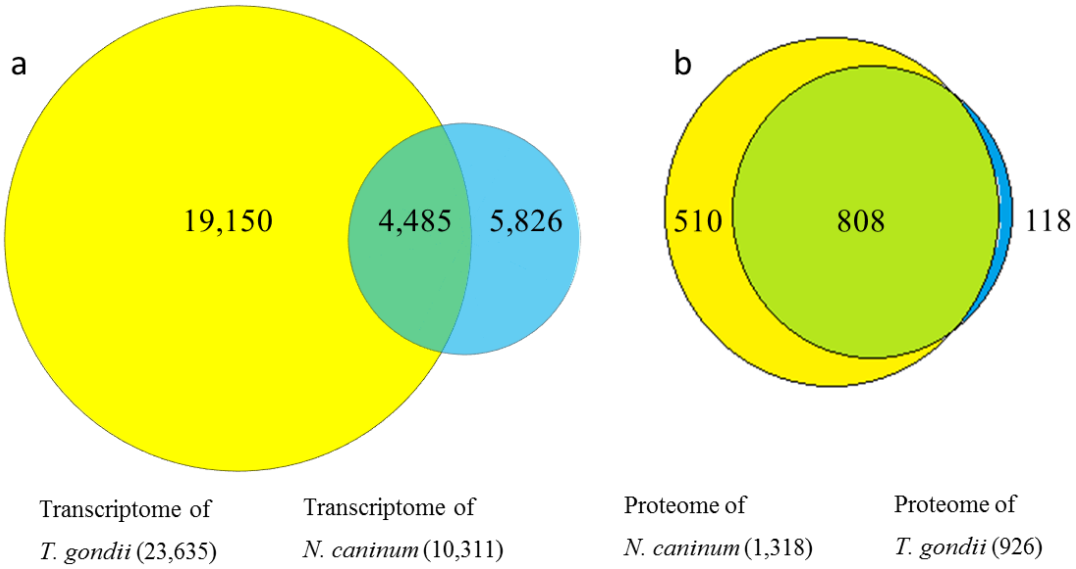

Figure 5.3: Total number of identified transcripts and proteins from host cell infected with *T. gondii* and *N. caninum* at 16 hr p.i. a: total number of transcripts and overlap of one gene to one transcript between infection with *T. gondii* and *N. caninum*. b: total number of proteins and overlap between infection with *T. gondii* and *N. caninum*.

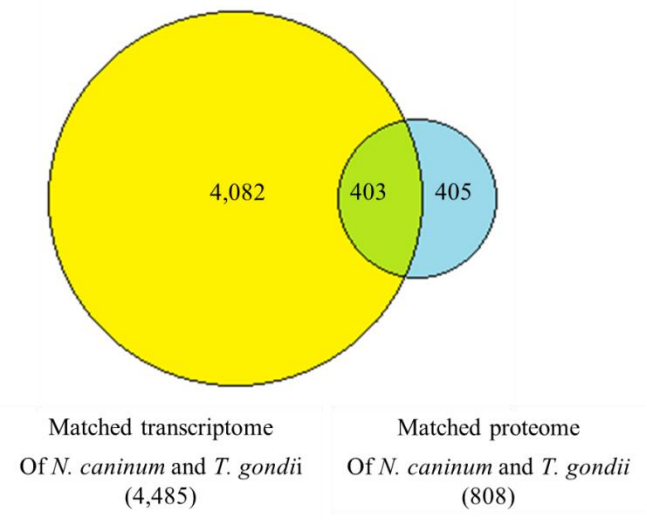

Figure 5.4: Total number of overlapped transcripts and proteins from host cell infected with *T. gondii* and *N. caninum* at 16 hr p.i.

5.3.3. Functional analysis of the transcripts and proteins between host cells infected with *T. gondii* and *N. caninum*

5.3.3.1. Overlapped transcripts in response to infection with *T. gondii* and *N. caninum*

The overlapped 403 gene IDs from transcripts of host cell infected with *T. gondii* and *N. caninum* were analysed for enriched biological processes (BP) using DAVID tool. Based on the fold change (FC) value of the analysed transcripts of *T. gondii* to *N. caninum* infections, the 403 transcripts were divided into three groups; host transcripts with greater than two folds expression in *T. gondii* infection than in *N. caninum* infection, host transcripts with greater than two folds expression in *N. caninum* infection and transcripts that do not exhibit significant expression changes ($\geq$ - 2 and $\leq$ + 2) between the two infections. 100 (25 %) transcripts were highly expressed in *T. gondii* infection while 22 (5 %) transcripts were found highly expressed in *N. caninum* infection (Figure 5.5). The high similarity of 70 % (281 transcripts) of the expressed host transcripts indicates a generally similar host response upon infection of the two parasites.

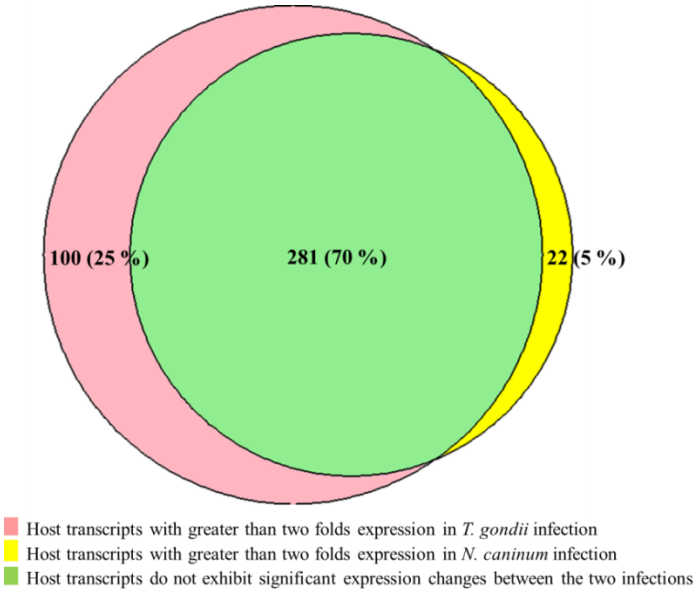

Figure 5.5: Total number of transcripts of host cell infected with *T. gondii* and *N. caninum*. Transcripts divided based on the cut-off applied, host transcripts with greater than two folds expression in *T. gondii* infection than in *N. caninum* infection, host transcripts with greater than two folds expression in *N. caninum* infection and transcripts that do not exhibit significant expression changes (≥ - 2 and ≤ + 2) between the two infections.

5.3.3.1.1. Biological processes enriched from host transcripts significantly overexpressed in *N. caninum* infection

Enriched biological processes were analysed using DAVID tool for host transcripts that significantly overexpressed in *N. caninum* infection. Figure 5.6 shows the biological processes with enrichment fold, while Table 5.1 shows the host transcripts associated with each BP and Appendix Table VII shows the detailed information about each BP enriched. BPs enriched for these transcripts are mostly associated with negative regulation of cellular protein metabolic process and protein catabolic process. In addition, transcripts associated with positive regulation of inflammatory response to pathogen were also enriched in *N. caninum* infection. *T. gondii* type I and III strains were found to negatively regulate inflammatory response of the host cells mediated by cytokine IL-12 (Ong *et al.*, 2010; Saeij *et al.*, 2007; Yamamoto *et al.*, 2009).

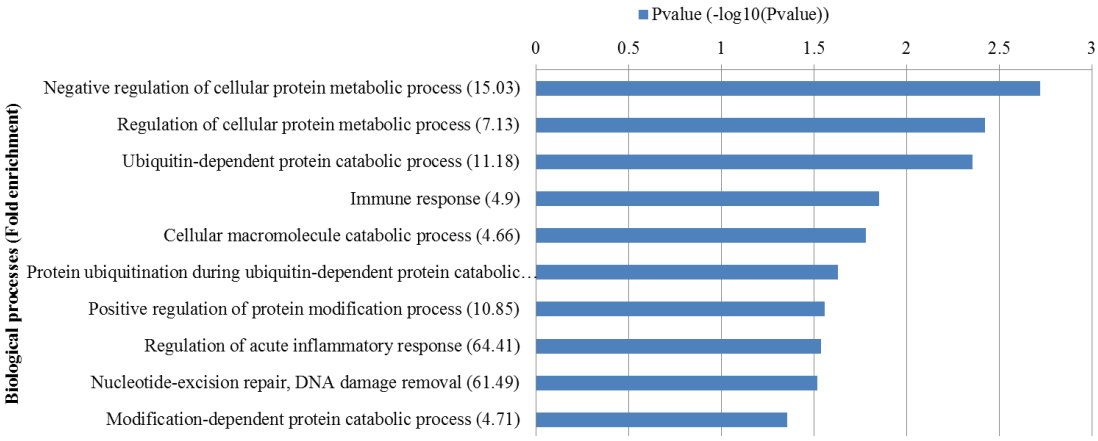

Figure 5.6: Biological processes enriched for host transcripts significantly overexpressed in *N. caninum* infection

Table 5.1: Biological processes enriched from host transcripts significantly overexpressed in *N. caninum* infection.

Biological processes	**Gene IDs**	**Protein name**
Negative regulation of cellular protein metabolic process	P43686	26S protease regulatory subunit 6B, PSMC4
	P17980	26S protease regulatory subunit 6A, PSMC3
	P38919	Eukaryotic initiation factor 4A-III, EIF4A3
	P01023	Alpha-2-macroglobulin, A2M
	Q16531	DNA damage-binding protein 1, DDB1
Positive regulation of protein metabolic process	P43686	26S protease regulatory subunit 6B, PSMC4
	P17980	26S protease regulatory subunit 6A, PSMC3
	P60033	CD81 antigen, CD81
Positive regulation of acute inflammatory response and immune responses	P30443	HLA class I histocompatibility antigen, A-1 alpha chain, HLA-A
	Q86WV6	Stimulator of interferon genes protein, TMEM173
	Q01628	Interferon-induced transmembrane protein 3, IFITM3
	P01024	Complement C3, C3
	P02794	Ferritin heavy chain, FTH1
	P01023	Alpha-2-macroglobulin, A2M

5.3.3.1.2. Biological processes enriched from host transcripts significantly overexpressed in *T. gondii* infection

The enriched biological processes from host transcripts significantly overexpressed in *T. gondii* infection were also analysed in DAVID tool. Figure 5.7 shows the biological processes with enrichment fold, while Table 5.2 shows the host transcripts associated with each BP and Appendix Table VIII shows the detailed information about each BP enriched. Almost all the biological processes enriched associate with protein production which indicates that infected host cell is in high demand to build up more protein during infection with *T. gondii* than in *N. caninum*. The top ten biological processes enriched (Figure 5.7) associates with RNA processing, translation, PTM of protein, intracellular protein transport and protein targeting. In addition, molecules associated with anti-apoptosis were highly enriched in *T. gondii* infection; suggesting that it reprograms host cell to maintain infection long enough before egress.

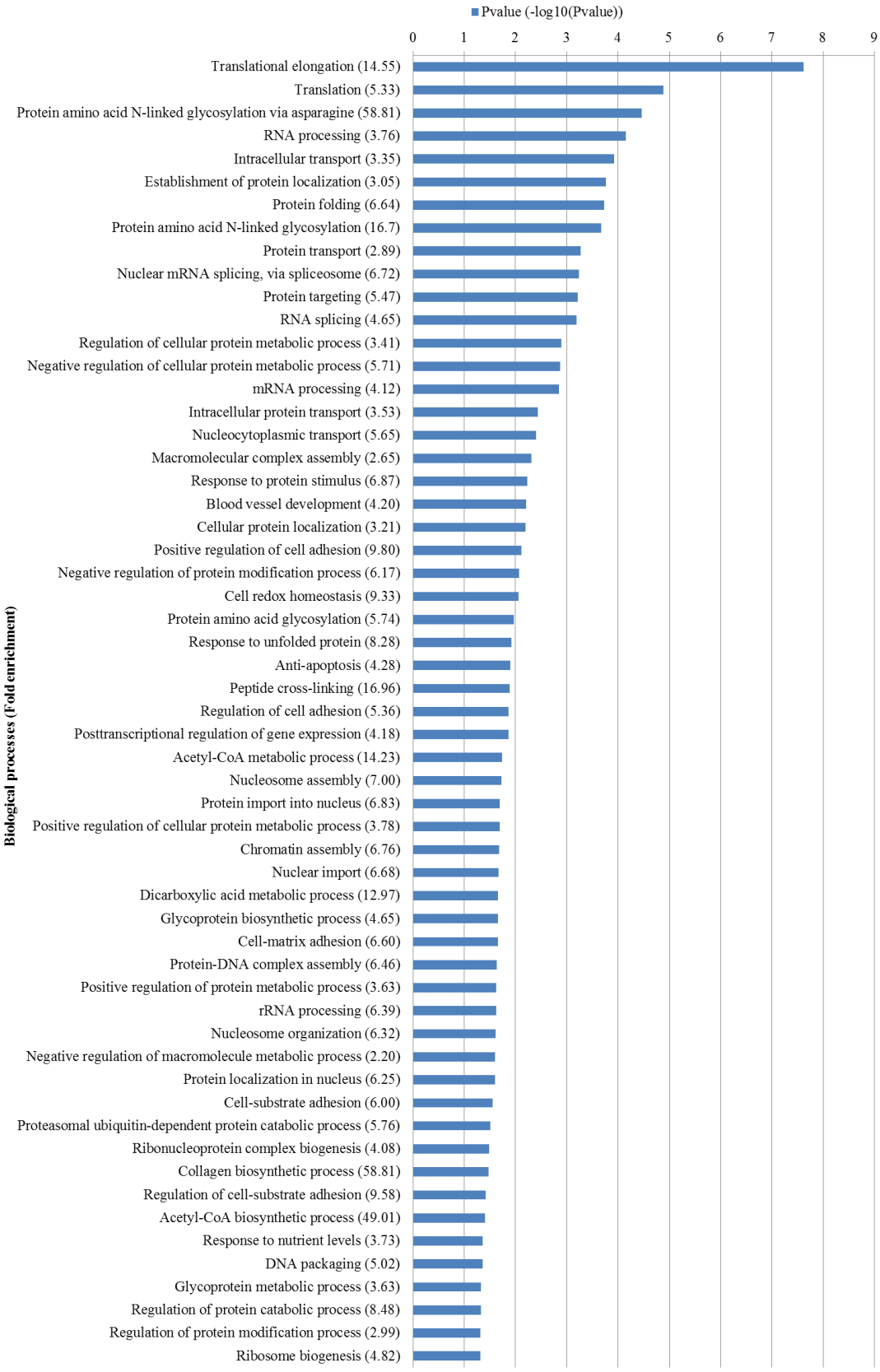

Figure 5.7: Biological processes based on pvalue enriched from DAVID tool for host transcripts significantly overexpressed in *T. gondii* infection

Table 5.2: Biological processes enriched from host transcripts significantly overexpressed in *T. gondii* infection.

Biological processes	Gene IDs	Protein name
RNA processes	Q9Y3F4	Serine-threonine kinase receptor-associated protein, STRAP
	Q9Y2X3	Nucleolar protein 58, NOP58
	O75533	Splicing factor 3B subunit 1, SF3B1
	Q07955	Serine/arginine-rich splicing factor 1, SRSF1
	P11940	Polyadenylate-binding protein 1, PABPC1
	Q08170	Serine/arginine-rich splicing factor 4,
	P62906	60S ribosomal protein L10a, RPL10A
	Q9UQ80	Proliferation-associated protein 2G4, PA2G4
	P62995	Transformer-2 protein homolog beta, TRA2B
	Q6P2Q9	Pre-mRNA-processing-splicing factor 8, PRPF8
	Q00839	Heterogeneous nuclear ribonucleoprotein U, HNRNPU
	P38159	RNA-binding motif protein, X chromosome, RBMX
Translation elongation	P36578	60S ribosomal protein L4, RPL4
	P07814	Bifunctional glutamate/proline-tRNA ligase, EPRS
	P05387	60S acidic ribosomal protein P2, RPLP2
	P62750	60S ribosomal protein L23a, RPL23A
	P35268	60S ribosomal protein L22, RPL22
	P84098	60S ribosomal protein L19, RPL19
	P61247	40S ribosomal protein S3a, RPL3A
	P62906	60S ribosomal protein L10a, RPL10A
	Q02878	60S ribosomal protein L6, RPL6
	P62081	40S ribosomal protein S7, RPS7
	P62851	40S ribosomal protein S25, RPS25
	P41091	Eukaryotic translation initiation factor 2 subunit 3, EIF2S3
Protein folding	P11142	Heat shock cognate 71 kDa protein, HSPAB
	Q14554	Protein disulfide-isomerase A5, PDIA5
	P08238	Heat shock protein HSP 90-beta, HSP90AB1
	P14625	Endoplasmin, HSP90B1
	P78371	T-complex protein 1 subunit beta, CCT2
	P17987	T-complex protein 1 subunit alpha, TCP1
	P49257	Protein ERGIC-53, LMAN1
	P38646	Stress-70 protein, mitochondrial, HSPA9
Glycosylation	Q8TCJ2	Dolichyl-diphosphooligosaccharide-protein glycosyltransferase subunit STT3B, STT3B
	P04843	Dolichyl-diphosphooligosaccharide-protein glycosyltransferase subunit 1, RPN1
	Q9H0U3	Magnesium transporter protein 1, MAGT1
	P46977	Dolichyl-diphosphooligosaccharide-protein glycosyltransferase subunit STT3A, STT3A
	Q16706	Alpha-mannosidase 2, MAN2A1
	Q16706	Alpha-mannosidase 2, MAN2A1
Protein targeting and transporting	P09936	Ubiquitin carboxyl-terminal hydrolase isozyme L1,UCHL1
	Q01105	Protein SET, SET
	P53007	Tricarboxylate transport protein, mitochondrial, SLC25A1
	Q14974	Importin subunit beta-1, KPNB1
	P49257	Protein ERGIC-53, LMAN1
	Q9Y2X3	Nucleolar protein 58, NOP58
	P43307	Translocon-associated protein subunit alpha, SSR1
	P38646	Stress-70 protein, mitochondrial
	P09038	Fibroblast growth factor 2, FGF2
	P27348	14-3-3 protein theta, YWHAQ
	P11142	Heat shock cognate 71 kDa protein, HSPA8

	P61106	Ras-related protein Rab-14, RAB14
	P62258	14-3-3 protein epsilon, YWHAE
	P62826	GTP-binding nuclear protein Ran, RAN
	Q00610	Clathrin heavy chain 1, CLTC
	P02452	Collagen alpha-1(I) chain, COL1A1
	Q9NP72	Ras-related protein Rab-18, RAB18
	P13667	Protein disulfide-isomerase A4, PDIA4
	P17301	Integrin alpha-2, ITGA2
	P14625	Endoplasmin, HSP90B1
Cellular macromolecular complex assembly	Q07955	Serine/arginine-rich splicing factor 1, SRSF1
	P0C0S5	Histone H2A.Z, H2AFZ
	P07814	Bifunctional glutamate/proline-tRNA ligase, EPRS
	Q14974	Importin subunit beta-1, KPNB1
	Q01105	Protein SET, SET
	P21980	Protein-glutamine gamma-glutamyltransferase 2, TGM2
	P17987	T-complex protein 1 subunit alpha, TCP1
	P07305	Histone H1.0, H1F0
	Q9NVA2	Septin-11, SEPT11
	Q9BUF5	Tubulin beta-6 chain, TUBB6
	Q5SSJ5	Heterochromatin protein 1-binding protein 3, HP1BP3
	Q16181	Septin-7, SEPT7
Regulation of cellular protein metabolic processes	P09038	Fibroblast growth factor 2, FGF2
	P48556	26S proteasome non-ATPase regulatory subunit 8, PSMD8
	O43242	26S proteasome non-ATPase regulatory subunit 3, PSMD3
	Q13200	26S proteasome non-ATPase regulatory subunit 2, PSMD2
	Q01105	Protein SET, SET
	P08238	Heat shock protein HSP 90-beta, HSP90AB1
	P17301	Integrin alpha-2, ITGA2
	P62258	14-3-3 protein epsilon, YWHAE
	Q9UQ80	Proliferation-associated protein 2G4, PA2G4
	P07996	Thrombospondin-1, THBS1
	P04792	Heat shock protein beta-1, HSPH1
Anti-apoptosis	P21980	Protein-glutamine gamma-glutamyltransferase 2, TGM2
	P14625	Endoplasmin, HSP90B1
	P09429	High mobility group protein B1, HMGB1
	P07996	Thrombospondin-1, THBS1
	P04792	Heat shock protein beta-1, HSPB1
	P38646	Stress-70 protein, mitochondrial, HSPA9

5.3.3.2. Overlapped proteome in response to infection with *T. gondii* and *N. caninum*

The overlapped 403 proteins IDs from host cell infected with *T. gondii* and *N. caninum* were analysed for enriched biological processes using DAVID tool as performed for host transcripts. The 403 proteins were divided into three groups using the same criteria as transcriptome data analysis. In total, 116 (29 %) proteins were highly expressed in *T. gondii* infection while 98 (24 %) proteins were found highly expressed in *N. caninum* infection. The lower similarity of 47 % (192 proteins) at protein level than transcript level in response to infection with these parasites indicates a more divergent protein response upon infection of the two parasites as shown in Figure 5.8.

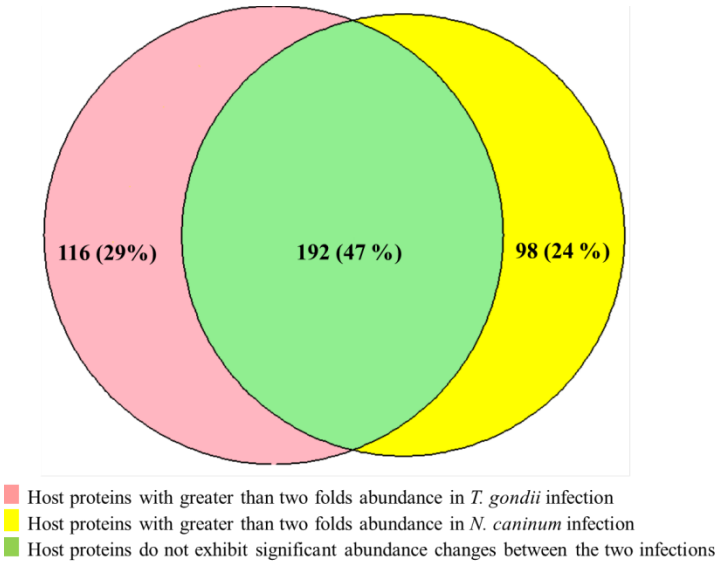

Figure 5.8: Total number of proteins of host cell infected with *T. gondii* and *N. caninum*. Proteins divided based on the cut-off applied, host proteins with greater than two folds expression in *T. gondii* infection than in *N. caninum* infection, host proteins with greater than two folds expression in *N. caninum* infection and proteins that do not exhibit significant expression changes (≥ - 2 and ≤ + 2) between the two infections.

The quantified proteins matched between *T. gondii* and *N. caninum* infections are presented in the volcano plot below (figure 5.9). Highly expressed host proteins upon *T. gondii* infection (top-right of the plot) include positive regulation of translation processes; while the highly expressed host proteins upon *N. caninum* infection (top-left of the plot) includes molecules associated with energy and protein production (Figure 5.9). To understand the enriched biological processes of these

proteins and to compare with transcriptomics data, same functional analysis was performed using DAVID tool.

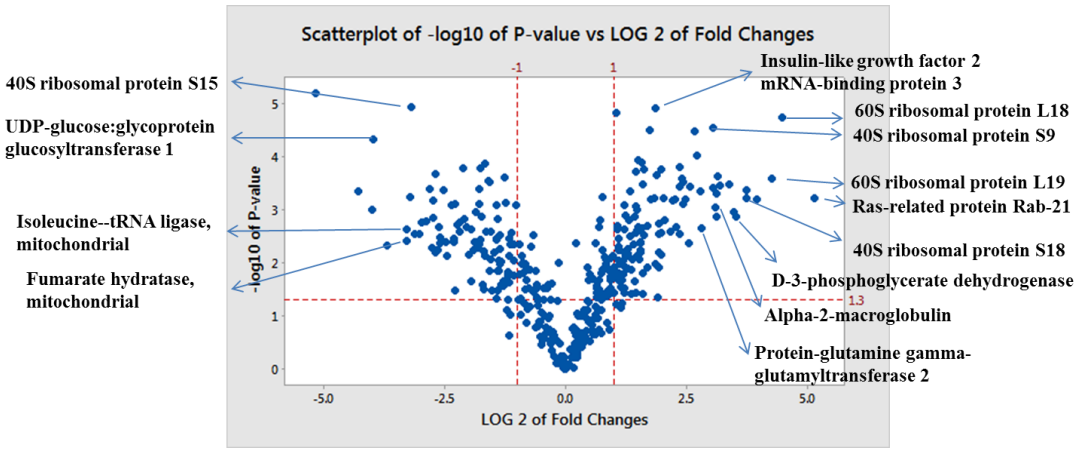

Figure 5.9: Volcano plot of quantified host proteins infected with *T. gondii* and *N. caninum* at 36 hr p.i. The volcano plot shows p-value versus FC of quantified proteins of host cell infected with the two parasites. Red dash line on y-axis at 1.3 is equal to p-value of 0.05. Red dash line at + 1 and - 1 on x-axis are equivalent to FC of host proteins. Host proteins located at the top-right corner are highly expressed in *T. gondii* infection; while host proteins on the top-left corner are highly expressed in *N. caninum* infection.

5.3.3.2.1. Biological processes enriched from host proteins significantly expressed in *N. caninum* infection

The biological processes enriched for host proteins significantly overexpressed in *N. caninum* are shown in Figure 5.10, Table 5.3 and Appendix Table III. Figure 5.10 shows the BP with enrichment fold, while Table 5.3 shows the host transcripts associated with each BP and Appendix Table IX shows the detailed information about each BP enriched. The BPs enriched show that the overexpressed proteins in *N. caninum* infection are involved in generation of precursor metabolites and energy such as monosaccharide catabolic processes, glycolysis, aerobic respiration, coenzyme catabolic process and tricarboxylic acid cycle. In addition, proteins associated with protein production and processing are overexpressed in *N. caninum* infection such as translation processes, protein transport and targeting and protein folding.

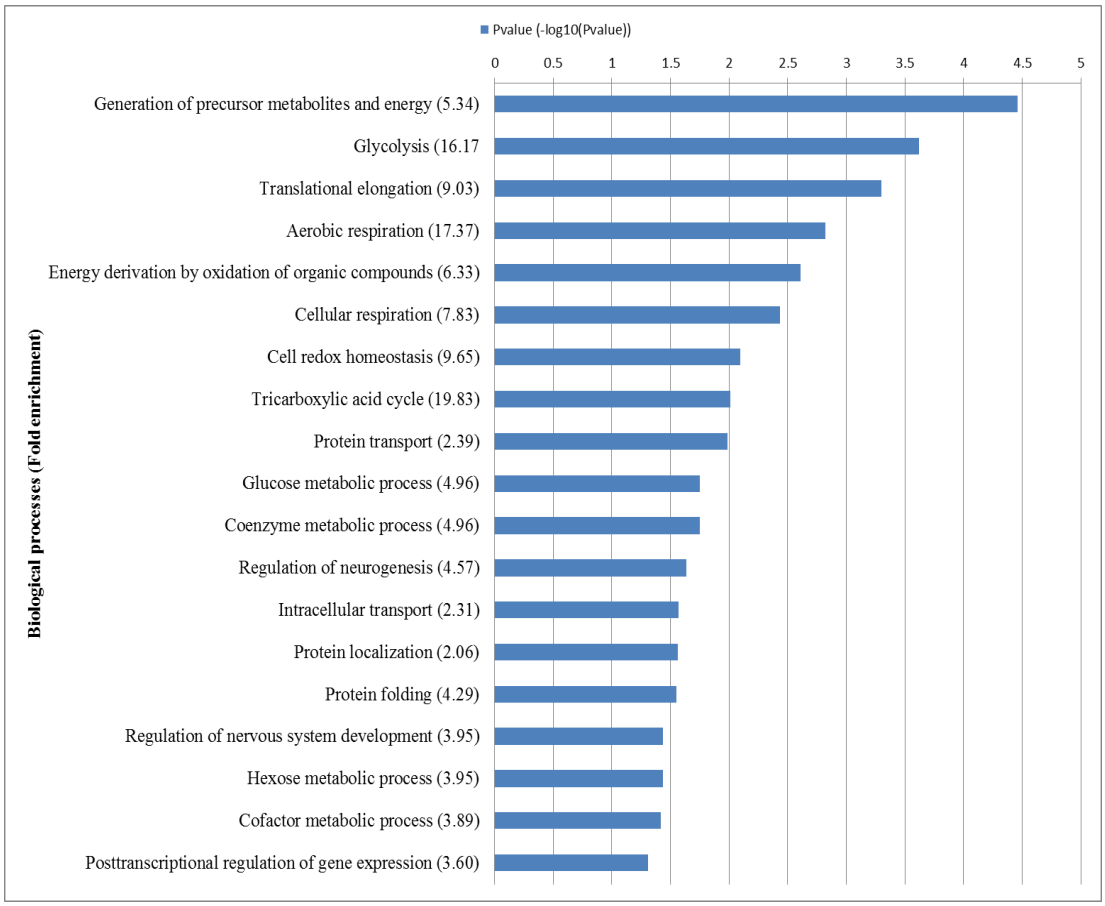

Figure 5.10: Biological processes enriched in DAVID tool from host proteins significantly overexpressed in *N. caninum* infection

Table 5.3: Table 5.3: Biological processes enriched from host proteins significantly overexpressed in *N. caninum* infection at 36 hr p.i.

Biological processes	**Gene IDs**	**Protein name**
Generation of precursor metabolites and energy	Q5JWF2	Guanine nucleotide-binding protein G(s) subunit alpha isoforms XLas, GNAS
	P31040	Succinate dehydrogenase [ubiquinone] flavoprotein subunit, mitochondrial, SDHA
	P04406	Glyceraldehyde-3-phosphate dehydrogenase, GAPDH
	P60174	Triosephosphate isomerase, TPI1
	P49821	NADH dehydrogenase [ubiquinone] flavoprotein 1, mitochondrial, NDUFV1
	P00558	Phosphoglycerate kinase 1, PGK1
	P06733	Alpha-enolase, ENO1
	P07954	Fumarate hydratase, mitochondrial, FH
	O75390	Citrate synthase, mitochondrial, CS
	P22695	Cytochrome b-c1 complex subunit 2, mitochondrial, UQCRC2
	P17858	ATP-dependent 6-phosphofructokinase, liver type, PFKL
	O00764	Pyridoxal kinase, PDXK
Translation processes	P26641	Elongation factor 1-gamma, EEF1G
	P61513	60S ribosomal protein L37a, RPL37A
	P27635	60S ribosomal protein L10, RPL10
	P46778	60S ribosomal protein L21, RPL21
	P35268	60S ribosomal protein L22, RPL22
	P62841	40S ribosomal protein S15, RPS15
	Q9NSE4	Isoleucine--tRNA ligase, mitochondrial, IARS2
Intracellular protein transport and targeting	Q5JWF2	Guanine nucleotide-binding protein G(s) subunit alpha isoforms XLas, GNAS
	P13667	Protein disulfide-isomerase A4, PDIA4
	P27348	14-3-3 protein theta, YWHAQ
	O75396	Vesicle-trafficking protein SEC22b, SEC22B
	Q01082	Spectrin beta chain, non-erythrocytic 1, SPTBN1
	P62258	14-3-3 protein epsilon, YWHAE
	P46459	Vesicle-fusing ATPase, NSF
	Q9Y5X1	Sorting nexin-9, SNX9
	Q15363	Transmembrane emp24 domain-containing protein 2, TMED2
	P27797	Calreticulin, CALR
	O43707	Alpha-actinin-4, ACTN4
	P61981	14-3-3 protein gamma, YWHAG
Protein folding	Q15084	Protein disulfide-isomerase A6, PDIA6
	Q9NYU2	UDP-glucose:glycoprotein glucosyltransferase 1, UGGT1
	P48643	T-complex protein 1 subunit epsilon, CCT5
	P27797	Calreticulin, CALR
	O60884	DnaJ homolog subfamily A member 2, DNAJA2

5.3.3.2.2. Biological processes enriched from host proteins significantly overexpressed in *T. gondii* infection

The biological processes enriched using DAVID tool for the host proteins significantly overexpressed in *T. gondii* infection with enrichment fold are shown in Figure 5.11. Table 5.4 shows the host transcripts associated with each BP while Appendix Table X shows the detailed information about each BP enriched. Several biological processes were highly enriched such as translation processes, RNA processes, ribosomal biogenesis, protein transport and targeting, protein folding, phagocytosis and responses to inflammation.

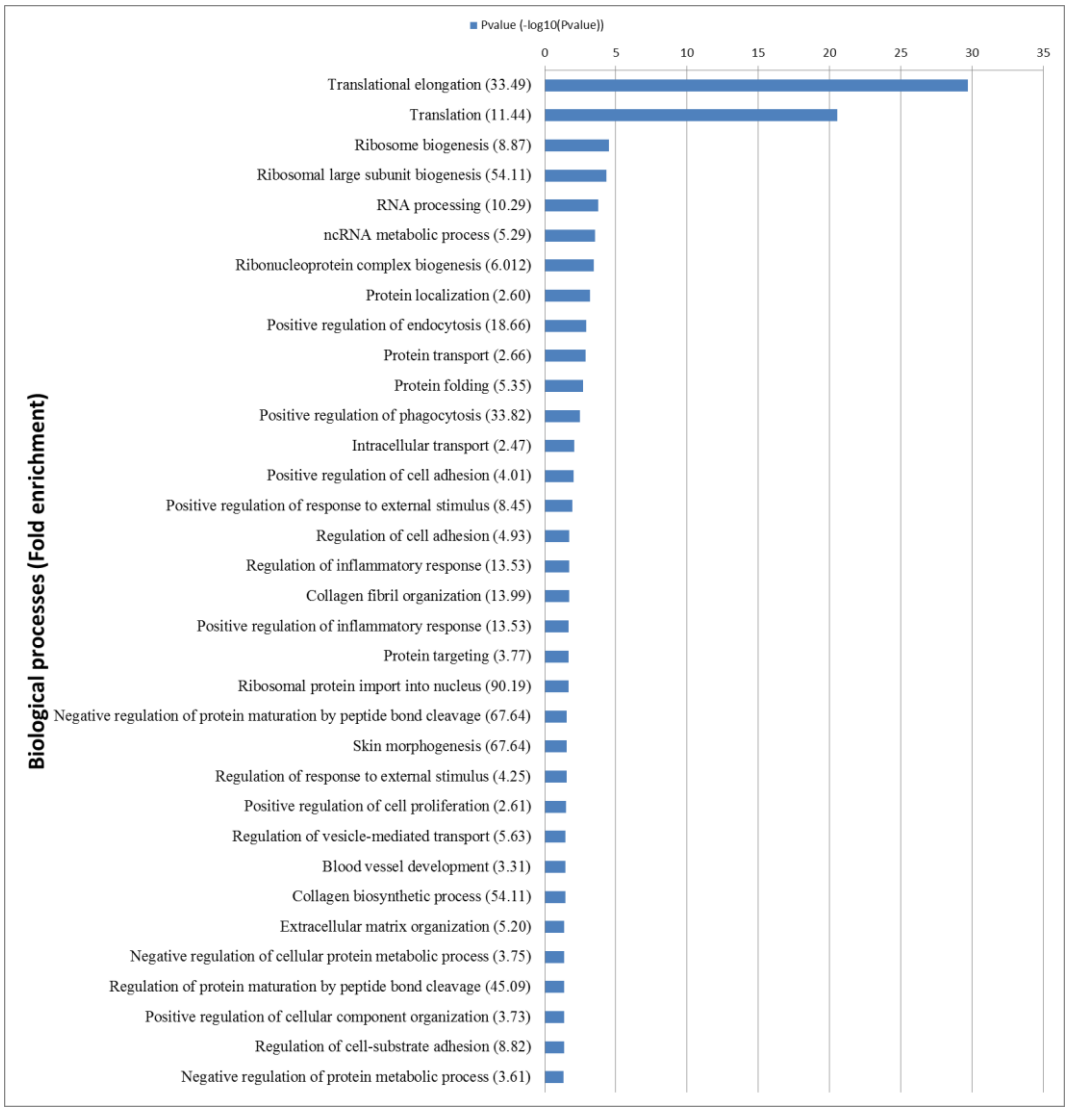

Figure 5.11: Biological processes enriched in David tool from host proteins significantly overexpressed in *T. gondii* infection

Table 5.4: Biological processes enriched from host proteins significantly overexpressed in *T. gondii* infection.

Biological processes	Gene IDs	Protein name
Translation processes	P18124	60S ribosomal protein L7, RPL7
	P14868	Aspartate-tRNA ligase, cytoplasmic, DARS
	P62750	60S ribosomal protein L23a, RPL23A
	Q07020	60S ribosomal protein L18, RPL18
	P62280	40S ribosomal protein S11, RPS11
	P62249	40S ribosomal protein S16, RPS16
	P62424	60S ribosomal protein L7a, RPL7A
	P84098	60S ribosomal protein L19, RPS19
	P62269	40S ribosomal protein S18, RPS18
	P61247	40S ribosomal protein S3a, RPS3A
	P62241	40S ribosomal protein S8, RPS8
	P62829	60S ribosomal protein L23, RPL23
	P47914	60S ribosomal protein L29, RPL29
	P61313	60S ribosomal protein L15, RPL15
	O00425	Insulin-like growth factor 2 mRNA-binding protein 3, IGF2BP3
	P62854	40S ribosomal protein S26, RPS26
	P62851	40S ribosomal protein S25, RPS25
	P46782	40S ribosomal protein S5, RPS5
	P46781	40S ribosomal protein S9, RPS9
	P15880	40S ribosomal protein S2, RPS2
	Q02543	60S ribosomal protein L18a, RPL18A
	P42766	60S ribosomal protein L35, RPL35
	P62913	60S ribosomal protein L11, RPL11
	P07814	Bifunctional glutamate/proline-tRNA ligase, EPRS
	P61254	60S ribosomal protein L26, RPL26
	Q02878	60S ribosomal protein L6, RPL6
	P18077	60S ribosomal protein L35a, RPL35A
	P40429	60S ribosomal protein L13a, RPL13A
Ribosomal biogenesis	P62249	40S ribosomal protein S16, RPS16
	P18124	60S ribosomal protein L7, RPL7
	P62424	60S ribosomal protein L7a, RPL7A
	P61254	60S ribosomal protein L26, RPL26
	P62913	60S ribosomal protein L11, RPL11
	P18077	60S ribosomal protein L35a, RPL35A
	O00567	Nucleolar protein 56, NOP56
	P22087	rRNA 2'-O-methyltransferase fibrillarin, FBL
RNA processes	P18124	60S ribosomal protein L7, RPL7
	P62913	60S ribosomal protein L11, RPL11
	P17844	Probable ATP-dependent RNA helicase DDX5, DDX5
	P31943	Heterogeneous nuclear ribonucleoprotein HFF cells, HNRNPH1
	O00567	Nucleolar protein 56, NOP56
	Q92841	Probable ATP-dependent RNA helicase DDX17, DDX17
	P22087	rRNA 2'-O-methyltransferase fibrillarin, FBL
	P62249	40S ribosomal protein S16, RPS16
	P11940	Polyadenylate-binding protein 1, PABPC1
	Q08170	Serine/arginine-rich splicing factor 4, SRSF4
	P61254	60S ribosomal protein L26, RPL26
	O75400	Pre-mRNA-processing factor 40 homolog A, PRPF40A
	P18077	60S ribosomal protein L35a, RPL35A
	Q15365	Poly(rC)-binding protein 1, PCBP1
Protein transporting and targeting	P61204	ADP-ribosylation factor 3, ARF3
	Q14974	Importin subunit beta-1, KPNB1

	Q9Y3Q3	Transmembrane emp24 domain-containing protein 3, TMED3
	Q9UL25	Ras-related protein Rab-21, RAB21
	P60033	CD81 antigen, CD81
	P61026	Ras-related protein Rab-10, RAB10
	P02452	Collagen alpha-1(I) chain, COL1A1
	Q9H444	Charged multivesicular body protein 4b, CHMP4B
	P62913	60S ribosomal protein L11, RPL11
	P43307	Translocon-associated protein subunit alpha, SSR1
	P35579	Myosin-9, MYH9
	P38646	Stress-70 protein, mitochondrial, HSPA9
	P61106	Ras-related protein Rab-14, RAB14
	P17301	Integrin alpha-2, ITGA2
	P48444	Coatomer subunit delta, ARCN1
	P62829	60S ribosomal protein L23, RPL23
	P62826	GTP-binding nuclear protein Ran, RAN
Protein folding	P23284	Peptidyl-prolyl cis-trans isomerase B, PPIB
	P78371	T-complex protein 1 subunit beta, CCT2
	P17987	T-complex protein 1 subunit alpha, TCP1
	P30533	Alpha-2-macroglobulin receptor-associated protein, LRPAP1
	Q9UBS4	DnaJ homolog subfamily B member 11, DNAJB11
	Q9Y230	RuvB-like 2, RUVBL2
	P38646	Stress-70 protein, mitochondrial, HSPA9
positive regulation of phagocytosis	P17301	Integrin alpha-2, ITGA2
	P01024	Complement C3, C3
	Q08431	Lactadherin, MFGE8

5.3.3.3. Overlapped phosphoproteome of host cell in response to infection with *T. gondii* and *N. caninum*

Table 5.5 shows the total number of the quantified host phosphoproteins matched with the host transcripts and proteins infected with *T. gondii* and *N. caninum*. In total, 57 out of 473 of the quantified phosphoproteins were matched with the quantified transcripts and proteins.

Table 5.5: Quantified phosphoproteins that match transcriptomic and proteomic datasets.

ID	Description	Max fold change	Infection with higher expression
Q14697	Neutral alpha-glucosidase AB	196.94	*T. gondii* infection
Q9UQ35	Serine/arginine repetitive matrix protein 2	7.63	*T. gondii* infection
Q9H3N1	Thioredoxin-related transmembrane protein 1	7.37	*T. gondii* infection
P08238	Heat shock protein HSP 90-beta	6.97	*T. gondii* infection
P04792	Heat shock protein beta-1	6.92	*T. gondii* infection
P29966	Myristoylated alanine-rich C-kinase substrate	6.85	*T. gondii* infection
P62081	40S ribosomal protein S7	6.14	*T. gondii* infection
Q9P035	Very-long-chain (3R)-3-hydroxyacyl-[acyl-carrier protein] dehydratase 3	4.08	*T. gondii* infection
Q15084	Protein disulfide-isomerase A6	3.73	*T. gondii* infection
Q9C0C2	182 kDa tankyrase-1-binding protein	3.35	*T. gondii* infection
Q14847	LIM and SH3 domain protein 1	3.26	*T. gondii* infection
P60174	Triosephosphate isomerase	2.58	*T. gondii* infection
P31943	Heterogeneous nuclear ribonucleoprotein H	2.34	*T. gondii* infection
P08670	Vimentin	2.27	*T. gondii* infection
Q07065	Cytoskeleton-associated protein 4	1.99	*T. gondii* infection
P67809	Nuclease-sensitive element-binding protein 1	1.97	*T. gondii* infection
Q16555	Dihydropyrimidinase-related protein 2	1.88	*T. gondii* infection
P48681	Nestin	1.70	*T. gondii* infection
P35221	Catenin alpha-1	1.57	*T. gondii* infection
P35606	Coatomer subunit beta'	1.45	*T. gondii* infection
Q9UMS6	Synaptopodin-2	1.31	*T. gondii* infection
Q9NR30	Nucleolar RNA helicase 2	1.27	*T. gondii* infection
P43307	Translocon-associated protein subunit alpha	1.21	*T. gondii* infection
Q03135	Caveolin-1	1.19	*T. gondii* infection
O00264	Membrane-associated progesterone receptor component 1	1.17	*T. gondii* infection
Q9UKM9	RNA-binding protein Raly	1.11	*T. gondii* infection
P23284	Peptidyl-prolyl cis-trans isomerase B	1.09	*T. gondii* infection
O94826	Mitochondrial import receptor subunit TOM70	1.09	*T. gondii* infection
P23396	40S ribosomal protein S3	1.04	*T. gondii* infection
P17858	6-phosphofructokinase, liver type	1.03	*T. gondii* infection
Q07666	KH domain-containing, RNA-binding, signal transduction-associated protein 1	1.02	*T. gondii* infection
Q9UBG0	C-type mannose receptor 2	1.02	*T. gondii* infection
Q9Y2X3	Nucleolar protein 58	1.01	*T. gondii* infection
P08648	Integrin alpha-5	1.00	*T. gondii* infection
Q6NZI2	Polymerase I and transcript release factor	11.07	*N. caninum* infection
P04406	Glyceraldehyde-3-phosphate dehydrogenase	4.39	*N. caninum* infection

Q14247	Src substrate cortactin	2.93	*N. caninum* infection
P08123	Collagen alpha-2(I) chain	1.67	*N. caninum* infection
Q969G5	Protein kinase C delta-binding protein	1.63	*N. caninum* infection
P50454	Serpin H1	1.62	*N. caninum* infection
P02794	Ferritin heavy chain	1.58	*N. caninum* infection
P68363	Tubulin alpha-1B chain	1.55	*N. caninum* infection
Q14204	Cytoplasmic dynein 1 heavy chain 1	1.49	*N. caninum* infection
P39023	60S ribosomal protein L3	1.46	*N. caninum* infection
Q00839	Heterogeneous nuclear ribonucleoprotein U	1.40	*N. caninum* infection
Q9Y490	Talin-1	1.39	*N. caninum* infection
O75396	Vesicle-trafficking protein SEC22b	1.34	*N. caninum* infection
Q9NZN4	EH domain-containing protein 2	1.30	*N. caninum* infection
Q01082	Spectrin beta chain, non-erythrocytic 1	1.22	*N. caninum* infection
P35579	Myosin-9	1.21	*N. caninum* infection
Q06210	Glutamine--fructose-6-phosphate aminotransferase [isomerizing] 1	1.16	*N. caninum* infection
P17302	Gap junction alpha-1 protein	1.14	*N. caninum* infection
P07814	Bifunctional glutamate/proline--tRNA ligase	1.13	*N. caninum* infection
Q13200	26S proteasome non-ATPase regulatory subunit 2	1.09	*N. caninum* infection
Q1KMD3	Heterogeneous nuclear ribonucleoprotein U-like protein 2	1.08	*N. caninum* infection
Q13425	Beta-2-syntrophin	1.07	*N. caninum* infection
O76021	Ribosomal L1 domain-containing protein 1	1.04	*N. caninum* infection

5.3.4. Integrated data analysis of 3omics

The integrated data analysis was performed to study the changes in 3omics (transcriptome, proteome and phosphoproteome) in response to infection with *T. gondii* and *N. caninum* at a system level. The criteria used to determine discrepancies between transcript and protein expressions was based on directions of genes with over two fold differences between infections e.g. when a transcript increased two fold in expression between *T. gondii* and *N. caninum* infection, the protein of the same transcript decreased two fold in expression. Results show that the majority (94 %) of transcriptome and proteome are following the same trends in *T. gondii* and *N. caninum* infections. However, 6 % of the transcriptome and proteome were regulated differently from both infections. The biological processes that these different molecules are associated are shown in Table 5.6. The majority of these molecules are associated with protein production and processing.

Table 5.6: differentially regulated transcripts and proteins of host cell infected with *T. gondii* and *N. caninum*.

Protein IDs	Description	Biological processes	FC in transcriptome	FC in proteome
Q969G5	Protein kinase C delta-binding protein, PRKCDBP	Circadian regulation of gene expression	2.133	0.375
P62258	14-3-3 protein epsilon, YWHAE	Protein targeting and transporting	2.14	0.195
Q9Y3I0	tRNA-splicing ligase RtcB homolog, RTCB	Cell-matrix adhesion	2.149	0.48
P30041	Peroxiredoxin-6, PRPDX6	Cell redox homeostasis,	2.275	0.294
P09936	Ubiquitin carboxyl-terminal hydrolase isozyme L1, UCHL1	Protein targeting and transporting	2.337	0.181
Q99536	Synaptic vesicle membrane protein VAT-1 homolog, VAT1	Negative regulation of mitochondrial fusion	2.343	0.141
P38159	RNA-binding motif protein, X chromosome, RBMX	RNA processes	2.477	0.397
P13667	Protein disulfide-isomerase A4, PDIA4	Intracellular protein transport and targeting	2.57	0.15
Q9NVA2	Septin-11, SEPT11	Cellular macromolecular complex assembly	2.661	0.344
Q16181	Septin-7, SEPT7	Cellular macromolecular complex assembly	2.796	0.318
P27348	14-3-3 protein theta, YWHAQ	Intracellular protein transport and targeting	3.481	0.249
P09429	High mobility group protein B1, HMGB1	Anti-apoptosis	3.563	0.301
Q96A33	Coiled-coil domain-containing protein 47, CCDC47	Calcium ion homeostasis	3.667	0.438
Q14980	Nuclear mitotic apparatus protein 1, NUMA1	Cell division	3.774	0.328
Q9UQ80	Proliferation-associated protein 2G4, PA2G4	Regulation of cellular protein metabolic processes	3.915	0.106
O75390	Citrate synthase, mitochondrial, CS	Generation of precursor metabolites and energy	4.316	0.411
P35555	Fibrillin-1, FBN1	Extracellular matrix organization	4.372	0.268
P05204	Non-histone chromosomal protein HMG-17, HMGN2	-	5.242	0.204
O94832	Unconventional myosin-Id,	Cellular	5.262	0.39

	MYO1D	localization		
P35268	60S ribosomal protein L22, RPL22	Translation processes	8.975	0.31
P01024	Complement C3, C3	Positive regulation of phagocytosis	0.38	2.234
P01023	Alpha-2-macroglobulin, A2M	Regulation of acute inflammatory response and immune responses	0.391	8.681
Q15113	Procollagen C-endopeptidase enhancer 1, PCOLCE	Proteolysis	0.405	5.126
Q8N357	Solute carrier family 35 member F6, SLC35F6	Positive regulation of cell proliferation	0.454	2.08
P60033	CD81 antigen, CD81	Protein transporting and targeting	0.482	2.127

The quantified host phosphoproteins (473) and proteins (403) were compared; total of 57 host phosphoproteins and proteins were matched. The criteria used to select different host cell expression were based on two folds expression (decreased or increased) in protein and one and a half fold expression in phosphoproteins. Lower fold changes applied to phosphoproteins is due to the fact these two parasites are closely related and often small proportion of a protein are phosphorylated, thus small changes happen in the protein phosphorylation potentially indicate great differences in response to these two parasites. Results show that the majority 86 % out of the 57 of the matched proteome and phosphoproteome are following the same trends in *T. gondii* and *N. caninum* infections. However, 14 % of the 57 matched phosphoproteome and proteome were regulated differently from both infections. The biological processes that these different molecules are associated are shown in Table 5.7. The majority of these molecules are associated with energy and protein production.

Table 5.7: Host phosphoproteins and proteins were significantly overexpresses differently in *T. gondii* and *N. caninum* infection.

Protein ID	**Description**	**Biological processes**	**FC in proteome**	**FC in phosphoproteome**
Q14697	Neutral alpha-glucosidase AB	post-translational protein modification	0.296	196.943
P29966	Myristoylated alanine-rich C-kinase substrate	Energy reserve metabolic process	0.453	6.854
Q15084	Protein disulfide-isomerase A6	Protein folding	0.451	3.730
P60174	Triosephosphate isomerase	Glycolytic process	0.115	2.581
P67809	Nuclease-sensitive element-binding protein 1	mRNA splicing	0.204	1.971
P68363	Tubulin alpha-1B chain	Cell division	3.829	0.646
P50454	Serpin H1	Collagen biosynthesis process	2.810	0.619
P08123	Collagen alpha-2(I) chain	Collagen fibril organisation	2.833	0.597

The quantified host transcripts (403) and phosphoproteins (473) were compared; total of 57 host phosphoproteins and transcripts were matched. The criteria used to select different host cell expression were based on two folds expression (decreased or increased) in transcripts and one and a half fold expression in phosphoproteins. Results show that the majority 96.5 % out of the 57 of the matched transcriptome and phosphoproteome are following the same trends in *T. gondii* and *N. caninum* infections. However, 3.5 % of the 57 matched transcriptome and phosphoproteome were regulated differently from both infections. The biological process that these different molecules are associated is circadian regulation of gene expression as shown in Table 5.8.

Table 5.8: Host transcriptome and phosphoproteome infected with *T. gondii* and *N. caninum*. These IDs were significantly overexpresses differently in transcriptome and phosphoproteome.

Protein ID	**Description**	**Biological processes**	**FC in transcriptome**	**FC in phosphoproteome**
Q969G5	Protein kinase C delta-binding protein	Circadian regulation of gene expression	2.133	0.615
Q00839	Heterogeneous nuclear ribonucleoprotein U	Circadian regulation of gene expression	2.353	0.713

5.4. DISCUSSION

The present study aimed to analyse and compare the host cell response to infection with *T. gondii* and *N. caninum* at system wide level using quantitative transcriptome, proteome and phosphoproteome data.

Total number of quantified host cell transcripts in *T. gondii* infection was twice that found in *N. caninum* infection (Figure 5.3). These differences could be related to the quality of a particular RNASeq experiment that had higher noise level than the other. However, this does not greatly influence the overall comparison between transcriptome and proteome as only half of the quantified host proteins were matched to the transcripts after one gene, one transcript criteria was used for the matching (Figure 5.4).

5.4.1. Host cell is selectively regulated to fulfil the parasites requirement

T. gondii scavenge essential host nutrition as amino acids, sugar, nucleobases and co-factors (Schwab *et al.*, 1994) and cholesterol (Coppens *et al.*, 2006; Coppens *et al.*, 2000). In this study, data analysis showed that at expression level of proteins associates with protein production (Figure 5.11) was highly up-regulated in host cell infected with *T. gondii* compared to *N. caninum* at 36 hr p.i. On the other hand, proteins associate with energy production (Figure 5.10) where down regulated compared to *N. caninum* at the same time point of infection. These proteins that regulate energy and protein production could indicate that parasites selectively direct host cell to fulfil their essential requirements. Protein regulation is related to the compensation of protein metabolism acquired by replicating parasites and to maintain housekeeping protein necessary for maintaining normal cellular functions (Jovanovic *et al.*, 2015). These results indicate that these parasites like other pathogens e.g. HIV (Wojcechowskyj *et al.*, 2013), not only take advantage of the host cell signalling pathway but also manipulate pathways to fulfil their requirements. Host cell regulation is potentially associated with the demands of the highly replicating tachyzoites during different phases of their development (Francia and Striepen, 2014). This is comparable with the studies of Blader *et al.* (2001) and Nelson *et al.* (2008), in that they found high gene modulation and host cell regulation in later time point (24 hr p.i.) than early infection. The results show that following

infection of host cell, parasite selectively control and manipulate the host cell and intimate host-parasite interaction to co-opt the requirement of the replicating tachyzoites.

5.4.2. *T. gondii* stimulates higher activity of protein production in host cell

Based on the biological processes enriched from host cell proteins significantly overexpressed in *T. gondii* infection; translation processes were found highly enriched in *T. gondii* infection (Figure 5. 9 and 5.10). Overexpression of proteins involved in translation could be related to the differences at host-parasite interaction to produce more proteins require for continuous replication of tachyzoites before egress at this time point. In addition, almost all the biological processes enriched were related to protein production particularly translation processes as shown in Figure 5.7. The dynamic of protein fold changes is directly regulated by high abundance of mRNA in infection with *T. gondii*. The result of the present study is comparable to the study of Jovanovic *et al.* (2015) where they found a relationship between relative fold changes of protein expression and abundance of mRNA in response to lipopolysaccharide in stimulated mouse dendritic cells. Investigation showed that during acute and chronic infection of mouse forebrain with *T. gondii*, the majority of the transcripts of the parasite that highly up-regulated were associated with transcription and translation processes (Pittman *et al.*, 2014). In addition, microarray analysis showed that host cell responded to infection with *T. gondii* through regulation of large number of genes associated with transcription and protein synthesis, targeting and degradation and signalling (Blader *et al.*, 2001). The results associated with protein production show the importance of protein regulation both transcriptionally and translationally during infection with these parasites. In addition, because division in these parasites are synchronised based on the doubling processes; high protein production could be related to the stage of the replication of tachyzoites e.g. at G1 phase tachyzoites starts to synthesis and build up more proteins before start mitosis as reviewed in Francia and Striepen (2014). The high up-regulation of protein production during infection with *T. gondii* potentially is related to the high demand of *T. gondii* replication at this time point than *N. caninum*.

5.4.3. *T. gondii* inhibits apoptosis and acute inflammatory response of host cell

T. gondii has evolved mechanisms to inhibit host cell apoptosis and evade immune system using arrays of effectors that allow its survival and host cell maintenance through avoiding tissue destruction by inflammatory responses of host (Lüder and Gross, 2005). In the present study, infection with *T. gondii* results in overexpression of anti-apoptosis transcripts (Table 5.2) more than infection with *N. caninum*. IFN-γ-treated murine fibroblasts infected with *T. gondii* were found to resist apoptosis whereas apoptosis was found in cells infected with *N. caninum*. The apoptosis of host cell with *N. caninum* was found associated with high induction of DNA fragmentation and increase in the activity of caspase-3 and -8 (Nishikawa *et al.*, 2002). In addition *N. caninum* was found to induce the ligand (FasL) of death receptor (Fas) in the presence or absence of IFN-γ treatment which is important in induction of extrinsic apoptotic pathway, suggesting that *N. caninum* induces apoptosis more readily than *T. gondii* (Nishikawa *et al.*, 2002). *T. gondii* protects infected cell from different apoptotic inducer such as actinomycin-D (Kim *et al.*, 2006) or cycloheximide in combination with actinomyocine-D or TNF-α through inhibition of caspases such as caspase 3, -8 and -9 (Goebel *et al.*, 1998). Thus the results of the present study provided supporting evidence that *T. gondii* inhibited apoptosis more than *N. caninum* infection.

In addition, host cell infected with *T. gondii* was found resulted in suppression of transcripts associated with acute inflammatory response more than *N. caninum* infection (Table 5.1). HFF cell infection with *T. gondii* type I and III at 18 hr p.i. was found associated with high phosphorylation of STAT3/6 more than infection with type II strain (Saeij *et al.*, 2007). In types I and III strain of *T. gondii*, ROP16 was found involved in direct and sustained phosphorylation and translocation of STAT3/6 into nucleus which consequently leading to inhibition of host cell early immune response mediated by cytokines, IL-12. While in Type II strain, phosphorylation (and activation) and translocation of STAT3 was found for only a short time and followed by induction of high IL-12p40 (Ong *et al.*, 2010; Saeij *et al.*, 2007; Yamamoto *et al.*, 2009). The results of these studies are comparable with the present study in that *T. gondii* types III strain was used in the experiment and that lower immune response was found compared to *N. caninum* infection. In addition,

other ROP proteins in *T. gondii* such as ROP18 was also found associated with virulence of these parasites. TgROP18 phosphorylates host cell IRGs necessary for destruction of PVM in infected cells while *N. caninum* does not due to pseudogenisation of *NcROP18* (Lei *et al.*, 2014; Reid *et al.*, 2012). The result of the present study suggests that differential induction of early immune response is associated with the regulation of virulence in *T. gondii* and *N. caninum*.

5.4.4. Integrated data analysis shows consistencies in response to infection with *T. gondii* and *N. caninum*

Regulation of eukaryotic gene expression is control by processes at system level that maintain balance between transcripts and proteins within cell for normal physiological state or in response to external stimuli. These processes associate with gene transcription, RNA processing, translation and protein life cycle (Jüschke *et al.*, 2013). In addition, lower correlation was also reported at 40 % between mRNA expression and protein abundance (De Sousa Abreu *et al.*, 2009; Maier *et al.*, 2009); suggested that several factors are contributing to the differences in the abundance of mRNA and protein that are controlled by post-transcriptional, translational and protein degradation (Vogel and Marcotte, 2012).

Host-pathogen interactions result in high protein expression which maintained by mRNA transcription and abundance (Jovanovic *et al.*, 2015). In the present study, a general agreement was reported between omics of host cell in response to infection with *T. gondii* and *N. caninum*. Thus the present study is comparable with the study of Jovanovic *et al.* (2015) in that transcriptome/proteome, proteome/phosphoproteome and transcriptome/phosphoproteome for matched transcripts and proteins from both *T. gondii* and *N. caninum* were very similar. This similarity is potentially associated with the fact that these two parasites possess remarkably conserved genomes and transcriptomes (Reid *et al.*, 2012).

Presence of differentially enriched pathway from phosphoproteome analysis such as mTOR signalling pathway and glycolysis/gluconeogenesis; biological processes such as protein and energy production, host cell response to apoptosis and inflammatory responses, suggest that these parasites selectively target and manipulate host cell system for their benefit.

5.4.5. Limitation of data analysis

In this data analysis, only one replicate of transcriptome data was available, for this purpose artificial replicates were generated. The latter was to meet the requirement of the software Normalyzer which does not affect the normalisation method performed for the transcripts data. Replicates offer more confidence to normally distributed data analysis. The quantified omics data were analysed without applying significant threshold as cut-off e.g. p-value <0.05 to individual value of transcripts, proteins and phosphoproteins after normalisation. Because of the fact that p-value was not possible to be generated from single replicate of the quantified transcripts.

5.4.6. Conclusion

In conclusion, host cell responses are determined by pathogen effectors; infection with *T. gondii* and *N. caninum* results in selective energy and protein induction of host cell to fulfil the requirement of highly dividing tachyzoites. These results indicate that these parasites synchronise their requirement due to continuous synchronous endodyogeny. Therefore energy is potentially produced first then followed by protein production; and determines the parasites to enter new cycle of cell division or to egress when there are not enough resources. In addition, integrated data analyses from omics of host cell show that the majority of omics trends of host cell in response to infection with these parasites are similar. The similarity in transcriptomics, proteomics and phosphoproteomics in response to infection with these parasites indicate that the molecular organisations of these parasites are preserved.

Chapter SIX: Discussion and future perspectives

6.1. DISCUSSION

T. gondii and *N. caninum* are closely related intracellular obligatory protozoan parasites. The genome, transcriptome and proteome are similar in both parasites; however there exist several biological differences between the two parasites including host range, zoonotic potential, transmission and virulence. The exact causes and mechanisms leading to these biological differences are yet to be fully elucidated. These parasites have to invade successfully and establish an infection within the host cell to survive, grow, differentiate and multiply. These biological activities require continuous interactions and communications between the host cell and the parasites which could potentially be responsible for the biological differences between *T. gondii* and *N. caninum*.

While there is more information about protein-protein interactions and multiple protein complexes in *T. gondii*, less is known about these in *N. caninum*. In addition, there are limited comparative host cell transcriptomics and proteomics studies in response to infection with the two parasites, and there is no comparative host phosphoproteomics study in response to infection with *T. gondii* and *N. caninum*. The aim of this study was to understand the cause of the biological differences between *T. gondii* and *N. caninum* through dissecting host-parasite interactions. The comparison of host-parasite interactions between the two parasites was performed through the implementation of advanced global analysis of tachyzoites MPCs and the host cell transcriptome, proteome and phosphoproteome during infection with the two parasites.

The results shown in this thesis support the hypothesis that there are differences in the host-parasite interactions in response to infection with *N. caninum* when compared to *T. gondii*. The main finding of the present study was the identification of the host pathways that are differentially expressed in response to infection with *T. gondii* and *N. caninum* and these are associated with energy and protein metabolisms such as glycolysis/gluconeogenesis and mTOR signalling pathways. The results of the present study are complementary to the findings from previous studies where differences were shown in the host innate immune responses and host cell necrosis during infection with the two parasites (Lei *et al.*, 2014;

Nishikawa *et al.*, 2002). The differences in host-parasite interactions at the qualitative and quantitative level are potentially associated with the differences in the virulence and transmission strategy of *T. gondii* and *N. caninum*.

In chapter two, BN-PAGE combined with LC MS/MS analysis was used for the comparative investigation of the whole tachyzoites PPIs and MPCs of *T. gondii* and *N. caninum* in their native state. Although the technique is used for one-step isolation and high resolution of separation of MPCs from different biological samples, it is laborious and requires optimisation for different biological samples from different organisms. The MPCs identified from BN-PAGE prepared from tachyzoites of both *T. gondii* and *N. caninum* were difficult to compare due to differences in protein separation on BN-PAGE. The differences could be due to non-specific interactions and/or migration of different MPCs to different molecular weight locations. Despite this, several different complexes were identified in *T. gondii* and *N. caninum* tachyzoites. In *T. gondii*, a complex that plays an important part in attachment [MIC6/1 and SAC1 (SRS29B)] was identified. The oligomerisation of proteins from different organelles and complex formation facilitates invasion of host cell collaboratively (Alexander *et al.*, 2005; Carruthers and Tomley, 2008). The interaction/co-localisation of MIC6/1 and SAG1 potentially indicates that these proteins function together in tachyzoites and facilitate attachment and invasion of host cells. In addition, three subunits (TgMyoA-MLC1-GAP45) of the glideosome were identified in *N. caninum*. This is in agreement with the findings of Frenal *et al.* (2010) on *T. gondii* and Sanders *et al.* (2007) from detergent-resistant membranes of *Plasmodium falciparum* schizonts. The similarity in the subunit of the glideosome of *T. gondii* and *N. caninum* potentially indicates that both parasites use the same cytoskeletal elements to power the gliding motility and invasion of host cells. However, further studies are needed to confirm the presence of other subunits of the glideosome in *N. caninum*.

Another important finding was the identification of proteins associated with MJ formation, which drive invasion of host cell by *N. caninum* and these include RON1, RON2, RON3, RON5, RON8, a ROP2 family member and ROP40. These results are in agreement with previous results from a proteomic analysis of rhoptry organelle fractions, showing several proteins from the rhoptry bulb and neck in *T.*

gondii namely TgRON1, 2, 3, and 4 (Bradley *et al.*, 2005) and in *N. caninum* - NcRON2, 3, 4, and 8 (Marugán-Hernández *et al.*, 2011). In addition RON2, 3, 4, 5 and 8 have been found to be associated with MJ formation in *T. gondii* and *N. caninum* tachyzoites (Alexander *et al.*, 2005; Sohn *et al.*, 2011; Straub *et al.*, 2009). Oligomerisation of these proteins inside the parasite rhoptry and beyond the parasite plasma membrane and their role in MJ formation suggests that these proteins are secreted as one macromolecule to help accelerate host cells invasion and establishment of an infection.

In chapter three, a pull-down assay has been used to study direct PPIs of *T. gondii* and *N. caninum* proteins (GRA2 and GRA7) with host cell lysate proteins and further analysed using LC-MS/MS. This method is more accurate to study PPIs than BN-PAGE because it uses expressed recombinant tagged proteins of interest as bait to pull-down prey proteins from targeted cell lysate. However purification of recombinant protein was found to be challenging. Recombinant GRA2 and GRA7 proteins from both parasites were expressed in transformed BL21 (DE3) competent cells; however, the expressed recombinant proteins were co-purified with other proteins from the expression system using Ni-NTA purification column. Expression and purification of GRA proteins was difficult due to the presence of multiple hydrophobic or amphipathic alpha helices (Bittame *et al.*, 2015). Therefore, several different methods were carried out to purify expressed recombinant GRA proteins such as using different growth media (LB, minimal media), different purification system (cobalt HisPur Resin kit) and purification under denaturing condition using 8 M urea. However, none of these methods resulted in the purification of the recombinant GRA proteins. In addition, a second step of purification was applied to the elution fraction of Ni-NTA HisTrap exploiting the solubility of these proteins using HPLC. The HPLC fractionation resulted in the successful purification of the recombinant TgGRA2. However, due to limitation of access to HPLC, the purification of more recombinant TgGRA2 protein was not possible.

Another key aim of this thesis was to understand the differences in host responses arising during infection with *T. gondii* and *N. caninum* through protein phosphorylation and signal transduction.

In chapter four, the phosphopeptides of host cell in response to infection with *T. gondii* and *N. caninum* at 20 hr p.i. were enriched and analysed by LC MS/MS. The identified phosphopeptides of host cells during infection with *T. gondii* and *N. caninum* were compared using label free quantitative phosphoproteomics. A previous study showed that *T. gondii* secretes an array of proteins and kinases into the infected host cells, suggesting that they play a role in phosphorylation and control of the parasite and/or host cell proteins (Treeck *et al.,* 2011). In addition, following *T. gondii* invasion and establishment of infection, PTMs of host proteins have been found to increase over time with protein phosphorylation in particular peaking at 24 hr p.i. (Nelson *et al.,* 2008). In this study, the total number of phosphorylated proteins in host cells during infection with *T. gondii* and *N. caninum* shows that the infected cells induce about twice more protein phosphorylations than non-infected cells. Three main differences were reported between the host protein phosphorylation during infection with *T. gondii* and *N. caninum*. Firstly, almost one third of the enriched phosphoproteome differed between cells infected with *T. gondii* and *N. caninum*. Secondly, approximately 21 % of identified phospho-motifs from significantly enriched phosphopeptides differed between cells infected with the two parasites. Thirdly, the pathway analysis showed a few pathways that were differentially enriched between infections with *T. gondii* and *N. caninum*; in particular, the mTOR and glycolysis/gluconeogenesis pathways were enriched in infection with *T. Gondii,* but not *N. caninum*. The differences in the phosphoproteome of host cells in response to infection as observed with both parasites are greater than the differences reported between the protein-coding genes, which is less than 5 % between both parasites (Reid *et al.,* 2012). Small differences in the protein phosphorylation of host cells by *T. gondii* and *N. caninum* were found to be responsible for great differences in the virulence of these parasites (Lei *et al.,* 2014). The differences found in the present study indicate that these parasites induce and/or manipulate the host canonical pathway and signalling cascades, such as the mTOR and the glycolysis/gluconeogenesis signalling pathways. The modulation of these pathways results in high energy production and protein expression which are highly required for tachyzoites division.

Results of the present study concerning the mTOR signalling pathway suggest that *T. gondii* and *N. caninum* phosphorylate the host mTOR substrates in a

parasite-dependent manner. These results are comparable with the study of Wang *et al.* (2009), which found that *T. gondii* phosphorylates the mTOR signalling pathway. In addition, based on the mTOR and glycolysis/gluconeogenesis signalling pathways, *T. gondii* appears to interact and manipulate more host cell proteins than *N. caninum* and thus, *T. gondii* induces more host cell response after 20 hr p.i. in vitro. Manipulation of these pathways during infection with *T. gondii* indicates that the host cell exerts more energy compared to infection with *N. caninum*. Thus, our results revealed high energy expenditure during *T. gondii* infection than *N. caninum* and this is probably related to the differences in virulence and transmission routes of *T. gondii* and *N. caninum*.

Development of more advanced tools and state of the art techniques for global analysis of genomic, transcriptomic and proteomic data allows researchers to study cells or organisms as a whole in systems biology. Systems biology allows the understanding of all the events arising in response to external or internal stimuli at a given time.

In chapter five, the comparative system-wide host cell responses to infection with *T. gondii* and *N. caninum* were analysed using quantitative transcriptomic, proteomic and phosphoproteomic data. Comparative quantitative analysis of the system-wide response of a host cell to infection with these parasites may uncover the mechanisms behind some of their biological differences. In this study, data analysis showed that significantly overexpressed transcripts and proteins in *T. gondii* and *N. caninum* infections perform markedly different tasks. The biological processes analysis of enriched host cell proteins and transcripts significantly overexpressed during infection with *T. gondii* showed that host cells build up more proteins in response to infection with *T. gondii* compared to *N. caninum* at 36 hr p.i. The proteins that were overexpressed were found to be the same ones involved in protein production (synthesis). On the one hand, the increase production of proteins is required for continuous replication of tachyzoites in *T. gondii* infection before egress at this time point (36 hr p.i.). On the other hand, proteins associated with energy production were down regulated in *T. gondii* compared to *N. caninum* at the same time point during infection. The selective regulation of proteins involved in energy and protein production by these parasites is potentially associated with their

multiplication requirements at this time point of infection. These results indicate that the parasites not only take advantage of the host cell signalling pathways, but also manipulate necessary pathways to fulfil their requirements. In addition, another key finding was that *T. gondii* infection resulted in the down regulation of acute inflammatory responses and induced the expression of anti-apoptotic transcripts in host cells to a greater degree compared to *N. caninum*. This is compatible with the results of Saeij *et al.* (2007), which found that infection with *T. gondii* type I and III in HFF cells at 18 hr p.i. resulted in the inhibition of the early immune responses of the host cells and these responses are mediated by the cytokine IL-12. In *T. gondii* type I and III, ROP16 was found to be involved in the direct and sustained phosphorylation and translocation of STAT3/6 into the host cell nucleus more than type II strain (Ong *et al.*, 2010; Saeij *et al.*, 2007; Yamamoto *et al.*, 2009). In addition, ROP18 in *T. gondii* was also found to phosphorylate the host cell IRGs necessary for the destruction of PVM in infected cells; while in *N. caninum*, this is not dependent on pseudogenisation of *NcROP18* (Lei *et al.*, 2014; Reid *et al.*, 2012). The result of the present study suggests that induction of early immune responses is associated with the regulation of virulence in *T. gondii* and *N. caninum*. In addition, early immune responses in *N. caninum* are potentially associated with the convertion of tachyzoites to tissue cysts and avoiding host immune response that would guarantee a successful transmission from infected mother to offspring's through vertical transmission.

6.2. FUTURE PERSPECTIVES

The comparative host-parasite interactions of *T. gondii* and *N. caninum* can be further investigated using different approaches. First of all, optimising BN-PAGE to study MPCs and PPIs of tachyzoites was not possible because of technical limitations. Therefore, we recommend optimising this promising technique to investigate the global PPIs and MPCs that are associated with different stages of the parasites, in particular tachyzoites and tissue cysts. Analyses of MPCs at different stages allow for a better understanding of the differences between different stages of the same parasite and between the same stages of the two parasites. In addition, dissecting the native MPCs of these parasites during and after invasion of the host cell is also critical to understand the proteins responsible for the interaction between

the parasite and the host cells. Mapping PPIs of apicomplexan parasites may be helpful to understand the biological differences between the two parasites. The PPIs database should contain the interactome of apicomplexan parasites based on manually curated interactions (reviewed from published papers) and computer-generated interactions (inferred). In addition, performing further genome-wide studies using different methods of analysing PPIs are also important such as Yeast two-hybrid, co-immunoprecipitation, protein microarray and also bioinformatics. Characterising the host-parasite interactome is one way to develop vaccines and identifying drug targets for the subsequent prevention and control of these parasites.

In order to study direct host-parasite interactions, other secretory proteins from the DGs as well as from other organelles such as rhoptries and micronemes from both parasites can be used to pull-down binding partners from the host cells. Different host cell types for *in vitro* pull-down should be used to confirm binding partners for different secretory proteins. In addition, co-immunoprecipitation can also be used besides pull-down assay to study and confirm wild type secretory proteins interaction with host cell during infection with the two parasites.

Further studies of protein phosphorylation patterns in host cells in response to infection with *T. gondii* and *N. caninum* are recommended. These studies should include different cell types such as macrophages, neuronal cells, myocytes and foetal cells of both human and animal origin to understand cell type-related differences in response to infection with these parasites. Moreover, *in vivo* models are recommended to study the host pathways regulation in response to infection with these parasites in the presence and absence of host immunity. In addition, we recommend using different strains from both parasites which may result in different host cell responses through host protein phosphorylation and signal transduction. It is important to enrich phosphopeptides from large amount of host protein extracts in response to infection with these parasites using SCX combined with IMAC or MOAC before using LC MS/MS. Longer runs of different fractions on LC MS/MS is also recommended to identify and quantify all peptides that phosphorylate in response to infection.

Using functional protein microarrays would be important to screen and identify substrates of parasite kinases within the host cell, which is a critical step for determining the target and downstream effectors of kinases and the signalling pathway involved (Smith *et al.*, 2011).

Finally, enrichment of different genome modifications such as histone acetylation and DNA methylation would be important to understand host genes regulation in response to infection.

6.3. CONCLUSION

In conclusion, the results of this project have provided new insights into the biological differences between *T. gondii* and *N. caninum*, especially through the analysis of host cell signalling pathways in response to infection at the systems biology level. The results indicated that host cell responses to infection with *T. gondii* and *N. caninum* are not only restricted to immune modulation and inhibition of apoptosis, but they also include a system-wide modulation of the host cell including transcription regulation, protein metabolism and PTMs. The phosphoproteome of host cells largely overlapped between infection with *T. gondii* and *N. caninum*: such results were expected due to the fact that the genome and transcriptome of both parasites are relatively similar (Reid *et al.*, 2012). However, differences in the phosphoproteome of host cells in response to infection with *T. gondii* and *N. caninum* were also observed and include the number of protein phosphorylations, phospho-motifs and signalling pathways. In addition, the quantified phosphopeptides were higher in *T. gondii* infection indicating that the host cell responds more to *T. gondii* compared to *N. caninum* and this could also mean that *T. gondii* manipulates more host cell signalling pathways as do *N. caninum* tachyzoites. These qualitative and quantitative differences in host-parasite interactions are potentially associated with the biological differences observed between these parasites, especially in terms of their virulence and transmission strategy.

APPENDIX

Table I: All proteins identified by MS analyses of in-gel digestion from BN-PAGE and SDS-PAGE of *N. caninum*. Based on Mascot scoring, ions scores > 31 of an individual peptide indicate identity or extensive homology ($p<0.05$).

Gel spot no.* (no. proteins identified)	Protein accession	Protein description	Protein score	Protein mass (Da)	No. of significant protein sequences	Protein coverage	*T. gondii* orthologue (Protein ID accession)**
1 (19)	NCLIV_034460	Hypothetical protein	341	65224	6	11.6	Cell division cycle 48 protein (TGME49_273090)
	NCLIV_001970	Unspecified product	171	67177	5	9.6	TgROP2 family member
	NCLIV_048570	Conserved hypothetical protein	151	28575	3	16.3	Gliding-associated protein 45 (GAP45) (TGME49_223940)
	NCLIV_049900	Hypothetical protein	106	93837	2	3.4	Myosin A (TGME49_235470)
	NCLIV_065750	Alpha 2 subunit of 20S proteasome (ISS), related	99	28771	3	11.6	-
	NCLIV_029420	Putative myosin light chain TgMLC1	98	25052	2	11.1	-
	NCLIV_019110	HSP90-like protein, related	73	97392	3	3.5	-
	NCLIV_048880	Proteasome subunit beta type-7, related	73	25629	2	9.5	-
	NCLIV_061160	Putative acid phosphatase	71	47250	1	3	-
	NCLIV_028230	Proteasome subunit alpha type-7, related	62	27566	1	5.7	-
	NCLIV_017470	Proteasome subunit alpha type, related	59	33463	1	3.7	-
	NCLIV_022220	Hypothetical protein	51	63784	2	3.1	Mitochondrial-processing peptidase beta subunit, putative (TGME49_202680)
	NCLIV_033230	SRS domain-containing protein	51	33911	1	4.7	-
	NCLIV_050470	Hypothetical protein	49	60165	2	3.2	Peptidase M16 family protein, putative (TGME49_236210)
	NCLIV_034470	Hypothetical protein	47	21721	1	4.2	No *T. gondii* orthologue is available
	NCLIV_003050	Putative myosin heavy chain	40	125340	1	1.3	-
	NCLIV_050770	Putative cation-transporting ATPase	34	244077	1	0.4	-
	NCLIV_042410	Putative sortilin	33	105595	1	1.3	-

	NCLIV_055490	Heat shock protein 70 (Precursor), related	31	73215	1	1.5	-
2 (12)	NCLIV_032770	Hypothetical protein	112	102113	3	4	Vacuolar proton-translocating ATPase subunit, putative (TGME49_232830)
	NCLIV_019110	HSP90-like protein, related	105	97392	4	6	-
	NCLIV_033230	SRS domain-containing protein	91	33911	2	8.8	-
	NCLIV_001970	Unspecified product	67	67177	3	5.2	TgROP2 family member
	NCLIV_003050	Putative myosin heavy chain	64	125340	1	0.9	-
	NCLIV_048590	Unspecified product	58	220934	1	0.8	Rhoptry neck protein RON3 (TGME49_223920)
	NCLIV_003650	Hypothetical protein	49	38097	1	4.2	Cytochrome c oxidase subunit, putative (TGME49_209260)
	NCLIV_029800	Conserved hypothetical protein	41	17170	1	7.1	Hypothetical protein (TGME49_257160)
	NCLIV_049080	Hypothetical protein	40	17718	1	5.3	Vacuolar ATP synthetase (TGME49_212310)
	NCLIV_042690	Putative vacuolar proton-translocating ATPase subunit	38	121381	1	0.8	-
	NCLIV_045350	Conserved hypothetical protein	36	108340	1	0.8	Hypothetical protein (TGME49_228060)
	NCLIV_016800	Putative TCP-1/cpn60 chaperonin family protein	31	63060	1	1.7	-
3 (15)	NCLIV_011410	Protein disulfide isomerase	227	53333	6	12.7	-
	NCLIV_024820	14-3-3 protein homolog	97	30961	4	15	-
	NCLIV_010200	Hypothetical protein	96	35538	1	3.8	Ribosomal protein RPL5 (TGME49_320050)
	NCLIV_021050	Unspecified product	77	93761	2	2	Subtilisin SUB1 (TGME49_204050)
	NCLIV_053840	Unspecified product	72	38965	1	3.1	Rhoptry protein ROP1 (TGME49_309590)
	NCLIV_047630	Putative 40S ribosomal protein S18	62	17979	2	12.7	-
	NCLIV_048020	Hypothetical protein	57	36545	1	3	Ribosomal protein RPSA (TGME49_266060)
	NCLIV_003440	Actin, related	53	42277	2	5.6	-

	NCLIV_020220	Putative elongation factor 2	51	94169	1	1.3	-
	NCLIV_054700	Putative uridine phosphorylase	47	33380	1	4	-
	NCLIV_028540	Conserved hypothetical protein	46	30255	1	2.9	Hypothetical protein (TGME49_255420)
	NCLIV_032290	SSU ribosomal protein S3P, related	41	26415	1	3.4	-
	NCLIV_043110	Putative interferon gamma-inducible protein 30	34	42952	1	3.1	-
	NCLIV_045350	Conserved hypothetical protein	32	108340	1	0.8	Hypothetical protein (TGME49_228060)
	NCLIV_008730	Hypothetical protein	31	18124	1	9	Ribosomal protein RPL12 (TGME49_254440)
4 (22)	NCLIV_011410	Protein disulfide isomerase	274	53333	9	18.2	-
	NCLIV_017370	Putative CAMP-dependent protein kinase regulatory subunit	92	43204	2	5.2	-
	NCLIV_010200	Hypothetical protein	76	35538	1	3.8	Ribosomal protein RPL5 (TGME49_320050)
	NCLIV_024870	Hypothetical protein	74	24203	1	5.2	Ribosomal protein RPL13 (TGME49_263050)
	NCLIV_021080	Hypothetical protein	72	28448	2	9.2	Ribosomal protein RPL8 (RPL8) (TGME49_204020)
	NCLIV_053840	Unspecified product	71	38965	1	3.1	Rhoptry protein ROP1 (TGME49_309590)
	NCLIV_011270	Hypothetical protein	69	45133	3	6.4	Phosphoglycerate kinase PGKI (TGME49_318230)
	NCLIV_046040	Hypothetical protein	60	18976	1	6.2	Ribosomal protein RPS11 (TGME49_226970)
	NCLIV_028540	Conserved hypothetical protein	53	30255	1	2.9	Hypothetical protein (TGME49_255420)
	NCLIV_024820	14-3-3 protein homolog	52	30961	2	7.5	-
	NCLIV_003440	Actin, related	51	42277	1	2.7	-
	NCLIV_021050	Unspecified product	47	93761	1	0.9	Subtilisin SUB1 (TGME49_204050)
	NCLIV_008730	Hypothetical protein	40	18124	1	9	Ribosomal protein RPL12 (TGME49_254440)

	NCLIV_029000	Conserved hypothetical protein	40	178459	1	1	Tetratricopeptide repeat-containing protein (TGME49_256100)
	NCLIV_025240	Putative Gbp1p protein	39	32118	1	3.4	-
	NCLIV_033680	Solute carrier family 25 (Mitochondrial carrier, dicarboxylate transporter), member 10, related	38	36863	1	2.4	-
	NCLIV_019970	Peptidyl-prolyl cis-trans isomerase A, related	38	19256	1	5.2	-
	NCLIV_048020	Hypothetical protein	37	36545	1	2.4	Ribosomal protein RPSA (TGME49_266060)
	NCLIV_046820	Putative pterin-4a-carbinolamine dehydratase	36	12022	1	12.4	-
	NCLIV_047990	Conserved hypothetical protein	35	932829	1	0.1	Phosphatidylinositol 3- and 4-kinase (TGME49_266010)
	NCLIV_000740	Class I chitinase, related	34	75107	1	1.6	-
	NCLIV_011550	Novel protein (Zgc:77155), related	33	24657	1	4.8	-
5 (2)	NCLIV_044550	Conserved hypothetical protein	37	205533	1	0.6	Myb family DNA-binding domain-containing protein (TGME49_306320)
	NCLIV_042860	Conserved hypothetical protein	32	259558	1	0.4	HEAT repeat-containing protein (TGME49_290990)
6 (4)	NCLIV_045350	Conserved hypothetical protein	42	108340	1	0.8	Hypothetical protein (TGME49_228060)
	NCLIV_053840	Unspecified product	40	38965	1	3.1	Rhoptry protein ROP1 (TGME49_309590)
	NCLIV_046230	Putative cgmp-inhibited 3~,5~-cyclic phosphodiesterase	35	317922	1	0.3	-
	NCLIV_040860	Tryptophanyl-trna synthetase, related	34	68374	1	1.3	-
7 (1)	NCLIV_045350	Conserved hypothetical protein	40	108340	1	0.8	Hypothetical protein (TGME49_228060)
8 (4)	NCLIV_070010	Hypothetical protein, conserved	209	329150	7	2.6	Rhoptry neck protein RON8 (TGME49_306060)
	NCLIV_042820	cDNA FLJ58099, highly similar to Homo sapiens clathrin, heavy polypeptide-like 1	99	196066	2	1.2	-

		(CLTCL1), transcript variant 1, mRNA, related					
	NCLIV_031970	Hypothetical protein	59	294704	3	1.4	Pre-mRNA processing splicing factor PRP8 (TGME49_231970)
	NCLIV_045350	Conserved hypothetical protein	43	108340	1	0.8	Hypothetical protein (TGME49_228060)
9 (6)	NCLIV_007800	Unspecified product	86	213846	2	1.7	Hypothetical protein (TGME49_253370)
	NCLIV_042820	cDNA FLJ58099, highly similar to Homo sapiens clathrin, heavy polypeptide-like 1 (CLTCL1), transcript variant 1, mRNA, related	53	196066	3	2	-
	NCLIV_038320	Unspecified product	46	122855	1	1.4	PAN domain-containing protein (TGME49_209920)
	NCLIV_045350	Conserved hypothetical protein	42	108340	1	0.8	Hypothetical protein (TGME49_228060)
	NCLIV_015430	Hypothetical protein	39	213813	1	0.7	protein disulfide-isomerase domain-containing protein (TGME49_238040)
	NCLIV_026260	GA26239, related	34	467672	1	0.2	-
10 (6)	NCLIV_042820	cDNA FLJ58099, highly similar to Homo sapiens clathrin, heavy polypeptide-like 1 (CLTCL1), transcript variant 1, mRNA, related	243	196066	9	5	-
	NCLIV_070010	Hypothetical protein, conserved	177	329150	10	3.4	Rhoptry neck protein RON8 (TGME49_306060)
	NCLIV_048590	Unspecified product	135	220934	8	4.1	Rhoptry neck protein RON3 (TGME49_223920)
	NCLIV_029100	Putative SET domain containing protein	37	140267	1	0.9	-
	NCLIV_045350	Conserved hypothetical protein	33	108340	1	0.8	Hypothetical protein (TGME49_228060)
	NCLIV_058530	Tetratricopeptide TPR_2 repeat protein, related	32	62544	1	1.9	-
11 (1)	NCLIV_045350	Conserved hypothetical protein	36	108340	1	0.8	Hypothetical protein

							(TGME49_228060)
12 (6)	NCLIV_064620	Unspecified product	215	165970	6	4.5	Rhoptry neck protein RON2 (TGME49_300100)
	NCLIV_025730	Conserved hypothetical protein	52	84225	1	1.3	Rhoptry neck protein RON10 (TGME49_261750)
	NCLIV_056900	AGAP005082-PA, related	43	1315974	1	0.1	-
	NCLIV_021870	Unspecified product	39	250434	1	0.4	AP2 domain transcription factor AP2VIIa-6 (TGME49_203050)
	NCLIV_045350	Conserved hypothetical protein	38	108340	1	0.8	Hypothetical protein (TGME49_228060)
	NCLIV_006290	Conserved hypothetical protein	34	466790	1	0.2	Hypothetical protein (TGME49_297210)
13 (4)	NCLIV_064620	Unspecified product	200	165970	6	4.5	Rhoptry neck protein RON2 (TGME49_300100)
	NCLIV_045350	Conserved hypothetical protein	48	108340	1	0.8	Hypothetical protein (TGME49_228060)
	NCLIV_032010	Putative protein phosphatase 2C	34	410004	1	0.2	-
	NCLIV_057960	Unspecified product	33	119961	1	1.1	Rhoptry protein ROP14 (TGME49_315220)
14 (6)	NCLIV_003050	Putative myosin heavy chain	158	125340	5	4.6	-
	NCLIV_021050	Unspecified product	100	93761	3	4.5	Subtilisin SUB1 (TGME49_204050)
	NCLIV_055360	Unspecified product	65	182101	2	2.1	Rhoptry neck protein RON5 (TGME49_311470)
	NCLIV_045350	Conserved hypothetical protein	36	108340	1	0.8	Hypothetical protein (TGME49_228060)
	NCLIV_043150	Conserved hypothetical protein	34	36835	1	3.1	Hypothetical protein (TGME49_291650)
	NCLIV_042410	Putative sortilin	32	105595	1	1.3	-
15 (5)	NCLIV_055360	Unspecified product	112	182101	4	2.6	Rhoptry neck protein RON5 (TGME49_311470)
	NCLIV_036700	Putative M16 family peptidase	65	158286	1	0.9	-
	NCLIV_019110	HSP90-like protein, related	53	97392	2	2.6	-
	NCLIV_021050	Unspecified product	38	93761	1	0.8	Subtilisin SUB1

							(TGME49_204050)
	NCLIV_048590	Unspecified product	32	220934	1	0.6	Rhoptry neck protein RON3 (TGME49_223920)
16 (3)	NCLIV_049900	Hypothetical protein	91	93837	1	1.8	myosin A (TGME49_235470)
	NCLIV_055360	Unspecified product	90	182101	2	2.4	Rhoptry neck protein RON5 (TGME49_311470)
	NCLIV_045350	Conserved hypothetical protein	34	108340	1	0.8	Hypothetical protein (TGME49_228060)
17 (4)	NCLIV_066100	Putative microtubule-binding protein	44	92401	1	1.9	-
	NCLIV_021050	Unspecified product	35	93761	1	1	Subtilisin SUB1 (TGME49_204050)
	NCLIV_045350	Conserved hypothetical protein	34	108340	1	0.8	Hypothetical protein (TGME49_228060)
	NCLIV_014060	Putative lysophospholipase	33	106908	1	0.8	-
18 (3)	NCLIV_001970	Unspecified product	134	67177	3	5.4	TgROP2 family member
	NCLIV_045350	Conserved hypothetical protein	51	108340	1	0.8	Hypothetical protein (TGME49_228060)
	NCLIV_060730	Unspecified product	44	61652	1	2.4	Rhoptry protein ROP5 (TGME49_308090)
19 (4)	NCLIV_054120	Unspecified product	98	121119	2	1.6	RON1 (TGME49_310010)
	NCLIV_028680	Putative apical membrane antigen 1	54	64401	1	1.4	-
	NCLIV_052500	Hypothetical protein	47	33213	1	4	Flavoprotein subunit of succinate dehydrogenase
	NCLIV_045350	Conserved hypothetical protein	40	108340	1	0.8	Hypothetical protein (TGME49_228060)
20 (2)	NCLIV_001970	Unspecified product	165	67177	5	6.9	TgROP2 family member
	NCLIV_045350	Conserved hypothetical protein	34	108340	1	0.8	Hypothetical protein (TGME49_228060)
21 (1)	NCLIV_045350	Conserved hypothetical protein	34	108340	1	0.8	Hypothetical protein (TGME49_228060)
22 (1)	NCLIV_048300	Hypothetical protein	40	634244	1	0.2	PHD-finger domain-containing protein (TGME49_224260)
23 (3)	NCLIV_042820	cDNA FLJ58099, highly similar to Homo	328	196066	9	4.9	-

		sapiens clathrin, heavy polypeptide-like 1 (CLTCL1), transcript variant 1, mRNA, related					
	NCLIV_048590	Unspecified product	84	220934	4	2.3	Rhoptry neck protein RON3 (TGME49_223920)
	NCLIV_030080	Putative peroxisomal multifunctional enzyme	35	36206	1	3.7	-
24 (4)	NCLIV_064620	Unspecified product	270	165970	10	7.8	TgRON2 (TGME49_300100)
	NCLIV_045350	Conserved hypothetical protein	49	108340	1	0.8	Hypothetical protein (TGME49_228060)
	NCLIV_061250	Putative acetoacetyl-coA synthetase	36	57747	1	1.4	-
	NCLIV_000760	Conserved hypothetical protein	33	35979	1	2.6	Hypothetical protein (TGME49_293790)
26 (6)	NCLIV_055360	Unspecified product	134	182101	8	4.9	Rhoptry neck protein RON2 (TGME49_300100)
	NCLIV_003050	Putative myosin heavy chain	82	125340	1	1.3	-
	NCLIV_019110	HSP90-like protein, related	76	97392	1	1.8	-
	NCLIV_042410	Putative sortilin	55	105595	1	1.3	-
	NCLIV_021050	Unspecified product	43	93761	1	1	Subtilisin SUB1 (TGME49_204050)
	NCLIV_048300	Hypothetical protein	34	634244	1	0.2	PHD-finger domain-containing protein (TGME49_224260)
27 (6)	NCLIV_049900	Hypothetical protein	70	93837	1	1.7	Myosin A (TGME49_235470)
	NCLIV_055360	Unspecified product	47	182101	2	1	TgRON5 (TGME49_311470)
	NCLIV_048300	Hypothetical protein	38	634244	1	0.2	PHD-finger domain-containing protein (TGME49_224260)
	NCLIV_019700	Conserved hypothetical protein	33	142302	1	0.6	Hypothetical protein (TGME49_280450)
	NCLIV_015150	Conserved hypothetical protein	32	30925	1	2.9	Hypothetical protein (TGME49_284570)
	NCLIV_044170	Putative myosin head motor domain-containing protein	31	202943	1	0.8	-
29 (10)	NCLIV_055490	Heat shock protein 70 (Precursor), related	67	73215	2	14.8	-
	NCLIV_061920	Putative zinc finger (CCCH type) protein	43	123026	1	2.5	-

	NCLIV_054120	Unspecified product	37	121119	1	2.6	RON1 (TGME49_310010)
30 (1)	NCLIV_001970	Unspecified product	235	67177	7	12.8	TgROP2 family member
31 (7)	NCLIV_001970	Unspecified product	220	67177	5	8.9	TgROP2 family member
	NCLIV_012920	Unspecified product	63	43319	2	4.8	TgROP40 (TGME49_291960)
	NCLIV_020840	Hypothetical protein	55	61971	1	2.1	ATPase synthase subunit alpha, putative
	NCLIV_027600	Conserved hypothetical protein	39	63711	1	2.2	Hypothetical protein (TGME49_258870)
	NCLIV_061250	Putative acetoacetyl-coA synthetase	38	57747	1	1.4	-
	NCLIV_025670	ATP synthase subunit beta, related	34	60327	1	1.8	-
	NCLIV_031670	Conserved hypothetical protein	33	66820	1	1.4	Hypothetical protein (TGME49_231410)
33 (9)	NCLIV_053580	50S ribosomal protein L4P, related	170	46046	6	15.8	-
	NCLIV_001970	Unspecified product	130	67177	6	9.9	TgROP2 family member
	NCLIV_047530	Conserved hypothetical protein	85	69818	2	4.6	Hypothetical protein (TGME49_225150)
	NCLIV_006180	Putative duplicated carbonic anhydrase	61	59137	2	3.8	-
	NCLIV_010710	SRS domain-containing protein	53	43258	1	3	-
	NCLIV_018120	Conserved hypothetical protein	45	75282	1	1.2	Hypothetical protein (TGME49_243378)
	NCLIV_061040	Hypothetical protein	43	50946	2	4.2	Dihydrolipoyllysine-residue succinyltransferase component of oxoglutarate dehydrogenase (TGME49_219550)
	NCLIV_012920	Unspecified product	42	43319	1	2.3	TgROP40 (TGME49_291960)
	NCLIV_061160	Putative acid phosphatase	33	47250	1	3.2	-
34 (8)	NCLIV_050470	Hypothetical protein	159	60165	5	8.3	Peptidase M16 family protein beta subunit, putative (TGME49_236210)
	NCLIV_022220	Hypothetical protein	124	63784	4	6.3	Mitochondrial-processing peptidase beta subunit, putative (TGME49_202680)
	NCLIV_048570	Conserved hypothetical protein	96	28575	2	11.5	Gliding-associated protein 45 (GAP45) (TGME49_223940)

	NCLIV_017370	Putative CAMP-dependent protein kinase regulatory subunit	93	43204	3	9.8	-
	NCLIV_061940	Hypothetical protein	88	52724	1	5.4	-
	NCLIV_011410	Protein disulfide isomerase	74	53333	1	2.5	-
	NCLIV_001970	Unspecified product	72	67177	3	5.4	TgROP2 family member
	NCLIV_046190	Multidomain chromatinic protein with the following architecture: 3x PHD-bromo-3xphd-SET domain and associated cysteine cluster at the C-terminus, related	35	718468	1	0.1	-
35 (5)	NCLIV_010600	Putative microneme protein MIC3	105	40366	3	8.5	
	NCLIV_011120	Malate dehydrogenase, related	48	34237	1	3.5	-
	NCLIV_060660	SRS domain-containing protein	38	39552	1	3.4	-
	NCLIV_018350	Conserved hypothetical protein	37	365390	1	0.3	Hypothetical protein (TGME49_243635)
37 (4)	NCLIV_019110	HSP90-like protein, related	436	97392	17	20.4	-
	NCLIV_028570	Conserved hypothetical protein	34	30412	1	2.8	Hypothetical protein (TGME49_255380)
	NCLIV_045350	Conserved hypothetical protein	33	108340	1	0.8	Hypothetical protein (TGME49_228060)
25, 28, 32, 36	No proteins identified						

* Gel spots 1-5 are from 1D BN-PAGE (Figure 2.3a) and spots 6-37 are from 2D BN/SDS-PAGE (Figure 2.3b) of *N. caninum*

** Orthologue name of *T. gondii* protein for uncharacterised (hypothetical protein, unspecified product and conserved hypothetical protein) *N. caninum* proteins.

Table II: All proteins identified by MS analyses of in-gel digestion from BN-PAGE and SDS-PAGE of *T. gondii*. Based on Mascot scoring, ions scores > 31 of an individual peptide indicate identity or extensive homology ($p<0.05$).

Gel spot no.* (no. proteins identified)	Protein accession	Protein description	Protein score	Protein mass	Protein sequences significance	Protein coverage
2 (1)	TGME49_308090	Rhoptry protein ROP5 (ROP5)	35	61403	1	2.9
3 (2)	TGME49_320220	Ubiquinol cytochrome c oxidoreductase, putative	113	55439	2	4.7
	TGME49_308090	Rhoptry protein ROP5 (ROP5)	70	61403	1	2.9
	TGME49_202680	Peptidase M16, alpha subunit, putative	59	62788	1	2.3
	TGME49_219320	Acid phosphatase GAP50 (GAP50)	58	46916	1	3
	TGME49_248160	Hypothetical protein	39	123821	1	0.7
4 (3)	TGME49_244560	Heat shock protein 90, putative	171	97159	5	7.8
	TGME49_219320	Acid phosphatase GAP50 (GAP50)	71	46916	1	3
	TGME49_248160	Hypothetical protein	40	123821	1	0.7
6 (3)	TGME49_201780	Microneme protein MIC2 (MIC2)	74	85030	2	3.5
	TGME49_248160	Hypothetical protein	47	123821	1	0.7
	TGME49_228250	Elongation factor Tu GTP binding domain-containing protein	31	123234	1	1.1
7 (6)	TGME49_233460	SAG-related sequence SRS29B (SRS29B)	157	35619	5	19.9
	TGME49_218520	Microneme protein MIC6 (MIC6)	66	37897	2	8
	TGME49_269190	Glyceraldehyde-3-phosphate dehydrogenase GAPDH2 (GAPDH2)	45	106249	1	1.4
	TGME49_248810	Nuclear factor NF7	39	54531	1	2.8
	TGME49_232350	Lactate dehydrogenase LDH1 (LDH1)	32	36206	1	3.6
9 (8)	TGME49_211680	Protein disulfide isomerase	304	53165	9	22.5
	TGME49_263090	14-3-3 protein	215	37490	8	23.8
	TGME49_266060	Ribosomal protein RPSA (RPSA)	54	31831	2	8

	TGME49_248390	Ribosomal protein RPL26 (RPL26)	52	16467	1	6.3
	TGME49_227620	Dense granule protein GRA2 (GRA2)	51	19960	1	5.9
	TGME49_262620	RNA recognition motif-containing protein	50	32022	1	3.7
	TGME49_254440	Ribosomal protein RPL12 (RPL12)	46	18092	1	6.6
	TGME49_226430	Reticulon protein	40	22401	1	5.1
10 (1)	TGME49_211680	Protein disulfide isomerase	499	53165	8	19.9
11 (2)	TGME49_221210	Cyclophilin	50	19703	1	7.8
	TGME49_215430	Hypothetical protein	32	27705	1	5.3
12 (2)	TGME49_290950	Clathrin heavy chain, putative	406	195918	8	5.9
	TGME49_257470	Myosin J	35	276135	1	0.4
14 (1)	TGME49_248160	Hypothetical protein	33	123821	1	0.7
19 (2)	TGME49_244560	Heat shock protein 90, putative	219	97159	5	7.9
	TGME49_248160	Hypothetical protein	37	123821	1	0.7
20 (2)	TGME49_248160	Hypothetical protein	48	123821	1	0.7
	TGME49_235470	Myosin A	32	93998	1	1.7
21 (2)	TGME49_247550	Heat shock protein HSP60 (HSP60)	70	61499	4	8.2
	TGME49_308090	Rhoptry protein ROP5 (ROP5)	46	61403	1	2.9
24 (2)	TGME49_221210	Cyclophilin	52	19703	1	7.8
	TGME49_242625	ATPase family associated with various cellular activities (AAA) subfamily protein	33	985689	1	0.1
1, 5, 8, 13, 15-18, 22-23	No proteins identified					

* Gel spots 1-11 are from 1D BN-PAGE (Figure 2.4a) and spots 12-24 are from 2D BN/SDS-PAGE (Figure 2.4b) of *T. gondii*

Table III: DNA sequences of recombinant GRA gene used for expression of recombinant proteins.

Gene name	Accession number	Gene sequences[1]
TgGRA2	TGME49_227620	ATGTTCGCCGTAAAACATTGTTTGCTGGTTGTTGCCGTTGGCGCCCTGGTCAACGTCTCGGTGAGGGCTGCCGAGT TTTCCGGAGTTGTTAACCAGGGACCAGTCGACGTGCCTTTCAGCGGTAAACCTCTTGATGAGAGAGCAGTTGGAGGAAAA GGTGAACATACACCACCACTCCCAGACGAGAGGCAACAAGAGCCAGAAGAACCGGTTTCCCAACGTGCATCCAGAGTGG CAGAACAACTGTTTCGCAAGTTCTTGAAGTTCGCTGAAAACGTCGGACAGCACAGTGAGAAGGCCTTCAAAAAAGCAAA GGTGGTGGCAGAAAAAGGCTTCACCGCGGCAAAAACGCACACGGTTAGGGGTTTCAAGGTGGCCAAAGAAGCAGCTGG AAGGGGCATGGTGACCGTTGGCAAGAAACTCGCGAATGTGGAGAGTGACAGAAGCACTACGACAACGCAGGCCCCCGA CAGCCCTAATGGCCTGGCAGAAACCCAGGCTCCAGTGGAGCCCCAACAGCGGGCCGCACACGTGCCCGTCCCAGACTTTT CGCAGTAA
TgGRA7	TGME49_203310	ATGGCCCGACACGCAATTTTTTTCGCGCTTTGTGTTTTAGGCCTGGTGGCGGCGGCTTTGCCCCAGTTCGCTACCG CGGCCACCGCGTCAGATGACGAACTGATGAGTCGAATCCGAAATTCTGACTTTTTCGATGGTCAAGCACCCGTTGACAGT CTCAGACCGACGAACGCCGGTGTCGACTCGAAAGGGACCGACGATCACCTCACCACCAGCATGGATAAGGCATCTGTAG AGAGTCAGCTTCCGAGAAGAGAGCCATTGGAGACGGAGCCAGATGAACAAGAAGAAGTTCATTTCAGGAAGCGAGGCG TCCGTTCCGACGCTGAAGTGACTGACGACAACATCTACGAGGAGCACACTGATCGTAAAGTGGTTCCGAGGAAGTCGGA GGGCAAGCGAAGCTTCAAAGACTTGCTGAAGAAGCTCGCGCTGCCGGCTGTTGGTATGGGTGCATCGTATTTTGCCGCTG ATAGAATTCTGCCGGAACTAACAGAGCAGCAACAGACAGGCGAAGAACCCCTAACCACCGGCCAGAATGTGAGCACTGT GTTAGGCTTCGCAGCGCTTGCTGCTGCCGCAGCGTTCCTTGGCATGGGTCTCACGAGGACGTACCGACATTTTTCCCCACG CAAAAACAGATCACGGCAGCCTGCACTCGAGCAAGAGGTGCCTGAATCAGGCAAAGATGGGGAGGATGCCCGCCAGTA G
NcGRA2	NCLIV_045650	ATGTTCACGGGGAAACGTTGGATACTTGTTGTTGCCGTTGGCGCCCTGGTCGGCGCCTCGGTAAAGGCAGCCGATT TTTCTGGCAGGGGAACCGTCAATGGACAGCCGGTTGGCAGCGGTTATTCCGGATATCCCCGTGGCGATGATGTTAGAGAA TCAATGGCTGCACCCGAAGATCTGCCAGGCGAGAGGCAACCGGAGACACCCACGGCGGAAGCTGTAAAACAGGCAGCG GCAAAAGCTTATCGATTACTCAAGCAGTTTACTGCGAAGGTCGGACAGGAAACTGAGAACGCCTACTACCACGTGAAGA AAGCGACAATGAAAGGCTTTGACGTTGCAAAAGACCAGTCGTATAAGGGCTACTTGGCCGTCAGGAAAGCCACAGCTAA GGGCCTGCAGAGCGCTGGCAAGAGCCTTGAGCTTAAAGAGTCGGCACCGACAGGCACTACGACTGCGGCGCCGACTGAA AAAGTGCCCCCCAGTGGCCCGCGATCAGGTGAAGTTCAGCGTACTCGTAAAGAGCAAAATGACGTGCAGCAAACCGCAG AGATGTTGGCTGAGGAAATTCTTGAGGCTGGGCTTAAGAAGGACGATGGAGAAGGACGGGGAACGCCAGAAGCTGAAG TCAATTAA
NcGRA7	NCLIV_021640	ATGGCCCGACAAGCAACCTTCATCGTGGCTCTGTGCGTTTGTGGACTGGCAATCGCGGGCCTGCCGAGGCTCGCT AGCGCTGGAGACTTGGCAACCGAACAGCATGAAGGGGACATCGGATATGGGGTTAGGGCATATGCCGGCGTTTCAAACT ATGACGGCGATGACGATGCTGCAGGAAACCCTGTCGACTCGGATGTGACTGACGATGCCATTACAGATGGTGAGTGGCC

		ACGTGTTGTATCGGGGCAGAAGCCGCACACGACTCAGAAAGGCAGCTTGATCAAGAAGCTGGCAGTACCGGTGGTCGGC GCTCTTACGTCGTATCTTGTTGCTGACAGGGTGCTGCCCGAGTTGACTTCTGCAGAAGAAGAAGGAACAGAGTCCATCCC CGGTAAAAAACGTGTCAAGACTGCCGTGGGCATAGCCGCGTTAGTTGCAGCAGCCGCATTTGCTGGATTGGGTCTCGCGA GAACATTCAGGCATTTCGTGCCAAAAAAGTCAAAGACGGTTGCGAGTGAGGACTCTGCGCTCGGAAACAGTGAAGAGCA GTATGTGGAAGGAACCGTGAACGGGAGCAGTGATCCGGAACAGGAGCGGGCGGGTGGGCCTCTTATCCCGGAAGGAGA CGAGCAGGAAGTAGACACCGAATAG
6 × Histidine-SUMO tag		ATGGGTCATCACCATCATCATCACGGGTCCCTGCAGGACTCAGAAGTCAATCAAGAAGCTAAGCCAGAGGTCAAGCCAG AAGTCAAGCCTGAGACTCACATCAATTTAAAGGTGTCCGATGGATCTTCAGAGATCTTCTTCAAGATCAAAAAGACCACT CCTTTAAGAAGGCTGATGGAAGCGTTCGCTAAAAGACAGGGTAAGGAAATGGACTCCTTAAGATTCTTGTACGACGGTAT TAGAATTCAAGCTGATCAGGCCCCTGAAGATTTGGACATGGAGGATAACGATATTATTGAGGCTCACCGCGAACAGATTG G

[1]The underlined nucleotides are signal peptides coding sequences that are not included in the recombinant genes.

Table IV: Quantified phosphopeptides enriched using TiO_2 using progenesis software from host cell infected by *T. gondii* and *N. caninum* at 20 hr p.i.

Protein Accession	Peptide score	Phosphorylated sequence	Modifications	Protein description	Max fold change	Highest mean condition	P value
Q8NC51|PAIRB_HUMAN	97.88	SKSEEAHAEDSVMDHHFR	[3] S+79.97	Plasminogen activator inhibitor 1 RNA-binding protein	Infinity	HFF-Tg*	2.81E-05
P43243|MATR3_HUMAN	0	RDSFDDRGPSLNPVLDYDHGSR	[3] S+79.97	Matrin-3	41.32084	HFF-Tg	4.66E-03
O43399|TPD54_HUMAN	99.86	VEEEIVTLR	[7] T+79.97	Tumor protein D54	29.11005	HFF-Tg	1.67E-04
P23588|IF4B_HUMAN	0	SQSSDTEQQSPTSGGGK	[1] S+79.97	Eukaryotic translation initiation factor 4B	26.03601	HFF-Tg	1.03E-04
Q8N6H7|ARFG2_HUMAN	8.05	HGTDLWIDNMSSAVPNHSPEKK	[11] S+79.97	ADP-ribosylation factor GTPase-activating protein 2	20.42531	HFF-Tg	2.13E-02
Q16643|DREB_HUMAN	97.18	MAPTPIPTRSPSDSSTASTPVAEQIER	[10] S+79.97	Drebrin	16.87304	HFF-Tg	1.38E-03
P27816|MAP4_HUMAN	80.57	KKPCSETSQIEDTPSSKPTLLANGGHGVEGSDTTGSPTEFLEEK	[4] C+58.01|[36] S+79.97	Microtubule-associated protein 4	14.16188	HFF-Tg	2.50E-04
P52926|HMGA2_HUMAN	75.61	KPAQEETEETSSQESAEED	[10] T+79.97|[12] S+79.97	High mobility group protein HMGI-C	9.943278	HFF-Tg	1.61E-03
Q9Y5K6|CD2AP_HUMAN	96.59	TSSSETEEKKPEKPLILQSLGPK	[4] S+79.97	CD2-associated protein	8.733796	HFF-Tg	1.42E-03
O60524|NEMF_HUMAN	99.94	LASKEESSNSSDSK	[3] S+79.97	Nuclear export mediator factor NEMF	8.114517	HFF-Tg	1.17E-02
Q9UNL2|SSRG_HUMAN	99.59	KLSEADNR	[3] S+79.97	Translocon-associated protein subunit gamma	7.629456	HFF-Tg	5.93E-04
Q9UQ35|SRRM2_HUMAN	0	YSHSGSSSPDTK	[6] S+79.97	Serine/arginine repetitive matrix protein 2	7.62512	HFF-Tg	3.05E-04
Q8IUD2|RB6I2_HUMAN	99.94	RTNSTGGSSGSSVGGGSGK	[4] S+79.97	ELKS/Rab6-interacting/CAST family member 1	7.058231	HFF-Tg	5.00E-03
P08238|HS90B_HUMAN	42.88	IEDVGSDEEDDSGKDKK	[6] S+79.97	Heat shock protein HSP 90-beta	6.971021	HFF-Tg	4.05E-03
P04792|HSPB1_HUMAN	99.9	GPSWDPFRDWYPHSR	[3] S+79.97	Heat shock protein beta-1	6.915229	HFF-Tg	8.39E-03

P29966|MARCS_HUMAN	78.87	VNGDASPAAAESGAK	[1] V+27.99|[12] S+79.97	Myristoylated alanine-rich C-kinase substrate	6.854313	HFF-Tg	1.08E-04
Q13459|MYO9B_HUMAN	99.94	KKPGDASSLPDAGLSPGSQVDSK	[15] S+79.97	Unconventional myosin-IXb	6.609514	HFF-Tg	4.06E-04
Q8TD16|BICD2_HUMAN	6.69	TSPGGRTSPEAR	[1] T+79.97|[8] S+79.97	Protein bicaudal D homolog 2	6.548232	HFF-Tg	3.43E-02
Q9H0D6|XRN2_HUMAN	99.94	KAEDSDSEPEPEDNVR	[5] S+79.97|[7] S+79.97	5'-3' exoribonuclease 2	6.272299	HFF-Tg	1.80E-02
Q07960|RHG01_HUMAN	99.78	SSSPELVTHLK	[3] S+79.97	Rho GTPase-activating protein 1	6.243514	HFF-Tg	5.20E-03
Q9NWV8|BABA1_HUMAN	99.9	TRSNPEGAEDR	[3] S+79.97	BRISC and BRCA1-A complex member 1	6.217384	HFF-Tg	3.59E-04
O60256|KPRB_HUMAN	93.55	LGIAVIHGEAQDAESDLVDGRHSPPMVR	[15] S+79.97	Phosphoribosyl pyrophosphate synthase-associated protein 2	5.859535	HFF-Tg	4.37E-02
Q9UKV3|ACINU_HUMAN	99.89	SSSISEEKGDSDDEKPR	[11] S+79.97	Apoptotic chromatin condensation inducer in the nucleus	5.837208	HFF-Tg	1.91E-03
O60716|CTND1_HUMAN	97.77	GSLASLDSLR	[2] S+79.97|[5] S+79.97	Catenin delta-1	4.955117	HFF-Tg	2.28E-02
P52569|CTR2_HUMAN	99.57	NLSSPFIFHEK	[3] S+79.97	Low affinity cationic amino acid transporter 2	4.76651	HFF-Tg	3.13E-03
Q8TBM8|DJB14_HUMAN	93.07	KPSGSGDQSKPNCTK	[3] S+79.97|[13] C+57.02	DnaJ homolog subfamily B member 14	4.718028	HFF-Tg	2.42E-02
Q8TF72|SHRM3_HUMAN	59.09	ERSGSMDNTSAR	[3] S+79.97	Protein Shroom3	4.060433	HFF-Tg	1.50E-03
Q12797|ASPH_HUMAN	97.98	SSGNSSSSGSGSGSTSAGSSSPGAR	[20] S+79.97	Aspartyl/asparaginyl beta-hydroxylase	3.967675	HFF-Tg	1.94E-02
Q9NYF8|BCLF1_HUMAN	54.29	ETQSPEQVKSEK	[2] T+79.97	Bcl-2-associated transcription factor 1	3.860327	HFF-Tg	2.12E-03
Q15084|PDIA6_HUMAN	99.95	DGELPVEDDIDLSDVELDDLGKDEL	[13] S+79.97	Protein disulfide-isomerase A6	3.729874	HFF-Tg	2.40E-02

O75351|VPS4B_HUMAN	99.6	EGQPSPADEKGNDSDGEGESDDPEK	[14] S+79.97	Vacuolar protein sorting-associated protein 4B	3.714813	HFF-Tg	2.36E-02
Q9C0C2|TB182_HUMAN	81.14	EHGVGGVSQCPEPGLR	[8] S+79.97|[10] C+58.01|[11] P+31.99	182 kDa tankyrase-1-binding protein	3.345621	HFF-Tg	4.90E-03
P46937|YAP1_HUMAN	97.35	GDSETDLEALFNAVMNPK	[3] S+79.97|[8] E+21.98	Yorkie homolog	3.232932	HFF-Tg	1.73E-02
Q8NEY8|PPHLN_HUMAN	99.95	DTSPSSGSAVSSSK	[3] S+79.97	Periphilin-1	3.197906	HFF-Tg	1.79E-02
P05386|RLA1_HUMAN	99.83	KEESEESDDDMGFGLFD	[7] S+79.97|[11] M+15.99	60S acidic ribosomal protein P1	3.102044	HFF-Tg	3.37E-03
Q96Q45|TM237_HUMAN	13.35	RPSEGNEPSTK	[10] T+79.97	Transmembrane protein 237	2.865537	HFF-Tg	1.96E-02
P60174|TPIS_HUMAN	81.96	KQSLGELIGTLNAAK	[3] S+79.97|[15] K+21.98	Triosephosphate isomerase	2.581143	HFF-Tg	9.38E-03
P40123|CAP2_HUMAN	56.39	SHTPSPTSPK	[3] T+79.97|[5] S+79.97	Adenylyl cyclase-associated protein 2	2.561357	HFF-Tg	2.22E-03
Q9Y2D5|AKAP2_HUMAN	92.99	TNGHSPSQPR	[1] T+79.97|[2] N+0.98	A-kinase anchor protein 2	2.432455	HFF-Tg	4.26E-03
O60271|JIP4_HUMAN	99.94	ERPISLGIFPLPAGDGLLTPDAQK	[19] T+79.97	C-Jun-amino-terminal kinase-interacting protein 4	2.355563	HFF-Tg	3.99E-02
P31943|HNRH1_HUMAN	95.5	HTGPNSPDTANDGFVR	[2] T+79.97	Heterogeneous nuclear ribonucleoprotein H	2.344253	HFF-Tg	3.57E-03
P61978|HNRPK_HUMAN	99.84	DYDDMSPR	[6] S+79.97	Heterogeneous nuclear ribonucleoprotein K	2.212441	HFF-Tg	1.68E-02
Q00613|HSF1_HUMAN	98.1	VEEASPGRPSSVDTLLSPTALIDSILR	[11] S+79.97	Heat shock factor protein 1	2.10717	HFF-Tg	9.50E-03
Q07065|CKAP4_HUMAN	99.92	GAHPSGGADDVAK	[5] S+79.97	Cytoskeleton-associated protein 4	1.988499	HFF-Tg	1.62E-03
Q86VR2|F134C_HUMAN	93.06	GQTPLTEGSEDLDGHSDPEESFAR	[21] S+79.97	Protein FAM134C	1.972753	HFF-Tg	1.95E-03

Q16555|DPYL2_HUMAN	97.84	TVTPASSAKTSPAK	[1] T+79.97|[7] S+79.97|[11] S+79.97	Dihydropyrimidinase-related protein 2	1.883443	HFF-Tg	2.77E-02
P05412|JUN_HUMAN	97.97	NSDLLTSPDVGLLK	[6] T+79.97	Transcription factor AP-1	1.841234	HFF-Tg	7.56E-03
Q9UPQ0|LIMC1_HUMAN	97.72	CSPTVAFVEFPSSPQLK	[1] C+57.02|[2] S+79.97	LIM and calponin homology domains-containing protein 1	1.754757	HFF-Tg	2.67E-02
P48681|NEST_HUMAN	97.29	ETLKSLGEEIQESLK	[5] S+79.97	Nestin	1.704636	HFF-Tg	7.41E-03
Q969E4|TCAL3_HUMAN	98	GTDDSPKDSQEDLQER	[2] T+79.97	Transcription elongation factor A protein-like 3	1.6973	HFF-Tg	3.06E-03
Q15942|ZYX_HUMAN	99.88	EKVSSIDLEIDSLSSLLDDMTK	[4] S+79.97|[20] M+15.99	Zyxin	1.670009	HFF-Tg	5.89E-03
P07355|ANXA2_HUMAN	0	STVHEILCKLSLEGDHSTPPSAYGSVK	[1] S+42.01|[8] C+57.02|[11] S+79.97	Annexin A2	1.630623	HFF-Tg	4.43E-02
O75822|EIF3J_HUMAN	97.92	AAAAAAAGDSDSWDADAFSVEDPVRK	[1] A+42.01|[10] S+79.97	Eukaryotic translation initiation factor 3 subunit J	1.609533	HFF-Tg	4.94E-02
P46821|MAP1B_HUMAN	99.93	SDISPLTPR	[4] S+79.97	Microtubule-associated protein 1B	1.58957	HFF-Tg	2.13E-03
Q86VM9|ZCH18_HUMAN	93.41	RPNTSPDRGSR	[4] T+79.97|[10] S+79.97	Zinc finger CCCH domain-containing protein 18	1.580815	HFF-Tg	6.61E-03
P35221|CTNA1_HUMAN	99.93	SRTSVQTEDDQLIAGQSAR	[1] S+79.97|[4] S+79.97	Catenin alpha-1	1.570152	HFF-Tg	4.89E-02
P04264|K2C1_HUMAN	53.81	SSGGSSSVK	[1] S+79.97	Keratin, type II cytoskeletal 1	1.539394	HFF-Tg	2.76E-02
P22059|OSBP1_HUMAN	81.44	GVAAAGPAPAPPTGGSGGSGAGGSGSAR	[24] S+79.97	Oxysterol-binding protein 1	169.1061	HFF-Nc**	4.28E-03
O00193|SMAP_HUMAN	97.47	SASPDDDLGSSNWEAADLGNEER	[1] S+79.97	Small acidic protein	22.31701	HFF-Nc	2.50E-02

Q9NQC3|RTN4_HUMAN	80.68	SDSPPRPQPAFK	[1] S+79.97	Reticulon-4	14.44466	HFF-Nc	7.77E-05
O15427|MOT4_HUMAN	99.81	LHKPPADSGVDLR	[8] S+79.97	Monocarboxylate transporter 4	14.37004	HFF-Nc	2.29E-04
Q05519|SRS11_HUMAN	0	TAGPGPSGGPGGGGGGGGGGGTEVIQ	[1] T+42.01|[7] S+79.97	Serine/arginine-rich splicing factor 11	12.54036	HFF-Nc	5.32E-04
Q8NE71|ABCF1_HUMAN	92.59	GGNVFAALIQDQSEEEEEEEKHPPKPAKPEK	[13] S+79.97	ATP-binding cassette sub-family F member 1	11.62282	HFF-Nc	2.55E-03
Q92538|GBF1_HUMAN	99.56	GYTSDSEVYTDHGRPGK	[4] S+79.97	Golgi-specific brefeldin A-resistance guanine nucleotide exchange factor 1	11.16622	HFF-Nc	4.24E-03
Q6NZI2|PTRF_HUMAN	98.07	RGSSPDVHALLEIT	[3] S+79.97|[4] S+79.97	Polymerase I and transcript release factor	11.07213	HFF-Nc	2.59E-04
Q15746|MYLK_HUMAN	99.94	KSSTGSPTSPLNAEK	[3] S+79.97|[6] S+79.97	Myosin light chain kinase, smooth muscle	4.604182	HFF-Nc	3.96E-03
P04406|G3P_HUMAN	0	VIHDNFGIVEGLMTTVHAITATQK	[20] T+79.97	Glyceraldehyde-3-phosphate dehydrogenase	4.391173	HFF-Nc	3.12E-03
Q14247|SRC8_HUMAN	7.34	TQTPPVSPAPQPTEERLPSSPVYEDAASFK	[1] T+79.97|[23] Y+79.97	Src substrate cortactin	2.927259	HFF-Nc	2.46E-03
Q8IWB9|TEX2_HUMAN	99.27	SLSTEVEPK	[3] S+79.97	Testis-expressed sequence 2 protein	2.626984	HFF-Nc	3.18E-02
P29692|EF1D_HUMAN	89.82	ATAPQTQHVSPMR	[10] S+79.97	Elongation factor 1-delta	2.260407	HFF-Nc	4.92E-02
Q9Y6F6|MRVI1_HUMAN	89.4	GLSWDSGPEEPGPR	[3] S+79.97	Protein MRVI1	2.144264	HFF-Nc	2.72E-02
P29590|PML_HUMAN	99.48	AVSPPHLDGPPSPR	[3] S+79.97|[12] S+79.97	Protein PML	2.10862	HFF-Nc	1.03E-03
Q3KQU3|MA7D1_HUMAN	98.09	ESAAPASPAPSPAPSPTPAPPQK	[2] S+79.97|[11] S+79.97|[15] S+79.97	MAP7 domain-containing protein 1	2.088762	HFF-Nc	1.79E-02
Q96CV9|OPTN_HUMAN	99.85	KNSAIPSELNEK	[3] S+79.97	Optineurin	2.082669	HFF-Nc	4.04E-02
Q8WWI1|LMO7_HUMAN	99.94	EDSFESLDSLGSR	[3] S+79.97	LIM domain only protein 7	1.993567	HFF-Nc	3.07E-03

P10644|KAP0_HUMAN	99.94	EDEISPPPPNPVVK	[5] S+79.97	cAMP-dependent protein kinase type I-alpha regulatory subunit	1.893618	HFF-Nc	2.08E-02
P42167|LAP2B_HUMAN	99.69	SSTPLPTISSSAENTR	[1] S+79.97	Lamina-associated polypeptide 2, isoforms beta/gamma	1.862157	HFF-Nc	3.97E-03
Q13439|GOGA4_HUMAN	99.94	TSSFTEQLDEGTPNR	[1] T+79.97	Golgin subfamily A member 4	1.83503	HFF-Nc	4.55E-03
O95817|BAG3_HUMAN	98.06	VPPAPVPCPPPSPGPSAVPSSPK	[8] C+57.02|[12] S+79.97|[20] S+79.97	BAG family molecular chaperone regulator 3	1.830106	HFF-Nc	2.47E-02
Q9H1E3|NUCKS_HUMAN	99.81	LKATVTPSPVK	[6] T+79.97	Nuclear ubiquitous casein and cyclin-dependent kinase substrate 1	1.823225	HFF-Nc	3.71E-02
O43294|TGFI1_HUMAN	99.87	KRPSLPSSPSPGLPK	[4] S+79.97|[10] S+79.97	Transforming growth factor beta-1-induced transcript 1 protein	1.81477	HFF-Nc	1.66E-02
P02545|LMNA_HUMAN	98.05	ASSHSSQTQGGGSVTKK	[2] S+79.97|[6] S+79.97	Prelamin-A/C	1.789225	HFF-Nc	2.22E-02
P21333|FLNA_HUMAN	96.67	RAPSVANVGSHCDLSLK	[4] S+79.97|[12] C+57.02	Filamin-A	1.739089	HFF-Nc	4.98E-03
P78559|MAP1A_HUMAN	99.93	VPSAPGQESPIPDPK	[9] S+79.97	Microtubule-associated protein 1A	1.688718	HFF-Nc	6.44E-03
Q96PE2|ARHGH_HUMAN	97.25	SLSDPIPQR	[3] S+79.97	Rho guanine nucleotide exchange factor 17	1.663462	HFF-Nc	2.32E-02
Q969G5|PRDBP_HUMAN	99.94	IQSGLGALSR	[3] S+79.97	Protein kinase C delta-binding protein	1.62541	HFF-Nc	1.44E-02
Q68CZ2|TENS3_HUMAN	99.93	KLSLGQYDNDAGGQLPFSK	[3] S+79.97	Tensin-3	1.621837	HFF-Nc	4.04E-02
O14558|HSPB6_HUMAN	99.93	RASAPLPGLSAPGR	[3] S+79.97	Heat shock protein beta-6	1.609559	HFF-Nc	9.53E-03
Q8IYB3|SRRM1_HUMAN	99.91	SRVSVSPGR	[4] S+79.97|[6] S+79.97	Serine/arginine repetitive matrix protein 1	1.585139	HFF-N	1.19E-03
P02794|FRIH_HUMAN	88.05	MGAPESGLAEYLFDKHTL	[1]	Ferritin heavy chain	1.579336	HFF-Nc	3.79E-02

		GDSDNES	M+15.99|[17] T+79.97				
Q641Q2|FA21A_HUMAN	93.21	SRPTSFADELAAR	[1] S+79.97|[5] S+79.97	WASH complex subunit FAM21A	1.559013	HFF-Nc	1.07E-02
Q14195|DPYL3_HUMAN	97.76	GSPTRPNPPVR	[2] S+79.97	Dihydropyrimidinase-related protein 3	1.558031	HFF-Nc	1.20E-02
P68363|TBA1B_HUMAN	99.83	SIQFVDWCPTGFK	[1] S+79.97|[8] C+57.02	Tubulin alpha-1B chain	1.548237	HFF-Nc	6.77E-03
Q8N3V7|SYNPO_HUMAN	99.94	AASPAKPSSLDLVPNLPK	[3] S+79.97	Synaptopodin	1.516943	HFF-Nc	2.82E-02
P29536|LMOD1_HUMAN	99.86	NSLSPATQR	[4] S+79.97	Leiomodin-1	1.50808	HFF-Nc	9.96E-03

* Maximum fold change of phosphopeptides quantified from host cell infected by *T. gondii* at 20 hr p.i.
** Maximum fold change of phosphopeptides quantified from host cell infected by *N. caninum* at 20 hr p.i.

Table V: Upstream analysis of quantified phosphopeptides from host cell infected with *T. gondii*

Upstream Regulator	Molecule Type	p-value of overlap	Target molecules in dataset
Integrin	Complex	8.36E-03	JUN
Lh	Complex	2.04E-02	ARHGAP1,CAP2 ,CTNND1
FSH	Complex	3.90E-02	ARHGAP1,CAP2 ,CTNND1
CXCL12	Cytokine	8.29E-03	JUN,MARCKS
MIF	Cytokine	3.03E-02	JUN
IL22	Cytokine	3.84E-02	KRT1
RNF187	Enzyme	5.58E-03	JUN
TRAF7	Enzyme	5.58E-03	JUN
DDX17	Enzyme	1.66E-02	JUN
DDX5	Enzyme	2.21E-02	JUN
UPF1	Enzyme	3.84E-02	HMGA2
FN1	Enzyme	4.38E-02	NES
Beta Secretase	Group	5.58E-03	NES
Pkg	Group	1.11E-02	JUN
ERK	Group	2.21E-02	DPYSL2,JUN
CACNA1C	Ion channel	8.36E-03	ANXA2
MAP3K3	Kinase	8.36E-03	JUN
MAPK12	Kinase	8.36E-03	JUN
PIK3C2B	Kinase	8.36E-03	KRT1
PINK1	Kinase	8.36E-03	NES
MAPK7	Kinase	8.36E-03	JUN
EGFR	Kinase	1.51E-02	HNRNPH1,MAR CKS
CSF1R	Kinase	1.66E-02	JUN
ERBB4	Kinase	2.21E-02	JUN
RARB	Ligand-dependent nuclear receptor	2.76E-02	KRT1
ESRRG	Ligand-dependent nuclear receptor	4.11E-02	TPI1
miR-142-3p (and other miRNAs w/seed GUAGUGU)	Mature microrna	8.36E-03	BCLAF1
miR-200b-3p (and other miRNAs w/seed AAUACUG)	Mature microrna	2.49E-02	MARCKS
let-7a-5p (and other miRNAs w/seed GAGGUAG)	Mature microrna	2.49E-02	HMGA2
miR-16-5p (and other miRNAs w/seed AGCAGCA)	Mature microrna	3.84E-02	ZYX
mir-375	Microrna	2.79E-03	YAP1
mir-33	Microrna	2.79E-03	HMGA2
mir-1	Microrna	4.11E-02	ANXA2
mir-8	Microrna	4.11E-02	YAP1
FILIP1L	Other	2.79E-03	HSF1
CCDC80	Other	2.79E-03	BCLAF1
SEMA3A	Other	5.58E-03	MAP1B
RPL15	Other	5.58E-03	HMGA2
PRR7	Other	8.36E-03	JUN
KLHL2	Other	8.36E-03	JUN
N4BP1	Other	8.36E-03	JUN
RPL5	Other	8.36E-03	HMGA2
RPS11	Other	1.11E-02	HMGA2

RPL11	Other	1.11E-02	HMGA2
RPS18	Other	1.11E-02	HMGA2
RPL35A	Other	1.11E-02	HMGA2
RPL12	Other	1.11E-02	HMGA2
RPS15	Other	1.39E-02	HMGA2
RPS12	Other	1.39E-02	HMGA2
ALCAM	Other	1.39E-02	YAP1
S100A10	Other	1.66E-02	ANXA2
THY1	Other	1.94E-02	NES
BAG1	Other	1.94E-02	JUN
MEMO1	Other	2.21E-02	JUN
TINCR	Other	2.21E-02	KRT1
SPARC	Other	2.21E-02	NES
PDCD4	Other	2.21E-02	JUN
FAT1	Other	2.49E-02	JUN
CD9	Other	2.76E-02	YAP1
PNN	Other	3.30E-02	JUN
CUL4B	Other	4.38E-02	TPI1
APP	Other	4.91E-02	NES
PTPRR	Phosphatase	1.66E-02	JUN
MEF2A	Transcription regulator	5.58E-03	JUN
MYC	Transcription regulator	1.25E-02	HSPB1,JUN,TPI1
TAF6	Transcription regulator	1.94E-02	JUN
NANOG	Transcription regulator	2.21E-02	HNRNPH1,MAP 1B
SATB1	Transcription regulator	2.62E-02	CTNNA1,RPLP1
HOXA13	Transcription regulator	3.30E-02	SHROOM3
CARM1	Transcription regulator	3.84E-02	KRT1
SNAI2	Transcription regulator	4.11E-02	NES
ATF2	Transcription regulator	4.38E-02	JUN
TCF7L2	Transcription regulator	4.65E-02	YAP1
ITGA5	Transmembrane receptor	1.66E-02	JUN
BCL2	Transporter	2.21E-02	NES
STAU1	Transporter	2.49E-02	KRT1

Table VI: Upstream analysis of quantified phosphopeptides from host cell infected with *N. caninum*

Upstream Regulator	Molecule Type	p-value of overlap	Target molecules in dataset
F Actin	Complex	1.86E-03	FLNA
IgG1	Complex	1.11E-02	CTTN
TNF	cytokine	4.74E-02	MYLK,PML,SYNPO
RALBP1	Enzyme	1.86E-03	GAPDH
PLCB1	Enzyme	1.86E-03	GAPDH
FTL	Enzyme	3.72E-03	FTH1
ACO1	Enzyme	7.43E-03	FTH1
SUZ12	Enzyme	8.60E-03	MAP7D1,TNS3
NEIL2	Enzyme	1.11E-02	GAPDH
NDUFA13	Enzyme	1.11E-02	CTTN
UBE3A	Enzyme	1.66E-02	PML
PIN1	Enzyme	2.39E-02	PML
PRMT1	Enzyme	2.58E-02	FTH1
POLR2A	Enzyme	4.73E-02	GAPDH
HCAR1	G-protein coupled receptor	7.43E-03	SLC16A3
Lamin b	Group	1.86E-03	LMNA
Actin	Group	5.58E-03	FLNA
VEGFC	Growth factor	1.86E-03	CTTN
MAPK9	Kinase	1.31E-04	GAPDH,LMNA,LMO7
PRKAR2A	Kinase	3.72E-03	PRKAR1A
PRKAR2B	Kinase	9.28E-03	PRKAR1A
SHC1	Kinase	2.21E-02	FTH1
ESRRG	Ligand-dependent nuclear receptor	2.76E-02	GAPDH
NR3C1	Ligand-dependent nuclear receptor	3.30E-02	BAG3,PRKAR1A,RTN4
NUBP1	Other	3.72E-03	FTH1
STMN1	Other	5.58E-03	TUBA1B
SMARCA4	Transcription regulator	3.38E-03	GAPDH,LMNA,MYLK
PIAS3	Transcription regulator	5.58E-03	FTH1
NFYC	Transcription regulator	7.43E-03	FTH1
FOSB	Transcription regulator	7.43E-03	FTH1
BARX2	Transcription regulator	1.30E-02	FLNA
TAF6	Transcription regulator	1.30E-02	GAPDH
NFYB	Transcription regulator	2.03E-02	FTH1
ATF1	Transcription regulator	2.58E-02	FTH1
CARM1	Transcription regulator	2.58E-02	FTH1
BACH1	Transcription regulator	2.58E-02	FTH1
NFE2L2	Transcription regulator	2.76E-02	FTH1
KMT2A	Transcription regulator	2.76E-02	BAG3

SMARCA2	Transcription regulator	2.94E-02	MYLK
ATF2	Transcription regulator	2.94E-02	MYLK
JUND	Transcription regulator	3.30E-02	FTH1
VHL	Transcription regulator	3.66E-02	FTH1
NFYA	Transcription regulator	3.66E-02	FTH1
GTF2B	Transcription regulator	3.84E-02	GAPDH
JUNB	Transcription regulator	4.02E-02	FTH1
HIF1A	Transcription regulator	4.12E-02	GAPDH,NUCKS1
HDAC6	Transcription regulator	4.20E-02	TGFB1I1
DRAP1	Transcription regulator	4.20E-02	GAPDH
IREB2	Translation regulator	5.58E-03	FTH1
CAV1	Transmembrane receptor	2.39E-02	PTRF
ABCB7	Transporter	5.58E-03	FTH1
HNRNPU	Transporter	1.11E-02	GAPDH
S100A6	Transporter	4.91E-02	TMPO

Table VII: Biological processes enriched from host transcripts significantly overexpressed in *N. caninum* infection at 36 hr p.i.

Biological processes	Count	%	PValue	Genes	List Total	Pop Hits	Pop Total	Fold Enrichment
Negative regulation of cellular protein metabolic process	4	17.39	0.001919	P43686, P17980, P38919, P01023	20	180	13528	15.031
Negative regulation of protein metabolic process	4	17.39	0.00214	P43686, P17980, P38919, P01023	20	187	13528	14.468
Regulation of cellular protein metabolic process	5	21.74	0.003794	P43686, P60033, P17980, P38919, P01023	20	474	13528	7.1350
Ubiquitin-dependent protein catabolic process	4	17.39	0.004433	Q16531, P43686, P17980	20	242	13528	11.180
Immune response	5	21.74	0.014087	P30443, Q86WV6, Q01628, P01024, P02794	20	690	13528	4.9014
Cellular macromolecule catabolic process	5	21.74	0.016644	Q16531, P43686, P17980, P38919	20	725	13528	4.6648
Macromolecule catabolic process	5	21.74	0.021324	Q16531, P43686, P17980, P38919	20	781	13528	4.3303
Protein ubiquitination during ubiquitin-dependent protein catabolic process	2	8.696	0.023624	Q16531	20	17	13528	79.576
Positive regulation of protein modification process	3	13.04	0.027854	P43686, P60033, P17980	20	187	13528	10.851
Regulation of acute inflammatory response	2	8.696	0.029105	P01024, P01023	20	21	13528	64.419
Nucleotide-excision repair, DNA damage removal	2	8.696	0.030471	Q16531	20	22	13528	61.490
Positive regulation of cellular protein metabolic process	3	13.04	0.041669	P43686, P60033, P17980	20	233	13528	8.7090
Modification-dependent macromolecule catabolic process	4	17.39	0.044396	Q16531, P43686, P17980	20	574	13528	4.7135
Modification-dependent protein catabolic process	4	17.39	0.044396	Q16531, P43686, P17980	20	574	13528	4.7135
Positive regulation of protein metabolic process	3	13.04	0.044957	P43686, P60033, P17980	20	243	13528	8.3506
Proteolysis involved in cellular protein catabolic process	4	17.39	0.049565	Q16531, P43686, P17980	20	600	13528	4.5093

Table VIII: Biological processes enriched from host transcripts significantly overexpressed in *T. gondii* infection at 36 hr p.i.

Biological processes	**Count**	**%**	**PValue**	**Genes**	**List Total**	**Pop Hits**	**Pop Total**	**Fold Enrichment**
Translational elongation	10	10	2.37E-08	P36578, P05387, P62750, P35268, P84098, P61247, P62906, Q02878, P62081, P62851	92	101	13528	14.558
Translation	12	12	1.32E-05	P36578, P07814, P05387, P62750, P35268, P84098, P61247, P62906, Q02878, P62081, P62851, P41091	92	331	13528	5.3308
Protein amino acid N-linked glycosylation via asparagine	4	4	3.42E-05	Q8TCJ2, P04843, Q9H0U3, P46977	92	10	13528	58.817
peptidyl-asparagine modification	4	4	3.42E-05	Q8TCJ2, P04843, Q9H0U3, P46977	92	10	13528	58.817
RNA processing	14	14	7.11E-05	Q9Y3F4, Q9Y2X3, O75533, P62081, O00567, Q07955, P11940, Q08170, P62906, Q9UQ80, P62995, Q6P2Q9, Q00839, P38159	92	547	13528	3.7634
Intracellular transport	15	15	1.18E-04	P09936, Q01105, P53007, Q14974, P49257, Q9Y2X3, P43307, P38646, P09038, P27348, P11142, P61106, P62258, P62826, Q00610	92	657	13528	3.3571
Establishment of protein localization	16	16	1.75E-04	Q14974, P49257, Q9Y2X3, P02452, Q9NP72, P43307, P38646, P13667, P09038, P27348, P61106, P17301, P14625, P62258, P62826, Q00610	92	769	13528	3.0594
Protein folding	8	8	1.87E-04	P11142, Q14554, P08238, P14625, P78371, P17987, P49257, P38646	92	177	13528	6.6460
Protein amino acid N-linked glycosylation	5	5	2.12E-04	Q8TCJ2, Q16706, P04843, Q9H0U3, P46977	92	44	13528	16.709
Protein transport	15	15	5.38E-04	Q14974, P49257, Q9Y2X3, P02452, Q9NP72, P43307, P38646, P13667, P09038, P27348, P61106, P14625, P62258, P62826, Q00610	92	762	13528	2.8945
RNA splicing, via transesterification reactions	7	7	5.73E-04	Q07955, Q08170, O75533, P62995, Q6P2Q9, Q00839, P38159	92	153	13528	6.7274
nuclear mRNA splicing, via spliceosome	7	7	5.73E-04	Q07955, Q08170, O75533, P62995, Q6P2Q9, Q00839, P38159	92	153	13528	6.7274
RNA splicing, via transesterification reactions with bulged adenosine as nucleophile	7	7	5.73E-04	Q07955, Q08170, O75533, P62995, Q6P2Q9, Q00839, P38159	92	153	13528	6.7274

Protein targeting	8	8	6.07E-04	P09038, P27348, Q14974, P62258, Q9Y2X3, P62826, P43307, P38646	92	215	13528	5.4713
RNA splicing	9	9	6.44E-04	Q07955, P11940, Q9Y3F4, Q08170, O75533, P62995, Q6P2Q9, Q00839, P38159	92	284	13528	4.6598
Protein localization	16	16	7.50E-04	Q14974, P49257, Q9Y2X3, P02452, Q9NP72, P43307, P38646, P13667, P09038, P27348, P61106, P17301, P14625, P62258, P62826, Q00610	92	882	13528	2.6674
Regulation of cellular protein metabolic process	11	11	0.001285	P09038, P48556, O43242, Q13200, Q01105, P08238, P17301, P62258, Q9UQ80, P07996, P04792	92	474	13528	3.4124
Negative regulation of cellular protein metabolic process	7	7	0.001336	P48556, O43242, Q13200, Q01105, P08238, P62258, P07996	92	180	13528	5.7183
mRNA processing	9	9	0.001418	Q07955, P11940, Q9Y3F4, Q08170, O75533, P62995, Q6P2Q9, Q00839, P38159	92	321	13528	4.1227
Negative regulation of protein metabolic process	7	7	0.001623	P48556, O43242, Q13200, Q01105, P08238, P62258, P07996	92	187	13528	5.5043
mRNA metabolic process	9	9	0.003424	Q07955, P11940, Q9Y3F4, Q08170, O75533, P62995, Q6P2Q9, Q00839, P38159	92	370	13528	3.5767
Intracellular protein transport	9	9	0.003655	P09038, P27348, Q14974, P62258, Q9Y2X3, Q00610, P62826, P43307, P38646	92	374	13528	3.5384
Nucleocytoplasmic transport	6	6	0.004011	P09038, Q14974, Q01105, Q9Y2X3, P62826, P38646	92	156	13528	5.6555
Nuclear transport	6	6	0.004234	P09038, Q14974, Q01105, Q9Y2X3, P62826, P38646	92	158	13528	5.5839
Macromolecular complex assembly	12	12	0.004925	Q07955, P0C0S5, P07814, Q14974, Q01105, P21980, P17987, P07305, Q9NVA2, Q9BUF5, Q5SSJ5, Q16181	92	665	13528	2.6534
Cellular macromolecular complex assembly	8	8	0.00557	Q07955, P0C0S5, Q14974, Q01105, P17987, P07305, Q9BUF5, Q5SSJ5	92	318	13528	3.6992
Response to protein stimulus	5	5	0.005838	P11142, O00299, P08238, P17301, P04792	92	107	13528	6.8711
Blood vessel development	7	7	0.006143	P09038, P21980, P02452, P15144, P02461, P07996, Q6UVK1	92	245	13528	4.2012
Cellular protein localization	9	9	0.006402	P09038, P27348, Q14974, P62258, Q9Y2X3, Q00610, P62826, P43307, P38646	92	411	13528	3.2199
Cellular macromolecule localization	9	9	0.006679	P09038, P27348, Q14974, P62258, Q9Y2X3, Q00610, P62826, P43307, P38646	92	414	13528	3.1965
Vasculature development	7	7	0.00689	P09038, P21980, P02452, P15144, P02461, P07996, Q6UVK1	92	251	13528	4.1008
Positive regulation of cell adhesion	4	4	0.007642	P21980, P17301, P07996, Q53GQ0	92	60	13528	9.8028
Macromolecular complex subunit	12	12	0.007945	Q07955, P0C0S5, P07814, Q14974, Q01105, P21980,	92	710	13528	2.4852

organization				P17987, P07305, Q9NVA2, Q9BUF5, Q5SSJ5, Q16181				
Negative regulation of protein modification process	5	5	0.008453	P48556, O43242, Q13200, Q01105, P62258	92	119	13528	6.1782
Cell redox homeostasis	4	4	0.008741	P30041, P13667, Q14554, P09622	92	63	13528	9.3360
Cellular macromolecular complex subunit organization	8	8	0.010225	Q07955, P0C0S5, Q14974, Q01105, P17987, P07305, Q9BUF5, Q5SSJ5	92	357	13528	3.2950
Protein amino acid glycosylation	5	5	0.010851	Q8TCJ2, Q16706, P04843, Q9H0U3, P46977	92	128	13528	5.7438
Biopolymer glycosylation	5	5	0.010851	Q8TCJ2, Q16706, P04843, Q9H0U3, P46977	92	128	13528	5.7438
Glycosylation	5	5	0.010851	Q8TCJ2, Q16706, P04843, Q9H0U3, P46977	92	128	13528	5.7438
Response to unfolded protein	4	4	0.012106	P11142, O00299, P08238, P04792	92	71	13528	8.2841
Anti-apoptosis	6	6	0.01261	P21980, P14625, P09429, P07996, P04792, P38646	92	206	13528	4.2828
Peptide cross-linking	3	3	0.013097	P21980, P02461, P07996	92	26	13528	16.966
Regulation of cell adhesion	5	5	0.013651	P21980, P17301, P02452, P07996, Q53GQ0	92	137	13528	5.3665
Postranscriptional regulation of gene expression	6	6	0.013868	P11940, P17301, Q9UQ80, Q00839, P07996, P04792	92	211	13528	4.1813
Acetyl-CoA metabolic process	3	3	0.018337	P36957, P09622, O75390	92	31	13528	14.230
Nucleosome assembly	4	4	0.018964	P0C0S5, Q01105, P07305, Q5SSJ5	92	84	13528	7.0020
Protein import into nucleus	4	4	0.020175	P09038, Q14974, Q9Y2X3, P62826	92	86	13528	6.8392
Positive regulation of cellular protein metabolic process	6	6	0.020409	P09038, P48556, O43242, Q13200, P17301, P07996	92	233	13528	3.7865
Chromatin assembly	4	4	0.020796	P0C0S5, Q01105, P07305, Q5SSJ5	92	87	13528	6.7606
Nuclear import	4	4	0.021427	P09038, Q14974, Q9Y2X3, P62826	92	88	13528	6.6837
Dicarboxylic acid metabolic process	3	3	0.021837	P36957, P09622, O75390	92	34	13528	12.974
Glycoprotein biosynthetic process	5	5	0.021859	Q8TCJ2, Q16706, P04843, Q9H0U3, P46977	92	158	13528	4.6532
Cell-matrix adhesion	4	4	0.022069	Q14112, P17301, Q9Y3I0, P02461	92	89	13528	6.6086
Protein-DNA complex assembly	4	4	0.023384	P0C0S5, Q01105, P07305, Q5SSJ5	92	91	13528	6.4634
Positive regulation of protein metabolic process	6	6	0.023955	P09038, P48556, O43242, Q13200, P17301, P07996	92	243	13528	3.6307
rRNA processing	4	4	0.024058	Q9Y2X3, P62081, Q9UQ80, O00567	92	92	13528	6.3931
Nucleosome organization	4	4	0.024741	P0C0S5, Q01105, P07305, Q5SSJ5	92	93	13528	6.3244
Negative regulation of macromolecule metabolic process	11	11	0.025376	P09038, P48556, O43242, P27348, Q13200, Q01105, P08238, P62258, Q9UQ80, P09429, P07996	92	734	13528	2.2036
Protein localization in nucleus	4	4	0.025436	P09038, Q14974, Q9Y2X3, P62826	92	94	13528	6.2571
rRNA metabolic process	4	4	0.026855	Q9Y2X3, P62081, Q9UQ80, O00567	92	96	13528	6.1268

Cell-substrate adhesion	4	4	0.028317	Q14112, P17301, Q9Y3I0, P02461	92	98	13528	6.0017
Proteasomal ubiquitin-dependent protein catabolic process	4	4	0.031364	P48556, O43242, Q13200, P14625	92	102	13528	5.7664
Proteasomal protein catabolic process	4	4	0.031364	P48556, O43242, Q13200, P14625	92	102	13528	5.7664
Ribonucleoprotein complex biogenesis	5	5	0.033135	Q07955, Q9Y2X3, P62081, Q9UQ80, O00567	92	180	13528	4.0845
Collagen biosynthetic process	2	2	0.033189	P02452, P02461	92	5	13528	58.817
Regulation of cell-substrate adhesion	3	3	0.038255	P02452, P07996, Q53GQ0	92	46	13528	9.5897
Acetyl-CoA biosynthetic process	2	2	0.039695	P36957, P09622	92	6	13528	49.014
Response to nutrient levels	5	5	0.043805	P48681, O00299, P17301, P02786, P02452	92	197	13528	3.7320
DNA packaging	4	4	0.044256	P0C0S5, Q01105, P07305, Q5SSJ5	92	117	13528	5.0271
Glycoprotein metabolic process	5	5	0.047271	Q8TCJ2, Q16706, P04843, Q9H0U3, P46977	92	202	13528	3.6396
Regulation of protein catabolic process	3	3	0.047765	O43242, Q13200, P08238	92	52	13528	8.4832
Regulation of protein modification process	6	6	0.048688	P09038, P48556, O43242, Q13200, Q01105, P62258	92	295	13528	2.9907
Ribosome biogenesis	4	4	0.049057	Q9Y2X3, P62081, Q9UQ80, O00567	92	122	13528	4.8210

Table IX: Biological processes enriched from host proteins significantly overexpressed in *N. caninum* infection at 36 hr p.i.

Biological processes	**Count**	**%**	**P-value**	**Genes**	**List total**	**Pop. hits**	**Pop. total**	**Fold enrichment**
Generation of precursor metabolites and energy	11	11	3.48E-05	Q5JWF2, P31040, P04406, P60174, P49821, P00558, P06733, P07954, O75390, P22695, P17858	89	313	13528	5.342
Glycolysis	5	5	2.41E-04	P04406, P60174, P00558, P06733, P17858	89	47	13528	16.17
Translational elongation	6	6	5.04E-04	P26641, P61513, P46778, P35268, P62841, P27635	89	101	13528	9.03
Glucose catabolic process	5	5	5.43E-04	P04406, P60174, P00558, P06733, P17858	89	58	13528	13.1
Hexose catabolic process	5	5	0.001472	P04406, P60174, P00558, P06733, P17858	89	69	13528	11.01
Monosaccharide catabolic process	5	5	0.0011654	P04406, P60174, P00558, P06733, P17858	89	71	13528	10.7
Aerobic respiration	4	4	0.0014977	P31040, P07954, O75390, P22695	89	35	13528	17.37
Alcohol catabolic process	5	5	0.0018996	P04406, P60174, P00558, P06733, P17858	89	81	13528	9.383
Cellular carbohydrate catabolic process	5	5	0.0022668	P04406, P60174, P00558, P06733, P17858	89	85	13528	8.941
Energy derivation by oxidation of organic compounds	6	6	0.00246	Q5JWF2, P31040, P49821, P07954, O75390, P22695	89	144	13528	6.333
Cellular respiration	5	5	0.0036569	P31040, P49821, P07954, O75390, P22695	89	97	13528	7.835
Carbohydrate catabolic process	5	5	0.0055361	P04406, P60174, P00558, P06733, P17858	89	109	13528	6.972
Cell redox homeostasis	4	4	0.0079737	P30041, P13667, Q15084, P32119	89	63	13528	9.651
Tricarboxylic acid cycle	3	3	0.0096858	P31040, P07954, O75390	89	23	13528	19.83
Acetyl-CoA catabolic process	3	3	0.0096858	P31040, P07954, O75390	89	23	13528	19.83
Protein transport	12	12	0.0102774	Q5JWF2, P13667, P27348, O75396, Q01082, P62258, P46459, Q9Y5X1, Q15363, P27797, O43707, P61981	89	762	13528	2.394
Establishment of protein localization	12	12	0.0109586	Q5JWF2, P13667, P27348, O75396, Q01082, P62258, P46459, Q9Y5X1, Q15363, P27797, O43707, P61981	89	769	13528	2.372
Coenzyme catabolic process	3	3	0.0122863	P31040, P07954, O75390	89	26	13528	17.54
Acetyl-CoA metabolic process	3	3	0.017214	P31040, P07954, O75390	89	31	13528	14.71
Cofactor catabolic process	3	3	0.017214	P31040, P07954, O75390	89	31	13528	14.71
Glucose metabolic process	5	5	0.0176227	P04406, P60174, P00558, P06733, P17858	89	153	13528	4.967
Coenzyme metabolic process	5	5	0.0176227	P31040, P60174, O00764, P07954, O75390	89	153	13528	4.967
Dicarboxylic acid metabolic process	3	3	0.0205088	P31040, P07954, O75390	89	34	13528	13.41
Translation	7	7	0.0207888	P26641, P61513, P46778, P35268, Q9NSE4, P62841,	89	331	13528	3.215

				P27635				
Regulation of neurogenesis	5	5	0.022999	P12956, P27797, P13010, P61158, P61981	89	166	13528	4.578
Intracellular transport	10	10	0.0267528	Q5JWF2, P27348, O75396, P09936, Q01082, P62258, Q9Y5X1, P27797, P62841, P61981	89	657	13528	2.314
Protein localization	12	12	0.0274781	Q5JWF2, P13667, P27348, O75396, Q01082, P62258, P46459, Q9Y5X1, Q15363, P27797, O43707, P61981	89	882	13528	2.068
Protein folding	5	5	0.0282516	Q15084, Q9NYU2, P48643, P27797, O60884	89	177	13528	4.294
Regulation of nervous system development	5	5	0.0364823	P12956, P27797, P13010, P61158, P61981	89	192	13528	3.958
Hexose metabolic process	5	5	0.0364823	P04406, P60174, P00558, P06733, P17858	89	192	13528	3.958
Cofactor metabolic process	5	5	0.0382782	P31040, P60174, O00764, P07954, O75390	89	195	13528	3.897
Regulation of cell development	5	5	0.0446271	P12956, P27797, P13010, P61158, P61981	89	205	13528	3.707
Posttranscriptional regulation of gene expression	5	5	0.0487042	Q7KZF4, P67809, Q92616, P27797, Q9UQ80	89	211	13528	3.602

Table X: Biological processes enriched from host proteins significantly overexpressed in *T. gondii* infection at 36 hr p.i.

Biological processes	Count	%	P-value	Genes	List total	Pop. hits	Pop. total	Fold enrichment
Translational elongation	25	22	1.85E-30	P18124, P62750, Q07020, P62280, P62249, P62424, P84098, P62269, P61247, P62241, P62829, P47914, P61313, P62854, P62851, P46782, P46781, P15880, Q02543, P42766, P62913, P61254, Q02878, P18077, P40429	100	101	13528	33.49
Translation	28	24	2.90E-21	P18124, P14868, P62750, Q07020, P62280, P62249, P62424, P84098, P62269, P61247, P62241, P62829, P47914, P61313, O00425, P62854, P62851, P46782, P46781, P15880, Q02543, P42766, P62913, P07814, P61254, Q02878, P18077, P40429	100	331	13528	11.44
Ribosome biogenesis	8	7	3.06E-05	P62249, P18124, P62424, P61254, P62913, P18077, O00567, P22087	100	122	13528	8.871
Ribosomal large subunit biogenesis	4	3	4.40E-05	P18124, P61254, P62913, P18077	100	10	13528	54.11
rRNA processing	7	6	5.66E-05	P62249, P18124, P61254, P62913, P18077, O00567, P22087	100	92	13528	10.29
rRNA metabolic process	7	6	7.19E-05	P62249, P18124, P61254, P62913, P18077, O00567, P22087	100	96	13528	9.864
RNA processing	14	12	1.71E-04	P18124, P62913, P17844, P31943, O00567, Q92841, P22087, P62249, P11940, Q08170, P61254, O75400, P18077, Q15365	100	547	13528	3.462
ncRNA metabolic process	9	8	2.80E-04	P62249, P18124, P07814, P14868, P61254, P62913, P18077, O00567, P22087	100	230	13528	5.294
Ribonucleoprotein complex biogenesis	8	7	3.49E-04	P62249, P18124, P62424, P61254, P62913, P18077, O00567, P22087	100	180	13528	6.012
Establishment of protein localization	16	14	4.50E-04	P61204, Q14974, Q9Y3Q3, Q9UL25, P61026, P02452, Q9H444, P62913, P43307, P35579, P38646, P61106, P17301, P48444, P62829, P62826	100	769	13528	2.815
Protein localization	17	15	6.34E-04	P61204, Q14974, Q9Y3Q3, Q9UL25, P60033, P61026, P02452, Q9H444, P62913, P43307, P35579, P38646, P61106, P17301, P48444, P62829, P62826	100	882	13528	2.607
Positive regulation of endocytosis	4	3	0.0012099	P17301, P01024, P08962, Q08431	100	29	13528	18.66
Protein transport	15	13	0.0012634	P61204, Q14974, Q9Y3Q3, Q9UL25, P61026, P02452, Q9H444, P62913, P43307, P35579, P38646, P61106, P48444, P62829, P62826	100	762	13528	2.663
Protein folding	7	6	0.001890	P23284, P78371, P17987, P30533, Q9UBS4, Q9Y230, P38646	100	177	13528	5.35

			8					
ncRNA processing	7	6	0.0024918	P62249, P18124, P61254, P62913, P18077, O00567, P22087	100	187	13528	5.064
Positive regulation of phagocytosis	3	3	0.0033359	P17301, P01024, Q08431	100	12	13528	33.82
Regulation of phagocytosis	3	3	0.0059508	P17301, P01024, Q08431	100	16	13528	25.37
Intracellular transport	12	10	0.0084672	Q969X5, P61106, Q14974, P12236, P62829, P48444, P02792, P62913, P62826, P43307, P35579, P38646	100	657	13528	2.471
Positive regulation of cell adhesion	4	3	0.0096231	P21980, P17301, P07996, Q53GQ0	100	60	13528	9.019
Regulation of endocytosis	4	3	0.0100679	P17301, P01024, P08962, Q08431	100	61	13528	8.871
Positive regulation of response to external stimulus	4	3	0.0114734	P21980, P17301, P01024, P07996	100	64	13528	8.455
Regulation of cell adhesion	5	4	0.0180812	P21980, P17301, P02452, P07996, Q53GQ0	100	137	13528	4.937
Regulation of inflammatory response	4	3	0.0181826	P21980, P17301, P01024, P01023	100	76	13528	7.12
Collagen fibril organization	3	3	0.0189304	P02452, P50454, P08123	100	29	13528	13.99
Positive regulation of inflammatory response	3	3	0.0201871	P21980, P17301, P01024	100	30	13528	13.53
Protein targeting	6	5	0.0207653	Q14974, P62829, P62913, P62826, P43307, P38646	100	215	13528	3.775
Ribosomal protein import into nucleus	2	2	0.0217958	Q14974, P62829	100	3	13528	90.19
Negative regulation of protein maturation by peptide bond cleavage	2	2	0.028956	P07996, P01023	100	4	13528	67.64
Skin morphogenesis	2	2	0.028956	P02452, P08123	100	4	13528	67.64
Regulation of response to external stimulus	5	4	0.0292627	P21980, P17301, P01024, P07996, P01023	100	159	13528	4.254

Positive regulation of cell proliferation	8	7	0.0321097	P21980, P17301, P60033, P06703, Q13488, P43307, Q08431, P46781	100	414	13528	2.614
Regulation of vesicle-mediated transport	4	3	0.0333068	P17301, P01024, P08962, Q08431	100	96	13528	5.637
Blood vessel development	6	5	0.0338887	P21980, P02452, P07996, Q6UVK1, P35579, P08123	100	245	13528	3.313
Collagen biosynthetic process	2	2	0.0360644	P02452, P50454	100	5	13528	54.11
Vasculature development	6	5	0.0370154	P21980, P02452, P07996, Q6UVK1, P35579, P08123	100	251	13528	3.234
Extracellular matrix organization	4	3	0.0407301	P02452, P50454, P08123, Q53GQ0	100	104	13528	5.203
Negative regulation of cellular protein metabolic process	5	4	0.0430622	P48556, P62333, O00425, P07996, P01023	100	180	13528	3.758
Regulation of protein maturation by peptide bond cleavage	2	2	0.0431212	P07996, P01023	100	6	13528	45.09
Regulation of protein processing	2	2	0.0431212	P07996, P01023	100	6	13528	45.09
Positive regulation of cellular component organization	5	4	0.0437969	P17301, P01024, P08962, Q08431, P60981	100	181	13528	3.737
Regulation of cell-substrate adhesion	3	3	0.0445538	P02452, P07996, Q53GQ0	100	46	13528	8.823
Negative regulation of protein metabolic process	5	4	0.0483533	P48556, P62333, O00425, P07996, P01023	100	187	13528	3.617

REFERENCES

Achbarou, A., Mercereau-Puijalon, O., Sadak, A., Fortier, B., Leriche, M.A., Camus, D., Dubremetz, J.F. (1991). Differential targeting of dense granule proteins in the parasitophorous vacuole of *Toxoplasma gondii*. *Parasitology*, 103 Pt 3 (3): 321-329.

Adjogble, K.D., Mercier, C., Dubremetz, J.F., Hucke, C., Mackenzie, C.R., Cesbron-Delauw, M.F., Daubener, W. (2004). GRA9, a new *Toxoplasma gondii* dense granule protein associated with the intravacuolar network of tubular membranes. *Int J Parasitol*, 34 (11): 1255-1264.

Aikawa, M., Miller, L.H., Johnson, J., Rabbege, J. (1978). Erythrocyte entry by malarial parasites. A moving junction between erythrocyte and parasite. *Journal of Cell Biology*, 77 (1): 72-82.

Alaganan, A., Fentress, S.J., Tang, K., Wang, Q., Sibley, L.D. (2014). *Toxoplasma* GRA7 effector increases turnover of immunity-related GTPases and contributes to acute virulence in the mouse. *Proc Natl Acad Sci U S A*, 111 (3): 1126-1131.

Alberts, B. (1998). The cell as a collection of protein machines: Preparing the next generation of molecular biologists. *Cell*, 92 (3): 291-294.

Alexander, D.L., Mital, J., Ward, G.E., Bradley, P., Boothroyd, J.C. (2005). Identification of the moving junction complex of *Toxoplasma gondii*: a collaboration between distinct secretory organelles. *PLoS Pathogens*, 1 (2):

Alms, G.R., Sanz, P., Carlson, M., Haystead, T.A. (1999). Reg1p targets protein phosphatase 1 to dephosphorylate hexokinase II in *Saccharomyces cerevisiae*: characterizing the effects of a phosphatase subunit on the yeast proteome. *EMBO J*, 18 (15): 4157-4168.

Altschul, S.F., Madden, T.L., Schaffer, A.A., Zhang, J., Zhang, Z., Miller, W., Lipman, D.J. (1997). Gapped BLAST and PSI-BLAST: a new generation of protein database search programs. *Nucleic Acids Res*, 25 (17): 3389-3402.

Andersson, L., Porath, J. (1986). Isolation of phosphoproteins by immobilized metal (Fe3+) affinity chromatography. *Anal Biochem*, 154 (1): 250-254.

Arnau, J., Lauritzen, C., Petersen, G.E., Pedersen, J. (2006). Current strategies for the use of affinity tags and tag removal for the purification of recombinant proteins. *Protein Expression and Purification*, 48 (1): 1-13.

Arraiano, C.M., Maquat, L.E. (2003). Post-transcriptional control of gene expression: Effectors of mRNA decay. *Molecular Microbiology*, 49 (1): 267-276.

Arrizabalaga, G., Boothroyd, J.C. (2004). Role of calcium during *Toxoplasma gondii* invasion and egress. *Int J Parasitol*, 34 (3): 361-368.

Asai, T., Howe, D.K., Nakajima, K., Nozaki, T., Takeuchi, T., Sibley, L.D. (1998). *Neospora caninum*: Tachyzoites express a potent type-I nucleoside triphosphate hydrolase, but lack nucleoside diphosphate hydrolase activity. *Experimental Parasitology*, 90 (3): 277-285.

Atkinson, R.A., Ryce, C., Miller, C.M., Balu, S., Harper, P.A., Ellis, J.T. (2001). Isolation of *Neospora caninum* genes detected during a chronic murine infection. *Int J Parasitol*, 31 (1): 67-71.

Aurrecoechea, C., Barreto, A., Brestelli, J., Brunk, B.P., Cade, S., Doherty, R., Fischer, S., Gajria, B., Gao, X., Gingle, A., Grant, G., Harb, O.S., Heiges, M., Hu, S., Iodice, J., Kissinger, J.C., Kraemer, E.T., Li, W., Pinney, D.F., Pitts, B., Roos, D.S., Srinivasamoorthy, G., Stoeckert, C.J., Wang, H., Warrenfeltz,

S. (2013). EuPathDB: the eukaryotic pathogen database. *Nucleic Acids Res*, 41 (Database issue): D684-691.

Bahrami, B.F., Ataie-Kachoie, P., Pourgholami, M.H., Morris, D.L. (2014). p70 Ribosomal protein S6 kinase (Rps6kb1): an update. *J Clin Pathol*, 67 (12): 1019-1025.

Bai, X., Ma, D., Liu, A., Shen, X., Wang, Q.J., Liu, Y., Jiang, Y. (2007). Rheb activates mTOR by antagonizing its endogenous inhibitor, FKBP38. *Science*, 318 (5852): 977-980.

Bandini, L.A., Neto, A.F., Pena, H.F., Cavalcante, G.T., Schares, G., Nishi, S.M., Gennari, S.M. (2011). Experimental infection of dogs (*Canis familiaris*) with sporulated oocysts of *Neospora caninum*. *Vet Parasitol*, 176 (2-3): 151-156.

Barber, J.S., Trees, A.J. (1996). Clinical aspects of 27 cases of neosporosis in dogs. *Vet Rec*, 139 (18): 439-443.

Behnke, M.S., Fentress, S.J., Mashayekhi, M., Li, L.X., Taylor, G.A., Sibley, L.D. (2012). The polymorphic pseudokinase ROP5 controls virulence in *Toxoplasma gondii* by regulating the active kinase ROP18. *PLoS Pathog*, 8 (11): e1002992.

Bennion, B.J., Daggett, V. (2003). The molecular basis for the chemical denaturation of proteins by urea. *Proc Natl Acad Sci U S A*, 100 (9): 5142-5147.

Berggard, T., Linse, S., James, P. (2007). Methods for the detection and analysis of protein-protein interactions. *Proteomics*, 7 (16): 2833-2842.

Besteiro, S., Dubremetz, J.F., Lebrun, M. (2011). The moving junction of apicomplexan parasites: a key structure for invasion. *Cell Microbiol*, 13 (6): 797-805.

Besteiro, S., Michelin, A., Poncet, J., Dubremetz, J.F., Lebrun, M. (2009). Export of a *Toxoplasma gondii* rhoptry neck protein complex at the host cell membrane to form the moving junction during invasion. *PLoS Pathogens*, 5 (2):

Bhavsar, A.P., Guttman, J.A., Finlay, B.B. (2007). Manipulation of host-cell pathways by bacterial pathogens. *Nature*, 449 (7164): 827-834.

Bittame, A., Effantin, G., Petre, G., Ruffiot, P., Travier, L., Schoehn, G., Weissenhorn, W., Cesbron-Delauw, M.F., Gagnon, J., Mercier, C. (2015). *Toxoplasma gondii*: biochemical and biophysical characterization of recombinant soluble dense granule proteins GRA2 and GRA6. *Biochem Biophys Res Commun*, 459 (1): 107-112.

Black, M.W., Arrizabalaga, G., Boothroyd, J.C. (2000). Ionophore-resistant mutants of *Toxoplasma gondii* reveal host cell permeabilization as an early event in egress. *Molecular and Cellular Biology*, 20 (24): 9399-9408.

Blader, I.J., Manger, I.D., Boothroyd, J.C. (2001). Microarray analysis reveals previously unknown changes in *Toxoplasma gondii*-infected human cells. *J Biol Chem*, 276 (26): 24223-24231.

Bochtler, M., Ditzel, L., Groll, M., Hartmann, C., Huber, R. (1999). The proteasome. *Annu Rev Biophys Biomol Struct*, 28 295-317.

Bodenmiller, B., Mueller, L.N., Mueller, M., Domon, B., Aebersold, R. (2007). Reproducible isolation of distinct, overlapping segments of the phosphoproteome. *Nat Methods*, 4 (3): 231-237.

Bonhomme, A., Maine, G.T., Beorchia, A., Burlet, H., Aubert, D., Villena, I., Hunt, J., Chovan, L., Howard, L., Brojanac, S., Sheu, M., Tyner, J., Pluot, M., Pinon, J.M. (1998). Quantitative immunolocalization of a P29 protein (GRA7), a new antigen of *Toxoplasma gondii*. *The journal of histochemistry*

and cytochemistry : official journal of the Histochemistry Society, 46 (12): 1411-1422.

Boothroyd, J.C., Hehl, A., Knoll, L.J., Manger, I.D. (1998). The surface of *Toxoplasma*: more and less. *Int J Parasitol*, 28 (1): 3-9.

Bougdour, A., Durandau, E., Brenier-Pinchart, M.P., Ortet, P., Barakat, M., Kieffer, S., Curt-Varesano, A., Curt-Bertini, R.L., Bastien, O., Coute, Y., Pelloux, H., Hakimi, M.A. (2013). Host cell subversion by *Toxoplasma* GRA16, an exported dense granule protein that targets the host cell nucleus and alters gene expression. *Cell Host and Microbe*, 13 (4): 489-500.

Bougdour, A., Tardieux, I., Hakimi, M.A. (2014). *Toxoplasma* exports dense granule proteins beyond the vacuole to the host cell nucleus and rewires the host genome expression. *Cell Microbiol*, 16 (3): 334-343.

Bradley, P.J., Ward, C., Cheng, S.J., Alexander, D.L., Coller, S., Coombs, G.H., Dunn, J.D., Ferguson, D.J., Sanderson, S.J., Wastling, J.M., Boothroyd, J.C. (2005). Proteomic analysis of rhoptry organelles reveals many novel constituents for host-parasite interactions in *Toxoplasma gondii*. *J Biol Chem*, 280 (40): 34245-34258.

Braun, L., Brenier-Pinchart, M.P., Yogavel, M., Curt-Varesano, A., Curt-Bertini, R.L., Hussain, T., Kieffer-Jaquinod, S., Coute, Y., Pelloux, H., Tardieux, I., Sharma, A., Belrhali, H., Bougdour, A., Hakimi, M.A. (2013). A *Toxoplasma* dense granule protein, GRA24, modulates the early immune response to infection by promoting a direct and sustained host p38 MAPK activation. *The Journal of experimental medicine*, 210 (10): 2071-2086.

Braun, L., Travier, L., Kieffer, S., Musset, K., Garin, J., Mercier, C., Cesbron-Delauw, M.F. (2008). Purification of *Toxoplasma* dense granule proteins reveals that they are in complexes throughout the secretory pathway. *Mol Biochem Parasitol*, 157 (1): 13-21.

Braun, P., Gingras, A.C. (2012). History of protein-protein interactions: from egg-white to complex networks. *Proteomics*, 12 (10): 1478-1498.

Braun, R. (2014). Systems analysis of high-throughput data. In: Corey, S.J., Kimmel, M., Leonard, J.N. (Eds.). *A systems biology approach to blood*. New York: Springer, 153-187.

Butcher, B.A., Fox, B.A., Rommereim, L.M., Kim, S.G., Maurer, K.J., Yarovinsky, F., Herbert, D.R., Bzik, D.J., Denkers, E.Y. (2011). *Toxoplasma gondii* rhoptry kinase ROP16 activates STAT3 and STAT6 resulting in cytokine inhibition and arginase-1-dependent growth control. *PLoS Pathog*, 7 (9): e1002236.

Butt, T.R., Edavettal, S.C., Hall, J.P., Mattern, M.R. (2005). SUMO fusion technology for difficult-to-express proteins. *Protein Expression and Purification*, 43 (1): 1-9.

Buxton, D., Innes, E.A. (1995). A commercial vaccine for ovine toxoplasmosis. *Parasitology*, 110 Suppl (SUPPL.): S11-16.

Buxton, D., McAllister, M.M., Dubey, J.P. (2002). The comparative pathogenesis of neosporosis. *Trends Parasitol*, 18 (12): 546-552.

Cama, V.A., Ross, J.M., Crawford, S., Kawai, V., Chavez-Valdez, R., Vargas, D., Vivar, A., Ticona, E., Navincopa, M., Williamson, J., Ortega, Y., Gilman, R.H., Bern, C., Xiao, L. (2007). Differences in clinical manifestations among *Cryptosporidium* species and subtypes in HIV-infected persons. *The Journal of infectious diseases*, 196 (5): 684-691.

Camacho-Carvajal, M.M., Wollscheid, B., Aebersold, R., Steimle, V., Schamel, W.W. (2004). Two-dimensional Blue native/SDS gel electrophoresis of multi-protein complexes from whole cellular lysates: a proteomics approach. *Mol Cell Proteomics*, 3 (2): 176-182.

Carey, K.L., Donahue, C.G., Ward, G.E. (2000). Identification and molecular characterization of GRA8, a novel, proline-rich, dense granule protein of *Toxoplasma gondii*. *Mol Biochem Parasitol*, 105 (1): 25-37.

Carey, K.L., Jongco, A.M., Kim, K., Ward, G.E., Carey, K.L., Jongco, A.M., Kim, K., Ward, G.E. (2004). The *Toxoplasma gondii* Rhoptry Protein ROP4 Is Secreted into the Parasitophorous Vacuole and Becomes Phosphorylated in Infected Cells. *Eukaryotic cell*, 3 (5): 1320-1330.

Carruthers, V., Boothroyd, J.C. (2007). Pulling together: an integrated model of *Toxoplasma* cell invasion. *Curr Opin Microbiol*, 10 (1): 83-89.

Carruthers, V.B., Sibley, L.D. (1997). Sequential protein secretion front three distinct organelles of *Toxoplasma gondii* accompanies invasion of human fibroblasts. *European Journal of Cell Biology*, 73 (2): 114-123.

Carruthers, V.B., Sibley, L.D. (1999). Mobilization of intracellular calcium stimulates microneme discharge in *Toxoplasma gondii*. *Mol Microbiol*, 31 (2): 421-428.

Carruthers, V.B., Tomley, F.M. (2008). Microneme proteins in apicomplexans. *Subcell Biochem*, 47 33-45.

Carter, C.J. (2009). Schizophrenia susceptibility genes directly implicated in the life cycles of pathogens: Cytomegalovirus, influenza, herpes simplex, rubella, and *Toxoplasma gondii*. *Schizophrenia Bulletin*, 35 (6): 1163-1182.

Cavalcante, G.T., Monteiro, R.M., Soares, R.M., Nishi, S.M., Alves Neto, A.F., Esmerini Pde, O., Sercundes, M.K., Martins, J., Gennari, S.M. (2011). Shedding of *Neospora caninum* oocysts by dogs fed different tissues from naturally infected cattle. *Vet Parasitol*, 179 (1-3): 220-223.

Cesbron-Delauw, M.F. (1994). Dense-granule organelles of *Toxoplasma gondii*: Their role in the Host-Parasite relationship. *Parasitology Today*, 10 (8): 293-296.

Charif, H., Darcy, F., Torpier, G., Cesbron-Delauw, M.F., Capron, A. (1990). *Toxoplasma gondii*: characterization and localization of antigens secreted from tachyzoites. *Exp Parasitol*, 71 (1): 114-124.

Chaussabel, D., Semnani, R.T., McDowell, M.A., Sacks, D., Sher, A., Nutman, T.B. (2003). Unique gene expression profiles of human macrophages and dendritic cells to phylogenetically distinct parasites. *Blood*, 102 (2): 672-681.

Chawade, A., Alexandersson, E., Levander, F. (2014). Normalyzer: a tool for rapid evaluation of normalization methods for omics data sets. *J Proteome Res*, 13 (6): 3114-3120.

Cho, K., Kim Jin, Y., Park Gun, W., Kang, T., Yoon, J., Byun, K., Yoo Jong, S. (2012). Quantitative Phosphoproteomics of the Human Neural Stem Cell Differentiation into Oligodendrocyte by Mass Spectrometry. *Mass Spectrometry Letters*, 3 (4): 93-100.

Chou, M.F., Schwartz, D. (2011). Using the scan-x Web site to predict protein post-translational modifications. In: Baxevanis, A.D. (Eds.). *Curr Protoc Bioinformatics*. New York: John Wiley & Sons, Unit 13.16.

Citri, A., Yarden, Y. (2006). EGF-ERBB signalling: towards the systems level. *Nature reviews. Molecular cell biology*, 7 (7): 505-516.

Cole, C., Barber, J.D., Barton, G.J. (2008). The Jpred 3 secondary structure prediction server. *Nucleic Acids Res*, 36 (Web Server issue): W197-201.

Cole, R.A., Lindsay, D.S., Blagburn, B.L., Dubey, J.P. (1995). Vertical transmission of *Neospora caninum* in mice. *J Parasitol*, 81 (5): 730-732.

Collins, C.R., Withers-Martinez, C., Hackett, F., Blackman, M.J. (2009). An inhibitory antibody blocks interactions between components of the malarial invasion machinery. *PLoS Pathogens*, 5 (1):

Collins, M.O., Yu, L., Choudhary, J.S. (2007). Analysis of protein phosphorylation on a proteome-scale. *Proteomics*, 7 (16): 2751-2768.

Coppens, I., Dunn, J.D., Romano, J.D., Pypaert, M., Zhang, H., Boothroyd, J.C., Joiner, K.A. (2006). *Toxoplasma gondii* sequesters lysosomes from mammalian hosts in the vacuolar space. *Cell*, 125 (2): 261-274.

Coppens, I., Sinai, A.P., Joiner, K.A. (2000). *Toxoplasma gondii* exploits host low-density lipoprotein receptor- mediated endocytosis for cholesterol acquisition. *Journal of Cell Biology*, 149 (1): 167-180.

Cox, J., Mann, M. (2011). Quantitative, high-resolution proteomics for data-driven systems biology. *Annual Review of Biochemistry*, 80 273-299.

Craig, R., Beavis, R.C. (2004). TANDEM: Matching proteins with tandem mass spectra. *Bioinformatics*, 20 (9): 1466-1467.

Darcy, F., Deslee, D., Santoro, F., Charif, H., Auriault, C., Decoster, A., Duquesne, V., Capron, A. (1988). Induction of a protective antibody-dependent response against toxoplasmosis by in vitro excreted/secreted antigens from tachyzoites of *Toxoplasma gondii*. *Parasite Immunol*, 10 (5): 553-567.

Davison, H.C., Otter, A., Trees, A.J. (1999a). Significance of *Neospora caninum* in British dairy cattle determined by estimation of seroprevalence in normally calving cattle and aborting cattle. *Int J Parasitol*, 29 (8): 1189-1194.

Davison, H.C., Otter, A., Trees, A.J. (1999b). Estimation of vertical and horizontal transmission parameters of *Neospora caninum* infections in dairy cattle. *Int J Parasitol*, 29 (10): 1683-1689.

de Graaf, E.L., Giansanti, P., Altelaar, A.F., Heck, A.J. (2014). Single-step enrichment by Ti4+-IMAC and label-free quantitation enables in-depth monitoring of phosphorylation dynamics with high reproducibility and temporal resolution. *Mol Cell Proteomics*, 13 (9): 2426-2434.

De Sousa Abreu, R., Penalva, L.O., Marcotte, E.M., Vogel, C. (2009). Global signatures of protein and mRNA expression levels. *Molecular BioSystems*, 5 (12): 1512-1526.

Dejgaard, K., Theberge, J.F., Heath-Engel, H., Chevet, E., Tremblay, M.L., Thomas, D.Y. (2010). Organization of the Sec61 translocon, studied by high resolution native electrophoresis. *J Proteome Res*, 9 (4): 1763-1771.

Demain, A.L., Vaishnav, P. (2009). Production of recombinant proteins by microbes and higher organisms. *Biotechnology Advances*, 27 (3): 297-306.

DeMartino, G.N., Slaughter, C.A. (1999). The proteasome, a novel protease regulated by multiple mechanisms. *J Biol Chem*, 274 (32): 22123-22126.

Di Cristina, M., Spaccapelo, R., Soldati, D., Bistoni, F., Crisanti, A. (2000). Two conserved amino acid motifs mediate protein targeting to the micronemes of the apicomplexan parasite *Toxoplasma gondii*. *Mol Cell Biol*, 20 (19): 7332-7341.

Dijkstra, T., Barkema, H.W., Eysker, M., Hesselink, J.W., Wouda, W. (2002a). Natural transmission routes of *Neospora caninum* between farm dogs and cattle. *Veterinary Parasitology*, 105 (2): 99-104.

Dijkstra, T., Barkema, H.W., Hesselink, J.W., Wouda, W. (2002b). Point source exposure of cattle to *Neospora caninum* consistent with periods of common housing and feeding and related to the introduction of a dog. *Vet Parasitol*, 105 (2): 89-98.

Donahue, C.G., Carruthers, V.B., Gilk, S.D., Ward, G.E. (2000). The *Toxoplasma* homolog of *Plasmodium* apical membrane antigen-1 (AMA-1) is a microneme protein secreted in response to elevated intracellular calcium levels. *Molecular and Biochemical Parasitology*, 111 (1): 15-30.

Du, J., An, R., Cheng, L., Chen, Y., Shen, J.L. (2013). Screening of host cell proteins that interact with *Toxoplasma gondii* ROP18 via yeast two-hybrid system. *Chinese journal of parasitology and parasitic diseases*, 31 (1): 18-22.

Dubey, J.P. (1998). Advances in the life cycle of *Toxoplasma gondii*. *Int J Parasitol*, 28 (7): 1019-1024.

Dubey, J.P. (2003). Review of *Neospora caninum* and neosporosis in animals. *Korean J Parasitol*, 41 (1): 1-16.

Dubey, J.P. (2004). Toxoplasmosis - a waterborne zoonosis. *Vet Parasitol*, 126 (1-2): 57-72.

Dubey, J.P. (2009). Toxoplasmosis in sheep--the last 20 years. *Vet Parasitol*, 163 (1-2): 1-14.

Dubey, J.P. (2013). The History and Life Cycle of *Toxoplasma gondii*. In: Weiss, L.M., Kim, K. (Eds.). *Toxoplasma gondii: The Model Apicomplexan - Perspectives and Methods*. Amsterdam: Elsevier Ltd, 1-17.

Dubey, J.P., Barr, B.C., Barta, J.R., Bjerkas, I., Bjorkman, C., Blagburn, B.L., Bowman, D.D., Buxton, D., Ellis, J.T., Gottstein, B., Hemphill, A., Hill, D.E., Howe, D.K., Jenkins, M.C., Kobayashi, Y., Koudela, B., Marsh, A.E., Mattsson, J.G., McAllister, M.M., Modry, D., Omata, Y., Sibley, L.D., Speer, C.A., Trees, A.J., Uggla, A., Upton, S.J., Williams, D.J., Lindsay, D.S. (2002). Redescription of *Neospora caninum* and its differentiation from related coccidia. *Int J Parasitol*, 32 (8): 929-946.

Dubey, J.P., Beattie, C.P. (1988). *Toxoplasmosis of Animals and Man.* Boca Raton: CRC Press.

Dubey, J.P., Hattel, A.L., Lindsay, D.S., Topper, M.J. (1988). Neonatal *Neospora caninum* infection in dogs: isolation of the causative agent and experimental transmission. *J Am Vet Med Assoc*, 193 (10): 1259-1263.

Dubey, J.P., Knickman, E., Greene, C.E. (2005). Neonatal *Neospora caninum* infections in dogs. *Acta Parasitologica*, 50 (2): 176-179.

Dubey, J.P., Lindsay, D.S. (1989). Transplacental *Neospora caninum* infection in dogs. *Am J Vet Res*, 50 (9): 1578-1579.

Dubey, J.P., Lindsay, D.S. (1996). A review of *Neospora caninum* and neosporosis. *Vet Parasitol*, 67 (1-2): 1-59.

Dubey, J.P., Lindsay, D.S., Speer, C.A. (1998). Structures of *Toxoplasma gondii* tachyzoites, bradyzoites, and sporozoites and biology and development of tissue cysts. *Clin Microbiol Rev*, 11 (2): 267-299.

Dubey, J.P., Schares, G., Ortega-Mora, L.M. (2007). Epidemiology and control of neosporosis and *Neospora caninum*. *Clin Microbiol Rev*, 20 (2): 323-367.

Dubey, J.P., Tiao, N., Gebreyes, W.A., Jones, J.L. (2012). A review of toxoplasmosis in humans and animals in Ethiopia. *Epidemiol Infect*, 140 (11): 1935-1938.

Dubremetz, J.F., Achbarou, A., Bermudes, D., Joiner, K.A. (1993). Kinetics and pattern of organelle exocytosis during *Toxoplasma gondii*/host-cell interaction. *Parasitol Res*, 79 (5): 402-408.

Dunn, J.D., Ravindran, S., Kim, S.K., Boothroyd, J.C. (2008). The *Toxoplasma gondii* dense granule protein GRA7 is phosphorylated upon invasion and forms an unexpected association with the rhoptry proteins ROP2 and ROP4. *Infection and Immunity*, 76 (12): 5853-5861.

Egan, S.E., Weinberg, R.A. (1993). The pathway to signal achievement. *Nature*, 365 (6449): 781-783.

El Hajj, H., Demey, E., Poncet, J., Lebrun, M., Wu, B., Galéotti, N., Fourmaux, M.N., Mercereau-Puijalon, O., Vial, H., Labesse, G., Dubremetz, J.F. (2006). The ROP2 family of *Toxoplasma gondii* rhoptry proteins: Proteomic and genomic characterization and molecular modeling. *Proteomics*, 6 (21): 5773-5784.

El Hajj, H., Lebrun, M., Arold, S.T., Vial, H., Labesse, G., Dubremetz, J.F. (2007). ROP18 is a rhoptry kinase controlling the intracellular proliferation of *Toxoplasma gondii*. *PLoS Pathogens*, 3 (2):

Ellis, J.T., Ryce, C., Atkinson, R., Balu, S., Jones, P., Harper, P.A. (2000). Isolation, characterization and expression of a GRA2 homologue from *Neospora caninum*. *Parasitology*, 120 (Pt 4) (4): 383-390.

Elmore, S.A., Jones, J.L., Conrad, P.A., Patton, S., Lindsay, D.S., Dubey, J.P. (2010). *Toxoplasma gondii*: epidemiology, feline clinical aspects, and prevention. *Trends Parasitol*, 26 (4): 190-196.

Fandino, A.S., Rais, I., Vollmer, M., Elgass, H., Schagger, H., Karas, M. (2005). LC-nanospray-MS/MS analysis of hydrophobic proteins from membrane protein complexes isolated by blue-native electrophoresis. *Journal of mass spectrometry : JMS*, 40 (9): 1223-1231.

Fayer, R., Gasbarre, L., Pasquali, P., Canals, A., Almeria, S., Zarlenga, D. (1998). *Cryptosporidium parvum* infection in bovine neonates: dynamic clinical, parasitic and immunologic patterns. *Int J Parasitol*, 28 (1): 49-56.

Fenyö, D., Beavis, R.C. (2003). A method for assessing the statistical significance of mass spectrometry-based protein identifications using general scoring schemes. *Analytical Chemistry*, 75 (4): 768-774.

Ferrell, K., Wilkinson, C.R., Dubiel, W., Gordon, C. (2000). Regulatory subunit interactions of the 26S proteasome, a complex problem. *Trends Biochem Sci*, 25 (2): 83-88.

Ficarro, S.B., McCleland, M.L., Stukenberg, P.T., Burke, D.J., Ross, M.M., Shabanowitz, J., Hunt, D.F., White, F.M. (2002). Phosphoproteome analysis by mass spectrometry and its application to *Saccharomyces* cerevisiae. *Nat Biotechnol*, 20 (3): 301-305.

Ficarro, S.B., Parikh, J.R., Blank, N.C., Marto, J.A. (2008). Niobium(V) oxide (Nb2O5): application to phosphoproteomics. *Anal Chem*, 80 (12): 4606-4613.

Fischer, H.G., Stachelhaus, S., Sahm, M., Meyer, H.E., Reichmann, G. (1998). GRA7, an excretory 29 kDa *Toxoplasma gondii* dense granule antigen released by infected host cells. *Mol Biochem Parasitol*, 91 (2): 251-262.

Forler, D., Kocher, T., Rode, M., Gentzel, M., Izaurralde, E., Wilm, M. (2003). An efficient protein complex purification method for functional proteomics in higher eukaryotes. *Nat Biotechnol*, 21 (1): 89-92.

Francia, M.E., Striepen, B. (2014). Cell division in apicomplexan parasites. *Nature reviews. Microbiology*, 12 (2): 125-136.

Frenal, K., Polonais, V., Marq, J.B., Stratmann, R., Limenitakis, J., Soldati-Favre, D. (2010). Functional dissection of the apicomplexan glideosome molecular architecture. *Cell Host Microbe*, 8 (4): 343-357.

Frenkel, J.K. (1973). *Toxoplasma* in and around us. *BioScience*, 23 (6): 343-352.

Frenkel, J.K., Dubey, J.P., Miller, N.L. (1970). *Toxoplasma gondii* in cats: Fecal stages identified as coccidian oocysts. *Science*, 167 (3919): 893-896.

Freyre, A., Bonino, J., Falcon, J., Castells, D., Correa, O., Casaretto, A. (1999). The incidence and economic significance of ovine toxoplasmosis in Uruguay. *Vet Parasitol*, 81 (1): 85-88.

Gajria, B., Bahl, A., Brestelli, J., Dommer, J., Fischer, S., Gao, X., Heiges, M., Iodice, J., Kissinger, J.C., Mackey, A.J., Pinney, D.F., Roos, D.S., Stoeckert, C.J., Jr., Wang, H., Brunk, B.P. (2008). ToxoDB: an integrated *Toxoplasma gondii* database resource. *Nucleic Acids Res*, 36 (Database issue): D553-556.

Galinski, M.R., Barnwell, J.W. (1996). *Plasmodium vivax*: Merozoites, invasion of reticulocytes and considerations for malaria vaccine development. *Parasitol Today*, 12 (1): 20-29.

Garavelli, J.S. (2004). The RESID Database of Protein Modifications as a resource and annotation tool. *Proteomics*, 4 (6): 1527-1533.

Gaskins, E., Gilk, S., DeVore, N., Mann, T., Ward, G., Beckers, C. (2004). Identification of the membrane receptor of a class XIV myosin in *Toxoplasma gondii*. *The Journal of cell biology*, 165 (3): 383-393.

Geer, L.Y., Markey, S.P., Kowalak, J.A., Wagner, L., Xu, M., Maynard, D.M., Yang, X., Shi, W., Bryant, S.H. (2004). Open Mass Spectrometry Search Algorithm. *Journal of Proteome Research*, 3 (5): 958-964.

Gendrin, C., Mercier, C., Braun, L., Musset, K., Dubremetz, J.F., Cesbron-Delauw, M.F. (2008). *Toxoplasma gondii* uses unusual sorting mechanisms to deliver transmembrane proteins into the host-cell vacuole. *Traffic*, 9 (10): 1665-1680.

Ghazalpour, A., Bennett, B., Petyuk, V.A., Orozco, L., Hagopian, R., Mungrue, I.N., Farber, C.R., Sinsheimer, J., Kang, H.M., Furlotte, N., Park, C.C., Wen, P.Z., Brewer, H., Weitz, K., Camp, D.G., 2nd, Pan, C., Yordanova, R., Neuhaus, I., Tilford, C., Siemers, N., Gargalovic, P., Eskin, E., Kirchgessner, T., Smith, D.J., Smith, R.D., Lusis, A.J. (2011). Comparative analysis of proteome and transcriptome variation in mouse. *PLoS Genet*, 7 (6): e1001393.

Gilk, S.D., Gaskins, E., Ward, G.E., Beckers, C.J.M. (2009). GAP45 phosphorylation controls assembly of the *Toxoplasma* myosin XIV complex. *Eukaryotic Cell*, 8 (2): 190-196.

Goebel, S., Luder, C.G., Lugert, R., Bohne, W., Gross, U. (1998). *Toxoplasma gondii* inhibits the in vitro induced apoptosis of HL-60 cells. *The Tokai journal of experimental and clinical medicine*, 23 (6): 351-356.

Gomase, V., Akella, R. (2009). Phosphoproteomics: Recent advances in analytical techniques. *International Journal of Pharmaceuticals Analysis*,

González, J., Ramalho-Pinto, F.J., Frevert, U., Ghiso, J., Tomlinson, S., Scharfstein, J., Corey, E.J., Nussenzweig, V. (1996). Proteasome activity is required for the stage-specific transformation of a protozoan parasite. *Journal of Experimental Medicine*, 184 (5): 1909-1918.

Graus-Porta, D., Beerli, R.R., Daly, J.M., Hynes, N.E. (1997). ErbB-2, the preferred heterodimerization partner of all ErbB receptors, is a mediator of lateral signalling. *The EMBO Journal*, 16 (7): 1647-1655.

Greer, E.L., Oskoui, P.R., Banko, M.R., Maniar, J.M., Gygi, M.P., Gygi, S.P., Brunet, A. (2007). The energy sensor AMP-activated protein kinase directly regulates the mammalian FOXO3 transcription factor. *J Biol Chem*, 282 (41): 30107-30119.

Gruhler, A., Olsen, J.V., Mohammed, S., Mortensen, P., Faergeman, N.J., Mann, M., Jensen, O.N. (2005). Quantitative phosphoproteomics applied to the yeast pheromone signalling pathway. *Mol Cell Proteomics*, 4 (3): 310-327.

Gutman, J., Guarner, J. (2010). Pediatric malaria: 8-year case series in Atlanta, Georgia, and review of the literature. *Journal of Travel Medicine*, 17 (5): 334-338.

Hajj, H.E., Lebrun, M., Fourmaux, M.N., Vial, H., Dubremetz, J.F. (2006). Characterization, biosynthesis and fate of ROP7, a ROP2 related rhoptry protein of *Toxoplasma gondii*. *Mol Biochem Parasitol*, 146 (1): 98-100.

Halonen, S.K., Weiss, L.M. (2013). Toxoplasmosis. In: Gurd, J.M., Kischka, U., Marshall, A.G. (Eds.). *Handbook of clinical neurology*. Oxford: Oxford University Press, 125-145.

Hasnain, S.E., Begum, R., Ramaiah, K.V.A., Sahdev, S., Shajil, E.M., Taneja, T.K., Mohan, M., Athar, M., Sah, N.K., Krishnaveni, M. (2003). Host-pathogen interactions during apoptosis. *Journal of Biosciences*, 28 (3): 349-358.

Hastie, C.J., McLauchlan, H.J., Cohen, P. (2006). Assay of protein kinases using radiolabeled ATP: A protocol. *Nature protocols*, 1 (2): 968-971.

Hay, N., Sonenberg, N. (2004). Upstream and downstream of mTOR. *Genes and Development*, 18 (16): 1926-1945.

Hay, R.T. (2007). SUMO-specific proteases: a twist in the tail. *Trends in Cell Biology*, 17 (8): 370-376.

He, L., Hannon, G.J. (2004). MicroRNAs: small RNAs with a big role in gene regulation. *Nature reviews. Genetics*, 5 (7): 522-531.

He, X.L., Grigg, M.E., Boothroyd, J.C., Garcia, K.C. (2002). Structure of the immunodominant surface antigen from the *Toxoplasma gondii* SRS superfamily. *Nat Struct Biol*, 9 (8): 606-611.

Hehl, A.B., Lekutis, C., Grigg, M.E., Bradley, P.J., Dubremetz, J.F., Ortega-Barria, E., Boothroyd, J.C., Hehl, A.B., Lekutis, C., Grigg, M.E., Bradley, P.J., Dubremetz, J.F., Ortega-Barria, E., Boothroyd, J.C. (2000). *Toxoplasma gondii* Homologue of *Plasmodium* Apical Membrane Antigen 1 Is Involved in Invasion of Host Cells. *Infection and Immunity*, 68 (12): 7078-7086.

Heintzelman, M.B., Schwartzman, J.D. (1997). A novel class of unconventional myosins from *Toxoplasma gondii*. *J Mol Biol*, 271 (1): 139-146.

Hemphill, A., Gajendran, N., Sonda, S., Fuchs, N., Gottstein, B., Hentrich, B., Jenkins, M. (1998). Identification and characterisation of a dense granule-associated protein in *Neospora caninum* tachyzoites. *Int J Parasitol*, 28 (3): 429-438.

Hemphill, A., Gottstein, B., Kaufmann, H. (1996). Adhesion and invasion of bovine endothelial cells by *Neospora caninum*. *Parasitology*, 112 (Pt 2) (2): 183-197.

Hemphill, A., Vonlaufen, N., Naguleswaran, A. (2006). Cellular and immunological basis of the host-parasite relationship during infection with *Neospora caninum*. *Parasitology*, 133 (Pt 3): 261-278.

Hemphill, A., Vonlaufen, N., Naguleswaran, A., Keller, N., Riesen, M., Guetg, N., Srinivasan, S., Alaeddine, F. (2004). Tissue culture and explant approaches to studying and visualizing *Neospora caninum* and its interactions with the host cell. *Microscopy and microanalysis : the official journal of Microscopy Society of America, Microbeam Analysis Society, Microscopical Society of Canada*, 10 (5): 602-620.

Herm-Götz, A., Weiss, S., Stratmann, R., Fujita-Becker, S., Ruff, C., Meyhöfer, E., Soldati, T., Manstein, D.J., Geeves, M.A., Soldati, D. (2002). *Toxoplasma gondii* myosin A and its light chain: A fast, single-headed, plus-end-directed motor. *EMBO Journal*, 21 (9): 2149-2158.

Hjerten, S. (1962). Chromatographic separation according to size of macromolecules and cell particles on columns of agarose suspensions. *Arch Biochem Biophys*, 99 (3): 466-475.

Hoff, E.F., Carruthers, V.B. (2002). Is *Toxoplasma* egress the first step in invasion? *Trends in Parasitology*, 18 (6): 251-255.

Hogg, P.J. (2003). Disulfide bonds as switches for protein function. *Trends in Biochemical Sciences*, 28 (4): 210-214.

Homer, M.J., Aguilar-Delfin, I., Telford Iii, S.R., Krause, P.J., Persing, D.H. (2000). Babesiosis. *Clinical Microbiology Reviews*, 13 (3): 451-469.

Huang, D.W., Sherman, B.T., Lempicki, R.A. (2008). Systematic and integrative analysis of large gene lists using DAVID bioinformatics resources. *Nat. Protocols*, 4 (1): 44-57.

Hunter, T., Cooper, J.A. (1985). Protein-tyrosine kinases. *Annu Rev Biochem*, 54 897-930.

Huynh, M.H., Rabenau, K.E., Harper, J.M., Beatty, W.L., Sibley, L.D., Carruthers, V.B. (2003). Rapid invasion of host cells by *Toxoplasma* requires secretion of the MIC2-M2AP adhesive protein complex. *EMBO J*, 22 (9): 2082-2090.

Hynes, N.E., Lane, H.A. (2005). ERBB receptors and cancer: the complexity of targeted inhibitors. *Nature reviews. Cancer*, 5 (5): 341-354.

Hynes, N.E., MacDonald, G. (2009). ErbB receptors and signalling pathways in cancer. *Curr Opin Cell Biol*, 21 (2): 177-184.

Inoki, K., Zhu, T., Guan, K.L. (2003). TSC2 Mediates Cellular Energy Response to Control Cell Growth and Survival. *Cell*, 115 (5): 577-590.

Jacobs, D., Dubremetz, J.F., Loyens, A., Bosman, F., Saman, E. (1998). Identification and heterologous expression of a new dense granule protein (GRA7) from *Toxoplasma gondii*. *Mol Biochem Parasitol*, 91 (2): 237-249.

Jacot, D., Soldati-Favre, D. (2012). Does protein phosphorylation govern host cell entry and egress by the Apicomplexa? *International journal of medical microbiology : IJMM*, 302 (4-5): 195-202.

Jacquet, A., Coulon, L., De Neve, J., Daminet, V., Haumont, M., Garcia, L., Bollen, A., Jurado, M., Biemans, R. (2001). The surface antigen SAG3 mediates the attachment of *Toxoplasma gondii* to cell-surface proteoglycans. *Mol Biochem Parasitol*, 116 (1): 35-44.

Jain, S., Singh, R., Gupta, M.N. (2004). Purification of recombinant green fluorescent protein by three-phase partitioning. *Journal of chromatography. A*, 1035 (1): 83-86.

Jensen, L.J., Gupta, R., Blom, N., Devos, D., Tamames, J., Kesmir, C., Nielsen, H., Staerfeldt, H.H., Rapacki, K., Workman, C., Andersen, C.A., Knudsen, S., Krogh, A., Valencia, A., Brunak, S. (2002). Prediction of human protein function from post-translational modifications and localization features. *J Mol Biol*, 319 (5): 1257-1265.

Jewett, T.J., Sibley, L.D. (2003). Aldolase forms a bridge between cell surface adhesins and the actin cytoskeleton in apicomplexan parasites. *Molecular Cell*, 11 (4): 885-894.

Jewett, T.J., Sibley, L.D. (2004). The *Toxoplasma* proteins MIC2 and M2AP form a hexameric complex necessary for intracellular survival. *J Biol Chem*, 279 (10): 9362-9369.

Johnson, E.S. (2004). Protein modification by SUMO. *Annu Rev Biochem*, 73 355-382.

Joiner, K.A., Fuhrman, S.A., Miettinen, H.M., Kasper, L.H., Mellman, I. (1990). *Toxoplasma gondii*: fusion competence of parasitophorous vacuoles in Fc receptor-transfected fibroblasts. *Science*, 249 (4969): 641-646.

Jones, J.L., Dubey, J.P. (2010). Waterborne toxoplasmosis--recent developments. *Exp Parasitol*, 124 (1): 10-25.

Jones, S., Thornton, J.M. (1995). Protein-protein interactions: a review of protein dimer structures. *Progress in biophysics and molecular biology*, 63 (1): 31-65.

Jovanovic, M., Rooney, M.S., Mertins, P., Przybylski, D., Chevrier, N., Satija, R., Rodriguez, E.H., Fields, A.P., Schwartz, S., Raychowdhury, R., Mumbach, M.R., Eisenhaure, T., Rabani, M., Gennert, D., Lu, D., Delorey, T., Weissman, J.S., Carr, S.A., Hacohen, N., Regev, A. (2015). Immunogenetics. Dynamic profiling of the protein life cycle in response to pathogens. *Science*, 347 (6226): 1259038.

Jung, C., Lee, C.Y., Grigg, M.E. (2004). The SRS superfamily of *Toxoplasma* surface proteins. *Int J Parasitol*, 34 (3): 285-296.

Jüschke, C., Dohnal, I., Pichler, P., Harzer, H., Swart, R., Ammerer, G., Mechtler, K., Knoblich, J.A. (2013). Transcriptome and proteome quantification of a tumor model provides novel insights into post-transcriptional gene regulation. *Genome Biology*, 14 (11):

Karsten, V., Qi, H., Beckers, C.J.M., Reddy, A., Dubremetz, J.F., Webster, P., Joiner, K.A. (1998). The protozoan parasite *Toxoplasma gondii* targets proteins to dense granules and the vacuolar space using both conserved and unusual mechanisms. *Journal of Cell Biology*, 141 (6): 1323-1333.

Keeley, A., Soldati, D. (2004). The glideosome: A molecular machine powering motility and host-cell invasion by Apicomplexa. *Trends in Cell Biology*, 14 (10): 528-532.

Keller, N., Naguleswaran, A., Cannas, A., Vonlaufen, N., Bienz, M., Björkman, C., Bohne, W., Hemphill, A. (2002). Identification of a *Neospora caninum* microneme protein (NcMIC1) which interacts with sulfated host cell surface glycosaminoglycans. *Infection and Immunity*, 70 (6): 3187-3198.

Keller, N., Riesen, M., Naguleswaran, A., Vonlaufen, N., Stettler, R., Leepin, A., Wastling, J.M., Hemphill, A. (2004). Identification and characterization of a *Neospora caninum* microneme-associated protein (NcMIC4) that exhibits unique lactose-binding properties. *Infection and Immunity*, 72 (8): 4791-4800.

Khaminets, A., Hunn, J.P., Könen-Waisman, S., Zhao, Y.O., Preukschat, D., Coers, J., Boyle, J.P., Ong, Y., Boothroyd, J.C., Reichmann, G., Howard, J.C. (2010). Coordinated loading of IRG resistance GTPases on to the *Toxoplasma gondii* parasitophorous vacuole. *Cellular Microbiology*, 12 (7): 939-961.

Kim, J.Y., Ahn, M.H., Jun, H.S., Jung, J.W., Ryu, J.S., Min, D.Y. (2006). *Toxoplasma gondii* inhibits apoptosis in infected cells by caspase inactivation and NF-κB activation. *Yonsei Medical Journal*, 47 (6): 862-869.

Komili, S., Silver, P.A. (2008). Coupling and coordination in gene expression processes: a systems biology view. *Nature reviews. Genetics*, 9 (1): 38-48.

Kondapalli, L., Soltani, K., Lacouture, M.E. (2005). The promise of molecular targeted therapies: protein kinase inhibitors in the treatment of cutaneous malignancies. *J Am Acad Dermatol*, 53 (2): 291-302.

Kumar, A., Srivastava, S., Kumar Mishra, R., Mittal, R., Hosur, R.V. (2006). Residue-level NMR view of the urea-driven equilibrium folding transition of SUMO-1 (1-97): native preferences do not increase monotonously. *J Mol Biol*, 361 (1): 180-194.

Kusnadi, A.R., Hood, E.E., Witcher, D.R., Howard, J.A., Nikolov, Z.L. (1998). Production and Purification of Two Recombinant Proteins from Transgenic Corn. *Biotechnology Progress*, 14 (1): 149-155.

Kweon, H.K., Hakansson, K. (2006). Selective zirconium dioxide-based enrichment of phosphorylated peptides for mass spectrometric analysis. *Anal Chem*, 78 (6): 1743-1749.

Labruyere, E., Lingnau, M., Mercier, C., Sibley, L.D. (1999). Differential membrane targeting of the secretory proteins GRA4 and GRA6 within the parasitophorous vacuole formed by *Toxoplasma gondii*. *Molecular and Biochemical Parasitology*, 102 (2): 311-324.

Lamarque, M.H., Papoin, J., Finizio, A.L., Lentini, G., Pfaff, A.W., Candolfi, E., Dubremetz, J.F., Lebrun, M. (2012). Identification of a new rhoptry neck complex RON9/RON10 in the Apicomplexa parasite *Toxoplasma gondii*. *PLoS One*, 7 (3): e32457.

Laplante, M., Sabatini, D.M. (2012). MTOR signalling in growth control and disease. *Cell*, 149 (2): 274-293.

Larsen, M.R., Thingholm, T.E., Jensen, O.N., Roepstorff, P., Jørgensen, T.J.D. (2005). Highly selective enrichment of phosphorylated peptides from peptide mixtures using titanium dioxide microcolumns. *Molecular and Cellular Proteomics*, 4 (7): 873-886.

Lasonder, E., Green, J.L., Camarda, G., Talabani, H., Holder, A.A., Langsley, G., Alano, P. (2012). The *Plasmodium falciparum* schizont phosphoproteome reveals extensive phosphatidylinositol and cAMP-protein kinase A signalling. *J Proteome Res*, 11 (11): 5323-5337.

Lasserre, J.P., Sylvius, L., Joubert-Caron, R., Caron, M., Hardouin, J. (2010). Organellar protein complexes of Caco-2 human cells analyzed by two-dimensional blue native/SDS-PAGE and mass spectrometry. *J Proteome Res*, 9 (10): 5093-5107.

Le Blanc, J.C.Y., Hager, J.W., Ilisiu, A.M.P., Hunter, C., Zhong, F., Chu, I. (2003). Unique scanning capabilities of a new hybrid linear ion trap mass spectrometer (Q TRAP) used for high sensitivity proteomics applications. *Proteomics*, 3 (6): 859-869.

Lebrun, M., Carruthers, V.B., Cesbron-Delauw, M.F. (2007). *Toxoplasma* secretory proteins and their roles in cell invasion and intracellular survival. In: Weiss, L.M., Kim, K. (Eds.). *Toxoplasma gondii*. London: Elsevier Ltd, 265-316.

Lecordier, L., Mercier, C., Torpier, G., Tourvieille, B., Darcy, F., Liu, J.L., Maes, P., Tartar, A., Capron, A., Cesbron-Delauw, M.F. (1993). Molecular structure of a *Toxoplasma gondii* dense granule antigen (GRA 5) associated with the parasitophorous vacuole membrane. *Mol Biochem Parasitol*, 59 (1): 143-153.

Lee, B.H., Kim, W.H., Jeong, J., Yoo, J., Kwon, Y.K., Jung, B.Y., Kwon, J.H., Lillehoj, H.S., Min, W. (2010). Prevalence and cross-immunity of Eimeria species on Korean chicken farms. *Journal of Veterinary Medical Science*, 72 (8): 985-989.

Lei, T., Wang, H., Liu, J., Nan, H., Liu, Q. (2014). ROP18 is a key factor responsible for virulence difference between *Toxoplasma gondii* and *Neospora caninum*. *PLoS ONE*, 9 (6):

Lekutis, C., Ferguson, D.J., Grigg, M.E., Camps, M., Boothroyd, J.C. (2001). Surface antigens of *Toxoplasma gondii*: variations on a theme. *Int J Parasitol*, 31 (12): 1285-1292.

Li, Y., Corradetti, M.N., Inoki, K., Guan, K.L. (2004). TSC2: filling the GAP in the mTOR signalling pathway. *Trends Biochem Sci*, 29 (1): 32-38.

Liddell, S., Lally, N.C., Jenkins, M.C., Dubey, J.P. (1998). Isolation of the cDNA encoding a dense granule associated antigen (NCDG2) of *Neospora caninum*. *Mol Biochem Parasitol*, 93 (1): 153-158.

Lindsay, D.S., Dubey, J.P., Duncan, R.B. (1999b). Confirmation that the dog is a definitive host for *Neospora caninum*. *Veterinary Parasitology*, 82 (4): 327-333.

Lindsay, D.S., Upton, S.J., Dubey, J.P. (1999a). A structural study of the *Neospora caninum* oocyst. *Int J Parasitol*, 29 (10): 1521-1523.

Liu, G., Cui, X., Hao, P., Yang, D., Liu, J., Liu, Q. (2013). GRA 14, a novel dense granule protein from *Neospora caninum*. *Acta Biochim Biophys Sin (Shanghai)*, 45 (7): 607-609.

Lourido, S., Shuman, J., Zhang, C., Shokat, K.M., Hui, R., Sibley, L.D. (2010). Calcium-dependent protein kinase 1 is an essential regulator of exocytosis in *Toxoplasma*. *Nature*, 465 (7296): 359-362.

Lu, P., Vogel, C., Wang, R., Yao, X., Marcotte, E.M. (2007). Absolute protein expression profiling estimates the relative contributions of transcriptional and translational regulation. *Nature Biotechnology*, 25 (1): 117-124.

Lüder, C.G.K., Gross, U. (2005). Apoptosis and its modulation during infection with *Toxoplasma gondii*: Molecular mechanisms and role in pathogenesis. In: Diane, E., Griffin, M.D. (Eds.). *Current topics in microbiology and immunology*. Berlin Heidelberg: Springer, 219-237.

Luft, B.J., Remington, J.S. (1992). Toxoplasmic encephalitis in AIDS. *Clinical infectious diseases : an official publication of the Infectious Diseases Society of America*, 15 (2): 211-222.

Luo, R., Fang, L., Jin, H., Wang, D., An, K., Xu, N., Chen, H., Xiao, S. (2014). Label-free quantitative phosphoproteomic analysis reveals differentially regulated proteins and pathway in PRRSV-infected pulmonary alveolar macrophages. *J Proteome Res*, 13 (3): 1270-1280.

Magno, R.C., Straker, L.C., De Souza, W., Attias, M. (2005). Interrelations between the parasitophorous vacuole of *Toxoplasma gondii* and host cell organelles. *Microscopy and Microanalysis*, 11 (2): 166-174.

Maier, T., Güell, M., Serrano, L. (2009). Correlation of mRNA and protein in complex biological samples. *FEBS Letters*, 583 (24): 3966-3973.

Mann, M., Jensen, O.N. (2003). Proteomic analysis of post-translational modifications. *Nat Biotechnol*, 21 (3): 255-261.

Marblestone, J.G., Edavettal, S.C., Lim, Y., Lim, P., Zuo, X., Butt, T.R. (2006). Comparison of SUMO fusion technology with traditional gene fusion systems: Enhanced expression and solubility with SUMO. *Protein Science*, 15 (1): 182-189.

Marley, J., Lu, M., Bracken, C. (2001). A method for efficient isotopic labeling of recombinant proteins. *J Biomol NMR*, 20 (1): 71-75.

Marugán-Hernández, V., Álvarez-García, G., Tomley, F., Hemphill, A., Regidor-Cerrillo, J., Ortega-Mora, L.M. (2011). Identification of novel rhoptry proteins in *Neospora caninum* by LC/MS-MS analysis of subcellular fractions. *Journal of Proteomics*, 74 (5): 629-642.

Masatani, T., Matsuo, T., Tanaka, T., Terkawi, M.A., Lee, E.G., Goo, Y.K., Aboge, G.O., Yamagishi, J., Hayashi, K., Kameyama, K., Cao, S., Nishikawa, Y., Xuan, X. (2013). TgGRA23, a novel *Toxoplasma gondii* dense granule protein associated with the parasitophorous vacuole membrane and intravacuolar network. *Parasitology International*, 62 (4): 372-379.

Matagne, A., Dobson, C.M. (1998). The folding process of hen lysozyme: A perspective from the 'new view'. *Cellular and Molecular Life Sciences*, 54 (4): 363-371.

McAllister, M.M., Dubey, J.P., Lindsay, D.S., Jolley, W.R., Wills, R.A., McGuire, A.M. (1998). Dogs are definitive hosts of *Neospora caninum*. *Int J Parasitol*, 28 (9): 1473-1478.

McCann, C.M., Vyse, A.J., Salmon, R.L., Thomas, D., Williams, D.J., McGarry, J.W., Pebody, R., Trees, A.J. (2008). Lack of serologic evidence of *Neospora caninum* in humans, England. *Emerg Infect Dis*, 14 (6): 978-980.

Meissner, M., Reiss, M., Viebig, N., Carruthers, V.B., Toursel, C., Tomavo, S., Ajioka, J.W., Soldati, D. (2002a). A family of transmembrane microneme proteins of *Toxoplasma gondii* contain EGF-like domains and function as escorters. *Journal of Cell Science*, 115 (3): 563-574.

Meissner, M., Schlüter, D., Soldati, D. (2002b). Role of *Toxoplasma gondii* myosin a in powering parasite gliding and host cell invasion. *Science*, 298 (5594): 837-840.

Melo, M.B., Jensen, K.D., Saeij, J.P. (2011). *Toxoplasma gondii* effectors are master regulators of the inflammatory response. *Trends Parasitol*, 27 (11): 487-495.

Mercier, C., Adjogble, K.D.Z., Däubener, W., Delauw, M.F.C. (2005). Dense granules: Are they key organelles to help understand the parasitophorous vacuole of all apicomplexa parasites? *Int J Parasitol*, 35 (8): 829-849.

Mercier, C., Cesbron-Delauw, M.F. (2015). *Toxoplasma* secretory granules: One population or more? *Trends in Parasitology*, 31 (2): 60-71.

Mercier, C., Dubremetz, J.F., Rauscher, B., Lecordier, L., Sibley, L.D., Cesbron-Delauw, M.F. (2002). Biogenesis of nanotubular network in *Toxoplasma* parasitophorous vacuole induced by parasite proteins. *Mol Biol Cell*, 13 (7): 2397-2409.

Mercier, C., Lecordier, L., Darcy, F., Deslee, D., Murray, A., Tourvieille, B., Maes, P., Capron, A., Cesbron-Delauw, M.F. (1993). Molecular characterization of a dense granule antigen (Gra 2) associated with the network of the parasitophorous vacuole in *Toxoplasma gondii*. *Mol Biochem Parasitol*, 58 (1): 71-82.

Michelin, A., Bittame, A., Bordat, Y., Travier, L., Mercier, C., Dubremetz, J.F., Lebrun, M. (2009). GRA12, a *Toxoplasma* dense granule protein associated with the intravacuolar membranous nanotubular network. *Int J Parasitol*, 39 (3): 299-306.

Miernyk, J.A., Thelen, J.J. (2008). Biochemical approaches for discovering protein-protein interactions. *The Plant journal : for cell and molecular biology*, 53 (4): 597-609.

Mineo, T.W., Carrasco, A.O., Marciano, J.A., Werther, K., Pinto, A.A., Machado, R.Z. (2009). Pigeons (*Columba livia*) are a suitable experimental model for *Neospora caninum* infection in birds. *Vet Parasitol*, 159 (2): 149-153.

Ming, X.F., Burgering, B.M.T., Wennström, S., Claesson-Welsh, L., Heldin, C.H., Bos, J.L., Kozma, S.C., Thomas, G. (1994). Activation of p70/p85 S6 kinase by a pathway independent of p21ras. *Nature*, 371 (6496): 426-429.

Montoya, J.G., Remington, J.S. (2008). Management of *Toxoplasma gondii* infection during pregnancy. *Clinical infectious diseases : an official publication of the Infectious Diseases Society of America*, 47 (4): 554-566.

Mordue, D.G., Desai, N., Dustin, M., Sibley, L.D. (1999). Invasion by *Toxoplasma gondii* establishes a moving junction that selectively excludes host cell plasma membrane proteins on the basis of their membrane anchoring. *Journal of Experimental Medicine*, 190 (12): 1783-1792.

Mordue, D.G., Håkansson, S., Niesman, I., David Sibley, L. (1999a). *Toxoplasma gondii* resides in a vacuole that avoids fusion with host cell endocytic and exocytic vesicular trafficking pathways. *Experimental Parasitology*, 92 (2): 87-99.

Morris, M.T., Cheng, W.C., Zhou, X.W., Brydges, S.D., Carruthers, V.B. (2004). *Neospora caninum* expresses an unusual single-domain Kazal protease inhibitor that is discharged into the parasitophorous vacuole. *Int J Parasitol*, 34 (6): 693-701.

Moudy, R., Manning, T.J., Beckers, C.J. (2001). The Loss of Cytoplasmic Potassium upon Host Cell Breakdown Triggers Egress of *Toxoplasma gondii*. *Journal of Biological Chemistry*, 276 (44): 41492-41501.

Nagamune, K., Moreno, S.N., Chini, E.N., Sibley, L.D. (2008). Calcium regulation and signalling in apicomplexan parasites. *Subcell Biochem*, 47 70-81.

Naguleswaran, A., Alaeddine, F., Guionaud, C., Vonlaufen, N., Sonda, S., Jenoe, P., Mevissen, M., Hemphill, A. (2005). *Neospora caninum* protein disulfide isomerase is involved in tachyzoite-host cell interaction. *Int J Parasitol*, 35 (13): 1459-1472.

Naguleswaran, A., Cannas, A., Keller, N., Vonlaufen, N., Björkman, C., Hemphill, A. (2002). Vero cell surface proteoglycan interaction with the microneme protein NcMIC3 mediates adhesion of *Neospora caninum* tachyzoites to host cells unlike that in *Toxoplasma gondii*. *Int J Parasitol*, 32 (6): 695-704.

Naguleswaran, A., Muller, N., Hemphill, A. (2003). *Neospora caninum* and *Toxoplasma gondii*: a novel adhesion/invasion assay reveals distinct differences in tachyzoite-host cell interactions. *Exp Parasitol*, 104 (3-4): 149-158.

Nelson, M.M., Jones, A.R., Carmen, J.C., Sinai, A.P., Burchmore, R., Wastling, J.M. (2008). Modulation of the host cell proteome by the intracellular apicomplexan parasite *Toxoplasma gondii*. *Infection and Immunity*, 76 (2): 828-844.

Nett, I.R., Martin, D.M., Miranda-Saavedra, D., Lamont, D., Barber, J.D., Mehlert, A., Ferguson, M.A. (2009). The phosphoproteome of bloodstream form *Trypanosoma brucei*, causative agent of African sleeping sickness. *Mol Cell Proteomics*, 8 (7): 1527-1538.

Neville, D.C.A., Rozanas, C.R., Price, E.M., Gruis, D.B., Verkman, A.S., Townsend, R.R. (1997). Evidence for phosphorylation of serine 753 in CFTR using a novel metal- ion affinity resin and matrix-assisted laser desorption mass spectrometry. *Protein Science*, 6 (11): 2436-2445.

Ngounou Wetie, A.G., Sokolowska, I., Woods, A.G., Roy, U., Deinhardt, K., Darie, C.C. (2014). Protein-protein interactions: switch from classical methods to proteomics and bioinformatics-based approaches. *Cellular and molecular life sciences : CMLS*, 71 (2): 205-228.

Nishikawa, Y., Makala, L., Otsuka, H., Mikami, T., Nagasawa, H. (2002). Mechanisms of apoptosis in murine fibroblasts by two intracellular protozoan parasites, *Toxoplasma gondii* and *Neospora caninum*. *Parasite Immunol*, 24 (7): 347-354.

Nishikawa, Y., Xuan, X., Nagasawa, H., Igarashi, I., Fujisaki, K., Otsuka, H., Mikami, T. (2000). Monoclonal antibody inhibition of *Neospora caninum* tachyzoite invasion into host cells. *Int J Parasitol*, 30 (1): 51-58.

Nooren, I.M., Thornton, J.M. (2003). Diversity of protein-protein interactions. *EMBO J*, 22 (14): 3486-3492.

Nuhse, T.S., Stensballe, A., Jensen, O.N., Peck, S.C. (2003). Large-scale analysis of in vivo phosphorylated membrane proteins by immobilized metal ion affinity chromatography and mass spectrometry. *Mol Cell Proteomics*, 2 (11): 1234-1243.

Ojo, K.K., Reid, M.C., Siddaramaiah, L.K., Müller, J., Winzer, P., Zhang, Z., Keyloun, K.R., Vidadala, R.S.R., Merritt, E.A., Hol, W.G.J., Maly, D.J., Fan, E., Van Voorhis, W.C., Hemphill, A. (2014). *Neospora caninum* calcium-dependent protein kinase 1 is an effective drug target for neosporosis therapy. *PLoS ONE*, 9 (3):

Oka, O.B., Bulleid, N.J. (2013). Forming disulfides in the endoplasmic reticulum. *Biochimica et biophysica acta*, 1833 (11): 2425-2429.

Okada, T., Marmansari, D., Li, Z.M., Adilbish, A., Canko, S., Ueno, A., Shono, H., Furuoka, H., Igarashi, M. (2013). A novel dense granule protein, GRA22, is involved in regulating parasite egress in *Toxoplasma gondii*. *Molecular and Biochemical Parasitology*, 189 (1-2): 5-13.

Olsen, J.V., Mann, M. (2004). Improved peptide identification in proteomics by two consecutive stages of mass spectrometric fragmentation. *Proc Natl Acad Sci U S A*, 101 (37): 13417-13422.

Ong, Y.C., Reese, M.L., Boothroyd, J.C. (2010). *Toxoplasma* rhoptry protein 16 (ROP16) subverts host function by direct tyrosine phosphorylation of STAT6. *J Biol Chem*, 285 (37): 28731-28740.

Orru, S., Caputo, I., D'Amato, A., Ruoppolo, M., Esposito, C. (2003). Proteomics identification of acyl-acceptor and acyl-donor substrates for transglutaminase in a human intestinal epithelial cell line. Implications for celiac disease. *J Biol Chem*, 278 (34): 31766-31773.

Paré, J., Thurmond, M.C., Hietala, S.K. (1997). *Neospora caninum* antibodies in cows during pregnancy as a predictor of congenital infection and abortion. *Journal of Parasitology*, 83 (1): 82-87.

Paugam, A., Creuzet, C., Dupouy-Camet, J., Roisin, M.P. (2001). Evidence for the existence of a proteasome in *Toxoplasma gondii*: intracellular localization and specific peptidase activities. *Parasite*, 8 (4): 267-273.

Pawson, T. (1995). Protein modules and signalling networks. *Nature*, 373 (6515): 573-580.

Payne, T.M., Molestina, R.E., Sinai, A.P. (2003). Inhibition of caspase activation and a requirement for NF=KB function in the *Toxoplasma gondii*-mediated blockade of host apoptosis. *Journal of Cell Science*, 116 (21): 4345-4358.

Perco, P., Mühlberger, I., Mayer, G., Oberbauer, R., Lukas, A., Mayer, B. (2010). Linking transcriptomic and proteomic data on the level of protein interaction networks. *Electrophoresis*, 31 (11): 1780-1789.

Perera, P.K., Gasser, R.B., Firestone, S.M., Anderson, G.A., Malmo, J., Davis, G., Beggs, D.S., Jabbar, A. (2014). Oriental theileriosis in dairy cows causes a significant milk production loss. *Parasit Vectors*, 7 (1): 73.

Petroulakis, E., Mamane, Y., Le Bacquer, O., Shahbazian, D., Sonenberg, N. (2006). mTOR signalling: Implications for cancer and anticancer therapy. *British Journal of Cancer*, 94 (2): 195-199.

Pfeiffer, K., Gohil, V., Stuart, R.A., Hunte, C., Brandt, U., Greenberg, M.L., Schagger, H. (2003). Cardiolipin stabilizes respiratory chain supercomplexes. *J Biol Chem*, 278 (52): 52873-52880.

Pinkse, M.W.H., Uitto, P.M., Hilhorst, M.J., Ooms, B., Heck, A.J.R. (2004). Selective isolation at the femtomole level of phosphopeptides from proteolytic digests using 2D-NanoLC-ESI-MS/MS and titanium oxide precolumns. *Analytical Chemistry*, 76 (14): 3935-3943.

Pittman, K.J., Aliota, M.T., Knoll, L.J. (2014). Dual transcriptional profiling of mice and *Toxoplasma gondii* during acute and chronic infection. *BMC genomics*, 15 (1): 806.

Posewitz, M.C., Tempst, P. (1999). Immobilized gallium(III) affinity chromatography of phosphopeptides. *Anal Chem*, 71 (14): 2883-2892.

Prehna, G., Ivanov, M.I., Bliska, J.B., Stebbins, C.E. (2006). Yersinia Virulence Depends on Mimicry of Host Rho-Family Nucleotide Dissociation Inhibitors. *Cell*, 126 (5): 869-880.

Rabenau, K.E., Sohrabi, A., Tripathy, A., Reitter, C., Ajioka, J.W., Tomley, F.M., Carruthers, V.B. (2001). TgM2AP participates in *Toxoplasma gondii* invasion of host cells and is tightly associated with the adhesive protein TgMIC2. *Molecular Microbiology*, 41 (3): 537-547.

Ramaprasad, A., Mourier, T., Naeem, R., Malas, T.B., Moussa, E., Panigrahi, A., Vermont, S.J., Otto, T.D., Wastling, J., Pain, A. (2015). Comprehensive evaluation of *Toxoplasma gondii* VEG and *Neospora caninum* LIV genomes with tachyzoite stage transcriptome and proteome defines novel transcript features. *PLoS One*, 10 (4): e0124473.

Rath, A., Glibowicka, M., Nadeau, V.G., Chen, G., Deber, C.M. (2009). Detergent binding explains anomalous SDS-PAGE migration of membrane proteins. *Proc Natl Acad Sci U S A*, 106 (6): 1760-1765.

Reid, A.J., Vermont, S.J., Cotton, J.A., Harris, D., Hill-Cawthorne, G.A., Konen-Waisman, S., Latham, S.M., Mourier, T., Norton, R., Quail, M.A., Sanders, M., Shanmugam, D., Sohal, A., Wasmuth, J.D., Brunk, B., Grigg, M.E., Howard, J.C., Parkinson, J., Roos, D.S., Trees, A.J., Berriman, M., Pain, A., Wastling, J.M. (2012). Comparative genomics of the apicomplexan parasites *Toxoplasma gondii* and *Neospora caninum*: Coccidia differing in host range and transmission strategy. *PLoS Pathog*, 8 (3):

Reiss, M., Viebig, N., Brecht, S., Fourmaux, M.N., Soete, M., Di Cristina, M., Dubremetz, J.F., Soldati, D. (2001). Identification and characterization of an escorter for two secretory adhesins in *Toxoplasma gondii*. *The Journal of cell biology*, 152 (3): 563-578.

Rosenshine, I., Donnenberg, M.S., Kaper, J.B., Finlay, B.B. (1992). Signal transduction between enteropathogenic *Escherichia coli* (EPEC) and epithelial cells: EPEC induces tyrosine phosphorylation of host cell proteins

to initiate cytoskeletal rearrangement and bacterial uptake. *The EMBO Journal*, 11 (10): 3551-3560.

Rosowski, E.E., Lu, D., Julien, L., Rodda, L., Gaiser, R.A., Jensen, K.D.C., Saeij, J.P.J. (2011). Strain-specific activation of the NF-κB pathway by GRA15, a novel *Toxoplasma gondii* dense granule protein. *Journal of Experimental Medicine*, 208 (1): 195-212.

Saeij, J.P., Boyle, J.P., Coller, S., Taylor, S., Sibley, L.D., Brooke-Powell, E.T., Ajioka, J.W., Boothroyd, J.C. (2006). Polymorphic secreted kinases are key virulence factors in toxoplasmosis. *Science*, 314 (5806): 1780-1783.

Saeij, J.P., Coller, S., Boyle, J.P., Jerome, M.E., White, M.W., Boothroyd, J.C. (2007). *Toxoplasma* co-opts host gene expression by injection of a polymorphic kinase homologue. *Nature*, 445 (7125): 324-327.

Saeij, J.P.J., Boyle, J.P., Boothroyd, J.C. (2005). Differences among the three major strains of *Toxoplasma gondii* and their specific interactions with the infected host. *Trends in Parasitology*, 21 (10): 476-481.

Saffer, L.D., Mercereau-Puijalon, O., Dubremetz, J.F., Schwartzman, J.D. (1992). Localization of a *Toxoplasma gondii* rhoptry protein by immunoelectron microscopy during and after host cell penetration. *The Journal of protozoology*, 39 (4): 526-530.

Sanders, P.R., Cantin, G.T., Greenbaum, D.C., Gilson, P.R., Nebl, T., Moritz, R.L., Yates, J.R., 3rd, Hodder, A.N., Crabb, B.S. (2007). Identification of protein complexes in detergent-resistant membranes of *Plasmodium falciparum* schizonts. *Mol Biochem Parasitol*, 154 (2): 148-157.

Sanli, T., Steinberg, G.R., Singh, G., Tsakiridis, T. (2014). AMP-activated protein kinase (AMPK) beyond metabolism: A novel genomic stress sensor participating in the DNA damage response pathway. *Cancer Biology and Therapy*, 15 (2): 159-169.

Saouros, S., Edwards-Jones, B., Reiss, M., Sawmynaden, K., Cota, E., Simpson, P., Dowse, T.J., Jakle, U., Ramboarina, S., Shivarattan, T., Matthews, S., Soldati-Favre, D. (2005). A novel galectin-like domain from *Toxoplasma gondii* micronemal protein 1 assists the folding, assembly, and transport of a cell adhesion complex. *J Biol Chem*, 280 (46): 38583-38591.

Schagen, F.H., Rademaker, H.J., Rabelink, M.J., van Ormondt, H., Fallaux, F.J., van der Eb, A.J., Hoeben, R.C. (2000). Ammonium sulphate precipitation of recombinant adenovirus from culture medium: an easy method to increase the total virus yield. *Gene Ther*, 7 (18): 1570-1574.

Schagger, H. (2001). Blue-native gels to isolate protein complexes from mitochondria. *Methods Cell Biol*, 65 231-244.

Schagger, H., Bentlage, H., Ruitenbeek, W., Pfeiffer, K., Rotter, S., Rother, C., Bottcher-Purkl, A., Lodemann, E. (1996). Electrophoretic separation of multiprotein complexes from blood platelets and cell lines: technique for the analysis of diseases with defects in oxidative phosphorylation. *Electrophoresis*, 17 (4): 709-714.

Schagger, H., Cramer, W.A., Von Jagow, G. (1994). Analysis of molecular masses and oligomeric states of protein complexes by blue native electrophoresis and isolation of membrane protein complexes by two-dimensional native electrophoresis. *Analytical Biochemistry*, 217 (2): 220-230.

Schagger, H., Jagow, G.v. (1991). Blue native electrophoresis for isolation of membrane protein complexes in enzymatically active form. *Anal. Biochem.*, 199 (223-231):

Schagger, H., von Jagow, G. (1991). Blue native electrophoresis for isolation of membrane protein complexes in enzymatically active form. *Anal Biochem*, 199 (2): 223-231.

Schwab, J.C., Beckers, C.J.M., Joiner, K.A. (1994). The parasitophorous vacuole membrane surrounding intracellular *Toxoplasma gondii* functions as a molecular sieve. *Proceedings of the National Academy of Sciences of the United States of America*, 91 (2): 509-513.

Segal, E.D., Falkow, S., Tompkins, L.S. (1996). Helicobacter pylori attachment to gastric cells induces cytoskeletal rearrangements and tyrosine phosphorylation of host cell proteins. *Proc Natl Acad Sci U S A*, 93 (3): 1259-1264.

Sessler, N., Krug, K., Nordheim, A., Mordmuller, B., Macek, B. (2012). Analysis of the *Plasmodium falciparum* proteasome using Blue Native PAGE and label-free quantitative mass spectrometry. *Amino Acids*, 43 (3): 1119-1129.

Seward, R.J., Perlman, D.H., Berg, E.A., Hu, J., Costello, C.E. 2004. Methyl esterification of peptides prior to immobilized metal-ion affinity chromatography: determination of optimal time time course and side products. In: 52nd ASMS Conference on Mass Spectrometry and Allied Topics, May 23-27, Nashville, Tennessee.

Shahbazian, D., Parsyan, A., Petroulakis, E., Hershey, J., Sonenberg, N. (2010). eIF4B controls survival and proliferation and is regulated by proto-oncogenic signalling pathways. *Cell Cycle*, 9 (20): 4106-4109.

Shankavaram, U.T., Reinhold, W.C., Nishizuka, S., Major, S., Morita, D., Chary, K.K., Reimers, M.A., Scherf, U., Kahn, A., Dolginow, D., Cossman, J., Kaldjian, E.P., Scudiero, D.A., Petricoin, E., Liotta, L., Lee, J.K., Weinstein, J.N. (2007). Transcript and protein expression profiles of the NCI-60 cancer cell panel: An integromic microarray study. *Molecular Cancer Therapeutics*, 6 (3): 820-832.

Sharma, S.V., Settleman, J. (2009). ErbBs in lung cancer. *Exp Cell Res*, 315 (4): 557-571.

Shaw, M.K., He, C.Y., Roos, D.S., Tilney, L.G. (2000). Proteasome inhibitors block intracellular growth and replication of *Toxoplasma gondii*. *Parasitology*, 121 (1): 35-47.

Shchemelinin, I., Šefc, L., Nečas, E. (2006). Protein kinases, their function and implication in cancer and other diseases. *Folia Biologica*, 52 (3): 81-101.

Shi, L., Chowdhury, S.M., Smallwood, H.S., Yoon, H., Mottaz-Brewer, H.M., Norbeck, A.D., McDermott, J.E., Clauss, T.R., Heffron, F., Smith, R.D., Adkins, J.N. (2009). Proteomic investigation of the time course responses of RAW 264.7 macrophages to infection with *Salmonella enterica*. *Infect Immun*, 77 (8): 3227-3233.

Shi, Y. (2009). Serine/threonine phosphatases: mechanism through structure. *Cell*, 139 (3): 468-484.

Shui, W., Gilmore, S.A., Sheu, L., Liu, J., Keasling, J.D., Bertozzi, C.R. (2009). Quantitative Proteomic Profiling of Host−Pathogen Interactions: The Macrophage Response to *Mycobacterium tuberculosis* Lipids. *Journal of Proteome Research*, 8 (1): 282-289.

Sibley, L.D., Niesman, I.R., Parmley, S.F., Cesbron-Delauw, M.F. (1995). Regulated secretion of multi-lamellar vesicles leads to formation of a tubulovesicular network in host-cell vacuoles occupied by *Toxoplasma gondii*. *Journal of Cell Science*, 108 (4): 1669-1677.

Sibley, L.D., Pfefferkorn, E.R., Boothroyd, J.C. (1991). Proposal for a uniform genetic nomenclature in *Toxoplasma gondii*. *Parasitology Today*, 7 (12): 327-328.

Sinai, A.P. (2014). The *Toxoplasma gondii* Parasitophorous Vacuole Membrane: A Multifunctional Organelle in the Infected Cell. In: Weiss, L.M., Kim, K. (Eds.). *Toxoplasma gondii*. Boston: Academic Press, 375-387.

Sinai, A.P., Joiner, K.A. (1997). Safe haven: the cell biology of nonfusogenic pathogen vacuoles. *Annu Rev Microbiol*, 51 415-462.

Sinai, A.P., Joiner, K.A. (2001). The *Toxoplasma gondii* protein ROP2 mediates host organelle association with the parasitophorous vacuole membrane. *The Journal of cell biology*, 154 (1): 95-108.

Sinai, A.P., Webster, P., Joiner, K.A. (1997). Association of host cell endoplasmic reticulum and mitochondria with the *Toxoplasma* grondii parasitophorous vacuole membrane: A high affinity interaction. *Journal of Cell Science*, 110 (17): 2117-2128.

Smith, M.G., Ptacek, J., Snyder, M. (2011). Kinase substrate interactions. In: Wu, C.J. (Eds.). *Protein microarray for disease analysis, methods and protocols*. London: Springer, 201-212.

Sohn, C.S., Cheng, T.T., Drummond, M.L., Peng, E.D., Vermont, S.J., Xia, D., Cheng, S.J., Wastling, J.M., Bradley, P.J. (2011). Identification of novel proteins in *Neospora caninum* using an organelle purification and monoclonal antibody approach. *PLoS ONE*, 6 (4): e18383.

Soldati, D., Dubremetz, J.F., Lebrun, M. (2001). Microneme proteins: structural and functional requirements to promote adhesion and invasion by the apicomplexan parasite *Toxoplasma gondii*. *Int J Parasitol*, 31 (12): 1293-1302.

Song, C., Chiasson, M.A., Nursimulu, N., Hung, S.S., Wasmuth, J., Grigg, M.E., Parkinson, J. (2013). Metabolic reconstruction identifies strain-specific regulation of virulence in *Toxoplasma gondii*. *Molecular Systems Biology*, 9

Speer, C.A., Clark, S., Dubey, J.P. (1998). Ultrastructure of the oocysts, sporocysts, and sporozoites of *Toxoplasma gondii*. *J Parasitol*, 84 (3): 505-512.

Speer, C.A., Dubey, J.P., McAllister, M.M., Blixt, J.A. (1999). Comparative ultrastructure of tachyzoites, bradyzoites, and tissue cysts of *Neospora caninum* and *Toxoplasma gondii*. *Int J Parasitol*, 29 (10): 1509-1519.

Stern, D.F. (2001). Phosphoproteomics. *Exp Mol Pathol*, 70 (3): 327-331.

Sterner, D.E., Berger, S.L. (2000). Acetylation of histones and transcription-related factors. *Microbiology and molecular biology reviews : MMBR*, 64 (2): 435-459.

Straub, K.W., Cheng, S.J., Sohn, C.S., Bradley, P.J. (2009). Novel components of the Apicomplexan moving junction reveal conserved and coccidia-restricted elements. *Cell Microbiol*, 11 (4): 590-603.

Straub, K.W., Peng, E.D., Hajagos, B.E., Tyler, J.S., Bradley, P.J. (2011). The moving junction protein RON8 facilitates firm attachment and host cell invasion in *Toxoplasma gondii*. *PLoS Pathog*, 7 (3): e1002007.

Su, Y., Li, X., Ji, W., Sun, B., Xu, C., Li, Z., Qian, G., Su, C. (2014). Small molecule with big role: MicroRNAs in cancer metastatic microenvironments. *Cancer Letters*, 344 (2): 147-156.

Suss-Toby, E., Zimmerberg, J., Ward, G.E. (1996). *Toxoplasma* invasion: The parasitophorous vacuole is formed from host cell plasma membrane and

pinches off via a fission pore. *Proceedings of the National Academy of Sciences of the United States of America*, 93 (16): 8413-8418.

Swamy, M., Siegers, G.M., Minguet, S., Wollscheid, B., Schamel, W.W. (2006). Blue native polyacrylamide gel electrophoresis (BN-PAGE) for the identification and analysis of multiprotein complexes. *Science's STKE : signal transduction knowledge environment*, 2006 (345): pl4.

Tenter, A.M., Heckeroth, A.R., Weiss, L.M. (2000). *Toxoplasma gondii*: from animals to humans. *Int J Parasitol*, 30 (12-13): 1217-1258.

Tie, J., Fan, D. (2011). Big roles of microRNAs in tumorigenesis and tumor development. *Histol Histopathol*, 26 (10): 1353-1361.

Tomley, F.M., Soldati, D.S. (2001). Mix and match modules: structure and function of microneme proteins in apicomplexan parasites. *Trends Parasitol*, 17 (2): 81-88.

Torrey, E.F., Yolken, R.H., Torrey, E.F., Yolken, R.H. (2013). *Toxoplasma* oocysts as a public health problem. *Trends in Parasitology*, 29 (8): 380-384.

Travier, L., Mondragon, R., Dubremetz, J.F., Musset, K., Mondragon, M., Gonzalez, S., Cesbron-Delauw, M.F., Mercier, C. (2008). Functional domains of the *Toxoplasma* GRA2 protein in the formation of the membranous nanotubular network of the parasitophorous vacuole. *Int J Parasitol*, 38 (7): 757-773.

Treeck, M., Sanders, J.L., Elias, J.E., Boothroyd, J.C. (2011). The phosphoproteomes of *plasmodium falciparum* and *Toxoplasma gondii* reveal unusual adaptations within and beyond the parasites' boundaries. *Cell Host and Microbe*, 10 (4): 410-419.

Trees, A.J., Davison, H.C., Innes, E.A., Wastling, J.M. (1999). Towards evaluating the economic impact of bovine neosporosis. *Int J Parasitol*, 29 (8): 1195-1200.

Trees, A.J., Williams, D.J. (2005). Endogenous and exogenous transplacental infection in *Neospora caninum* and *Toxoplasma gondii*. *Trends Parasitol*, 21 (12): 558-561.

Trinidad, J.C., Specht, C.G., Thalhammer, A., Schoepfer, R., Burlingame, A.L. (2006). Comprehensive identification of phosphorylation sites in postsynaptic density preparations. *Mol Cell Proteomics*, 5 (5): 914-922.

Tsalikis, J., Croitoru, D.O., Philpott, D.J., Girardin, S.E. (2013). Nutrient sensing and metabolic stress pathways in innate immunity. *Cellular Microbiology*, 15 (10): 1632-1641.

Tyler, J.S., Boothroyd, J.C. (2011). The C-terminus of *Toxoplasma* RON2 provides the crucial link between AMA1 and the host-associated invasion complex. *PLoS Pathogens*, 7 (2): e1001282.

Urbaniak, M.D., Martin, D.M., Ferguson, M.A. (2013). Global quantitative SILAC phosphoproteomics reveals differential phosphorylation is widespread between the procyclic and bloodstream form lifecycle stages of *Trypanosoma brucei*. *Journal of proteome research*, 12 (5): 2233-2244.

Villen, J., Beausoleil, S.A., Gerber, S.A., Gygi, S.P. (2007). Large-scale phosphorylation analysis of mouse liver. *Proc Natl Acad Sci U S A*, 104 (5): 1488-1493.

Villen, J., Gygi, S.P. (2008). The SCX/IMAC enrichment approach for global phosphorylation analysis by mass spectrometry. *Nat Protoc*, 3 (10): 1630-1638.

Vogel, C., Marcotte, E.M. (2012). Insights into the regulation of protein abundance from proteomic and transcriptomic analyses. *Nature reviews. Genetics*, 13 (4): 227-232.

von Mering, C., Krause, R., Snel, B., Cornell, M., Oliver, S.G., Fields, S., Bork, P. (2002). Comparative assessment of large-scale data sets of protein-protein interactions. *Nature*, 417 (6887): 399-403.

Walduck, A., Rudel, T., Meyer, T.F. (2004). Proteomic and gene profiling approaches to study host responses to bacterial infection. *Curr Opin Microbiol*, 7 (1): 33-38.

Wang, Y., Weiss, L.M., Orlofsky, A. (2009). Intracellular parasitism with *Toxoplasma gondii* stimulates mammalian-target-of-rapamycin-dependent host cell growth despite impaired signalling to S6K1 and 4E-BP1. *Cell Microbiol*, 11 (6): 983-1000.

Wastling, J.M., Armstrong, S.D., Krishna, R., Xia, D. (2012). Parasites, proteomes and systems: Has Descartes' clock run out of time? *Parasitology*, 139 (9): 1103-1118.

Wastling, J.M., Xia, D. (2013). Proteomics of *Toxoplasma gondii*. In: Weiss, L.M., Kim, K. (Eds.). *Toxoplasma gondii: The Model Apicomplexan - Perspectives and Methods: Second Edition*. Amsterdam and Boston: Elsevier/Academic Press, 731-754.

Weilhammer, D.R., Iavarone, A.T., Villegas, E.N., Brooks, G.A., Sinai, A.P., Sha, W.C. (2012). Host metabolism regulates growth and differentiation of *Toxoplasma gondii*. *Int J Parasitol*, 42 (10): 947-959.

Weissenböck, H., Dubey, J.P., Suchy, A., Sturm, E. (1997). Neosporosis causing encephalomalacia and myocarditis in young dogs. *Wiener Tierarztliche Monatsschrift*, 84 (8): 233-237.

Westra, D.F., Welling, G.W., Koedijk, D.G., Scheffer, A.J., The, T.H., Welling-Wester, S. (2001). Immobilised metal-ion affinity chromatography purification of histidine-tagged recombinant proteins: a wash step with a low concentration of EDTA. *Journal of chromatography. B, Biomedical sciences and applications*, 760 (1): 129-136.

Wieduwilt, M.J., Moasser, M.M. (2008). The epidermal growth factor receptor family: biology driving targeted therapeutics. *Cellular and molecular life sciences : CMLS*, 65 (10): 1566-1584.

Wiens, O., Xia, D., von Schubert, C., Wastling, J.M., Dobbelaere, D.A., Heussler, V.T., Woods, K.L. (2014). Cell cycle-dependent phosphorylation of *Theileria annulata* schizont surface proteins. *PLoS One*, 9 (7): e103821.

Williams, D.J.L., Hartley, C.S., Björkman, C., Trees, A.J. (2009). Endogenous and exogenous transplacental transmission of *Neospora caninum* - How the route of transmission impacts on epidemiology and control of disease. *Parasitology*, 136 (14): 1895-1900.

Wilson-Grady, J.T., Villen, J., Gygi, S.P. (2008). Phosphoproteome analysis of fission yeast. *J Proteome Res*, 7 (3): 1088-1097.

Wittig, I., Braun, H.P., Schagger, H. (2006). Blue native PAGE. *Nat Protoc*, 1 (1): 418-428.

Wojcechowskyj, J.A., Didigu, C.A., Lee, J.Y., Parrish, N.F., Sinha, R., Hahn, B.H., Bushman, F.D., Jensen, S.T., Seeholzer, S.H., Doms, R.W. (2013). Quantitative phosphoproteomics reveals extensive cellular reprogramming during HIV-1 entry. *Cell Host Microbe*, 13 (5): 613-623.

Wolschin, F., Wienkoop, S., Weckwerth, W. (2005). Enrichment of phosphorylated proteins and peptides from complex mixtures using metal oxide/hydroxide affinity chromatography (MOAC). *Proteomics*, 5 (17): 4389-4397.

Woodbine, K.A., Medley, G.F., Moore, S.J., Ramirez-Villaescusa, A., Mason, S., Green, L.E. (2008). A four year longitudinal sero-epidemiology study of *Neospora caninum* in adult cattle from 114 cattle herds in south west England: associations with age, herd and dam-offspring pairs. *BMC Vet Res*, 4 35.

Wullschleger, S., Loewith, R., Hall, M.N. (2006). TOR signalling in growth and metabolism. *Cell*, 124 (3): 471-484.

Xia, D., Sanderson, S.J., Jones, A.R., Prieto, J.H., Yates, J.R., Bromley, E., Tomley, F.M., Lal, K., Sinden, R.E., Brunk, B.P. (2008). The proteome of *Toxoplasma gondii*: integration with the genome provides novel insights into gene expression and annotation. *Genome biology*, 9 (7): R116.

Yamamoto, M., Standley, D.M., Takashima, S., Saiga, H., Okuyama, M., Kayama, H., Kubo, E., Ito, H., Takaura, M., Matsuda, T., Soldati-Favre, D., Takeda, K. (2009). A single polymorphic amino acid on *Toxoplasma gondii* kinase ROP16 determines the direct and strain-specific activation of Stat3. *The Journal of experimental medicine*, 206 (12): 2747-2760.

Yang, T.E.T., Nelson, P.S., Bush, G.L., Meyer, D.I., Kain, S.R. (1997). An immobilized Co2+ affinity matrix for purification of 6xhistidine-tagged proteins. *American Biotechnology Laboratory*, 15 (1): 12-14.

Yang, Y., Hu, M., Yu, K., Zeng, X., Liu, X. (2015). Mass spectrometry-based proteomic approaches to study pathogenic bacteria-host interactions. *Protein & Cell*, 6 (4): 265-274.

Yarden, Y., Sliwkowski, M.X. (2001). Untangling the ErbB signalling network. *Nature reviews. Molecular cell biology*, 2 (2): 127-137.

Zhai, B., Villen, J., Beausoleil, S.A., Mintseris, J., Gygi, S.P. (2008). Phosphoproteome analysis of Drosophila melanogaster embryos. *J Proteome Res*, 7 (4): 1675-1682.

Zhang, H., Compaore, M.K.A., Lee, E.g., Liao, M., Zhang, G., Sugimoto, C., Fujisaki, K., Nishikawa, Y., Xuan, X. (2007). Apical membrane antigen 1 is a cross-reactive antigen between *Neospora caninum* and *Toxoplasma gondii*, and the anti-NcAMA1 antibody inhibits host cell invasion by both parasites. *Molecular and Biochemical Parasitology*, 151 (2): 205-212.

Zheng, B., He, A., Gan, M., Li, Z., He, H., Zhan, X. (2009). MIC6 associates with aldolase in host cell invasion by *Toxoplasma gondii*. *Parasitol Res*, 105 (2): 441-445.

Zinecker, C.F., Striepen, B., Tomavo, S., Dubremetz, J.F., Schwarz, R.T. (1998). The dense granule antigen, GRA2 of *Toxoplasma gondii* is a glycoprotein containing O-linked oligosaccharides. *Molecular and Biochemical Parasitology*, 97 (1-2): 241-246.

Zolnierowicz, S., Bollen, M. (2000). Protein phosphorylation and protein phosphatases. *EMBO J*, 19 (4): 483-488.

Zoncu, R., Efeyan, A., Sabatini, D.M. (2011). mTOR: from growth signal integration to cancer, diabetes and ageing. *Nature reviews. Molecular cell biology*, 12 (1): 21-35.

Zuo, X., Li, S., Hall, J., Mattern, M.R., Tran, H., Shoo, J., Tan, R., Weiss, S.R., Butt, T.R. (2005). Enhanced expression and purification of membrane proteins by

SUMO fusion in *Escherichia coli*. *Journal of Structural and Functional Genomics*, 6 (2-3): 103-111.